Integrating Meal and Exercise into Personalized Glucoregulation Models: Metabolic Dynamics and Diabetic Athletes

Sofie Schunk
Marquette University

INTEGRATING MEAL AND EXERCISE INTO PERSONALIZED GLUCOREGULATION
MODELS: METABOLIC DYNAMICS AND DIABETIC ATHLETES

by

Sofie W. Schunk, B.S.

A Thesis submitted to the Faculty of the Graduate School, Marquette University, in
Partial Fulfillment of the Requirements for the Degree of Master of Biomedical
Engineering

Milwaukee, Wisconsin

December 2015

ABSTRACT
INTEGRATING MEAL AND EXERCISE INTO PERSONALIZED GLUCOREGULATION
MODELS: METABOLIC DYNAMICS AND DIABETIC ATHLETES

Sofie W. Schunk, B.S.

Marquette University, 2015

Diabetes affects nearly 26 million Americans, according to the American Diabetes Association, with as many as three million Americans who have Type 1 Diabetes (ADA, 2015). Type 1 Diabetes (T1D) is autoimmune and characterized by little to no insulin production whereas Type 2 Diabetes (T2D) concerns insulin resistance and inability to use produced insulin. Factors contributing to current diabetes management and regulation include exercise type, daily movement activities, and distinct tissue compartment metabolism, each challenging to model in a robust and comprehensive manner. Past models are highly limited in regard to exercise and varying glucose fluctuations dependent on type, intensity, and duration. Modeling could greatly enhance factors that contribute to diabetes management—currently, T1D is managed with a pump and/or injections, informed by constant blood glucose monitoring.

This thesis addresses knowledge gaps in the management and etiology of diabetes through development of a novel dynamic mathematical model informing controller design and implementation (artificial pancreas, continuous glucose monitors, and pumps). Diet and meal content on the basis of varying glycemic index and on the effects of activity and exercise, with lifestyle habit implications are a main focus. Emphasis is placed on model personalization with a T1D athlete example. The following model and case study implement specific aims:

- 10th order model designed in Matlab with 4 interrelated sub-models to integrate meal diversity, exercise activities, and personalized body composition.
    - 3-State Glucose Compartmental Model
    - 2-State Control Mechanisms: Insulin and Glucagon
    - 2-State Digestion Model
    - 2-State Exogenous Insulin Control
    - Skeletal Muscle Model with Mitochondrial State
    - Nonlinear relations including Hill Functions
- A 2 Phase Case Study, IRB approved for a Type 1 athletic 23-year-old female to evaluate and develop the model.

Results illustrate effects of meal type (slow vs. fast glycemic index) and exercise/activity based glucose-glycogen consumption on blood plasma glucose predictions and hormonal control action for both non-diabetic and diabetic model versions. Current challenges are addressed with model personalization, providing input flexibility for body mass, muscle ratio, stress, and types of diabetes (T1D, T2D) informing artificial pancreas design and possible sports performance applications.

ACKNOWLEDGMENTS

Sofie W. Schunk

I would like to thank and recognize:

- Dr. Jack Winters for the constant and tireless feedback, meetings, knowledge, and care for the success of the project as my advisor.
  - Dr. Winters' students tested the model with use as part of a class project, giving key controller insights.

- Dr. Said Audi, and Dr. Sandra Hunter for serving on my committee.

- Dr. Paula Papanek, Christopher Sundberg, and laboratory members for assisting with anaerobic threshold testing and DXA body composition scans.

- Other Type 1 Diabetic athletes that I have communicated with and ran with, encouraging me as they experience similar management issues and have shared unique and personalized knowledge: John Klika, DSP athletes, etc.
  - This was my personal motivation for the project.

- My family and friends for their continuous love, patience, and inspiration to finish my degree pursuing something with personal motivation.

- The Marquette President's Running Club for joining me on a few of my case study exercise sessions and giving me guidance and inspiration to pursue running at a higher level.

- Marquette University Athletics Al McGuire Center and Todd Smith for allowing me to use their facility during exercise sessions.

- Dexcom (San Diego location) for the opportunity to present my ideas and for use of their G4 Platinum Continuous Glucose Monitor as part of the Phase 2 Case Study.

- Bob Hanische of Peak Performance Professionals for providing initial insight and knowledge on diabetes and exercise in terms of Type 1 and Type 2.

This thesis is dedicated to people with Type 1 diabetes and their families, as well as my family and friends, who inspire me to pursue my passion of bettering the diabetic community and encourage those to pursue their dreams despite having diabetes.

TABLE OF CONTENTS

LIST OF TABLES

LIST OF FIGURES

GLOSSARY

AP, Artificial Pancreas
AT, Anaerobic Threshold
BG, Blood Glucose
bpm, Beats Per Minute
CGM, Continuous Glucose Monitor
CHO, Carbohydrate
C_{gm}**,** Glucagon Control Parameter, Muscle Tissue Gain, scaled to pg/dl (*Cgb* in code)
C_{gnm}**,** Glucagon Control Parameter, Non-Muscle Tissue Gain, scaled to pg/dl (*Cga*)
C_{inm}**,** Insulin Control Parameter, Non-Muscle Tissue Gain (*Cia* in code)
C_{im}**,** Insulin Control Parameter, Muscle Tissue Gain (*Cib* in code)
ECF, Extracellular Fluid
FFA, Free Fatty Acid
GI, Glycemic Index
GLC, Glucagon
GLUT2, Non-Muscle Glucose Transporter
GLUT4, Muscle Glucose Transporter
G_{efff}, Non-Linear Hill Controller for Rate of x_d entering x_g (*Gabs* in code)
G_{effs}, Non-Linear Hill Controller for Rate of x_{ds} entering x_d path (*Gslow* in code)
G_{exer}, Blood Glucose Loss with Muscle Demand Gradient (*Gmgrad* in code)
$G_{ex\text{-}Total}$, Total Aerobic Exercise Glucose Consumption (kcal/hr)
G_{metm}, Basal Metabolic Elimination Rate to Muscle Tissue, Scaled by w_m (g/hr)
G_{metnm}, Basal Metabolic Elimination Rate to Non-Muscle Tissue, Scaled by w_{nm} (g/hr)
HR, Heart Rate (bpm), inputted as *u5*
k_{greft}**,** Reference Threshold for BG for Non-Muscle Flux Direction (mg/dl)
IMTG, Intramuscular Triglyceride
k_{fast}, Meal GI Parameter (Scale of 0-100)
$k_{s\text{-}ds}$, Half-Way Value for Hill Control, Slow Digestive Pathway (Rising)
rattype1i, Ratio of T1D (Decimal Percent, Remaining Insulin Production)
rattype1g, Ratio of T1D (Decimal Percent, Remaining Glucagon Production)
RER, Respiratory Exchange Ratio
T1D, Type 1 Diabetes
T2D, Type 2 Diabetes
u1fast, Input Representing Fast Absorbing Carbohydrate Path, in kcal/hr
u1slow, Input Representing Slow Absorbing Carbohydrate Path, in kcal/hr
u2, Input Representing Insulin Injection
u3, Input Representing Aerobic Exercise (same as u_{exer}), in kcal/hr
u4, Input Representing Anaerobic Exercise (same as u_{daily}), in kcal/hr
u5, Input Representing External Heart Rate Data, in bpm
u_{carb}**,** Input Representing Proportion of Carbohydrate (*fraccarb* in code)
u_{daily}**,** Input Representing Daily Activity (same as *u4*), in kcal/hr
u_{exer}**,** Input Representing Aerobic Exercise (same as *u3*), in kcal/hr
u_{fast}**,** Input Representing Fast Carbohydrate (*u1fast* in code), in kcal/hr
u_{inj}**,** Input Representing Insulin Injection (same as *u2*)

u_{slow}, Input Representing Slow Carbohydrate (***u1slow*** in code), in kcal/hr

uHM, Input Representing Hormonal Action as a Stress Ratio (*stressor* parameter)

VO2max, Maximal Aerobic Capacity

w_{bm}, Scaling Parameter of BG to Glucose Muscle Tissue (*wratm* in code) [g/kg muscle]

w_{bt}, Scaling Parameter of BG to Glucose Non-Muscle Tissue (*wratt* in code) [g/kg]

w_m, Muscle Mass (kg)

w_{mito}, Mitochondrial Mass, as a Ratio of Muscle Mass (***rat***$_{mito}$) (kg)

w_{nm}, Non-Muscle Mass (kg)

x_d, State Representing Glucose Digestive Forward Flow Final Path (g/hr)

x_{ds}, State Representing Low Glycemic Index (Slow) Forward Glucose Path (g/hr)

x_g, State Representing Blood Glucose (mg/dl)

$\dot{x}_g$, State Representing Blood Glucose Derivative (mg/dl)

x_{gn}, State Representing Endogenous Glucagon Control Action in Blood Plasma (pg/dl)

x_i, State Representing Endogenous Insulin Control Action in Blood Plasma (mU/dl)

$x_{inj\text{-}nm}$, State Representing Exogenous Insulin Delivery: Non-Monomeric (mU/hr)

$x_{inj\text{-}m}$, State Representing Exogenous Insulin Delivery: Monomeric (mU/hr)

x_m, State Representing Muscle Tissue (g/kg)

x_{mito}, State Representing Mitochondria (g/kg)

x_{nm}, State Representing Non-Muscle Tissue (g/kg)

1. INTRODUCTION

It can be argued that glucose, in its many forms, is the most important substrate in the body, providing energy for human organ functions and all processes. Hence, a thorough mechanistic and quantitative understanding of blood glucose (BG) regulation would help provide insight into those factors that contribute to diabetes. Further, predictive modeling algorithms can predict BG effects of various lifestyles. Clinicians and diabetes educators need to be able to quantitatively explain effects of diet choice, athletics, and activity level—currently, as seen with many diabetic patients, it is trial and error as to controlling influences of lifestyle factors. Factors include exercise variants, daily movement activities, tissue compartment metabolism, level of athleticism, and meal type distinction and diet habits. Models could aide in predicting athletic performance for all individuals, not just those with disease and/or diabetes. There is a need for a robust and comprehensive lifestyle model, as current models reviewed throughout Chapter 2 are limited, or fail to recognize the importance of, modeling all influential factors.

A novel nonlinear 10-state lumped compartmental model is presented in Chapter 3 that aims to address these challenges, and is designed to provide flexibility for variable body mass, muscle ratio, mitochondrial volume, body composition, metabolism and Type 1 and Type 2 diabetes. The model is intended for both research and clinical use, particularly diabetes educators, and to inform delivery design of current artificial pancreas mechanisms, as well as develop continuous glucose monitor (CGM) feedback and prediction based on current

activity and/or diet. It is motivated by the concept that a diabetic should be able to manage BG with exercise, diet, and dual-hormonal control based on algorithm feedback of a personalized model, similar to that of machine learning mechanisms. Chapter 4, which takes an important step towards extending the general BG regulation model of Chapter 3 to a new personalized version, particularly for trained athletes with Type 1 diabetes. Chapter 3 remains innovative in regard to digestive and non-muscle/muscle compartmental storage dynamics.

Chapter 4 is innovative in creating a *multidisciplinary* model of mass and energy flow dynamics (common to mechanical engineering mechanisms) of the novel glucose model combined with concepts of exercise physiology. When daily choices become habitual, a lifestyle body *type* is present—for example, one could be athletic, lean, overweight, inactive, or active. Exercise physiologists are able to quantify metabolic differences in basal metabolism properties of various body types, which could inform a personalized model. Chapter 4 uses an athletic Type 1 female as an example for future adaptive modeling and device learning mechanisms. Mechanisms involve an additional state to enhance skeletal muscle dynamics in the form of mitochondrial consumption. Additionally, a stressor parameter and input associated with elevated intensity and exercise stress allows for improvement for certain types of exercise modeling, such as high intensity interval training (circuits) or sprints.

Future directions and applications for clinical use are found in Chapter 5. The ultimate goal is to better inform clinicians to educate people with diabetes appropriately in regard to glucose regulation on the basis of lifestyle choices that

may become habitual. This is possible with better understanding of lifestyle types in hope that a library of personalized adaptive models can be created. It is intended that current device technologies will become robust in that each can 'learn' its user to eliminate guesswork of bolus corrections, often used for appearance of hypo- and hyperglycemia. Such models can inform CGM 'trends,' or inform a patient where their BG is headed, based on causation effects of lifestyle inputs. A particular user profile, if robust, could drive overall trends and baselines with instantaneous inputs (i.e. meal GI, stress, and/or exercise) affecting immediate BG.

2. BACKGROUND

2.1 Overview of Disease

Tight regulation of BG is required for adequate metabolic function in humans. Common target BG ranges have included a tight range of 80-120 mg/dl that is ideal for organ performance and brain function, requiring ~130 g/day of glucose (ADA and National Academy of Sciences, 2005). A high BG, or hyperglycemia, results in long-term complications and defines the concept of *diabetes*: elevated fasting BG levels. On the other hand, hypoglycemia, or low BG <60 mg/dl, can occur in all individuals with lack of carbohydrate intake and/or exercise, but is especially dangerous for people with diabetes relying on exogenous sources. Glucoregulation modeling allows for concise predictive BG algorithms, based on controller design and an understanding of human physiologic pathways and hormonal control. A broader 'acceptable' glucose range of 70-180 mg/dl is suggested for modeling

because of undesirable side effects of too tightly regulating BG, especially for active

people with diabetes and minimal model based insulin devices that fail to recognize

that increased insulin sensitivity and glucose consumption are dependent on

activity type (Macdonald, 1987 and McDonald, 2013). Non-diabetic comparisons of

BG response can help inform proper control via insulin and/or other solutions for

BG control: exercise, diet, and other lifestyle activities. The imperative need for

regulation is best explained by *lack* of regulation as common to those with a

disability, such as Type 1 or Type 2 Diabetes.

2.1.1 Type 1 and Type 2 Diabetes

In the process of medical device development, particularly those that replace

(either partially or completely) a lost biological function, it is imperative to

understand the physiology behind control mechanisms involved and the underlying

cause. According to the American Diabetes Association (ADA), Diabetes affects about

9.3% (29.1 million) of the U.S. population in 2012 and is on the rise; however, it is

important to note that only 5% of the 9.3% (1.25 million Americans) have Type 1

diabetes (T1D). People with Type 1 diabetes fail to produce insulin, or at a reduced

amount. People with Type 2 diabetes (T2D) produce insulin (usually in excess) but

do not use insulin *properly*, or have developed insulin resistance. Other key

differences in regard to model purposes include reduced glucagon action in T1D,

body weight differences (T2D particularly), and resting basal insulin, blood, and

tissue glucose levels. Treatment includes continuous monitoring and insulin

administration and/or pills to prevent long-term health complications such as skin

and eye degeneration, neuropathy, ketosis, and foot complications and short-term hypo- and hyperglycemia.

2.2   Historical Literature Review: Response Data and Older Models

Many models focus on varying aspects of blood plasma glucose regulation. Typically BG concentration is the main dynamic model compartment, with models ranging from very simple (2 total compartments) to complex. All have their advantages and disadvantages, but from the present perspective, lack some key states and processes. This section reviews past modeling strategies, and provides a context for the proposed improvements, as such models help address knowledge gaps in the etiology of people with Type 1 and Type 2 diabetes, often informing controller design. Table 2.1 outlines current BG regulation models as an evolutionary process.

One of the most cited original models, focusing on simplification, results from a classic 3-state "Bergman minimal model" with two states including insulin dynamics and glucose (Bergman, 1981). Bergman quantified insulin sensitivity with 3 compartments representing plasma insulin, remote insulin and plasma glucose concentrations. The model focuses on the insulin-dependent patient, assuming all insulin is infused exogenously and then promotes uptake of plasma glucose into the hepatic (liver) and periphery tissues, using the form of ordinary differential equations, multiplicative states, and about 7 known parameters. Extensions of the Bergman minimal model include a minimal exercise model adding a critical threshold value (on the basis of VO2max) that drives hepatic glucose production

and glycogenolysis during exercise characterized by intensity and duration (Roy, 2007). These changes are reflected with added terms of the plasma glucose equation of the Bergman minimal model. Further, in a review of various differential equation approaches, Makroglou et al. (2006) presents delay modeling approaches including those by Sturis et al. (1991), integro-differential equations, and partial differential equations (Makroglou, 2006). The integro-differential equation approach is key for modeling intravenous glucose tolerance test dynamics after recognizing the widely used minimal model is improper in qualitative behavior, as the base parameter is equal to the basal glucose level. A more realistic delay and dynamic model is needed, recognized by many (i.e. Li, 2001 or Mukhopadhyay, 2004) and can also be improved with Hill Kinetics, particularly Michaelis-Menten, as used in the Chapter 3 model structure of this thesis (Gesztelyi, 2012). These additions will address fundamental limitations with added states to further insulin dynamics and the particular need to recognized delays and oscillations (Makroglou, 2006).

Core compartmental improvements to Bergman's model (other than diet and exercise) include a 5-state model adding insulin (in liver) and added glucagon states (Sorensen, 1985 and Northrop, 2000). Sorenson, as an integral part of a chemical engineering Ph.D. dissertation, implemented a mass balance model taking into account blood flow, compartmental exchange (with a focus on organs), and metabolic processes adding and removing glucose, insulin, and glucagon of a 70 kg non-diabetic individual. Clinical studies informed model parameters and estimation curves, partially shown Figure 2.1a-b below. Key insights include the modeling of glucagon in the form of an ordinary differential equation (ODE) with

characterization as a result of an extensive series of rat studies. In addition to Sorenson, Northrop also proposed a model for glucoregulation in an *Introduction to Complexity and Complex Systems* (Northrop, 2011). This nonlinear model does not address exercise, but has a main focus of various hormonal factors, such as Leptin, insulin, and glucagon (GLC). GLC production is modeled as a simple, first-order loss kinetics with a static, nonlinear function providing the GLC rate input to the GLC loss dynamics ODE. The mathematical modeling of the three main sources of glucose (diet, gluconeogenesis, and the breakdown of stored liver and muscle glycogen to glucose) is a strong point of this model. Northrop, 2011, particularly focuses on hormone kinetics, separating cells into insulin-sensitive and non-insulin sensitive (see Figure 2.1c-d), with hepatic glucose flux that depends on insulin, GLC, leptin and other regulatory hormones, not only BG. However, it fails to decipher between *types* of glucose input, which will be a focus of the Chapter 3 model in addition to modeling complexities in a simplified manner. These glucagon models are compared to and validate the Schunk-Winters glucagon model in Section 3.5.3.
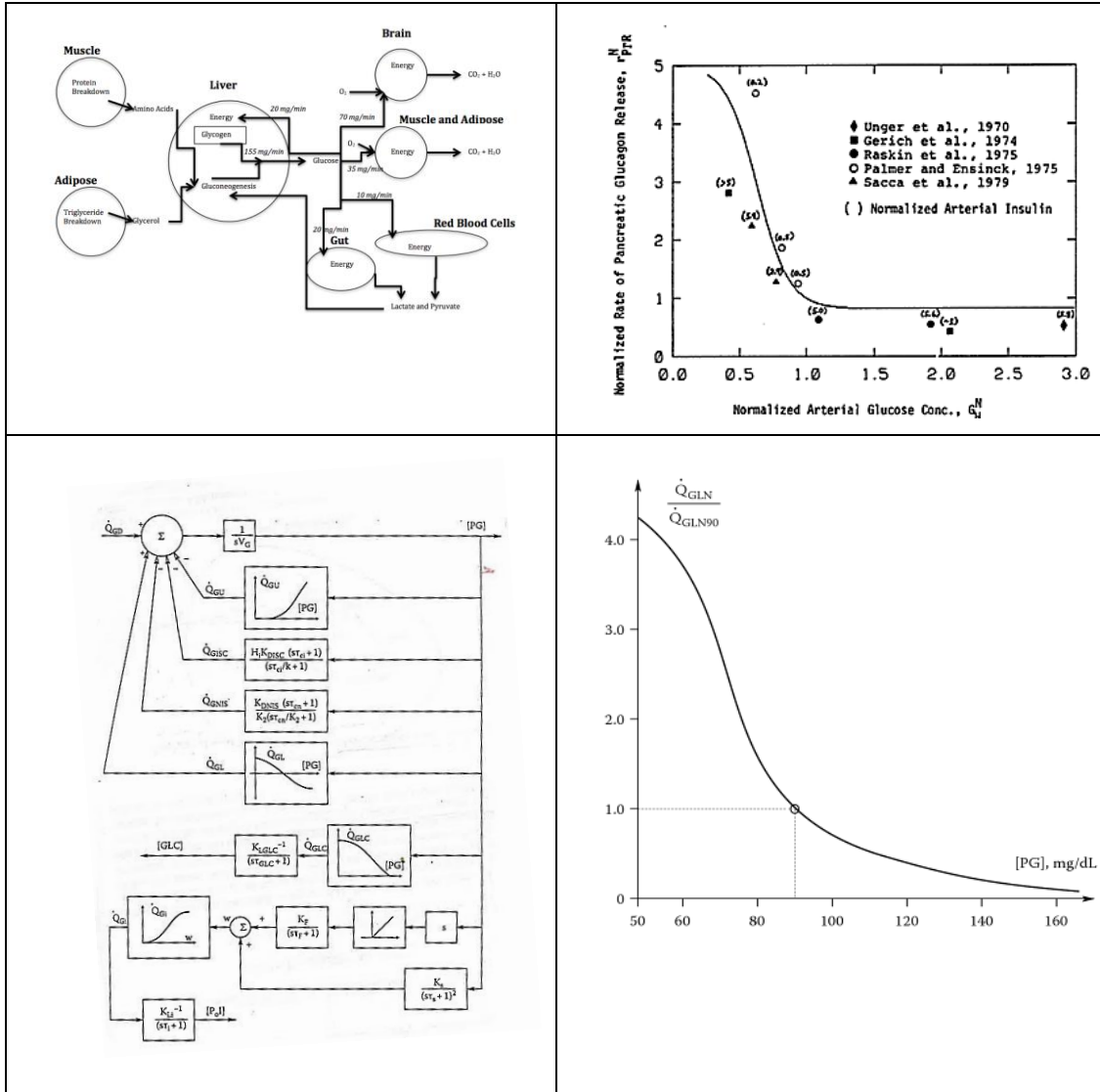
Figure 2.1: Sorenson (1985) and Northrop (2000) Blood Glucose Regulation Block Diagrams and Glucagon Plots. Upper Plots (a,b): Adapted from Sorenson (1985) blood glucose regulation model (left) and associated plot of normalized rate of glucagon release as a function of normal arterial glucose concentration (right). Lower Plots: From Northrop (2000) blood glucose regulation block diagram model (left) with glucose loss rates in urine, into insulin-sensitive cells, into non-insulin-sensitive cells, and a hepatic glucose flux that depends on hormones insulin, glucagon, and leptin. Normalized glucagon secretion as a function of steady-state plasma glucose concentration is shown on the right with half-life of glucagon is 10 minutes.

Higher-order models were developed that similarly utilized Bergman mass-flow relations but instead utilized logistic complexities and Bernoulli-Langevin expressions for hepatic glucose production and characterizing exogenous insulin

profiles and delays, respectively (Neelakanta, 2006 and Sankaranarayanan, 2012).

Neelakanta et al., 2006, clinically validates hepatic glucose production on the basis

of plasma glucose and hepatic insulin concentration. A University of Colorado group

added and characterized insulin infusion profiles under necessity to characterize

infusion risks (Sankaranarayanan, 2012). A variety of potential hypoglycemic

scenario events were modeled including taking an excessive amount of insulin or

taking a bolus too early in regard to glucose ingestion (also, miscalculation of CHO

content or GI considerations). Potential hyperglycemic scenarios tested included

meal-bolus discrepancy and discrepancy between a meal's predicted GI and actual

GI (i.e. higher than expected). It was concluded that planned meal times vs. actual

meal times indicated the highest risk for hypoglycemia, when patient's seemed to

take a bolus far in advance of actually consuming foodstuff. This ideology that

insulin must be taken sufficiently in advance of a meal (15 minutes suggested by

clinicians, but should vary with GI) indicates an insulin absorption delay. Li and

colleagues, 2006, denote two explicit time delays: insulin secretion from beta cells

as a series of complex processes including inherent delays of GLUT2, potassium

channels, etc. on the range of 5-15 min and a time lag of the effect of hepatic glucose

production with a magnitude of half-maximal suppression between 11 to 22

minutes and half-maximal recovery between 54 to 119 minutes (Li, 2006). Perhaps

more importantly are the sigmoidal shapes of associated functions, f_1-f_4, informed

by literature and similar to nonlinearities present in the Schunk-Winters model.

These shapes are shown in Figure 2.2 below.
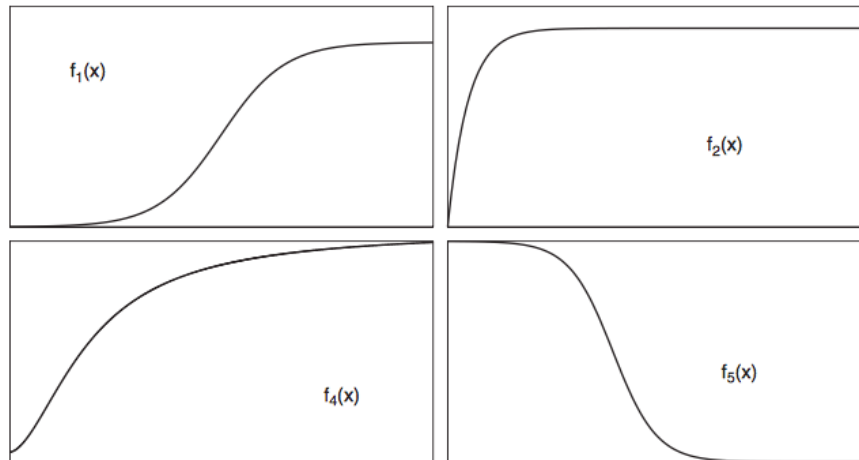
Figure 2.2: Li (2006) Function Shapes. Function shapes of respected states are plotted against BG concentration indicated by f_1: insulin production simulated by glucose concentration, f_2: insulin-dependent glucose consumers, dependent on BG alone, f_4: insulin-dependent glucose uptake, and f_5: glucose production controlled by insulin concentration (from Li, 2006).

Time delays are found amongst many of the other models as well, not only in regards to insulin action and injections, but with digestive absorption and energy and mass conservation pathways and will be discussed in Sections 2.3.1 and 2.3.2.

Most models idealize diet as a single glucose input source, ignoring the 'quality' of carbohydrates. Once filtered through the digestive system, there is a rate of appearance of glucose into the bloodstream. Newer models utilize 2-3 states to capture this digestive process, but fail to distinguish between carbohydrate type and varying absorption rates (Dalla Man, 2014, and Hernandez-Ordonez, 2008). Leading up, in 2007, Cobelli and colleagues developed an advanced 12-state model for studying the effects of carbohydrates (meal) an extension approved by the FDA as a preclinical trial tool for controller design used extensively (Cobelli, 2009 and Kotachev, 2010). More recently, the addition of glucagon control action resulted in a 16th-order model with 7 additional parameters (Dalla Man, 2014). The model

implements simulations representing a diversity of "virtual" users. This work evolved into a FDA approved simulator for evaluating controllers for T1D management (Kotachev, 2010 and Dalla Man, 2014). One significant limitation is that it is still intended for a single meal implemented as a bolus dose of carbohydrates.

The transient dynamics of glucose appearance is strongly influenced by foodstuff composition, with measures such as glycemic index (GI) to document the reality of peak glucose influx ranging from minutes to hours after ingestion (Monro, 2008). Low glycemic foodstuff results in a slower breakdown (less of the "sugar high" spike in BG). The "sugar high" idea is long-standing and is characterized as a strong blood insulin influx in response to high glycemic foods, triggering a sudden "crash" in BG owing to increased flux into tissues for storage (mostly in liver and muscle and adipose) and via energy conversion pathways into fats (Jenkins, 1981, Wolfe, 1998, and Walsh, 2014). Only one group (Yamamoto, 2014) addressed the need for deciphering between a food's GI, which is well known to effect the rate at which foodstuff is absorbed (Mohammed, 2004). In modeling meal absorption, Yamomoto (2014) addresses glycemic index and associated insulin effect based on replicated literature curves. A state-space representation form is used for the carbohydrate metabolism subsystem, which distinguishes between rapidly absorbing glucose (RAG) and slowly absorbing glucose (SAG). It is determined that 95% of RAG is absorbed within 20 minutes, with SAG between 20-120 minutes. Therefore, SAG utilizes a 20-minute time delay, with a time constant of about 21 minutes (vs. 4.2 for RAG). There is also a first-order gastric emptying delay related

to the time required to pass from the stomach to the duodenum. However, this

particular model is limited in its other 'lifestyle' inputs such as exercise and utilizes

only the Bergman minimal insulin model for subcutaneous insulin (Bergman, 1981

and Shimoda, 1997). Figure 2.3 below shows the comparison to 'staple' foods with

known glycemic index values—the glucose-equivalent value takes into account fiber

content and the known glucose relative (GR) function, with white bread as the

reference food and expressed as a percentage with respect to 50 grams of glucose.

This is important for simulation, as 50 grams of each staple food was used.
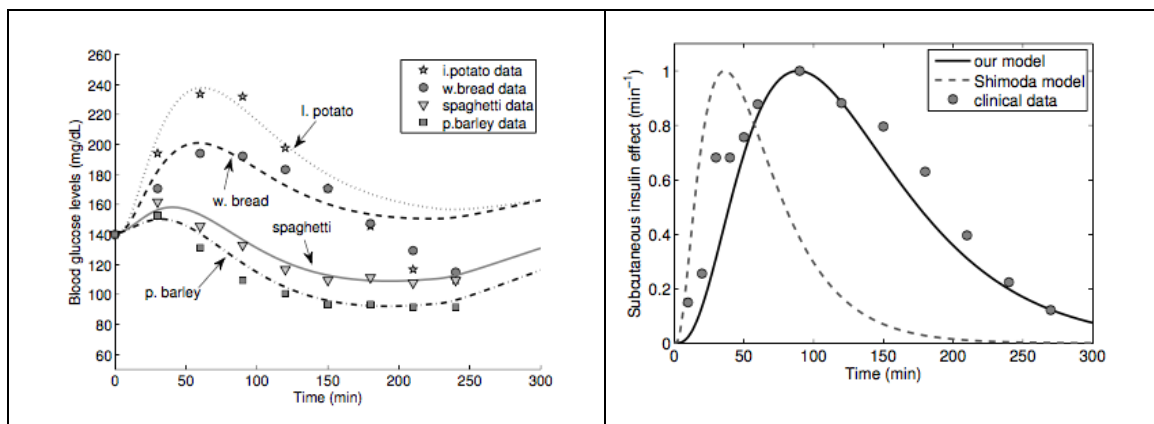
Figure 2.3: Yamamoto (2014) Meal Simulation Model with Insulin. *Left:* Simulation of four staple foods with the proposed model compared to clinical data from Mohammed et al., 2004 (Yamamoto, 2014). *Right:* Simulation of subcutaneous insulin effect, as compared to clinical data used for Bergman model verification purposes (Yamamoto, 2014).

Neelakanta et al., 2006, used early Cobelli theoretical formulations and

clinical data to form simulated results based on the modified and adapted complex

systems approach outlined in their model (Neelakanta, 2006 and Cobelli, 1985). The

main focus of this model is on hormonal controllers, specifically insulin and

glucagon, to indicate statistical bounds on BG concentration and the rate of

appearance of glucose in the blood plasma (Neelakanta, 2006). The improvements by Cobelli's group are implemented in a simulation model of the glucose-insulin system in normal life conditions for use in diabetes research (Dalla Man, 2007 and Cobelli, 2009). The general model consists of 12-13 states, with an emphasis on compartmental insulin kinetics and uni-directional glucose stomach states implemented in MatLab and Simulink. Advantages of the Cobelli model include accurate experimental parameter values and the use of Hill kinetics, introducing a realistic non-linearity approach of parameters and states.

Exercise as an input to the models is only recent and has been kept as a simple and single input. In fact, 3 different exercise models were proposed and implemented *in silico* (Cobelli, 2009)*.* This 2009 version by the *Cobelli* group implemented three additional 'test' inputs for exercise, outlined in Models A-C. Model A assumed that exercise causes a rapid on-and-off increase in insulin-independent glucose clearance and a rapid-on/slow-off effect on insulin sensitivity. Model B relaxes the assumption that exercise causes a rapid on-and-off increase in insulin-independent glucose clearance. Model C is similar to model A, but also assumes that insulin action is increased in proportion to the duration and intensity of exercise. It was determined, in assessment of quality of each prediction model, that Models A and B predict different levels of exercise (based on heart rate) have the same effect on glucose utilization and Model C predicts a reasonable glucose infusion rate during euglycemic-hyperinsulinemic clamp simulations for both mild and moderate exercise. However, other literature suggests that exercise intensity, or different levels of exercise, does in fact have implications on glucose utilization and

therefore Models A and B are limited compared to the Schunk-Winters exercise model (i.e. Brooks, 1994). Heart rate (HR) is also debatable as an accurate measure of exercise level, as HR tends to fluctuate with other factors and is intrinsic to an individual. Hence, most exercise physiologists use factors such as percent of aerobic capacity. That being said, HR can be an accurate predictor if an anaerobic threshold and/or VO2max stress test has been performed and correlations between HR and particular training zones have been determined. It can help better inform exercise activity level and effort, as well as stress. This is further discussed in Chapter 4.

Perhaps the first model to successfully demonstrate the importance to model exercise, as a function of working tissue uptake, plasma insulin, and hepatic glucose release, was Roy (2007). However, the model is limited in that hepatic production is the only additional means by which glucose is available with exercise and the insulin model is minimal. Hernandez-Ordonez (2007) furthered exercise model validation at low and moderate intensities and the redistribution of blood flow but do not seem to address the effect of meals and/or varying metabolic properties of individuals. Duun-Henrikson (2013) used a linear, three-compartment insulin model and simply varied absorption rate as a function of exercise intensity and duration.

In 2013, a group associated with *Cobelli* and colleagues modified the *in silico* 2009 Padova type 1 simulator (Cobelli, 2009) to incorporate the effect of physical activity after demonstrating a doubling of insulin activity (Schiavon, 2013). Subjects were allocated into two groups: one in the absence of and one with different degrees of reductions and durations of basal insulin infusion rates—it was shown that an effective strategy is to reduce basal insulin by 50% 90 minutes prior to exercise and

30% during exercise to avoid hypoglycemia. However, this is not possible in regard to current artificial pancreas design, and exercise type and intensity are not accounted for, both of which my further adjust what changes need to be made in insulin dosing before, during, and after exercise. This will be a partial focus of Chapter 4, after exercise and the metabolic properties associated with muscle demand are modeled and able to predict proper BG control.

Originally, a 4th/5th classroom model formed by Dr. Jack Winters for a biocontrol systems course (BIEN 3301) starting in 2012 forms the basis of the 9th/10th order Schunk-Winters model proposed in this thesis. The original model contains 4-5 states, and included breaking tissue into separate muscle and non-muscle compartments, the typical BG compartment, a simple 1st-order stomach glucose filter, an insulin state viewed as a controller, and an optional 5th state for 1st-order dynamics for exogenous insulin delivery (could be external for people with diabetes). Advantages of this model include, but are not limited to, a basic component for sensitivity to exercise via a glucose input sink, which acts as a forefront for future modeling. This model is successful in modeling the severe effects that are common to most people with diabetes; distinct parameter changes are used to separately model Type 1 and Type 2 diabetes. Disadvantages included lack of non-insulin control and other key hormonal regulators of BG including glucagon, GLUT4 and GLUT2. Exercise is also limited to a subjective intensity scale. Meals are limited to only magnitude and duration as input parameters.

In summary, models tend to move from utilizing simplified compartment 'minimal models,' such as Sorensen (1978) focusing on nonlinear organ glucose

demand and Bergman (1981), the first base compartmental insulin model, to those that exist as a *system*, or multiple states involving dual-control and/or separate volume-based compartments with varying metabolic properties. Wilinska (2005) performed an extensive study evaluating and validating insulin models, including acceptable linear models (Shimoda, 1997), more complex and nonlinear compartmental models (Hovorka, 2004), and those using Michaelis-Menten kinetics which form a strong core componentry of the Chapter 3 and 4 insulin compartment structure. Many of these are shown in Table 2.1. Other models focus on the effect of metabolic variations and compartment loss/fluxes due to temperature, thyroid hormones, urine loss, and mechanical workload (Northrop, 2000).

The Schunk-Winters model addresses significant knowledge gaps in terms of digestive absorption pathways and exercise characterization, which are limited in most models above (e.g., Cobelli, 2009, Dalla Man, 2014, Yamamoto, 2014, and Roy, 2007).

Table 2.1: Evolutionary Summary of Glucoregulation Models *(NL = Nonlinear, L = Linear)*

Source	Model Structure	Strengths	Limitations	Relevance
		Cobelli Group		
Cobelli et al, 1985	• 5 State • Glucose Subsystem (first order): production and utilization (L) • Glucagon Subsystem (first order): secretion, distribution and metabolism(NL-rate) • Insulin Subsystem (3rd order): distribution and metabolism of portal and peripheral infusion by input to liver and plasma compartments (NL)	• Dynamic model of the glucose regulation system enabled minimal insulin profile with peripheral insulin infusion to be computed.	• Not adaptable to all types of normal and diabetic subjects. • Meal input is limited to single carbohydrate source as digestive dynamics lack.	• Provides basis for minimal insulin model and Cobelli group development.
Dalla Man et al, May 2007	• 12 State • Glucose Subsystem: insulin-independent utilization and insulin-dependent utilization • Insulin Subsystem: liver and plasma • Stomach: solid phases, and gut • Adipose and Muscle (NL)	• Glucose-Insulin model graphical interface • Insulin control at organ/tissue and whole body levels • Type 1 and Type 2 Recognition	• Does not account for varying metabolic properties across tissues • Meal input limited to simple carbohydrates. • No input for exercise/activity	• Matlab/Simulink simulation parameters and graphs for a normal, type 2, type 1 subject • Meal input and both open and closed loop controls available.
Dalla Man et al, October 2007	• 16th Order adding digestive dynamics (ingestion and absorption) based on concentration and flux • Same compartments as Dalla Man, May 2009, with 36 parameters (normal and type 2)	• Meals into quasi-model sub-systems: Glucose, Insulin, Muscle and Adipose, Gastro-Intestinal • Mixed Meal	• Not performed for Type 1; only Type 2, normal • Muscle and Adipose Tissue are in one compartment • Stress hormone/ glucagon not considered	• Rate of appearance parameters are similar and provides rate of appearance and production graphs for comparison.
Dalla Man et al, 2009	• Utilizes 16th order (2007) model at rest • Exercise dynamics: 8 parameters, key being hepatic glucose effectiveness and hepatic insulin sensitivity	• Addition of physical activity via 3 models in steady and non-steady (after a meal) state	• Only short term exercise and do not properly characterize intensity	Some useful exercise parameters on the basis of heart rate are provided; comparative curves (validation lacking)

Kovatchev et al, 2009	• Computer simulation environment: glucose-insulin model (Cobelli et al, 2009), *In Silico* Sensor, *In Silico* Insulin Pump, Controller	• *In silico* testing of control algorithms linking CGM and insulin delivery	• Computer simulation only • Only insulin delivery method model is FDA approved	• Insight into AP methods and comparative graphs provided for 24-hour plus simulations.
Kovatchev et al, 2010	• Testing of model-predictive control (MPC) algorithm in conjunction with CGM for 300 virtual subjects • Closed and Open Loop control comparison	• Extended 2009 *in silico* testing to include closed-loop control (better regulates at night) • Improved accuracy	• Only focus on type 1 diabetes	• Useful parameters and comparative graphs provided, especially using CGM data
Dalla Man et al, 2014	• New additions from 2007 Model (2009 Simulator): counterregulation updates (liver, muscle, and adipose tissue), new alpha cell and glucagon kinetics and delivery (3 additional compartments) (NL)	• Addition of glucagon • New rules for insulin to carbs ration and correction factor • Dual-Hormone control (vs. 2009 version)	• Results only show for a single meal and no exercise input capability is apparent	Glucagon secretion and following glucose appearance kinetics parameters; graphs for comparison
Other Models				
Sorenson, 1978	• Nonlinear, ~ 19 Variables • Additional Compartments: Brain, Vascular, Kidney, Renal and Peripheral Systems	• Glucagon (GLC) modeled as ODE • Mass-balance modeling approach focusing on compartmental exchange (organs)	• Parameters estimated from rat clinical trials (GLC is known to behave differently in humans)	• Glucagon modeling insights for validation • Incorporates compartments and blood flow similar to Schunk-Winters
Bergman, 1981	• 3 States, 7 parameters • 2 Insulin Compartments: plasma and interstitial • 1 Glucose Compartment: plasma and basal levels	• Glucose effectiveness and sensitivity. • Basic Insulin Model	• Minimal model	• Basis of many glucose regulation models in literature. • Minimal model that can be built off of.
Sturis et al (1991)	• 6 states • Negative feedback loops: insulin effect on glucose utilization and production and the effect of glucose on insulin secretion	• Introduction of insulin degradation time constants and time delays • Separates liver, brain and nerves, muscle and fat	• Lumps muscle and fat together in terms of delays—no way to separate exercise demand	• Understand oscillations via delays in feedback loops • Shape delay curves and inform time constants for various compartments

Shimoda, 1997 (from Wilinska, 2005)	• 3 Compartment Insulin, Linear • Depot (2 compartments) and Plasma Insulin • Saturable absorption rates and disappearance	• Michealis-Menten Kinetics similar to our model • Simplified	• No adaption to outside influential factors • Minimal	• Simplest form, with saturable effects while keeping a linear model; used by Yamamoto
Northrop et al, 2000	• 7 State • Glucose Compartment: loss urine (Linear) into ISCs (1st order linear) and NISCs (1st order Linear), hepatic glucose flux (hormone dependent) • Glucose Input from diet (bimodal, Linear) • Glucagon Production (NL-rate provides input to 1st order loss kinetics) • Portal Insulin (2 states, Linear and NL-saturated)	• Metabolic rate constant as a function of temperature, thyroid hormone concentration, epinephrine and mechanical work load if the cells are muscle. • Separate glucose sinks into insulin vs. non-insulin sensitive cells • Bimodal glucose input rate	• Validation and implementation • Limited in direct application to exercise	• Hormonal importance in regard to non-insulin mediated pathways, key during exercise and increased workload
Hovorka et al, 2004	• ~11 Variables; • Endogenous glucose production and renal filtration	• Evaluated using 15 clinical experiments in subjects with Type 1; strong glucose-insulin sub model	• Main focus is correcting during fasting conditions and overnight; no full day simulations	Insulin model useful for when depletion occurs with comparative plots
Li et al, 2006	• Core: Two Delay Differential Equations for glucose production/utilization and insulin production/clearance	• Time delays of insulin using mas conservation • Oscillation replication of glucose and insulin	• Only for type 1 and lacks a bit on meal input dynamics and glucose/energy homeostasis understanding	Comparative plots, especially regarding mass conservation and time delays
Neelkanta et al, 2006	• 4 Glucose Sinks: Insulin-Sensitive Cells (ISCs), Noninsulin-sensitive cells (NISCs), kidneys (urine loss), liver or muscle (storage) • Glucose Input: diet, stored fat/protein, glycogen • Insulin secretion is NL • Three Subsystems: • Glucose Subsystem: 5 NL rates • Insulin Subsystem: 5 quantity terms	• Liver glucose production based on glucose and insulin concentrations • Mass-Flow Model	• Validation and Implementation	Pertinent to predicting and quantifying the effect of hepatic gluconeogenesis based on current concentrations

	• Glucagon Subsystem: 2 quantities, 1 rate		
Roy et al, 2007	• Take three-compartment Bergman model and add exercise • Insulin dynamics adds circulatory removal, • Glucose uptake and hepatic glucose production (exercise induced) added	• Modeling exercise effects based on uptake of working tissue, plasma insulin, and hepatic glucose release	• Do not fully understand hepatic glucose production—this is the way exercise effects are modeled via increase/decrease which is not the case • Data from literature	• Provides insight that there is a need to model exercise • Experimental data from literature
Hernandex-Ordonez, et al, 2007	• 23rd order nonlinear dynamical system	• Validate low and moderate intensity exercise on existing glucose-insulin model; extrapolate for high intensity • Redistribution of blood flow with exercise	• Meal simulation is limited and not addressed • Stress hormones and trained vs. untrained parameters not present	Insight into glucose production segmentation: 50% glycogenolysis, 30% hepatic, and 20% renal; comparative plots
Duun-Henrikson et al, 2013	• Linear Three-Compartment Insulin Model: subcutaneous layer, deep tissues, and plasma	• Three-compartment artificial pancreas model • Absorption rate as a function of exercise intensity and duration	• Need validation for insulin appearance during exercise • Only focus on normal, but recognize Type 1 implications	Combine exercise idea into artificial pancreas application
Yamamoto et al, 2014	• 3 Compartments: Carbohydrate metabolism, subcutaneous insulin, glucose-insulin metabolism • Slowly Available Glucose: 2nd order delay system • 3-Compartment (Shimoda) Insulin Model • Bergman Minimal Model	• Model of digestion and absorption from carbohydrates based on the Glycemic Index	• Do not provide exercise and some error in regards to control algorithm discussion and state-space equations	Direct comparison to meal compartment model; type 1 applications
Sankaranarayanan et al, 2012	• Integration of 3 Models • Meal Absorption • Insulin Infusion Pump • Insulin-Glucose Regulation Model (Hovorka, Cobelli, Sorensen)	• Insulin infusion pump risks modeling and varying insulin curve shapes	• Case-study only • Assume food ingested has a single carbohydrate source with fixed high GI	Insulin infusion plots

2.3   Need for a Lifestyle Model

2.3.1   Lifestyle Influenced Modeling: Foodstuff Consumption

Foodstuff and varying absorption properties of foods are recognized throughout the nutrition community particularly in regard to glycemic index (GI). Yet, glucose compartmental models often have a *single* carbohydrate input source, with other mixed meal components assumed negligible in regard to BG effect (Dalla Man, 2007, Roy, 2007, and Kovatchev, 2010). One group does capture the kinetics behind GI, applying bioavailability concepts into rapidly and slowly available glucose (Yamamoto, 2014). Their model is implemented in a way to 'test' known GI foods and was recreated for comparison to the Schunk-Winters digestive compartment, outlined in the Chapter 4 case study. Clinical data is presented in regard to BG increment after ingestion of foods partitioned by GI and clinically prescribed insulin dosages—however, limitations still exist, especially in regard to starting states (Mohammed, 2003 and Sekigami, 2004). Similarities exist in transient response for varying glycemic index (i.e. blood sugar 'spike' for high GI vs. gradual to steady state) and insulin response effect—oftentimes, there is 'overshoot' in correction for low GI carbohydrate meals due to accommodation of fast insulin dynamics and time delay. Due to the simple fact *one type* of insulin is used for *any* CHO ingestion and varying digestive absorption paths, problems arise due to insulin delay and timing, which is investigated in Chapter 3.

Both models (Yamamoto, 2015, and Schunk-Winters, 2012) use a summing technique for the final digestive absorption state as seen in Figure 2.3 above. Glycemic impact curves, or "the weight of glucose inducing a glycemic response" on BG concentration are well documented for a variety of foods (Monro, 2008) and described in glucose forward flow implementation of Chapter 3 below. The motivation behind modeling GI ties into the need to model in conjunction with the subject's *other* habitual lifestyle habits. For example, by experience, a T1D individual can actually keep one's glucose within a target range solely by eating a low GI diet and exercising, although also dependent on whether or not the individual still produces *some* insulin. It was determined that lower GI foods are typically associated with higher fat and protein content (if overall caloric intake is kept consistent) and could aide in 'tight' BG control of the patient based on absorption properties (Jenkins, 1981) if known to the predictive algorithm.

The Dalla Man/Cobelli meal simulator model is used as additional reference and comparison to how most models simulate diet (Dalla Man, 2007). For the purpose of comparison and that models (other than Schunk-Winters) only display capability and literature curves for a defined carbohydrate bolus, all use the same input of 50g carbohydrate ingestion typically with an unknown GI (other than Kotachev, 2010), thereby making model replication somewhat limiting. Other studies, using a similar bolus (~50 g carbohydrate) demonstrate significantly reduced area (i.e. lower BG levels) under the BG curve post-prandial after a low-glycemic meal vs. a high-glycemic meal (Parillo, 2011).

2.3.2   Lifestyle Influenced Modeling: Integrating Diet and Physical Activity

Diet preference and lifestyle choice can influence substrate preference and utilization during exercise (and also rest) due to availability. This is particularly keen for adaptive modeling—if an individual eats a largely low GI diet (hence, most likely incorporating more fat and protein), bioavailability of CHO and glycogen stores are most likely decreased. However, a factor of adaptability must also be taken into consideration as if the person is also trained, CHO oxidation is decreased in general and glycogen 'sparing' occurs. This phenomenon suggests a low GI diet may be sufficient to avoid hypoglycemia due to increased fat oxidation and mitochondrial biogenesis in adapted and trained individuals (Kiens, 1993 and Hurley, 1986). On the other hand, a high carbohydrate and high GI diet will increase insulin production (possibly decrease sensitivity) and influence BG concentration and uptake flux into tissues (especially non-muscle if no muscle demand exists).

Glucose mass flow and direction is highly dependent on varying types of energy and tissue demand, particularly in regards to anaerobic vs. aerobic exercise, as well as daily activity. Substrate for work comes from four main sources of stored energy: muscle glycogen, free fatty acids (intramuscular, and via triglyceride breakdown from mostly adipose sites), liver glycogen, and in some cases muscle proteins (Powers, 2014). A catalyst, pyruvate dehydrogenase (PDH) has entered the research field as a key catalyst for the entry of CHO and its subsequent oxidation, in addition to the extensively studied relationship of oxygen uptake and carbon dioxide production as a fuel consumption estimate (CHO vs fat) (ACSM and Powers, 2014). Biochemically, fat requires more oxygen for oxidation (23 O_2 vs 6 O_2).

Greater activation (and hence CHO oxidation) occurs with increasing the glycolytic

flux and rate of pyruvate production, either by increasing muscle glycogen prior to

exercise or with higher epinephrine concentration. Similarly, myoplasm calcium

increases muscle activation and (indirectly) carbohydrate oxidation as it is released

from the sarcoplasmic reticulum during skeletal muscle contraction (Harmer, 2013).

Maximal oxygen uptake and the respiratory exchange ratio aid in characterizing the

point at which FFA vs CHO utilization turnover occurs, and can influence an

individual's basal metabolic parameters (Brooks, 1994). Variation in basal

metabolic rate explicitly demonstrates another need for a personalized adaptive

model, and in addition, it is imperative that glycolysis is understood in all forms.

Anaerobic glycolysis represents an integral component of CHO utilization at high

intensity contractions, yet the associated catalytic enzymes can be altered in regard

to physiological adaptations especially in regard to trained individuals (Ohlendieck,

2010). Aerobically, fuel oxidation assumes a mix of CHO and fat metabolism, thereby

directly requiring understanding prior to modeling the glucose regulation system.

Values such as Respiratory Exchange Ratio (RER) are direct measures of

characterizing fuel utilization if maximal oxygen uptake and ventilation parameters

are measured. An RER of 0.7 corresponds to fat oxidation while an RER of 1.0 or

higher directly correlates glucose oxidation, particularly at high intensity exercise

(Melzer, 2011). It appears trained individuals, or those who have underwent

submaximal training for extended periods of time, have a lower RER and hence

higher degree of fat utilization in addition to a higher capability to utilize muscle

triglycerides (Boyadjiev, 2004). Other mechanisms include an increased number of

mitochondria and GLUT4 translocation in muscle cells, as well as increased enzyme activity and decreased catecholamine effect (Boyadjiev, 2004, and Holloszy, 2011). Effects of training are discussed further in Chapter 4.

Formation of dynamic insulin modeling systems and associated absorption properties into the tissue and/or blood has been an intensive evolutionary process, core to most diabetic technology systems today. There are inherent time delays associated with insulin type, body composition, and environment (Walsh, 2014). For example, if one with high body fat content were to inject insulin into the abdomen vs. a slim athlete injecting insulin into the leg prior to physical activity, clearly the athlete would absorb and utilize insulin at a much faster rate. In fact, it is well documented that anything involved in increasing blood flow will increase insulin absorption rate, such as hot temperatures or any form of muscle activity (Walsh, 2014). This is in addition to time delays associated with dissociation and monomeric vs. non-monomeric absorption properties of insulin, and, changing pharmacodynamics of insulin action depending on the size of bolus if above a certain level (Walsh, 2014). It appears that if injected in a large proportion, there is a saturation factor and some insulin may be lost or not fully absorbed. Both issues can be taken into account while modeling insulin with the use of Hill and Michaelis-Menten kinetics—particularly if exogenous insulin is involved. In terms of modeling, it is proposed that the different types of insulin (injection) will take paths based peak timing and implemented as slower non-monomeric or faster monomeric (Li, 2006 and Diabetes Services, Inc.). If a subject is insulin-independent, a time delay is

still present and may vary due to anticipatory effects (or lack of) of diet, exercise, or any other factor affecting BG.

Physical activity increases the rate at which insulin effects occur, known as insulin sensitivity. It originally was hypothesized, although now currently debated, that tissue compartments could remain hypersensitive up to 48 hours post-exercise (MacDonald, 2006). This is a dangerous issue in regard to late-onset hypoglycemia, which could occur at night when the patient is unaware. However, there are other mechanisms of compensation, as typically diet is increased with intense exercise, and insulin sensitivity becomes an adaption of trained individuals, or routine, as fat oxidation increases therefore sparing glucose (Befroy, 2008). Maarbjerg, 2011, and colleagues outline many stimuli contributing to increased insulin signaling and sensitivity (hence, glucose uptake) including increased GLUT4 translocation in active muscles and fat cells dependent on the phosphorylation of protein TBC1D4, as well as decreased glycogen levels (Maarbjerg, 2011). As recently supported, these phenomena are present up to 4 hours after exercise, unlike the previously cited '48.'

Hormones, particularly catecholamine's epinephrine and norepinephrine, along with amylin and leptin, influence glucose energy flow amongst compartments and are not modeled mathematically, only recognized as influences in literature (Aronoff, 2004, and ACSM). Epinephrine has been known to cause bouts of hyperglycemia, characteristic of the 'fight or flight' response—glucose will flood into the bloodstream, aiding in the concept of an 'adrenaline rush.' This concept is difficult to model, and also occurs during exercise, especially in a high intensity or race setting (Tonoli, 2012). For that reason, studies have been done altering the

order of anaerobic/resistance training and aerobic training to decrease the effect of a BG 'spike' prior to the decrease in BG due to an aerobic session (Yardley, 2012). Training, particularly long endurance, also decreases catecholamine action in general, indicating a need for a personalized model. Amylin, also synthesized in beta-cells as with insulin, acts to suppress glucagon secretion and slow gastric emptying, thereby aiding in glucose appearance and disappearance in circulation (Aronoff, 2014). This complementary effect of amylin to insulin acts through the central nervous system and may prove to be important for diabetic modeling purposes. Leptin acts to regulate the amount of excess dietary calories stored as fat in fat cells versus the amount of glucose stored as glycogen in the liver and muscles (Northrop, 2011). Although not clearly associated with immediate glucose dynamics, leptin plays a role in fat accumulation based on an excess of carbohydrates, important for long-term modeling simulations.

Clinically, it does not yet seem possible to predict BG regulation of a diabetic athlete—diabetic athletes must discover themselves what is needed and when but with no real clinical guidance, only suggestions based on community tips and trial and error. For that reason, an algorithm intended to incorporate non-insulin (and glucagon) mediated physiologic mechanisms would be highly beneficial.

2.3.3   Lifestyle Influenced Remodeling: Types 1 and 2 Diabetes

All of the above mechanisms are occurring within a living biosystem that is inherently changing based on its use history, which reflects lifestyle. Thus various tissues of the body can remodel in structure and composition, including in response

to lifestyle behavior and/or clinical interventions. This in turn needs to be considered in clinical disease management. Two common examples are reviewed.

The current diabetes epidemic taking priority today involves obesity and its direct risk factor of Type 2 Diabetes. This is an example of *remodeling*: lifestyle choices lead to a change in body type, composition, and overall metabolic implications which can turn into insulin resistance, and hence disease. Accumulation of excess glucose in the blood due to over-eating and lack of exercise eventually (over a long-term period) leads to an over-production of insulin but the inability to utilize insulin properly, as glucose can no longer enter cells due to excess. Buildup often results in conversion to fat, an external *remodeling* symptom, and insulin resistance as an internal *remodeling* symptom. A lifestyle model, if performed for months, could predict implications of BG buildup with proper thresholds, tissue volume accumulation, and summation over a significant period of time. It has been proven that physical activity is a means of prevention and treatment for T2D; a *remodeling* back to a healthy lifestyle, practically reversing insulin resistance, is possible with increased skeletal muscle capitalization, increased muscular GLUT4 levels, hexokinase, and glycogen synthesis of chronic, daily aerobic exercise (Yavari, 2012). With informed models and predictors of these effects—particularly concerning tissue metabolism changes, GLUT4 flux, and decreased body mass—it is possible to inspire T2D to make these changes, as it is possible to decrease glucose accumulation and levels in general. Exercise-induced insulin sensitivity has attracted recent attention for designing effective lifestyle changes for T2D (Maarbjerg, 2011). With lifestyle models, this effect could be

demonstrated and would inform treatment plans and options useful in a clinical

setting.

Similarly, an athlete, especially if exercise habits are 6 (or greater) days per

week for extended time periods, will experience body composition remodeling.

Trained individuals have vastly different metabolic properties and substrate

utilization during rest and physical activity. Glucose is a key player—oftentimes, an

athlete relies more on fat oxidation than glucose oxidation while at lower intensities

of exercise and at rest. This involves changes such as increased mitochondrial

content, all of which are outlined in Chapter 4. It is important to note modeling

changes that would occur for a diabetic athlete—reliance on fat (vs. glucose),

increased muscle mass tissue volume, increased glycogen stores, and importance of

varying exercise intensity on substrate utilization (Melzer, 2011).

2.3.4   Artificial Pancreas Predictive Applications

It is recognized that there is a current need for innovative BG regulation models

correlating to the current diabetes epidemic. Many factors, mostly related to

treatment options, manipulate the basis for modeling approaches—diet, exercise,

and interventional technologies, such as insulin injection, pumps, continuous

glucose monitors (CGM's) and the recent concept of an artificial pancreas (AP).

Recently the AP system has evolved towards a two-sensor system, using two

Dexcom, Inc., glucose sensors (for comparative proportional error calculations) with

two pumps for independent delivery of insulin and glucagon controlled by a laptop

running a custom glucoregulation control model (Jacobs, 2011).   In this pilot

strategy, delivery occurred on the basis of weight, Hemoglobin A1C (HbA1C), meals, and carbohydrates, all of which factor into an estimation of insulin sensitivity and dependent on proportional error from target glucose levels. HbA1C is a common measure for how well-controlled one's BG has been for the previous 2-3 months, as it reflects average levels and whether or not red blood cells have become "glycated."

Further, Dexcom, a forerunner in the CGM technology field, has an initial AP design that is using BG models, such as the Cobelli et al. 2009 version as seen in Table 2.1(Garcia, 2013).

The concept of using BG dynamic models for AP controller algorithms makes considerable sense. The challenge is using models that are robust enough to capture the diverse events in life that affect BG, including forms of exercise. The models outlined in Chapter 3 and 4 of this thesis, particularly for personalized adaptation of an athlete in Chapter 4, possess capability of further informing AP technology for unique individuals. However, this is only possible by increasing the algorithm accuracy of trend prediction, possibly beginning with integrating extensive user profiles. An extensive user profile, that incorporates metabolic parameters (resting metabolism, body composition, exercise data to correlate heart rate, etc.) would generate a generic algorithm for a particular individual that then can be informed by instantaneous events (stress, exercise, foodstuff consumption).

Only in recent clinical studies has the need to adapt dual-hormone AP designs in regard to lifestyle, particularly exercise and trained individuals, been *addressed* (Haidar, 2013). In a recent clinical study, closed loop delivery guided by advanced algorithms was shown to improve short-term glucose control, shown with 15 T1D

adults who underwent a 24-hour simulation with 30 minutes of exercise (Haidar, 2013). However, this still is not sufficient to predict and inform a habitual lifestyle and parameter set of trained individuals (see Chapter 4). Limitations often involve instability of glucagon at room temperature; however, it is known that there are other non-hormone dependent pathways that aid in glucose and energy utilization during exercise.

Studies have demonstrated a need for adjusting basal insulin infusion rate prior to and during exercise—however, this has resulted in only a general suggestion, rather than personalized, for AP adaptation by an insulin reduction of about 50% (Shiavon, 2013). Clinicians typically advise people with diabetes, for ease, to stop insulin altogether during exercise. This may help avoid post-exercise late-onset hypoglycemia due to increased insulin sensitivity for long-term duration if exercise was of high caliber (MacDonald, 2006). However, as another AP application, a patient should not *have* to completely stop insulin (unless they are experiencing hypoglycemia) with a personalized model fine-tuned to individual metabolic parameters. It seems that insulin sensitivity is only a small implication of exercise and late-onset hypoglycemia; stress hormones and other contraindications as a result of training are other causes, especially if a 'false high' is accounted for at the beginning of exercise. For example, at the onset of exercise, as discussed, BG can elevate. If an AP device corrects for this, oftentimes a hypoglycemic episode ensues with the result of BG declining due to exercise demand in conjunction with an insulin bolus effect. Additionally, a group used the basic 3-compartment insulin model best suggested by Wilinska, 2005, and attempted to model the absorption

rate between subcutaneous and deeper tissue as a function of exercise intensity, realizing this was a major challenge to the current AP (Duun-Henriksen, 2013). However, their methodology is limited to two levels of exercise intensity, and does not address the influence of diet as another lifestyle parameter.

Heart rate is an easily obtainable metric and is well known to inform effort (if different than perceived) during exercise and also often elevates during various high-stress or active events. In the case of the proposed model, HR (if available) will be used to inform exercise and stress (hormonal) inputs, but will not be fully relied upon, mainly due to heart rate variability and interpersonal variations that must be quantified in order to deem HR accurate.

3. NOVEL MODELING APPROACH METHODOLOGY

3.1 Introduction

Modeling of the blood glucose regulation system will better inform diabetes management on the basis of predicting trends characterized by model inputs. Clinicians and diabetes educators need to be able to quantitatively explain effects of diet choice, athletics, and activity level, and how these relate to drug delivery choices. Exercise type, daily movement activities, tissue compartment metabolism, level of athleticism, meal type distinction and diet habits play a key role in BG prediction algorithms. There is a need for a robust and comprehensive model that simulates lifestyle choices, as current models are limited and fail to recognize importance of modeling all influential factors.

A goal of the model relates to improved BG prediction so that a particular individual has confidence in respective management. As personally seen with many diabetic patients, it is trial and error as to controlling influences of lifestyle factors— for example, physical and mental stress become task-dependent and can elicit vastly different responses amongst individuals. Similarly, a marathoner will treat a two-hour run as a 'walk in the park,' whereas another individual could experience physical and mental stress.

A novel nonlinear 10-state lumped compartmental model is presented that aims to address knowledge gaps that go beyond those addressed by other models, including the ability to provide flexibility for lifestyle choices, variable body mass, muscle ratio, and more logical parametric approaches for representing people with

Type 1 and Type 2 diabetes. The model is intended for both research and clinical use, particularly diabetes educators, and to inform delivery design of current artificial pancreas mechanism with a dual-hormone delivery, as well as develop continuous glucose monitor (CGM) feedback and prediction based on current activity and/or diet. It is motivated by the concept that a diabetic should be able to manage BG with exercise, diet, and dual-hormonal control based on algorithm feedback of a personalized model, similar to that of machine learning mechanisms.

3.2   Background

Many models have been proposed, focusing on varying aspects of blood plasma glucose (BG) regulation. Typically BG concentration is one of the compartments in a dynamic model, with models ranging from very simple (2 total compartments) to complex. Models tend to move from utilizing simplified compartment 'minimal models,' such as Bergman (1981), the iteration of a compartmental insulin model, to those that exist as a *system*, or multiple states involving dual-control and/or separate volume-based compartments with varying metabolic properties- Sorensen (1978) presents a complex model focusing on nonlinear organ glucose demand. Wilinska (2005) performed an extensive study evaluating and validating insulin models, including acceptable linear models (Shimoda, 1997), more complex and nonlinear compartmental models (Hovorka, 2004), and those using Michaelis-Menten kinetics, which form a strong core componentry of the proposed model. Other models focus on the effect of metabolic variations and compartment loss/fluxes due to temperature, thyroid hormones, urine loss, and mechanical

workload (Northrop, 2000). In addition to Sorenson, Northrop et al. implemented a system producing the hormone glucagon (GLC) as a simple, first-order loss kinetics with a static, nonlinear function providing the GLC rate input to the GLC loss dynamics ODE. Northrop particularly focuses on hormone kinetics, separating cells into insulin-sensitive and non-insulin sensitive, with hepatic glucose flux that depends on insulin, GLC, leptin and other regulatory hormones, not only BG.

The classic 3-state "Bergman minimal model" with two states including insulin dynamics and glucose (Bergman, 1981) is one of the most widely used core models. Bergman quantified insulin sensitivity with 3 compartments, representing plasma insulin, remote insulin and plasma glucose concentrations. Extensions to this model include a minimal exercise model adding a critical threshold value (on the basis of VO2max) that drives hepatic glucose production and glycogenolysis during exercise characterized by intensity and duration (Roy, 2007). These changes are reflected with added terms of the plasma glucose equation of the Bergman minimal model. Further, in a review of various differential equation approaches, Makroglou et al. (2006) presents delay modeling approaches including those by Sturis et al. (1991), integro-differential equations, and partial differential equations (Makroglou, 2006). The integro-differential equation approach is key for modeling intravenous glucose tolerance test dynamics after recognizing the widely used minimal model is improper in qualitative behavior, as the base parameter is equal to the basal glucose level. A more realistic dynamic model is needed, recognized by many (i.e. Li, 2001 or Mukhopadhyay, 2004) and can also be improved with use of Hill kinetics, including the special case of Michaelis-Menten, reviewed in Gesztelyi, 2012. These additions

will address fundamental limitations with added states to further insulin dynamics and the particular need to recognized delays and oscillations (Makroglou, 2006).

Hepatic glucose production and release is a large part of many models, often as a mildly-delayed dynamic response due to depleted glycogen stores and/or low BG levels. For example, Neelkanta (2006) proposed 4 glucose sinks: insulin-sensitive cells (ISCs), noninsulin-sensitive cells (NISCS), kidneys (urine loss) and liver or muscle (storage). It is possible to model liver storage and stimuli for glucose production when needed by using a lumped glucose/glycogen model and glucagon control, respectively. It becomes clear that liver can be modeled as a part of the non-muscle tissue compartment for the purposes of the Schunk-Winters model. Non-muscle tissue releases glucose mainly on the basis of glucagon-dependent (state-dependent) flux, or glycogen-to-glucose conversion particularly in regard to the liver. Glucagon directly modulates liver delivery rate.

Most models idealize diet as a single glucose input source, ignoring the 'quality' of carbohydrates. Once filtered through the digestive system, there is a rate of appearance of glucose into the bloodstream. Newer models utilize 2-3 states to capture this digestive process, but fail to distinguish between carbohydrate type and varying absorption rates (Dalla Man, 2014 and Hernandez-Ordonez, 2008). By 2007, Cobelli and colleagues developed an advanced 12-state model for studying the effects of carbohydrates (meal) an extension approved by the FDA as a preclinical trial tool for controller design used extensively (Cobelli, 2009 and Kotachev, 2010). More recently, the addition of glucagon control action resulted in a 16th-order model with 7 additional parameters (Dalla Man, 2014). The model implements simulations

representing a diversity of "virtual" users. This work evolved into a FDA approved simulator for evaluating controllers for T1D management and has made its way extensively into the modeling field today, forming a strong sense of nonlinear control in regard to insulin response for both T1D and T2D, as well as more recent additions of glucagon and exercise (Kotachev, 2010 and Dalla Man, 2014). One significant limitation is that it is still intended for a single meal implemented as a bolus dose of carbohydrates.

The transient dynamics of glucose appearance is strongly influenced by foodstuff composition, with measures such as GI to document the reality of peak glucose influx ranging from minutes to hours after ingestion (Monro, 2008). Low glycemic foodstuff results in a slower breakdown (less of the "sugar high" spike in BG). The control actions of insulin in response to high glycemic foods generates a strong blood insulin influx, and trigger a sudden "crash" in BG owing to increased flux into tissues for storage (mostly in liver and muscle and adipose) and via energy conversion pathways into fats (Walsh, 2014, Wolfe, 1998, and Jenkins, 1981). Only one current group (Yamamoto, 2014) appears to have addressed the need for deciphering between a food's glycemic index (GI), which is well known to effect the rate at which foodstuff is absorbed (Mohammed, 2004). In modeling meal absorption, Yamomoto (2014) addressed glycemic index and associated insulin effect based on replicated literature curves. A state-space representation form is used for the carbohydrate metabolism subsystem, which distinguishes between rapidly absorbing glucose (RAG) and slowly absorbing glucose (SAG). It was determined that 95% of RAG was absorbed within 20 minutes, with SAG between

20-120 minutes. SAG was modeled as a 20-minute time delay plus a time constant of about 21 minutes (vs. just a time constant of 4.2 min for RAG). There was also a first-order gastric emptying time constant related to the time required to pass from the stomach to the duodenum. However, this particular model is limited in its 'lifestyle' inputs such as exercise and utilizes only the Bergman minimal insulin model for subcutaneous insulin (Bergman, 1981 and Shimoda, 1997). Absorption dynamics are represented by critically-damped second-order plus delay system of the following form (Figure 3.1).

$$\frac{dx_R(t)}{dt} = \begin{bmatrix} 0 & 1 \\ -\dfrac{1}{T_{RAG}^2} & -\dfrac{2}{T_{RAG}} \end{bmatrix} x_R(t) + \begin{bmatrix} 0 \\ \dfrac{K_{RAG}}{T_{RAG}^2} \end{bmatrix} Glc^{RAG}(t),$$

$$G_{RAG}(t) = \begin{bmatrix} 1 & 0 \end{bmatrix} x_R(t) \tag{5}$$

$$\frac{dx_S(t)}{dt} = \begin{bmatrix} 0 & 1 \\ -\dfrac{1}{T_{SAG}^2} & -\dfrac{2}{T_{SAG}} \end{bmatrix} x_S(t) + \begin{bmatrix} 0 \\ \dfrac{K_{SAG}}{T_{SAG}^2} \end{bmatrix} Glc^{SAG}(t - \tau_{SAG}),$$

$$G_{SAG}(t) = \begin{bmatrix} 1 & 0 \end{bmatrix} x_S(t), \tag{6}$$

Figure 3.1: Yamamoto (2014) Glucose Absorption Equations. *From Yamamoto, 2014,* representing rapidly-absorbing glucose (RAG), x_{RAG}, and slowly-absorbing glucose dynamics), x_{SAG}, with time-constant T parameters of 4.22 min for RAG and 21.1 min for SAG with a 20-minute time delay for 95% total absorption. Values were obtained *in vitro.* Design specifications for RAG absorption include complete glucose absorption for an impulse food between 0-2o minutes and the area-under-the-curve of RAG glucose absorption equal to the glucose equivalent for the RAG regardless of the amount and GI of the food ingested.

3.3   Need for a New Lifestyle Model

It is evident that four major contributions need to be incorporated into novel BG models: glycemic index (GI) and digestive dynamics, glycogen/glucose lumped

into compartments, a muscle compartment that includes the effects of exercise and activity, and hybrid-control compartmental energetic model. Fast and slow nonlinear pathways, as informed by meal GI, should demonstrate a ratio of carbohydrates to protein and fat with respective Hill saturation dynamics affecting both absorption rate and substrate availability (Gesztelyi, 2012). Unlike many models, glycogen and glucose can allow to be lumped into compartments as one entity since the focus is on energy flux and storage. Glucagon and control-sensitive flux rates allow for a new and innovative way of accessing glucose without an additional state, particularly the liver. GLUT4 and GLUT2 pathways become particularly important, with glycogen stores following mass-conservation throughout all tissues and glucagon as the controller mechanism.

The separation of tissue into a non-muscle and muscle compartment allows accommodation for demand-based muscle metabolism, and different from constant glucose sinks of non-muscle. Not included under non-muscle is a steady glucose energy sink, particularly related to brain consumption.

The addition of a muscle compartment allows for varying muscle mass and body composition of individuals, and type and duration of exercise. Similarly, the addition of the internal muscle mitochondrial consumption state allows for ATP production on the basis of the amount of mitochondria present, as this is a parameter known to vary amongst individuals.

3.4   Methods

3.4.1   Model Structure

The overriding model design objective was an inherently robust model of the

human glucoregulation system, using the minimal set of state variables

(summarized in Figure 3.2) and parameters necessary to simulate diverse scenarios

with adjustability to composition variation and T1D and T2D. Appendix 7.1 lists all

flux input/output parameters and terms.
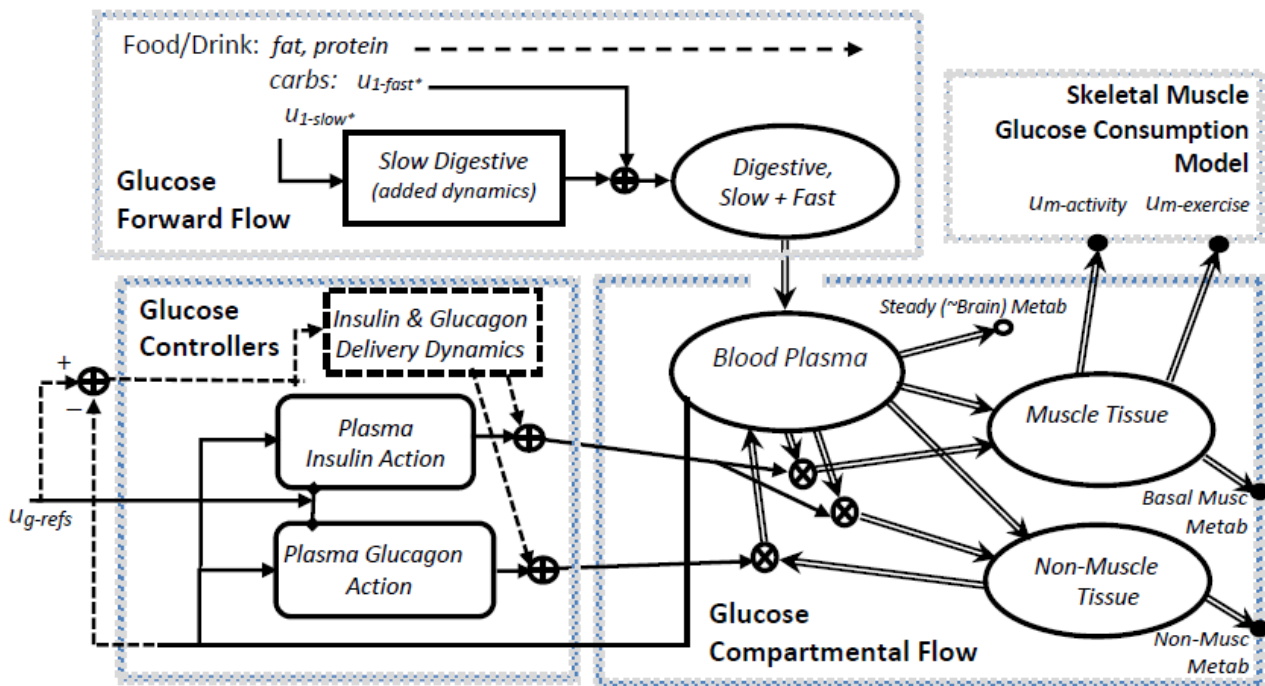
Figure 3.2: Schunk-Winters Compartmental Model Block Diagram and Structure. Thick lines represent material flow with storage and control action as unidirectional signals informed by rate parameters and oftentimes, nonlinear, by either Hill kinetics or multiplicative states. Dashed lines represent exogenous control, via injection or other external device. Nonlinear relations include both flux terms and heuristics that change fitting equations based on different state or input signal ranges.

3.4.2   Four Major Novel Contributions

The Schunk-Winters model addresses knowledge gaps found in literature,

focusing on four major contributions including both simplifications and

developments of past models: glycemic index and digestive dynamics, lumping

glycogen and glucose, addition of a muscle compartment and regulatory action, and

opportunity for a hybrid control-compartmental energetic model.

3.4.2.1   Glycemic Index and Digestive Dynamics

The inputs to this sub-model are rate and amount of oral ingestion of

foodstuff, with the carbohydrate fraction separated into 'fast' and a 'slow' inputs, as

informed by the estimated GI of meal components, available from many sources

(e.g., Monro, 2008 and Yamamoto, 2014). About 88-98% of carbohydrate is

absorbed (highest for pure high-GI carbohydrate ingestion, lowest for low-GI)

(Monro, 2008 and Yamamoto, 2014). Also inputted is the ratio of carbohydrate to

the total consumed energy including fat plus (especially) protein content in a meal

which can (mildly) influence rate of absorption and carbohydrate availability (as is

widely documented, and that Meal GI, universally, is a weighted sum of meal

constituents and associated food GI and carbohydrate (CHO) amount (Monro,

2008):

$$Meal\ GI = \frac{(GI_{FoodA} x\ g\ avail\ CHO_{FoodA}) + (GI_{FoodB} x\ g\ avail\ CHO_{FoodB}) + \cdots}{Total\ g\ avail\ CHO} \qquad [3.1]$$

The slow (low GI) signal enters a separate, slower digestive pathway that is

assumed to be first-order, but nonlinear in that the rate adjusts with the amount of

carbohydrate and overall material. The material flow state from this pathway

converges (sums) with the direct "fast" pathway to a final first-order digestive-

absorption process. This approach appears novel, although the concept of

mathematically distributing carbohydrate into rapidly and slowly available glucose

based on GI has been published recently, but with a different (linear) strategy, with

equations outlined in Figure 3.1 above, similar to Yamamoto et al, 2014 (Monro,

2008). Meals are inputted in regard to total carbohydrate content (kcal/hr with 4

calories per gram of carbohydrate) and proportion of fast, high GI, carbohydrate

content. Other parameters include a term for dietary thermogenesis (i.e. heat lost

during digestion, assumed a function of the slow pathway) and digestive

effectiveness ratios for fast (~98% absorption) and slow (~88% absorption)

digestive inputs due to food loss during digestion in the intestine and stomach, as

well as fiber and other foodstuff that is not fully absorbed (particularly for slow

CHO).

In regards to the calculation of GI, and for purposes of model validation, fiber

content should be subtracted in order to obtain the amount of 'available

carbohydrates.' Cooking and reheating food tends to raise GI, and this must be

controlled for to obtain a particular GI.

3.4.2.2 Glycogen/Glucose Lumped

Glucagon and control-sensitive flux rates, specifically GLUT2 (non-muscle

glucose transporter) and GLUT4 (muscle glucose transporter), represent a new and

innovative way of accessing glucose in the model without the need for an additional

state, typically liver. Both tissue compartments assume that glycogen is the compact

storage form of glucose and represented throughout the mass-conservation system

in all tissues assumed in the model—liver, muscle, adipose, etc. Unlike past models,

there is no state explicitly associated with hepatic production and glycogenesis;

however glucagon plays the role of control action as a function of non-muscle

storage (along with the associated flux) resulting in a 'lumped' modeling approach.

That being said, training can alter relative glycogen storage levels, particularly in

muscle, indicating glycogen stores will start higher and sparing often occurs

(Holloszy, 1984). It seems necessary to delineate between muscle and non-muscle

tissue as opposed to adding a liver state, as hepatic glycogenolysis and

gluconeogenesis can still be modeled with glucagon and GLUT2 action.

3.4.2.3 Muscle Compartment and Regulatory Action

Muscle is often lumped into the tissue compartment of most models, such as

'Muscle and Adipose Tissue' or 'Periphery' (Dalla Man, 2009 and Roy, 2007),

proposing significant limitations. Others simply use exercise as a glucose 'sink' and

decrease in BG (typically non-linear), increase in hepatic gluconeogenesis, storage,

and flux, and increase in insulin sensitivity (Northrop, 2000, and Neelkanta, 2006).

The proposed model addresses this knowledge gap by recognizing metabolic

differences of muscle vs. non-muscle tissue, and treating muscle as a separate

compartment.

Muscle glycogen storage can alter with diet and training, and act as an

immediate source of glucose for short-term, contraction-based activity. Storage

capacity of muscle glycogen in a healthy, non-obese, 70 kg male subject is about 350

grams, or at most 2% of total body volume (Holloszy, 1982). However, muscle

requires mass flow from BG, especially if a burst of anaerobic activity or high

intensity, >60% VO2max aerobic exercise, as glycogen stores are limited.

Contractions stimulate processes including phosphocreatine (PCr) shuttling, Ca^{2+}

flux from the sarcoplasmic reticulum, and GLUT4. Metabolism using PCr as fuel is a

glycolytic process particularly important in the first 3 minutes of ATP need and/or

demand (i.e. exercise or daily, anaerobic, activity). The delivery of glucose parallels

the activation of contraction (Gastin, 2001).

Plasma epinephrine, a powerful stimulator of cyclic AMP formation at the

onset of exercise as well and is primarily responsible for the onset of glycogenolysis

at exercise >80% VO2max (Kjaer, 1989), is not explicitly modeled as its own entity.

However, it is indirectly modeled through the nonlinear subtraction of fat in the fuel

demand mix.

Fat metabolism is another energy fuel source, and is often a factor of training

level as related to mitochondrial volume increase, which often occurs with aerobic

endurance training (Holloszy, 2011). Maximum proportion of fat fuel consumption

occurs at low to moderate intensity exercise (Holloszy, 1996). This concept results

in the nonlinear subtraction (as a reciprocal Hill function) for both tissue glucose

states. When fat is being utilized, glucose consumption will be reduced until

intensity or anaerobic activity increases or substrate availability is altered (Hurley,

1986).

The GLUT4 gradient and production of fuel mix (fat) are both modeled by nonlinear Hill kinetics on the basis of fat utilization curves found in literature (Brooks, 1994). Total aerobic exercise consumption is defined as subtracting the total fat fuel mix consumption from the total exercise input. The model assumes by default that fat oxidation has a maximum of 30% of total aerobic capacity, although with training, this could increase (Brooks, 1994). Total anaerobic exercise consumption is assumed by default to be 50 kcal/hr before switching to mitochondrial and aerobic. GLUT4, Ca^{2+}, and liver glycogenolysis are key regulators and pathways for glucose access during exercise without hormonal control (i.e. glucagon and insulin), although there is an important catecholamine effect as well.

Often exercise intensity fluctuates, and it would be useful to have a method for informing the model about fluctuating levels of muscular demand for glucose. Heart rate data from a smart watch and/or other form of continuous monitor, of available, can help inform exercise and activity input signals, helping sculpt perceived energy rate input pulses given in kcal/hr (*u3* and *u4*).

Various measurements of fitness level and correlation between substrate utilization, fat vs. carbohydrate fuel, during exercise of varying duration and intensity exists and will be further examined in Chapter 4 (i.e. Yardley, 2012). Other model capabilities involve individual fitness parameters and will be developed for model personalization features (Chapter 4). For example, knowing anaerobic threshold and VO2max of an individual allows characterization of heart rate 'zones' 1-5 ranging from 'light, recovery' exercise (zone 1) to above anaerobic threshold (zone 5). Often used in exercise physiology, zones can be correlated with respiratory

exchange ratio (RER) in which an RER = 0.7, often during zones 1-2, is mainly fat

utilization while zone 5, or RER $\geq$ 1.0, is mainly glucose utilization with a fuel mix in

between (Knoebel, 1984). Zones are often used in regard to exercise planning and

training, as they can be adjusted as one becomes trained, typically favoring higher

fat utilization at elevated heart rates and shifting zones upward (Millan, 2014).

There is the possibility that long durations of circuit training and/or

anaerobic exercise can elicit fuel mix responses as well; however, this is a current

debate. Heart rate (HR), assuming steady state, can be a rough crude indicator of the

amount of fat consumption, if HR zones are known and can provide an accurate

sense of intensity—further discussed in Chapter 4 as an additional external input.

3.4.2.4 Hybrid Control-Compartmental Energetic Model

A hybrid model enables the ability to have more realistic inputs than most

models. Inputs are all scaled to kcal/hr (exercise and activity) or g/hr (digestive

input, insulin) with easy conversion between each. Body composition data is easily

incorporated and scales various parameters that are influenced by body mass or

muscle/non-muscle compartment mass. Additionally, various types of insulin

resistance and type 1 effect scale the model. Lifestyle inputs also demonstrate the

need for GLUT2 and GLUT4 action, as many activities and scenarios allow even a

type 1 diabetic to be 'OK' without experience hypo- or hyperglycemia. For example,

a type 1 diabetic often can eat a low GI snack or exercise at a low intensity for an

extended duration without deviating from the target range due to other external

non-insulin, non-glucagon based pathways. Hill relations allow for maximum

saturation at known quantities and limits, as well as allow tuning for rate changes

due to a particular concentration without need for conversion, and are reviewed by

Gesztelyi, 2012.

3.4.3   Nonlinear Hill Kinetics for Saturating Rates and Signal Magnitudes

The model makes use of classic Hill saturating kinetics for rates and in some

cases signal magnitudes, and is reviewed by Gesztelyi, 2012:

$$F_{hill}(x, k_{max}, k_s, n) = \frac{k_{max}z^n}{k_s^n + x^n} \qquad [3.2]$$

where x is a state, k_{max} and k_s are maximum saturation and half-way x values, the Hill

coefficient n is 1 (Michaelis-Menten kinetics), 2, 4 or 6 (each with soft saturation at

both ends), and $z = x$ for rising and $z = k_s$ for falling curves (Hovorka, 2002).

For hormonal P-action signals where 10% rather than 50% of max helps design

resting values, we map:

$$k_s = [9^m k^n]^{1/n} \qquad [3.3]$$

where k=0.1 (10%) is the basis for hormone "reference" parameters, $m = 1$ for

rising, $m = -1$ for falling.

Nonlinearities of glucagon and insulin controllers (with added time delay for

insulin), meal absorption (slow and fast stomach states), tissue intolerance, and BG

loss muscle demand gradient all utilize Hill kinetics. Figure 3.3 demonstrates Hill

effects on BG based on insulin and glucagon controllers. In equations that follow,

Hill functions are seen throughout the following state equations, with values defined

in Appendix 7.1.
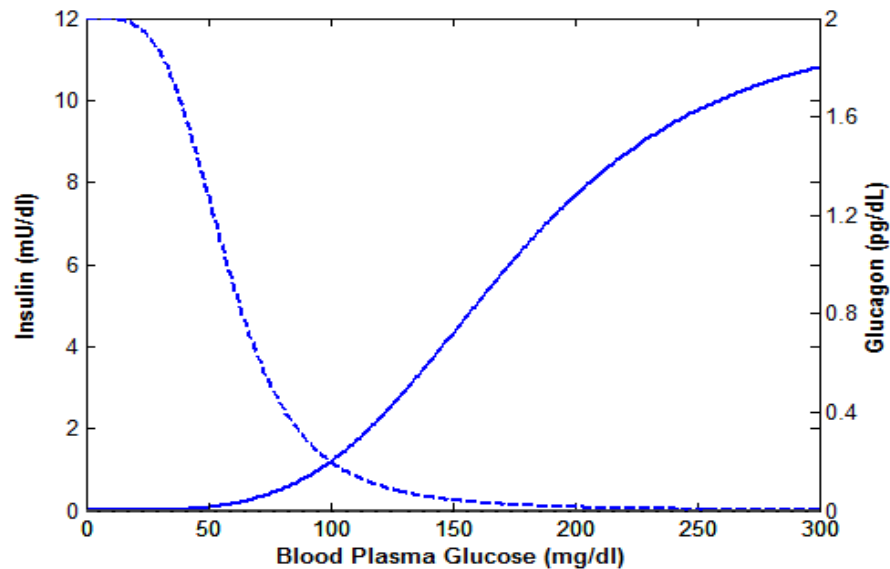
Figure 3.3: Insulin and Glucagon Hill Controllers. Insulin (solid) and glucagon (dashed) vs. blood plasma glucose concentration as implemented with Hill based controllers.

3.4.4 Glucose Compartmental Flow

A 3-compartment "process" model for glucose distributes most of body tissue volume (other than plasma glucose) into two compartments: skeletal muscle (~35-45% body weight (BW)) and non-muscle (~35-40% of BW). The non-muscle compartment represents unique features of tissues with specific glucose flux pathways within blood and/or storage capacity, including liver, adipose, cardiac and digestive. It does not include the volume of brain or blood erythrocytes (which are assumed to provide steady flux sinks), or extracellular fluid (ECF, the volume of the third compartment, "blood plasma/ECF").

Interface parameters based on relative mass are used to assure that states and fluxes are scaled appropriately between compartments. Appendix 7.1 provides non-muscle and muscle parameters influenced by respective BM contributions. Glucose compartmental relations of states $x_g, x_m \ and \ x_{nm}$ are represented by each flux and mass balance/flow term below with most terms nonlinear via use of Hill kinetics for rates or magnitudes, and multiplicative control action. A state-independent steady unidirectional glucose loss flux of (by default) 120g per day is used to represent the energy requirements of brain and erythrocytes, based on work by Roy (2002) and Melzer (2011). Additionally, there are two types of specialized fluxes that are a direct function of insulin or glucagon control action: a relatively small non-muscle flux sink associated with the slower-digestion pathway (developed below), and potentially much larger fluxes associated with muscle workload activities such as exercise (also developed below). The Schunk-Winters model scales to each person by BW ratios relative to defaults for BW (70 Kg), with similar ratios for non-muscle and muscle (see Appendix 7.1 Table for affected parameters). Muscle mass is also composed of mitochondrial mass, defined by a ratio parameter of percent muscle. This value becomes increasingly important with training and as discussed in Chapter 4.

The addition of a mitochondrial consumption state within the muscle compartment is motivated by the remarkable variation in energy demand and consumption during exercise and activity. This allows for varying rates between conversion pathways on the basis of total mitochondrial amount and fiber type distinction. Type 1 muscle fibers (slow oxidative) have high mitochondrial content

and are able to generate more work with less ATP utilization whereas Type 2 muscle fibers (fast glycolytic) require more immediate glucose as energy and have a lower mitochondrial content (Holloszy, 2011). Mitochondrial volume increases with endurance-trained individuals, as can energy transport capacity. For instance, one study found that a 2-fold increase in GLUT4 expression results in a 2-fold increase in glucose uptake at the same insulin concentration (Holloszy, 2011). This concept relates the idea that oftentimes walking, or simple daily activity, is beneficial for diabetes management, including those experiencing insulin resistance. For the purposes of our model, for the *x10* state, mitochondrial use of glucose *only* (despite mitochondria's important role in fat oxidation) is modeled to keep consistency with mass glucose conservation and kcal/hr inputs. The Kreb's cycle, which takes place in the mitochondrial matrix, is a precursor for oxidative phosphorylation and efficient generation of ATP from glucose fuel. We assume this process is most fully associated with aerobic exercise, the *u3* input of our model. On the other hand, anaerobic exercise and daily activity (*u4)* tend to use a less efficient ATP generation in glycolysis, or immediate glucose consumption in the cytoplasm. Any exercise involving fast-twitch glycolytic muscle fibers (often 'bursts' of activity) will utilize glycolysis. However, especially with long-lasting activity and/or anaerobic exercise, mitochondrial action will continue to take place as a more endured energy source but at a reduced proportion (parameter *kprop*).
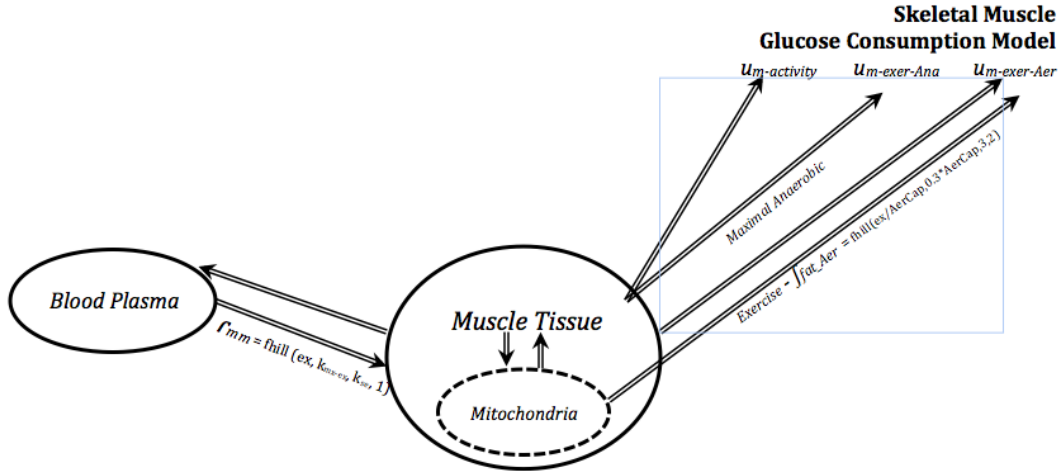
Figure 3.4: **Skeletal Muscle and Tissue Compartmental Model**.

Skeletal Muscle and Tissue Compartmental Model
$u_{m\text{-}activity}$: Daily Activity Muscle Input (kcal/hr)
$u_{m\text{-}exer\text{-}Ana}$: Anaerobic Exercise Muscle Input (kcal/hr)
$u_{m\text{-}exer\text{-}Aer}$: Aerobic Exercise Muscle Input (kcal/hr)
fat_Aer: Aerobic Fat Consumption (out of total exercise input) (kcal/hr)
AerCap: Maximal Aerobic Capacity (kcal/hr)

3.4.4.1   Blood Plasma Glucose State (mg/dl)

$$\frac{dx_g}{dt} = K_{bd}x_d - \left[\left(C_{i_{nm}}\left(\frac{k_{mx-nm}k_{tintol}}{k_{tintol}+x_{nm}}\right)^8 + C_{i_m}\left(\frac{k_{mx-m}k_{mintol}}{k_{mintol}+x_m}\right)^8\right)\right]x_g x_i + \left(C_{g_{nm}}+C_{g_m}\right)K_{gt}x_g x_{gn} -$$

$$\left[\left(\frac{k_{mx-ex}u_{exer}}{k_{s-ex}+u_{exer}}\right)^1\left(x_g-x_m\right)\right] - \frac{K_b}{w_{nm}} - \left(\frac{k_{g2max}x_g}{k_{greft}+x_g}\right)^2\left(x_g\right) \qquad [3.3]$$

where influxes are digestive (stomach) glucose (x_d) and glucagon controller

(x_{gn}, mostly via liver and controlled rates), with outfluxes of exercise loss (u_{exer}),

insulin (x_i, to tissues), brain consumption (K_b), bi-directional GLUT2 loss (liver,

intestines, etc.), muscle demand consumption.

Below is a key for Equation 3.3. Equations 3.4- 3.12 follow a similar scheme,

with terms and parameters defined in the Glossary and Appendix 7.1. In particular,

Hill parameters are denoted by k_s or $k_{mx,}$ referring to half-way saturation and

maximal saturation, respectively. Other subscripts inform on the basis of state or

parameter. For instance, a subscript '*m*' refers to muscle, or k_{greft} refers to the

parameter *greft.* Current state concentrations are denoted by *x* terms. The units of

each state are provided after each subheading or in the Glossary and Appendix 7.1.

$\frac{dx_g}{dt}$, Rate of Change in BG vs. Time (hr) [mg/dl]

K_{bd}, Conversion of Digestive Mass Flow (g/hr) into ECF (BG + interstitial) scaled by blood volume (in dl)   and with mass converted from g to mg

x_d, Glucose Digestive Forward Rate Path [g/hr]

C_{inm}, Insulin Control Parameter, Non-Muscle Tissue Gain [unitless]

k_{mx-nm}, Maximum Saturation for Non-Muscle Tissue Intolerance [/hr]

k_{tintol}, Reference Threshold for Non-Muscle Tissue [mg/dl]

x_{nm}, Non-Muscle Tissue State [g/kg]

k_{mx-m}, Maximum Saturation for Muscle Tissue Intolerance [/hr]

k_{mintol}, Reference Threshold for Muscle Tissue [mg/dl]

x_m, Muscle Tissue State [g/kg]

x_i, Endogenous Insulin Control Action in Blood Plasma (mU/dl)

$C_{g_{nm}}$, Glucagon Control Parmeter, Non-Muscle Tissue Gain [unitless]

C_{g_m}, Glucagon Control Parmeter, Muscle Tissue Gain [unitless]

K_{gt}, Basal Tissue Elimination Rate, Scaled to Grams (for Glucagon) [/hr]

x_i, Endogenous Glucagon Control Action in Blood Plasma (pg/dl)

k_{mx-ex}, Maximum Saturation for Muscle Tissue Gradient [/hr]

k_{s-ex}, Half-Way Saturation for Muscle Tissue Gradient [g/kg]

u_{exer}, Aerobic Exercise Input, *u3* [kcal/hr]

k_b, Blood Glucose to Steady Consumption Sink (mostly brain) [g/hr]*, scaled by k_{bd} conversion to mg/dl

w_{nm}, Non-Muscle Mass [kg]

k_{g2max}, Maximum Rate, GLUT2 Flux [/hr]

k_{greft}, Reference Threshold of BG for Non-Muscle Flux Direction [mg/dl]

Inputs ***u1-u4*** are in kcal/hr, consistent with an *energy flow* model. For

glucose, 4 Kcal of energy is assumed to have a one gram mass equivalent (1 g CHO =

4 kcal). Thus for rates, 1 g/hr of glucose flux maps to 4 Kcal/hr of glucose energy

flux. Any quantity that has units of kcal/hr will be divided by 4 in order to convert to

grams/hr.

3.4.4.2 Non-Muscle Tissue State (g/kg)

$$\frac{dx_{nm}}{dt} = \left[\left(\frac{k_{g2max}x_g}{k_{greft}+x_g}\right)^2(x_g) + C_{i_{nm}}\left(\frac{k_{mx-nm}k_{tintol}}{k_{tintol}+x_{nm}}\right)^8 x_g x_i - K_{gt}C_{g_{nm}}x_g x_{gn}\right]w_{bt} - \frac{[G_{met_{nm}}+(K_{carb}x_{ds})]}{w_{nm}}$$

[3.4]

where influxes are insulin-regulated BG delivery, brain requirement, bi-directional

GLUT2 gain (liver, intestines, etc.), and outfluxes are basal metabolic tissue loss and

glucagon-regulated delivery. Some are scaled by w_{bt}, based on blood volume and

non-muscle mass.

Scaling and conversion is similar to that of Equation 3.3. Parameter w_{bt} is

used for compartmental flux conversion with BG concentration (in mg/dl)

converted to amount in grams by using BG volume, then is normalized to the mass

of the segment (thus g/kg of non-muscle).

3.4.4.3 Muscle Tissue State (g/kg)

$$\frac{dx_m}{dt} = \left[\frac{(\frac{k_{mx-ex}u_{exer}}{k_{s-ex}+u_{exer}})^1(x_g-x_m)]}{G_{mb}} + C_{i_m}\left(\frac{k_{mx-m}k_{mintol}}{k_{mintol}+x_m}\right)^8 x_g x_i - C_{g_m}x_g x_{gn}\right]w_{bm} - \frac{G_{met_m}}{w_m} - $$
$$\frac{[u_{daily}+G_{exer}(u_{exer})]}{4w_m} - rat_{mito}x_{mito}$$

[3.5]

where influxes are insulin-managed BG delivery (scaled to this compartment) and

exercise-demanded BG delivery (scaled), and the outfluxes are basal metabolic

muscle loss, exercise-demanded muscle glucose consumption, and daily activity

related muscle glucose consumption.

Scaling and conversion is similar to that of Equation 3.3. Parameter w_{bm} is

used for compartmental flux conversion with BG concentration (in mg/dl)

converted to amount in grams by using BG volume, then is normalized to the mass of the segment (thus g/kg of muscle).

3.4.4.4   Mitochondrial State (g/kg)

$$\frac{dx_{mit}}{dt} = \left[\frac{k_{musc}(G_{ex-Total}+k_{prop}\frac{u_{daily}}{4}-x_m-x_{mit})}{4*w_{mit}} \right] \qquad [3.6]$$

where influxes are total exercise (anaerobic + aerobic) glucose consumption demand as a Hill function and daily activity and outfluxes are loss to muscle tissue (demand based) and mitochondrial consumption.

3.4.4.5   Glycogen Storage Approach

It is well known that glucose is stored as glycogen in almost all tissue compartments, with amount dependent on a variety of factors including habitual (and recent) diet (i.e. high carbohydrate vs. high protein and/or fat), health and athletic training status, as well as instantaneous demand of exercise. High dietary carbohydrate is a key reason for glycogenosis within the liver and muscle, the largest storage sites.

During high stress triggering events, whether it be a form of exercise requiring glucose or the 'fight-or-flight' mechanism elicited for another external stimulant, glycogenolysis typically occurs in the liver as shown in most models. Despite lack of an explicit liver state, the same effect is achieved with on-muscle demand contributing to a rise in BG on the basis of increased HR input (***u5)*** and/or glucagon controller response.

3.4.5   Glucose Forward Mass Flow

This sub-model is 2nd-order, with its output state being a mass flow rate of appearance of glucose into the blood plasma/extracellular fluid compartmental. The proportion of carbohydrates entering into the fast vs. slow absorption path is dependent on meal glycemic index (k_{fast}) and the total amount of carbohydrates inputted. There is a maximum saturation on how fast glucose can enter (if extremely high GI, absolute path, k_{max} or k_{abs}) and a limit on how much can be absorbed based on the filling and/or gastric emptying of the stomach in grams (slow path k_{min} value). Absorption is modeled with use of saturating Hill kinetics.
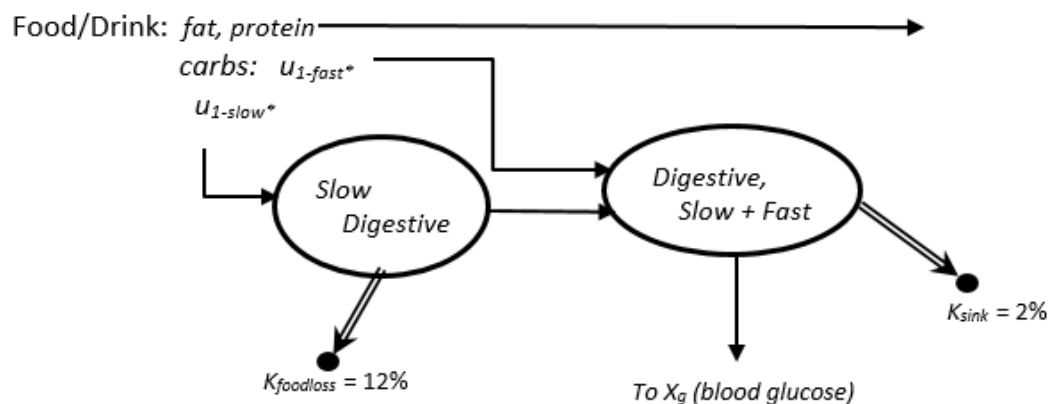
Digestive Lumped Compartmental Model

$u_{1-fast*}$: Fast Carbohydrate (High Glycemic) Glucose Input (kcal/hr)
$u_{1-slow*}$: Slow Carbohydrate (Low Glycemic) Glucose Input (kcal/hr)
$K_{foodloss}$: Food Input Not Absorbed (Fiber, etc.) (Decimal Percent)
K_{sink}: Foodstuff Lost Prior to Stomach Absorption (Intestines, etc.) (Decimal Percent)

Figure 3.5: Digestive Lumped Compartmental Model

3.4.5.1 Low Glycemic Index (Slow) Forward Glucose Path (g/hr)

$$\frac{dx_{ds}}{dt} = \left[K_{ugs} + \left(\frac{k_{ugs}x_{ds}}{k_{s-ds2}+x_{ds}}\right)^4\right] u_{carb} G_{eff_s}\left(\frac{u_{slow}}{4}\right) - x_{ds} \qquad [3.7]$$

where influxes are glucose input and slow stomach glucose state, and outflux is the

slow path that enters the final stomach path that follows. It is important to note that

scaling occurs by a factor of 4, as for glucose 1 g of CHO = 4 kcal.

3.4.5.2 Glucose Digestive Forward Flow Final Path (g/hr)

$$\frac{dx_d}{dt} = [u_d \left[\left(\frac{(k_{ugf}/2)x_d}{k_{s-d}+x_d}\right)^4 + \left(\frac{(k_{ugf}/2)x_d}{k_{s-d2}+x_d}\right)^4\right] G_{eff_f}\left(\frac{u_{fast}}{4}\right) + \left[K_{ugs} + \right.$$
$$\left. \left(\frac{k_{ugs}x_{ds}}{k_{s-ds2}+x_{ds}}\right)^4\right] G_{eff_s} x_{ds} - x_d] \qquad [3.8]$$

where the influxes are the glucose input (fast component) and the pre-filtered slow

component, each sculpted for lower rates outside of their respective digestive mid-

ranges, and the outflux is the output of the digestive process, i.e., the rate of glucose

entering the bloodstream.

3.4.6 Glucose Bio-Controllers

It is well known that x_g is regulated to reach homeostatic bounds of about 80

to 120 mg/dL (sometimes higher, if diabetic) largely through hormonal control

action. Endogenous insulin production within the pancreas and secretion into the

blood increases with high glucose concentration. Glucagon is a counter regulatory

hormone to insulin with similar mirroring dynamics for when x_g is low. Glucagon supplements the simplified hepatic glucose production process of this model.

Insulin and glucagon are implemented as nonlinear Hill controllers with n=4 to best replicate known literature curves (Sorenson, 1985, Northrop, 2000, and Duun-Henriksen,2013) and resting levels of about 10% of maximum. These can be viewed as nonlinear proportional action (P-action) controllers. Additionally, the insulin biocontroller is mildly delayed, and also includes implementation of a derivative action (D-action) control component (see Dalla Man, 2007, for former, Dalla Man, 2014, for latter).

Relative blood flow acts as an indirect controller in the fact that both glucose delivery from blood to different tissues and exogenous insulin delivery can both be affected. The rate of absorption of glucose into tissues from the blood is dependent on external factors that increase (or limit) blood flow, as well. Anything increasing blood flow to a certain tissue, such as heat or muscle activity, will increase glucose uptake rate into that type of tissue, of which insulin works as a signal. This mostly reflects changes in blood flow. For instance, with endurance exercise, there is redistribution of glucose towards muscle, heart, and skin if external temperature is increased, with internal organs can see a decrease. For example, during a long race, it is harder to digest foodstuff (the creation of 'gels' ensued) as flow becomes demand-based, with decreased flow for digestive processes. With higher flow perfusion to muscle and other glucose sources needed (i.e. liver), both insulin-dependent and non-insulin dependent fluxes should be up.

In another example, absorption may also be affected by excess tissue or an extremely large bolus within a short time frame, may result in limited or lowered absorption. This is modeled by adjusting the ratio of forward-rate parameters of the non-monomoric (slow) to monomeric (fast) parallel insulin pathways. Table 3.1 below outlines appropriate parameter adjustment. The addition of a Hill saturation controller accounts for high dosage boluses in a short time window—linearity is preserved at low dosages before becoming saturated (Figure 3.6).

Table 3.1: Factors Influencing Insulin Absorption Rate

	Increase Ratio (R_{effect})	**Decrease Ratio (R_{effect})**	**Increase Overall Magnitude (K_d)**	**Decrease Overall Magnitude (K_d)**
Effect	Slower absorption; non-monomeric absorption	Faster absorption; monomeric absorption	Faster Dissociation	Slower Dissociation
Physiologic Reasoning	Injection into excess tissue (i.e. abdomen), large bolus, Slow-Acting Type	Hot environment, muscle activity, lean tissue, Fast or Regular Insulin Type		Large bolus
Range of Value	0.6-1.0	0.1-0.6	0.02-0.1	0.005-0.02
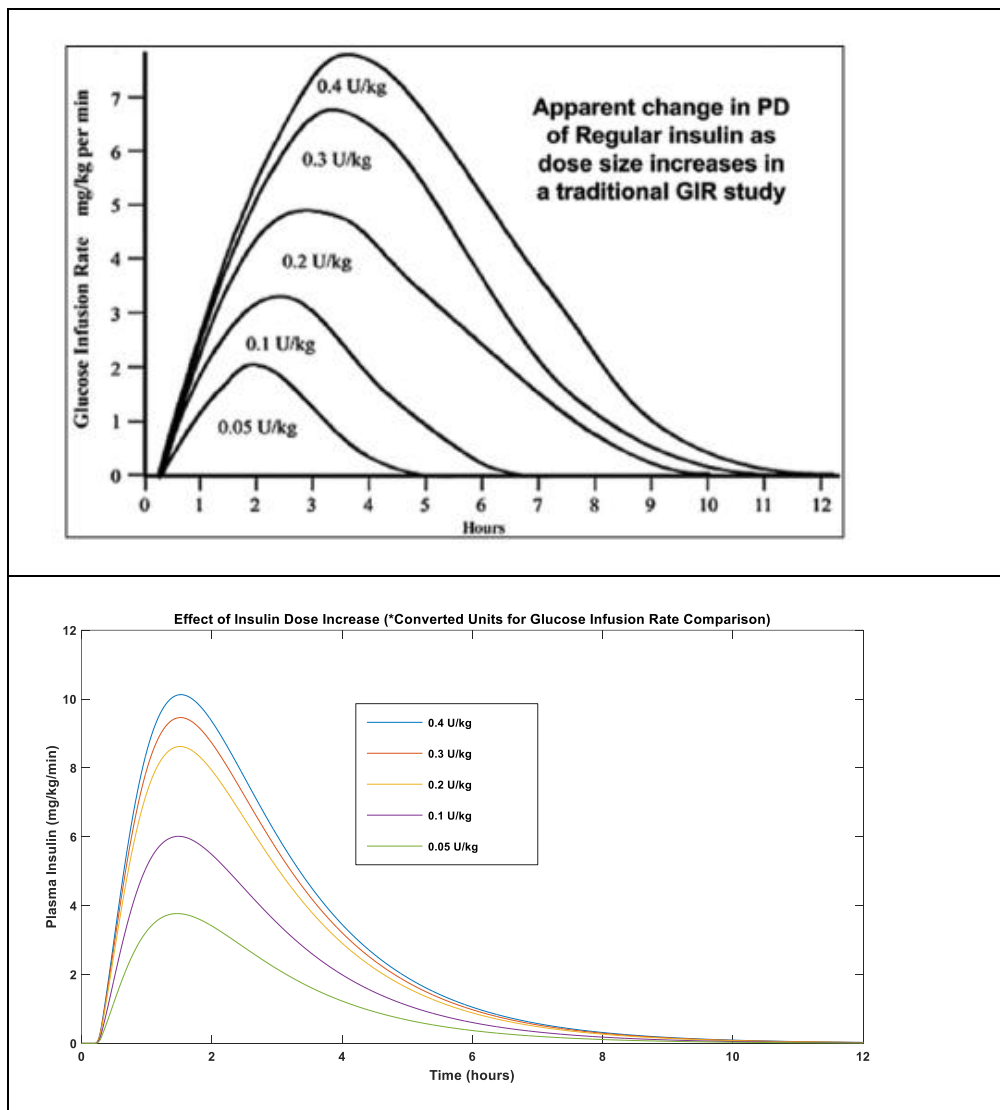
Figure 3.6 Effect of Dose Size on Insulin Pharmacodynamics. (Top): From Walsh, 2014: dose size changes pharmacodynamics of insulin. **(Bottom)** Recreated exogenous insulin saturation effect as bolus size increases (mainly due to predicted tissue absorption).

Exogenous insulin, particularly injections, can be of three types with varying peak effect and time delays—fast, regular, and long acting (Diabetes Services, Inc). Injection modeling here uses half sine waves to account for varying effects. Dosage depends on a clinically based sliding scale accounting for current x_g level and food GI. Peak rates and times used for curve shaping are as follows in Table 3.2.

Table 3.2: Action Times for Insulin (adapted from Diabetes Services, Inc)

Insulin	Starts	Peaks	Ends	Low Most Likely At:	Usage
Humolog/Novolog/ Apidira	10-20 min	1.5-2.5 hr	4.5-6 hr	2-5 hr	Designed to peak, covers meals, and lowers high BG's
Regular	30-45 min	2-3.5 hr	5-7 hr	3-7 hr	
Lantus	1-2 hr	6 hr	18-26 hr	5-10 hr	Designed for flatter and longest action, basal insulin action for keeping BG flat when fasting
Levemir	1-3 hr	8-10 hr	18-26 hr	8-16 hr	
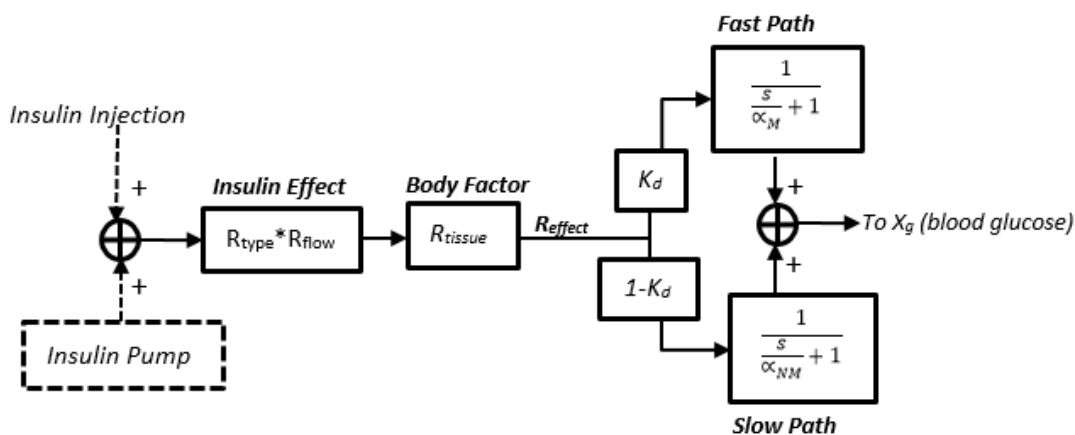
Insulin 'Black Box' Model

R_{effect}: Ratio of Non-Monomeric to Monomeric Insulin

R_{tissue}: Tissue Absorption Factor

R_{type}: Insulin Type Factor

R_{flow}: Blood Flow Factor

$K_{d:}$ Rate Constant of Insulin Dissociation

α_M: Rate Constant of Monomeric Insulin Absorption

α_{NM}: Rate Constant of Non-Monomeric Insulin Absorption

Figure 3.7: **Exogenous Insulin Model**

3.4.6.1   Endogenous Insulin Control Action in Blood Plasma (mU/dl)

$$\frac{dx_i}{dt} = K_{a2}x_{inj-m} + K_{a1}x_{inj-nm} + \left[rat_{type1i}\left(\frac{G_{refi}x_g}{k_{s-ins}+x_g}\right)^4 + rat_{type1i}\,K_{id}\dot{x}_g\right] - K_i x_i$$

[3.9]

3.4.6.2   Endogenous Glucagon Control Action in Blood Plasma (pg/dl)

$$\frac{dx_{gn}}{dt} = K_{gc}\left[rat_{type1i}\left(\frac{G_{refg}x_g}{k_{s-gn}+x_g}\right)^4 - x_{gn}\right]$$

[3.10]

3.4.6.3   Exogenous Insulin Delivery by Injection: Monomeric Absorption (mU/dl)

$$\frac{dx_{inj-m}}{dt} = K_d(x_{inj-nm} - k_{a2}*x_{inj-m})$$

[3.11]

3.4.6.4   Exogenous Insulin Delivery by Injection: Non-Monomeric Absorption (mU/dl)

$$\frac{dx_{inj-nm}}{dt} = -(K_d + k_{a1})*\left(x_{inj-nm}\right) + \left(\frac{hs_{max}*u_{inj}}{hs_{ks}+u_{inj}}\right)^1$$

[3.12]

3.4.6.5   Exogenous Glucagon

Exogenous glucagon would be an additional state, imperative to artificial pancreas function. A counter regulatory hormone to insulin must exist in order for AP technology to be possible. It is important to note that one limitation in including Glucagon in AP design is its short shelf life (Jacobs, 2011). New artificial pancreas (AP) research solutions (Jacobs, 2011) include one rather complex model (Neelkanta, 2006). Due to lack of data and substance instability as a part of current AP design, exogenous glucagon delivery is not included as a state in the Schunk-Winters model. However, if added, its inclusion would be simplified as a (linear or nonlinear) 1st-order process, making the overall model 11th-order. Due to glucagon's

fast dissociation, exogenous glucagon is indirectly modeled with non-muscle compartment action on the basis of hepatic glucose production (Jacobs, 2011).

3.4.7   Additional Hormonal Actions and Methods for Inclusion

Primary glucoregulatory hormones include insulin and glucagon, as is common to most models. However, it is known that there are other regulatory hormones for BG—three are noted here, each including a viable method for inclusion (e.g., as a multiplicative functional operating on one or more existing model parameters).

Amylin suppresses glucagon and works with insulin in circulating glucose by decreasing hepatic glucose output following ingestion, as well as slowing gastric emptying (Aronoff, 2014). Both insulin and amylin are produced by pancreatic β-cells, thereby will be absent in people with Type 1 diabetes and limited in Type 2. If adopted, a new real-time hormonal controller could naturally modulate the digestive rates (e.g., slow path) and thus the K_{ugf} parameter, and perhaps the glucagon rate for which glucose is used by tissue (i.e., modulate the C_{ga} parameter).

A second additional hormonal controller, also real-time and anticipatory, could involve sympathetic nervous system effects. Included would be catecholamine action in response to an exercise and/or emotional induced stress that enhances sympathetic drive. Enhanced sympathetic drive can result in a variety of measurable effects including elevated HR, pupil dilation, and increased blood flow and pressure. Oftentimes, an increase in BG is seen, even if brief. An approach for such additional control action would be to modulate the GLUT2-mediated flux between the non-

muscle and BG compartments. Hence, *stressorrat*, a parameter formed to scale

added stress other than only HR fluctuation is implemented for high-intensity and

increased stress training situations by increasing the rate at which glucose leaves x_g

from x_{nm} via the GLUT2 flux pathway in a multiplicative manner. *Greft* and *Kg2Max*

also have an effect as parameters involved in the GLUT2 Hill functional. *Stressorrat*

works to inform exercise of additional catecholamine action (and general

sympathetic neural system drive) that may be present.

This concept is further developed in Chapter 4, where high heart rate (within a

context) is proposed as a method to inform controller action.

The hormone leptin acts to regulate the amount of excess dietary calories

stored as fat in fat cells versus the amount of glucose stored as glycogen in the liver

and muscles (Northrop, 2011). The most significant location for leptin receptors is

on the pancreatic beta cells that secrete insulin. Leptin plays a role in fat

accumulation based on an excess of stored carbohydrates, important for long-term

modeling simulations, greater than 24-hours. The Schunk-Winters model has this

capability. This type of additional control would act as adaptive management,

particularly for long-term effects such as excess glucose building in tissues over

consecutive simulations (i.e. the ending state concentration is higher than first

initialized), as any longer-term buildup in either of the two tissue compartments is a

natural indicator of glycogen to fat transfer.

These new control action modulators are proposed here and developed in

Chapter 5 as future directions for the model.

3.4.8   Muscle State Inputs

Inputs to the muscle state relate to glucose fuel consumption associated with meeting muscle energy demands, here assumed to be of two forms. Inputs consume glucose and amount is scaled appropriately according to Table 3.3 on the basis of supply and demand.

Body composition inputs for the muscular state include muscle mass (out of total BW), mitochondrial volume, aerobic capacity, and knowledge of one's anaerobic threshold zones on the basis of a VO2max stress test. The latter is not required for the basic model, however, if HR is known, a more personalized and refined model input can be estimated. Table 3.3 below shows input variations.

Table 3.3: Exercise and Activity Input Characterization

Input	u_3	u_4	u_5 (if obtainable)
Characterization	• Primarily aerobic or during long duration anaerobic/circuit training • Continuous • HR is ramp-like • Can be sustained • Sufficient oxygen is provided to sustain for energy • Uses oxygen to burn CHO and fat for energy	• Primarily daily /training anaerobic-dominated activity, or "sprints" during longer exercise • Daily Activity, Weight Training • Fluctuating HR, characterize by spikes • Increase in glycolysis • Increase in lactic ace • Lower Oxygen requirement • Glucose = fuel	• HR input characterized by resting ($u_5 = 0$) and maximum ($u_5 = 1$) difference • Fluctuation or continuous is key to delineate between fuel mix type • Characterize anaerobic threshold and zones with VO2max stress test
Units	kcal/hr	kcal/hr	bpm

3.4.8.1 Exercise (*u3*)

Exercise, dependent on intensity (kcal/hr), duration (hr), and substrate availability (i.e. diet and fuel before and during), is inputted as either 1) aerobic or 2) anaerobic or a combination of both. The *u3* input primarily relates to aerobic exercise, as shown in Table 3.3. It is important to note that the combination, or fuel mix, of exercise is achieved by combining the activity input with aerobic exercise input on a scale of aerobic capacity.

Heart rate may also be inputted to better quantize the (potentially fluctuating) aerobic "pulse input" intensity (assuming zones are known), as well as characterize activity as anaerobic if HR fluctuations are present. Aerobic exercise is often continuous and ramp-like in behavior. Typically, aerobic exercise can be maintained, as sufficient oxygen is available for fat and carbohydrate consumption. Mitochondrial action is present, especially at low to moderate intensity.

3.4.8.2 Daily Activity (*u4*)

Considering a resting metabolic rate around 0.82, the typical human body derives more than half of its energy from fatty acids and the rest from glucose (Melzer, 2011); but many tissues (including muscle) can use whatever fuel is available. Activities requiring immediate energy typically utilize the phosphocreatine (PCr) shuttle and hence (indirectly) glucose utilization—this phenomena also is imperative to the onset of exercise. Many aspects of daily activity are often characterized as anaerobic, increasing glycolysis and glucose consumption

due to a low oxygen requirement (e.g., muscles recruitment that includes fast glycolytic fibers). Examples are certain team sports and work around the kitchen. In some cases lactic acid increases, and activity can be characterized as demonstrating fluctuating heart rate due to 'bursts' of energy demand. Circuit training and the end of a long aerobic session may present some characteristics of the *u4* input.

Daily activity is inputted in kcal/hr with maximum at around 200 kcal/hr, although dependent on aerobic capacity.

3.4.8.3   Heart Rate (*u5*)

One advantage of our modeling framework is that dietary and exercise inputs do not have to be bolus inputs, in contrast to most models (Dalla Man, 2007, and Yamamoto, 2015), but are energy rates that can be a function of time. Most common is a pulse input, i.e., an energy rate intensity over a time duration. Heart rate can be inputted into the model to help sculpt the u3 input. A standard heart rate monitor often measures at a frequency of 1/second, using units of beats per minute. This quantity is converted into model's time step, or 100 units/hour (1 unit = 36 seconds). Heart rate data at steady-state can be used to help quantify exercise intensity (and thus, potentially, u3 level), typically on the basis of anaerobic threshold zones, and heart rate fluctuations can be used to quantify a sudden stressful situation, or the onset of exercise (as well as circuit training or anaerobic exercise). Heart rate variability (HRV) due to breathing, etc. is not an issue as the time sampling unit is 36 seconds, significantly greater than the duration of HRV.

3.4.9   Summary of Default Parameters

For full description of parameters and values refer Appendix 7.1 and
Glossary. A majority of the core insulin sub-model was based off of literature curves
and clinical data from Cobelli (2007), Bergman (1981), Yamamaoto (2014), and
Hovorka (2004). The digestive sub-model was shaped on the basis of known
nutritional trends based on GI (Monro, 2008) and modeling approaches used by
Yamamoto (2014). Since the addition of GI digestive dynamics is new to the
modeling field, some personal clinical knowledge and data was also used for trend
shaping.

3.4.9.1   Parameter Adjustment: Person with T1D

The following parameters/relations in Table 3.4 are scaled by *rattype1i* (on a
scale from 0 to 1, with 0 being no insulin production):

Table 3.4: Type 1 Diabetic Parameter Adjustments for Insulin

Insulin initial state	1.0 mU/dl (default)
Insulin Controller	*GCi*
Residual Insulin Storage Controller	*GCid*
Muscle Flux Gradient	*Gmgrad*

The following parameters/relations in Table 3.5 are scaled by *rattype1g,* if
determined necessary (on a scale from 0 to 1, with 0 being no glucagon production):

Table 3.5: Type 1 Diabetic Parameter Adjustments for Glucagon

Glucagon initial state	70 pg/mL (default)
Glucagon Controller	*GCg*

It is not well-known the extent of diabetes on glucagon production; however, many other mechanisms (GLUT2/GLUT4 path, muscle contraction and calcium influx, etc.) are redundant with glucagon's primary actions: stimulating hepatic production and allowing glucose to enter the blood, that the effect of glucagon depletion is not as apparent as with insulin.

From personal experience working with a certified diabetes educator (CDE) it is often assumed that a T1D maintains normal glucagon production (i.e. rattype1g = 1.0). That being said, glucagon emergency injection kits are prescribed to T1D's in the case of hypoglycemia as this will be a more concentrated and faster action dose than pancreatic produced glucagon action (due to biological sensing time delays and potential for delayed hepatic glycogenolysis if BG is already low and no immediate glucose source exists). In the model there is opportunity to scale the amount of glucagon production present, although a default of 1.0 is used.

3.4.9.2   Parameter Adjustment: Person with T2D

Modeling insulin resistance would affect the absorption rate of glucose entering tissues. Insulin can be assumed to still be fully produced in the quantity needed for a given food intake (often excess); however, it will not be properly utilized, thereby resulting in elevated BG levels and eventually conversion into fats. In the model, some degree of insulin resistance can be related to the GLUT4 and GLUT2 gradients, since high tissue levels change this gradient. One study also suggests moderate weakness in select skeletal muscles due to a reduction in mitochondrial proteins in insulin-resistant fibers (Ohlendieck, 2010). As discussed

in Section 3.4.7, leptin acts to regulate body fat storage, a well-known indication of
T2D. The potential for an additional hormonal state could incorporate this
phenomenon, as supported by Northrop (2011) in a study in which exogenous
leptin has been used successfully to cause obese mice genetically lacking the ability
to produce leptin to lose weight.

General parameter adjustments for T2D simulation (Figure 3.19) typically
include an increased BW (and most likely non-muscle tissue) as well as decreased
mitochondrial volume and changes to lifestyle habits—higher caloric intake, high GI
food intake, decreased exercise and activity, etc. may be present.

3.5   Model Validation: Exogenous Insulin, Digestive, Muscle Activity

Section 3.5.1 demonstrates comparative validation of the insulin sub-model.
Figure 3.8 shows model capabilities of an exogenous insulin bolus *only* with no
other inputs. A 4 Unit bolus was compared to the normalized plasma insulin effect of
3 separate sets of data, with one being clinically based (red dashed in Figure 3.8
below) with the others being modeling approaches of two validated and
comprehensive studies (Yamamoto, 2014, and Shimoda, 2004). Figure 3.9 shows
BG, insulin, and glucagon replication an *in silico* T1D study by Dalla Man (2007) and
a variety of parameter variants overplotted (Table 3.6). Focus was on response rate
and magnitude. Figure 3.10 demonstrates model capabilities to scale based on the
ratio of remaining insulin production of a T1D and compares non-monomeric vs.
monomeric insulin injection response as in (Cobelli, 2009).

Section 3.5.2 demonstrates model digestive capabilities, particularly in regard to time response and magnitude. Some inputs of other models were not known, or did not exist, as many models do not account for GI or proportion of carbohydrates. However, in this case, an assumption of a mixed meal and moderate GI was used. Figure 3.11 highlights three key digestive studies (Dalla Man, 2007, Yamamoto, 2014, and Kotachev, 2010) and comparison to the Schunk-Winters model.

Section 3.5.3 compares the Schunk-Winters glucagon model to that of Sorenson (1985) and Northrop (2000) in Figure 3.12.

Section 3.6.5 demonstrates mitochondrial state effects in response to exercise input (Figure 15) in Figure 3.13.

3.5.1   Insulin Validation

Figure 3.8 compares Schunk-Winters insulin model to literature and clinical data. Data points were obtained from curves found in literature and overplotted in Matlab. Figure 3.9 demonstrates comparative model validation to Dalla Man (2014) in which certain parameters were varied over the course of 18 simulation runs, according to Table 3.6. Changed parameters (from default) are in bold. Figure 3.10 demonstrates the effect of varying insulin production and exogenous injection of both non-monomeric and monomeric insulin paths as in Cobelli (2007).
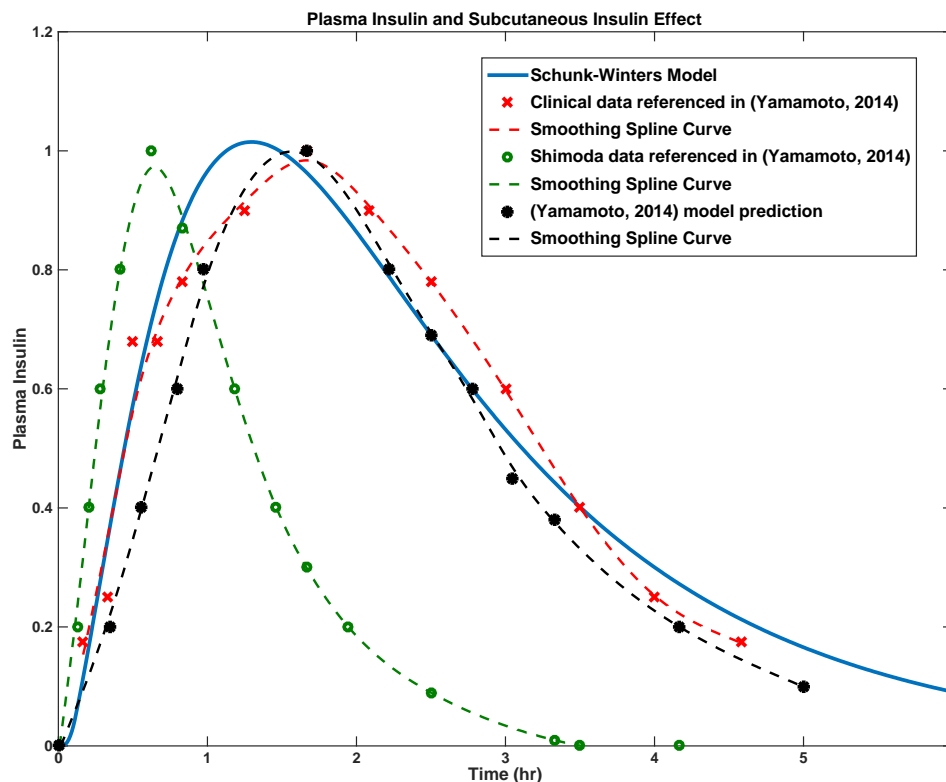
Figure 3.8: Insulin Submodel Validation and Literature Comparison. Comparative insulin validation approach with a constant input amongst all sources of a fast-acting insulin bolus (i.e. Lispro in most studies) at t = 0 (1 time unit in the Schunk-Winters model for a duration of 5 time units, or 3 minutes) of 80 U/hr, or ~4 Units. Yamamoto and Shimoda plot subcutaneous insulin effect (min^{-1}), or normalized so that the maximum peak is '1'. Clinical data is adapted from Swan (2009). All curves are adapted from picked data points of respective sources and fit using a smoothing spline function in Matlab.
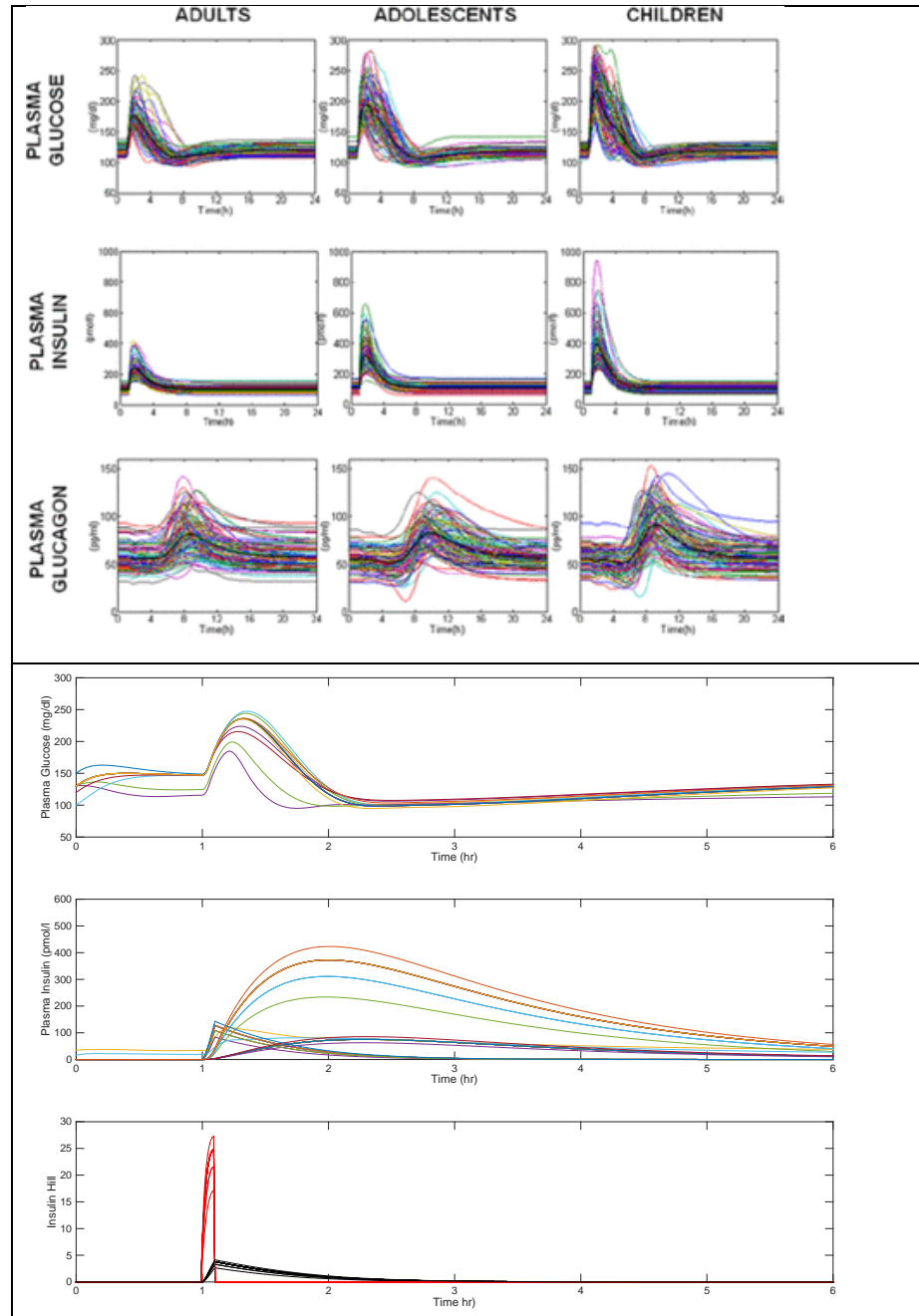
Figure 3.9: Model Validation with Parameter Adjustment to Dalla Man (2014). *Left:* Dalla Man (2014) simulated plasma glucose, insulin, and glucagon in 100 *in silico* T1DM adults, adolescents, and children. *Right:* Replication of Dalla Man (2014) using parameter variations listed in Table 3.6 below. The upper plot shows plasma glucose with the middle demonstrating effective plasma insulin based on exogenous bolus, also separated into monomeric and non-monomeric components (3 states are shown). The lower plot depicts Hill rate and magnitude insulin kinetics. Simulations varied mainly by BW to simulate adults vs. children with the lower plot showing insulin rate and magnitude controllers (Hill functions). The meal input was the same for both Dalla Man and Schunk-Winters, of 50g of carbohydrates at 8:00 AM (t = 1) and an optimal insulin bolus calculated according to patient's own carbohydrate to insulin ratio. Dalla Man focused on varying insulin sensitivity amongst patients, whereas in the *left* replication, variations focused on changing insulin sensitivity (or level of one's own insulin production) and BW parameters as well as muscle and non-muscle tissue mass.

Table 3.6: Parameter Simulation Variants for Dalla Man (2014) Validation (**Figure 3.9**)

BM (kg)	Muscle (kg)	Non-Muscle (kg)	Mitochondria to Muscle Ratio	Type 1 Ratio*	Starting BG (mg/dl)	Insulin Dose (U/hr)	Meal Magnitude (g CHO)
70	30	25	0.1	0	130	20	50
70	**35**	**20**	0.1	0	130	20	50
70	**25**	**30**	0.1	0	130	20	50
50	**21.5**	**18**	0.1	0	130	20	50
90	**38.7**	**32.4**	0.1	0	130	20	50
100	**43**	**36**	0.1	0	130	20	50
40	**21**	**18**	0.1	0	130	20	50
70	30	25	**0.2**	0	130	20	50
70	30	25	**0.05**	0	130	20	50
70	30	25	**0.3**	0	130	20	50
70	30	25	0.1	**0.5**	130	**10**	50
70	30	25	0.1	**0.25**	130	**15**	50
70	30	25	0.1	0	**100**	20	50
70	30	25	0.1	0	**120**	20	50
70	30	25	0.1	0	**150**	20	50
70	30	25	0.1	0	130	**15**	50
70	30	25	0.1	0	130	**25**	50

Note: The changed simulation parameters (from default) are highlighted in each respective column. Values were chosen both above and below the default on the basis of sensitivity.

*Type 1 ratio refers to the amount of insulin the T1D is still able to produce. A value of 0 = no insulin production and a value of 1.0 = non-diabetic production.
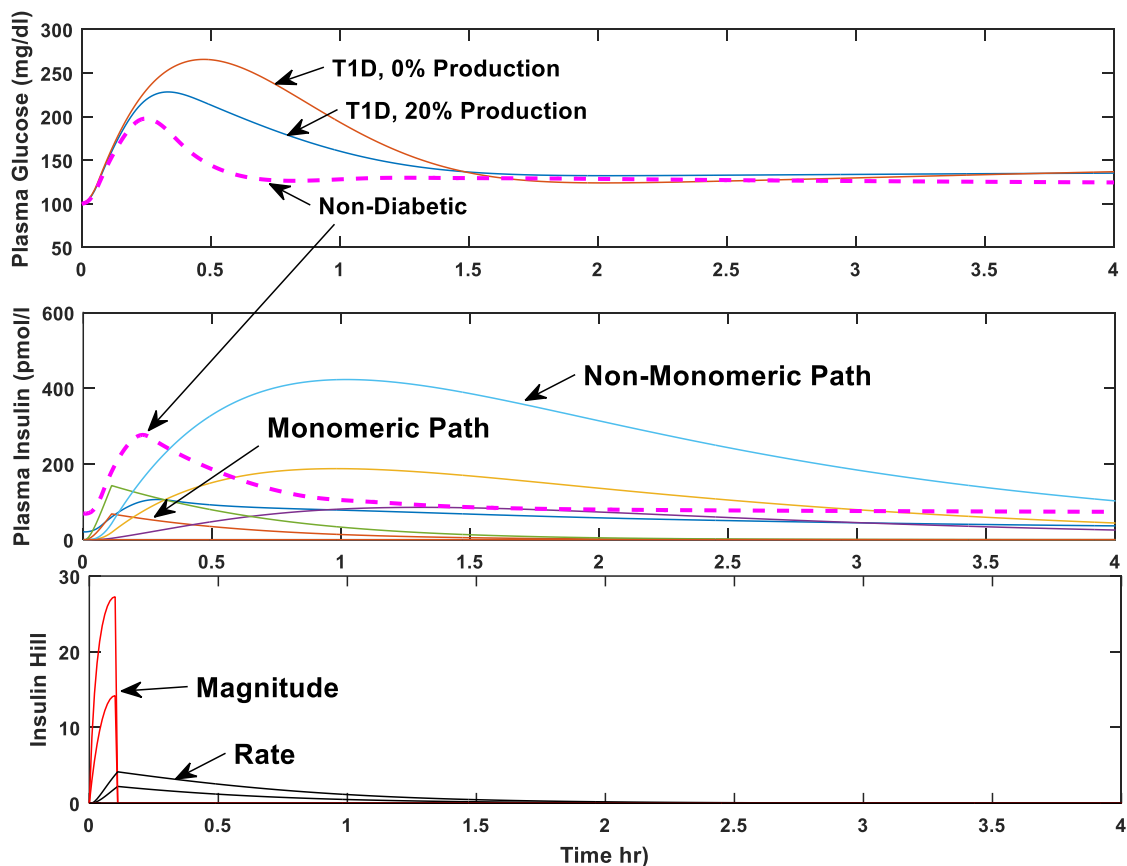
Figure 3.10: T1D Simulations Scaled by Percent Insulin Production. T1D simulations scaled by % remaining insulin production with 50g CHO input and simultaneous injection as in (Cobelli 2007). Insulin absorption controllers for exogenous input are shown.

3.5.2   Digestive Validation

Figure 3.11 demonstrates meal validation and effects of varying glycemic index and carbohydrate ratio as seen throughout literature. Figures in the left column compare overplots of digestive input, BG and insulin. The right column highlights replicated inputs.
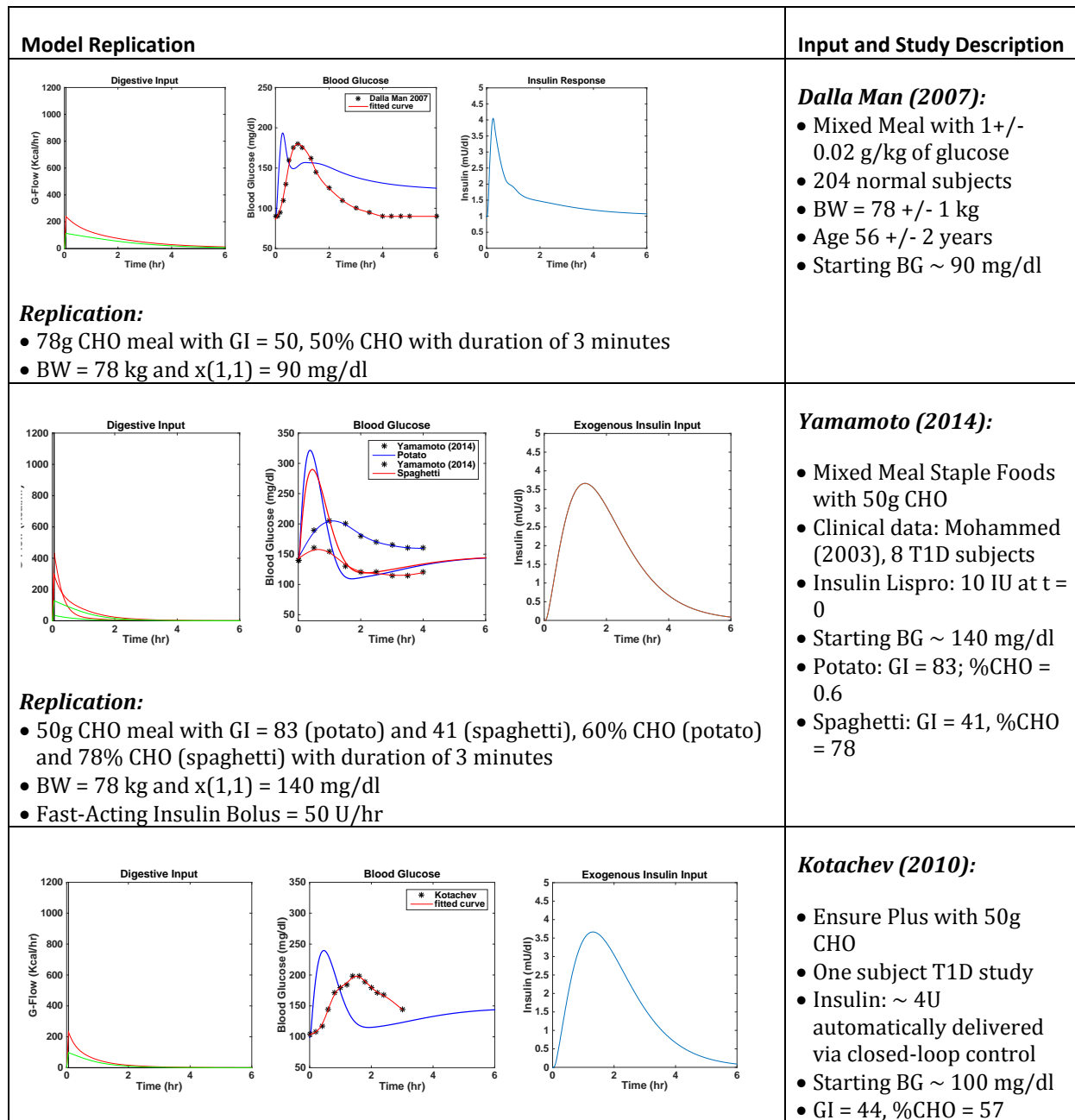
Figure 3.11: Digestive Submodel Validation and Literature Comparison

3.5.3 Glucagon Validation

Figure 3.12 demonstrates glucagon effect curves found in literature vs. blood

glucose concentration. The top two plots are found in literature, with the Schunk-

Winters model simulation on bottom. Note that glucagon is plotted vs. BG on the

right axis.
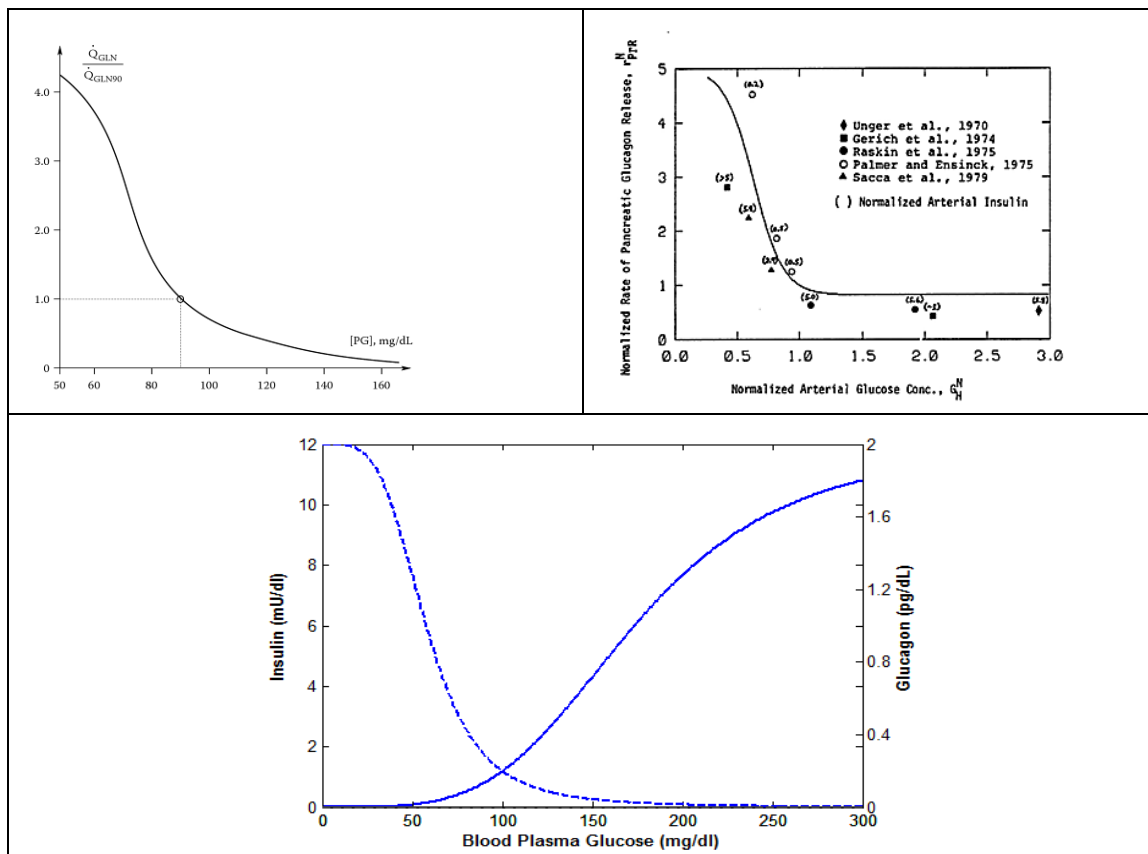
Figure 3.12: Glucagon Submodel Validation and Literature Comparison. Glucagon model comparison with Schunk-Winters model *(bottom)* validated by Northrop (2000) *(top left)* and Sorenson (1985) *(top right)* glucagon vs. blood plasma glucose plots. Note that the Schunk-Winters model plots glucagon (dashed) scaled on the right axis.

3.5.4   Mitochondrial State Validation

In order to see mitochondrial state effect, Figure 3.13 demonstrates a 2-hour

aerobic session with and without X_{mito} present. Exercise input appears to smooth

out, indirectly validating that the addition allows BG to rise due to increased ATP

efficiency, particularly during aerobic exercise. The mitochondrial state will be

further developed in Chapter 4. In Chapter 3, the state is relatively conservative and

sensitivity will be important in regards to athletes (Chapter 4) and increased

mitochondrial volume.
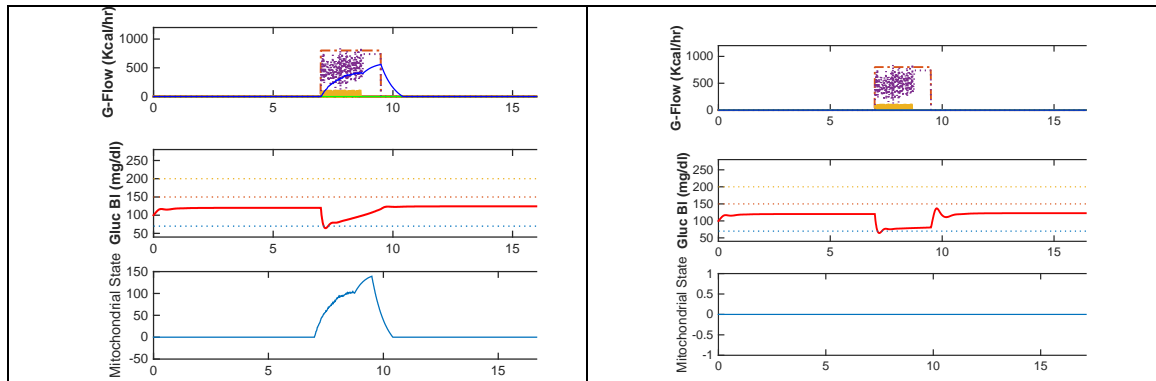
Figure 3.13: Mitochondrial State Validation. Two hour exercise session informed by HR input with (*left*) and without (*right)* mitochondrial state consumption present (lower plot).

3.6   Results: Sensitivity Analysis and Simulation Output

Parameter sensitivity analysis was performed for 23 of the 68 model

parameters, with emphasis on representative parameters for various relations (e.g.,

often 1 of 3 for most Hill functions). These can be separated into control/rate

parameters, threshold values, and scaling and maximum flux rates. Increments of $\pm$

10% were used to scale parameters from the nominal value, with behaviors

extracted from state trajectories that included peaks and magnitudes at strategic

times during strategic tasks, including pre- and post-meal, as well as pre- and post-

exercise. It is recognized that many forms of sensitivity analysis exist; however, this

approach was most applicable in that sensitivity of a given behavior (extracted from

state trajectories) to a particular parameter could be computed. In all cases

sensitivity coefficients were obtained using the following equation, defined by

Lehman et al, 1982:

$$\frac{(B_+ - B_-)/B_o}{(P_+ - P_-)/P_o}.$$ [3.13]

(B+-B_) refers to the change in state behavior of interest (i.e. x_g) and normalized to

make the quantity dimensionless, and *(P+-P_)* refers similarly to the parameter of

interest. Results for the default non-diabetic and Type I diabetic models are

provided in Appendices 7.6.1 and 7.6.2, respectively, for 4 tasks (see also Tables 3.9-

3.13):

- nominal steady-state level (*u1=u2=u3=u4=u5=0*),
- meal (u1 input only for non-diabetic, also u2 for Type 1 diabetic),
- snack (also *u1*, and *u2* for Type 1 diabetic), and
- moderate endurance exercise (*u3* input).

Table 3.7: Sensitivity Analysis Inputs

Meal	**Snack**	**Exercise**
• 700 kcal total • 30 minute duration • 175 g CHO (GI = 50, 50% CHO) • Simulation times: 0.3 hours before, 0.3 hours after ingestion, 1 hour post-meal	• 60 kcal total • 6 minute duration • 15 g CHO (GI = 80, 80% CHO) • Simulation times: 0.3 hours before, 0.3 hours after ingestion, 1 hour post-meal	• 600 kcal/hr for 1 hour • Aerobic Capacity = 1000 • Simulation times: 30 min before, halfway, 18 min after

In general, all states exhibited sensitivity to various parameters, but as might

be expected, it was very task-specific. For instance, there are several unidirectional

pathways: digestive submodel parameters would not be expected to influence the

response to exercise since *u1*=0, and exogenous insulin submodel parameters

would never influence non-diabetic model responses since *u2*=0. As certain state

equations are highly coupled either through compartmental or control modeling (e.g., x_g, x_{nm}, x_m, x_i, x_{gn}), it can be expected that all parameters entering into these relations will exhibit a degree of sensitivity. Some of the key results are highlighted in Tables 3.9-3.13 (parameters those with ***threshold of the value being greater than 0.4*** for a given behavior extracted from a given state trajectory) and Figures 3.14-3.15. Figure 3.16 includes a chart of overall most sensitive parameters for meal and exercise combined.

Insensitive parameters, and therefore reaching constant value in our model, are outlined in Table 3.8. Key values here for snack and meal are mitochondrial associated parameters, as well as k_{s-ds}, the 'half-way' Hill saturation value for the slow digestive pathway. In regards to exercise, constant parameters include those associated with the digestive compartment, as expected, with insulin parameters remaining relatively insensitive (see Table 3.13), as glucagon is the main controller.

Table 3.8: Constant Parameters (Sensitivity Consistently < 0.05)

Meal	Snack	Exercise
K_{a2}*	K_{a2}*	K_{a2}*
K_{a1}*	K_{a1}*	K_{a1}*
K_d*	K_d*	K_d*
K_{m-xex}	K_{m-xex}	K_{ugf}
Rat_ia	K_{se}	K_{se}
Hs_max	K_{sds}	K_{sds}
Hs_rate	Hs_max	Hs_max
Kprop	Hs_rate	Hs_rate
ratmito	Kprop	
	ratmito	

*These parameters are associated with injection and become sensitive when injection is present (i.e. T1D)

It was determined that steady-state levels of certain strategic states such as x_g (BG) are quite sensitive to certain parameters, especially those that directly or

indirectly affect BG, since this is the compartmental conduit through which x_g, x_{nm}, x_m, x_i, and x_{gn} interact. These important sensitivities are provided in Table 3.10 for the T1D model and 3.9 for the non-diabetic model, including both parameters associated with compartmental flow rates and with controller signals.

It was determined that GLUT4 was a main driver along with insulin controllers C_{ia} and C_{ib}. An example of state trajectories with variation in this parameter is provided in Figure 3.14. In another example, during exercise, *Kg2max* was key for stimulating glucagon action, summarized in Tables 3.11-3.13 looking in the X_{gn} column. Other sensitive parameters during exercise include the muscle gradient Hill parameter and reference threshold for muscle, *kmintol*, which also had sensitivity during meal as well. Scaling parameters, such as *wratt*, were also sensitive per their corresponding compartment (i.e. x_{nm}). Insulin elimination rate, K_i, was sensitive for the BG state in both meal and snack simulations, as expected.

Sensitivity analysis was also performed for both T1D simulations (Appendix 7.6.1), with key differences in that T1D show no sensitivity to certain plasma insulin controller parameters but have high sensitivity for most states in regard to injection parameters: k_d (insulin dissociation), k_{a1} (non-monomeric insulin forward rate) and k_{a2} (monomeric insulin forward rate). Additionally, exercise sensitivity behavior for T1D is diminished with *Cga*, *Kgt, ratmito, Kg2Max*, and *Grefg* as the only sensitive parameters. Hence, only non-diabetic sensitivity is shown with all sensitivity behaviors and simulations in Appendix 7.6 and is more inclusive due to a lower threshold (>0.4).

Table 3.9: Steady-State Sensitivity Analysis for Non-Diabetic with Basal Glucose Infusion of 50 kcal/hr

	X_g	X_{nm}	X_m	X_d	X_{ds}	X_i	X_{inj-m}	X_{gn}	X_{inj-nm}	X_{mito}
T = 24 hours	Ki 0.321 **Cga 1.336** **Kgt 1.339** Grefi 0.840 **Grefg 4.653** **Greft 2.726** **Kg2Max -1.144**	Ki -0.795 Cib 0.867 Cga 0.487 Kgt 0.472 **Grefi -2.047** **Grefg 1.632** Greft 0.978 Gbt 0.772 Kg2Max -0.412 Kmxex -0.644 Kse -0.463 KMintol 0.677	**Ki -2.278** **Cib 2.475** **Cga 1.309** **Kgt 1.267** **Grefi -5.857** **Grefg 4.380** **Greft 2.625** **Kg2Max -1.105** **Kmxex -1.837** **Kse -1.321** **KMintol 1.92** **Ratmito 1.648**	—	—	**Ki 1.878** Cga -0.890 Kgt -0.892 **Grefi 4.950** **Grefg -3.091** **Greft -1.816** Kg2Max 0.763	—	Cga -0.946 Kgt -0.948 Grefi -0.595 **Grefg 2.532** **Greft -1.929** Kg2Max 0.806	—	—
Steady-State Values	90 mg/dl	5 g/kg	10 g/kg	0	0	1.0*ratType1i	0	0.45*ratType1g	0	0

Table 3.10: Steady-State Sensitivity Analysis for T1D* with Basal Infusion of 0.75 kcal/hr and Basal Insulin 0.05 U/hr

	X_g	X_{nm}	X_m	X_d	X_{ds}	X_i	X_{inj-m}	X_{gn}	X_{inj-nm}	X_{mito}
T = 24 hours	**Cga 1.194** **Kgt 1.197** **Grefg 4.217** **Greft 2.635** **Kg2Max -1.207**	Gbt 0.819 Kd 0.436	Ki -0.640 Cib 0.642 Kmintol 0.458 **Kd 1.427** **Ratmito 2.038**	—	—	**Ki -1.270** **Ka2 -7.894** Ka1 0.462 **Kd 2.948**	**Ka2 -9.604** Ka1 0.462 **Kd 2.948**	**Cga -1.109** **Kgt -1.112** **Grefg 2.444** **Greft -2.442** **Kg2Max 1.114**	**Ka1 8.843** **Kd 108.100**	—
Steady-State Values	110 mg/dl	5 g/kg	10 g/kg	0	0	1.0*ratType1i	0	0.45*ratType1g	0	0

*Rattype1i = 0

Table 3.11: Non-Diabetic Meal Simulation Sensitivity Analysis

	X_g	X_{nm}	X_m	X_{ds}	X_i	X_{gn}
X_{max}^b	**Ki 1.149** Cia -0.733 Kugs 0.578 Kmintol -0.784	**Wratt 1.068** Kmintol -0.523	Cib 0.589 Kmintol 1.306	Kugs 0.662	Ki -0.796 Grefi 0.612 **Grefg -1.272**	—
X_{BM}^c	**Ki -1.879** **Cia -1.225** **Cib 3.090** **Cga 1.461** **Kgt 1.446** **Grefi -4.317** **Grefg 5.518** **Greft 1.872** Kg2Max -0.751 **Kmxex -1.233** Kse -0.921 **Kmintol -4.281** **Ratmito 1.079**	Ki -0.550 Cib 0.732 **Grefi -1.106** **Grefg 1.267** Gbt 0.504 Wratt 0.496 Kmintol 0.971	Ki -0.973 **Cib 1.296** Cga 0.620 Kgt 0.611 **Grefi -1.952** **Grefg 2.249** Greft 0.605 Kmxex -0.665 Kse -0.500 **Kmintol 1.690** Ratmito 0.645	—	**Ki -3.031** **Cia -1.147** **Cib 3.129** **Cga 1.311** **Kgt 1.296** **Grefi -4.489** **Grefg 4.857** **Greft 1.726** Kg2Max -0.707 **Kmxex -1.252** Kse -0.936 **Kmintol -4.060** **Ratmito 1.083**	**Ki -2.472** Cia -0.857 **Cib 3.297** Cga 0.768 Kgt 0.752 **Grefi -5.576** **Grefg 6.373**
X_{DMR}^d	—	**Ki -1.311** **Gbt 1.486** **Cia -1.131** **Kugf -1.035** **Cib 2.198** Wratt -0.486 Cga 0.796 **Kg2Max -1.315** Kgt 0.780 **Kmxex -1.125** **Grefi -2.666** Kse -0.848 **Grefg 2.966** **Kmintol 2.995** **Greft 0.894**	Ki -0.845 **Cib 1.201** Cga 0.533 Kgt 0.526 **Grefi -1.686** **Grefg 1.939** Greft 0.522 Kmxex -0.544 Kse -0.421 **Kmintol 1.622** Ratmito 0.506	Kugs 0.717	**Kid 0.890**	Ki -0.511 Cga 0.635 Kgt 0.636 **Grefi -1.025** **Grefg 1.301** Greft -0.615
X_{DMF}^e	Ki 0.546 Cia -0.431 Kid -0.402	**Wratt 1.077** Kmintol -0.456	Cib 0.649 **Kmintol 1.137**	K$_{ugs}$ 0.600	**Ki -1.165** Grefi 0.455 Grefg -0.621	Ki -0.451 Cga -0.608 Kgt -0.609 **Grefi -1.002** **Grefg 1.444** Greft -0.582

Table 3.12: Non-Diabetic Snack Simulation Sensitivity Analysis

	X_g	X_{nm}	X_m	X_d	X_{ds}	X_i	X_{gn}
X_{max}[b]	**Ki 1.380** Cia -0.618 **Cga 1.197** **Kgt 1.200** **Grefi 1.424** **Grefg 4.366** Greft 0.991	—	Ki -0.940 **Cib 1.327** Cga 0.633 Kgt 0.625 **Grefi -1.760** **Grefg 2.242** Greft 0.603	Kugf 0.549	**Kugs 0.972**	Ki -6.047 Cia -0.487 **Cga 1.927** **Kgt 1.932** **Grefi -8.041** **Grefg 6.924** Greft 1.307	—
X_{BS}[c]	Ki 0.776 Cia -0.479 Cga 0.920 Kgt 0.922 **Grefi 1.562** **Grefg 3.415** Greft 0.890	Ki -0.534 Cib 0.778 Cga 0.449 Kgt 0.444 **Grefi -1.049** **Greft 1.593** Greft 0.418 Gbt 0.451 Wratt 0.549 Kmintol 0.621	**Ki -1.014** **Cib 1.406** Cga 0.719 Kgt 0.710 **Grefi -1.994** **Grefg 2.534** Greft 0.666 Kmxex -0.684 Kse -0.513 **Kmintol 1.126** Ratmito 0.605	—	—	**Ki 54.629** **Cia 12.176** **Cib 7.400** **Cga -23.404** **Kgt -23.455** **Grefi 109.876** **Grefg -86.464** **Greft -22.650** **Kg2Max 6.985** **Kmxex -3.746** **Kse -2.814** **Kmintol 8.313**	Ki 0.866 Cia -0.531 **Cga 1.026** **Kgt 1.028** **Grefi 1.744** **Grefg -2.752** Greft 0.991
X_{DSR}[d]	Ki 0.774 Cia -0.479 Cga 0.921 Kgt 0.923 **Grefi 1.559** **Grefg 3.416** Greft 0.891	Ki -0.534 Cib 0.778 Cga 0.449 Kgt 0.444 **Grefi -1.049** **Greft 1.593** Greft 0.418 Gbt 0.451 Wratt 0.549 Kmintol 0.621	**Ki -1.014** **Cib 1.406** Cga 0.719 Kgt 0.710 **Grefi -1.994** **Grefg 2.534** Greft 0.666 Kmxex -0.684 Kse -0.513 **Kmintol 1.126** Ratmito 0.605	—	—	**Ki 54.629** **Cia 12.176** **Cib 7.400** **Cga -23.404** **Kgt -23.455** Grefi 109.876 Grefg -86.464 Greft -22.650 Kg2Max 6.985 Kmxex -3.746 **Kse -2.814** **Kmintol 8.313**	Ki 0.866 Cia -0.531 **Cga 1.026** **Kgt 1.028** Grefi 1.744 **Grefg -2.752** Greft 0.991
X_{DSf}[e]	Grefi 0.608 **Grefg 1.054**	Ki -0.547 Cib 0.797 Cga 0.451 Kgt 0.446 **Grefi -1.076** **Grefg 1.604** Wratt 0.535 Kmintol 0.653	**Ki -1.009** **Cib 1.399** Cga 0.711 Kgt 0.702 **Grefi -1.987** **Grefg 2.510** Greft 0.661 Kmxex -0.680 Kse -0.510 **Kmintol 1.152**	—	**Kugs 0.887**	Ki -0.852 Grefi -0.985 Grefg 0.619 Kugf 0.450 Kid 0.836	Grefi 0.510 **Grefg -1.046**

Table 3.13: Non-Diabetic Exercise Simulation Sensitivity Analysis

	X_g	X_{nm}	X_m	X_i	X_{gn}	X_{mito}
$X_{max}{}^b$	**Ki 1.819** **Grefg 4.594** **Cia -2.214** **Greft 1.611** **Cib -1.456** Kg2Max -0.522 **Cga 1.168** **Kmintol -1.315** **Kgt 1.170** **Kid -2.706** **Grefi 2.091**	—	Ki -0.550 Greft 0.675 Cib 0.994 Kmxex 0.591 **Cga 1.449** Kse -0.557 **Kgt 1.440** Kmintol 0.692 Grefi -0.993 **Ratmito -1.166** **Grefg 4.197**	**Ki -2.196** Cia -0.418 Cga 0.836 Kgt 0.839 **Grefi -2.160** **Grefg 2.902** Greft 0.541 Kmxex 0.915 Kid 0.745	**Ki 1.043** **Grefg -4.218** **Cia -1.337** **Greft 1.160** Cib -0.901 Kg2Max -0.458 **Cga 1.429** Kmintol -0.789 **Kgt 1.432** **Kid -1.682** **Grefi 1.412**	Grefg -0.201
$X_{BE}{}^f$	Ki 0.810 Cia -0.469 Cga 0.913 Kgt 0.915 **Grefi 1.629** **Grefg 3.388** Greft 0.877	Ki -0.403 Cib 0.708 Cga 0.525 Kgt 0.520 Grefi -0.738 **Grefg 1.797** Greft 0.464 Wratt 0.602	Ki -0.941 **Grefg 2.582** **Cib 1.404** Greft 0.666 **Cga 0.772** Kmxex -0.654 Kgt 0.763 Kse -0.489 **Grefi -1.756** Kmintol 0.903	—	Ki 0.916 Cia -0.527 **Cga 1.030** **Kgt 1.032** **Grefi 1.839** **Grefg -2.889** Greft 0.987	—
$X_{DE}{}^g$	Cga -0.951 Kgt -0.953 **Grefg -2.478** Kmxex 0.838	Cib 0.421 Cga 0.538 Kgt 0.535 Grefi -0.460 **Grefg 1.570** Wratt 0.743	Ki -0.533 **Grefg 2.902** Cib 0.893 Greft 0.572 Cga 0.976 Kse -0.432 Kgt 0.969 Kmintol 0.585 Grefi -0.996	**Ki 2.378** **Cga -1.293** **Kgt -1.297** **Grefi 3.298** **Grefg -3.808** Greft -0.541 Kmxex 0.475 Kid -0.911	**Kgt -1.197** **Kgt -1.199** **Grefg 1.085** Kmxex 0.874	Grefg -0.135
$X_R{}^h$	Cga 0.838 Kgt 0.840 Grefi 0.539 **Grefg 2.788** Greft 0.470 Kmxex 0.548 Kid -0.442	Cga 0.464 Kgt 0.461 **Grefg 1.355** Wratt 0.825	Ki -0.567 Greft 0.711 Cib 0.996 Kmxex 0.619 **Cga 1.539** Kse -0.589 **Kgt 1.529** Kmintol 0.673 **Grefi -1.059** **Ratmito -1.310** **Grefg 4.433**	Ki -0.958 Cga 0.614 Kgt 0.616 Grefi -0.910 **Grefg 2.101** Kmxex 0.827 **Kid 1.033**	Ki 0.509 **Cga 3.173** **Kgt 3.181** Grefi 0.890 **Grefg -2.388** Greft 0.983	Grefg 0.272
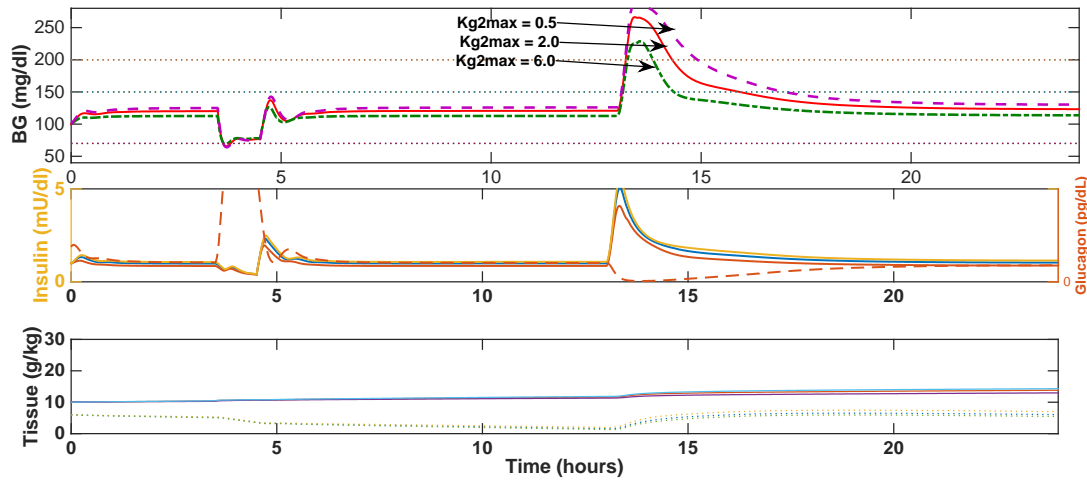
Figure 3.14: Non-Muscle Gradient Sensitivity Effect. Sensitivity effect of varying the GLUT2 non-muscle gradient parameter for a non-diabetic, Kg2Max, with an input of 600 kcal/hr exercise at t = 3.5 hours and a 700 kcal meal of duration 30 minutes (GI = 50, %CHO = 50) at t = 13 hours.
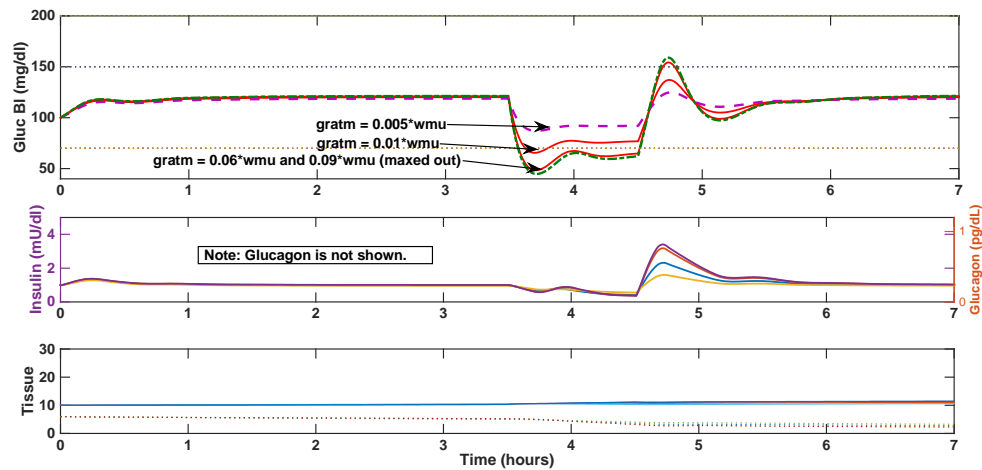
Figure 3.15: Muscle Gradient Sensitivity Effect. Sensitivity effect of varying the gratm muscle-blood glucose demand gradient parameter for a non-diabetic, with an input of 600 kcal/hr exercise at t = 3.5 hours.
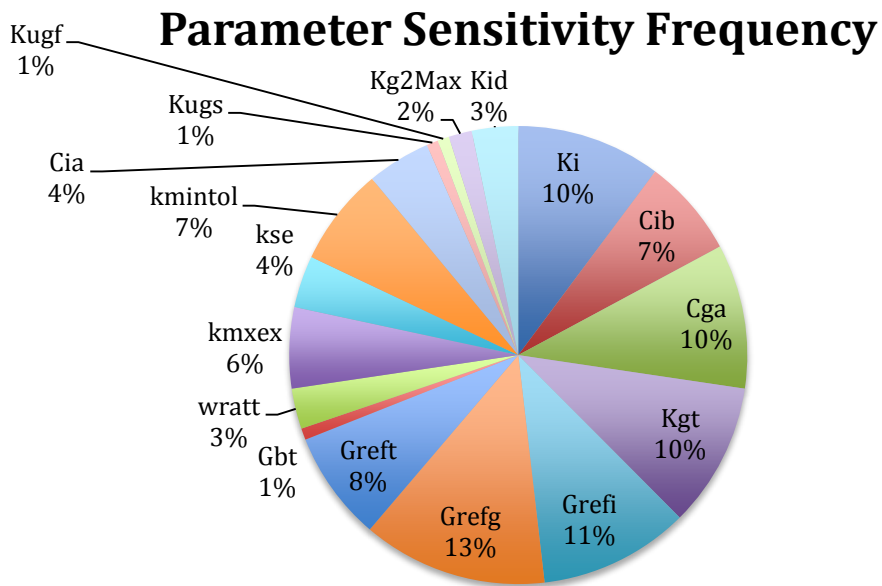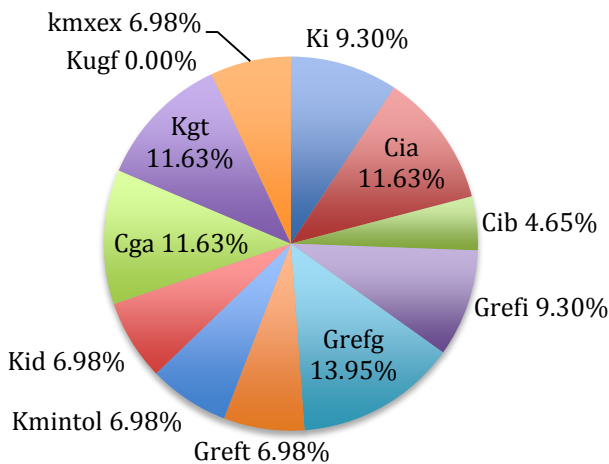
Figure 3.16: **Frequency of Most Sensitive Parameters.** Frequency of most sensitive parameters using total appearances over all sensitivity trials. The most sensitive in regard to x_g (G_{refg}, G_{reft}, K_{g2max}, and K_{g4max}) are also shown as a frequency plot. Bias is eliminated toward foodstuff but only including meal and exercise simulations (snack is ignored). ***Top:*** Meal and exercise simulations combined (overall sensitivity without bias toward meals and/or exercise). ***Bottom:*** X_g state sensitivity for both meal and exercise combined.

3.7 Model Predictions for 24-Hour Lifestyle Simulations

Section 3.7.1 demonstrates model digestive capabilities of varying GI vs. the proportion of carbohydrates in a mixed meal in Figure 3.17.

Section 3.7.2 demonstrates 24-hour simulation runs and overall model capabilities of a non-diabetic to that of a T1D (Figure 3.18) and results of a poor lifestyle and reaching T2D implications (Figure 3.19).

3.7.1 Low vs. High GI and Proportion of Carbohydrate Variation
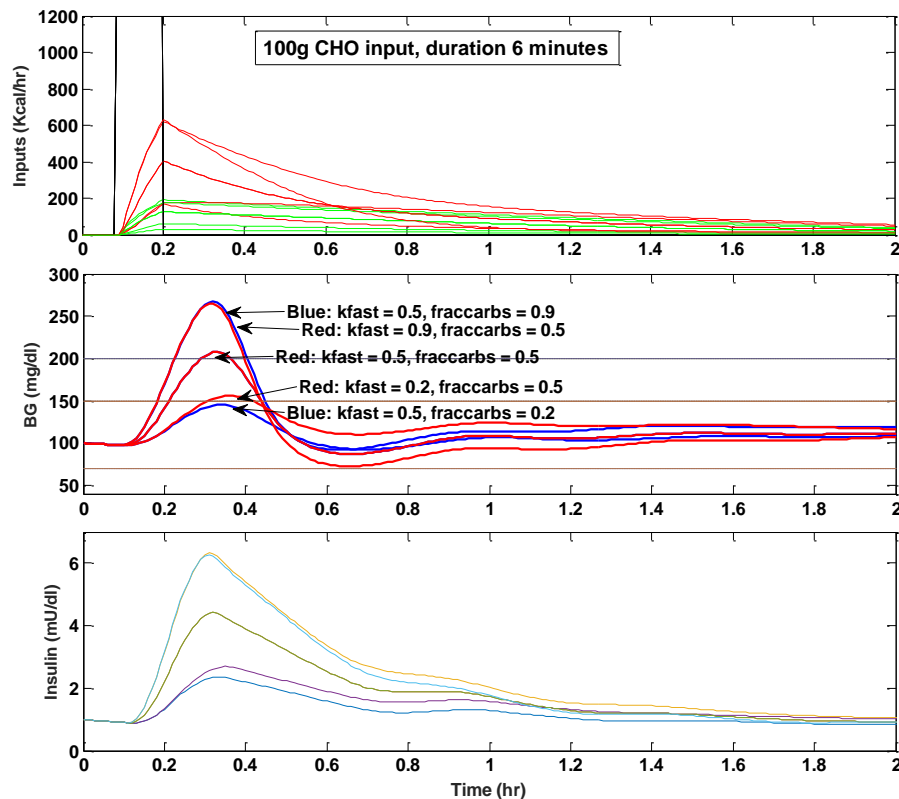
Figure 3.17: Low vs. High GI Foodstuff Comparison. Low vs. High GI foodstuff comparisons with *a)* kfast = 0.5 and 90% CHO vs. *b)* kfast = 0.5 and 20% CHO (blue BG curves) and varying GI with *c)* kfast = 0.9 and 50% CHO vs. *d)* kfast = 0.5 and 50% CHO vs. *e)* kfast = 0.2 and 50% CHO. Meal constants are for a non-diabetic subject all with 100g CHO input and a duration of 6 minutes. Note the black solid lines of the input plot is 'cut-off'' due to n input of 4000 kcal/hr for 6 minutes (i.e. 400 kcal or 100g of CHO).

3.7.2   24-Hour Simulation
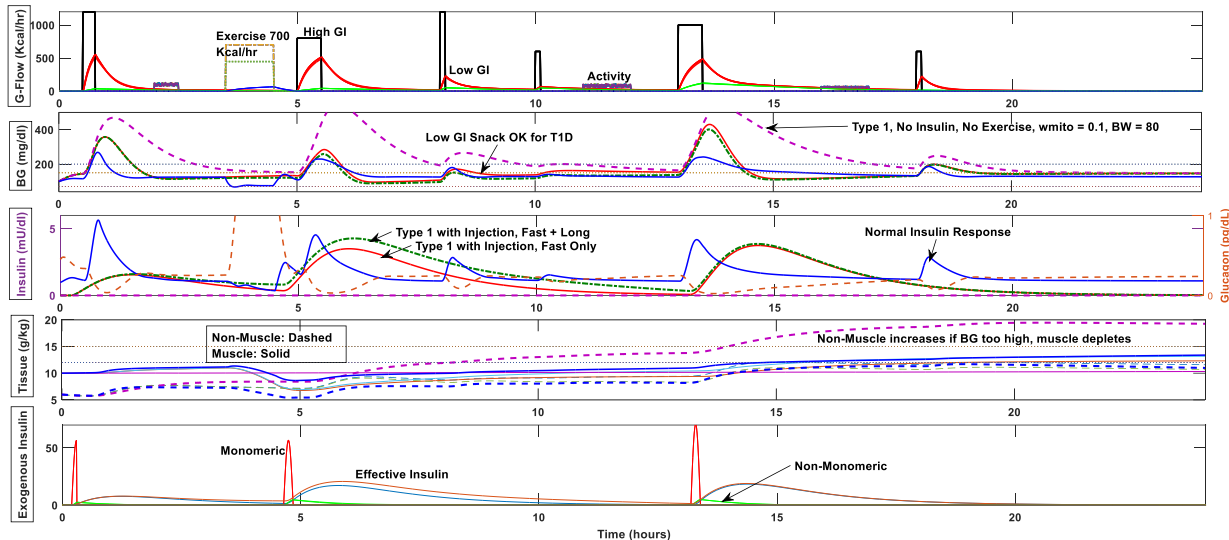
Figure 3.18: Non-Diabetic and T1D 24-Hour Simulations. Four 24-hour simulations: **1)** atypical T1D with no insulin injection or exercise (BW = 80kg, wmito = 0.1), **2)** Healthy T1D with meal rapid-acting injections and long-acting basal injection (*BW = 70, wmito =0.3*), **3)** same healthy T1D with no long-acting insulin, and **4)** non-diabetic with similar inputs as (2). Inputs (top plot) include 3 meals/3 snacks (black solid, red digestive state), 700 kcal/hr exercise. Muscle and non-muscle mass is kept consistent. A ***Healthy*** (large exercise, ~2000 kcal/day and mainly low GI meals) T1D shows natural regulation (good steady-state BG range) and can get 'better' than a non-diabetic with proper injection and timing (see second vs. third meal) and basal insulin. With lack of exercise and T1D glucose management, there is glycogen accumulation predicted, especially in non-muscle compartment.
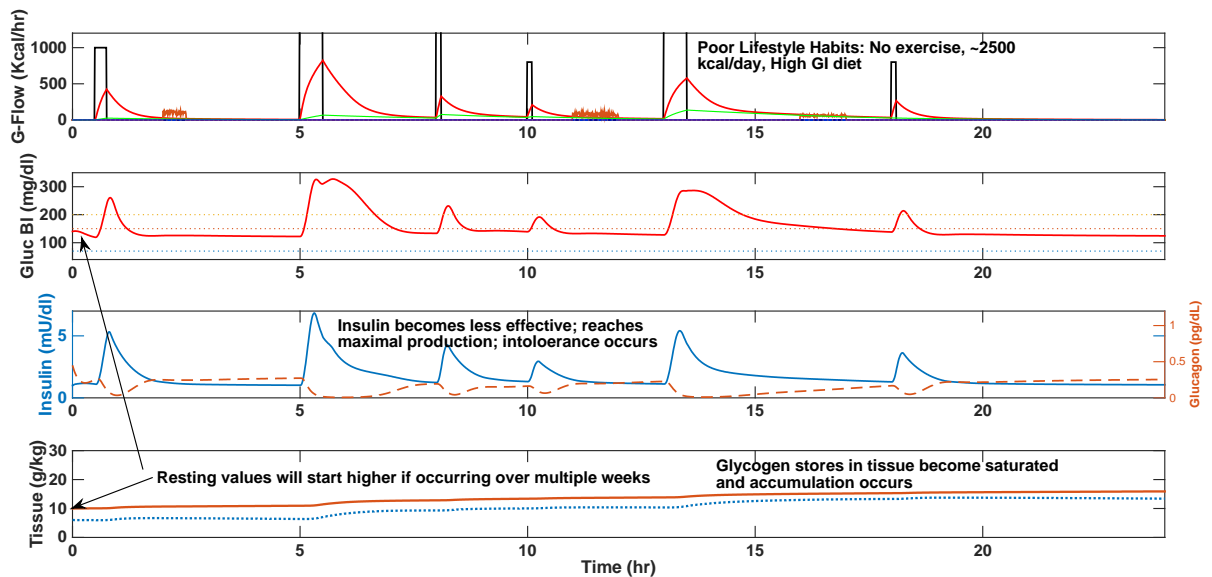
Figure 3.19: T2D Precursor 24-Hour Simulation. Effects of poor lifestyle habits and how, if continued over an extended period of time (>3 weeks), body *remodeling* could occur and be a T2D precursor model.

3.8   Discussion

The model aims to predict BG regulation based on various lifestyle choices and diabetes, while using the lowest possible number of states that can provide robust and personalized conditions and predictions.   Through its distinct framework, new perspectives are possible.

GI, often promoted as an influential factor in people with diabetes, is predicted to have a strong dynamic effect: a low glycemic diet (Figure 3.17) decreases glucose spikes while also predicting reasonable insulin control action and storage in muscle and non-muscle tissues. Low GI meal content tends to absorb slower, coinciding with the idea that whole grains, higher fiber, and unprocessed glucose will keep an individual feeling 'full' for longer. In the digestive validation section (Section 3.5.2) it is demonstrated particularly in the non-diabetic simulation, that there are two

peaks due to a separation of fast vs. slow carbohydrate absorption and hence rate of appearance into the blood stream (x_g)—this is common for mixed meals (i.e. *fraccarbs* <1.0). It is recognized that our model has faster insulin and meal transient dynamics than Dalla Man (2007) and Yamamoto (2014) in response to high-GI meals; however, on the basis of collected data (Chapter 4) and a variety of references supporting both cases (i.e. Dalla Man, 2007, vs. Shimoda, 2000) this is not recognized as a limitation.

Further, direct validation comparisons were limited in that our digestive submodel is more complex than most, with separation of absorption dynamics into two states, as well as influences of body composition. This made it difficult for direct comparison to Dalla Man (2007), as their 'mixed meal' could not be precisely replicated in our model without knowledge of glycemic index and fraction of carbs (50% was assumed for modeling purposes). The Dalla Man model and parameters are used by many others, and resulted in an FDA approved model—particularly for insulin, which validates our model in terms of magnitude and rate of increase for insulin response (Section 3.6.1). Our model is highly valid for mixed meals known in literature, with a slightly faster response to high-GI foodstuff than most, yet most models do not have capability of differentiating high-GI.

A key insight from model validation is that daily activity, exercise, dietary choices (GI) and body composition (including mitochondrial volume) are seen to be important for BG management. Further, in 24-hour simulations, there were frequently upward and downward drifts of glucose (mostly as glycogen)

concentration in the tissues which could be associated with lifestyle choices and, for people with diabetes, insulin management.

Steady-state sensitivity analysis (Tables 3.9 and 3.10) shows some high-sensitivity parameters when inputs (all u) are set to zero, explaining some steady-state adjustments that needed to be addressed. For example, it was found that due to an elevated starting value, glucagon was causing a drifting of BG upwards when t<1hr, hence the model was adjusted adding this baseline sensitivity. Insulin and glucagon controllers, along with GLUT2 and GLUT4 gradients, were consistently the most sensitive parameters at steady-state for a non-diabetic (states x_g, x_{nm}, and x_m). G_{ref} parameters were also sensitive, as expected (x_i and x_{gn}), for T1D as well. T1D steady-state sensitivity was focused on glucagon controllers (x_g, and x_{nm}), as well as GLUT2 gradient and basal tissue metabolism. Starting blood glucose value was set higher for a T1D at 137 mg/dl vs. 100 mg/dl for non-diabetic.

Sensitivity analysis (Tables 3.9-3.13) highlights some key aspects of the model: high sensitivity to adjustments of reference values for BG-tissue flux pathways (G_{ref}'s), especially to hormonal control action (as expected). This is true for BG and, importantly, more so for both tissue compartments. Other key sensitivity data relates to mitochondrial volume proportion in regards to exercise, and sensitivity to basal elimination rates particularly for non-muscle and in regard to insulin (Table 3.12 and 3.13). Meal and snack sensitivities (expressed mainly through the x_g, x_{nm}, x_m, x_{ds}, x_d, and x_i states) include mainly insulin control and non-muscle tissue scaling in addition to digestive forward rate controllers. Additionally, it is important to recognize that non-diabetics can still have a BG spike at the onset of a meal due to

this control (which is contradictory to what one believes) since with endogenous

insulin production there is no anticipatory effect (Figure 3.18).

Meal onset and insulin timing has relevance to T1D insulin sensitivity,

especially with timing: taking rapid-acting insulin 15 minutes prior to a meal (as

typically suggested clinically) was beneficial. However, the model predicts that a

T1D who does not take any insulin is able to slowly "regulate" BG, perhaps more

effectively than the experience of many T1D's; this is a byproduct of our

implementation of the GLUT2 pathway (and some residual production), which was

hard to fine-tune because of a lack of experimental data. T1D can take their insulin

as early as necessary, and theoretically could have better control than a non-

diabetic. However, that being said, spikes in non-diabetics tend to be brief, as

endogenous insulin acts much more rapidly than exogenous. T1D sensitivity

analysis additionally demonstrates exogenous insulin rate effects, particularly with

$k_{a1}, k_{a2},$ and k_d, the nonlinear fast and slow insulin and dissociation parameters,

respectively.

Perhaps the most novel insight from the model is the sensitivity of model

behavior to parameters associated with the GLUT2 and GLUT4 pathways, denoted

from Figure 3.14 and 3.15, both of which are known to be influenced by factors

other than hormonal control, including physical laws (e.g., the blood-tissue glucose

concentration gradient), and are predicted to influence relative balance between BG

states and tissue. This is further exemplified by increased sensitivity to *Kg2Max*

(Table 3.11) and muscle gradient parameters (i.e*. kse*). These insights, along with

manifold predictions of high tissue concentrations with certain lifestyle protocols

(including simulations not presented here), suggest new research directions for helping understand the complex phenomena called insulin intolerance, and by inference, the longer-term etiology of T2D as a function of lifestyle choices. With possible additions of a hormonal state, leptin would help shape glucose mass conservation via activation of conversion to fat (if in excess) and further more possibilities for personalized lifestyle implications and T2D.

In regard to model output limitations, because insulin, glucagon and corresponding glucose effect have a high model sensitivity in regard to control parameters (i.e. steady-state sensitivity coefficient for C_{ga} is ~1.8 and C_{ia} is ~0.3)—a slight input error would have a large effect on BG, decreasing accuracy.

Exercise also has a drastic effect and aids in BG control as seen in the 24-hour simulations. There is an influx from BG (which decreases) as muscle glycogen gradually becomes depleted (Figure 3.18) which in turn activates glucagon control (x_{gn}) in order for non-muscle glucose storage (mostly hepatic) to restore BG levels via glycogenolysis. Consequently, non-muscle tissue glucose (x_{nm}) decreases. Daily activity effects are less drastic as expected, but clearly influence glucose tissue stores, especially x_m, helping prevent meal-related buildup (Figures 3.18 and 3.19) and thus providing a natural form of advantageous glucose management.

The addition of a mitochondrial state allows for a smoother dynamic response and glucose transfer, particularly during aerobic exercise (Section 3.5.4, Figure 3.13), as seen with the ability for BG to rise during long duration exercise (i.e. more efficient glycolysis and ATP utilization at moderate intensities) when mitochondrial state is present (*left* of Figure 3.13) vs. when x_{mito} is set to 0 (*right).*

The antagonistic effects of insulin and glucagon control action are documented, important for both transient and steady state behavior. Exogenous insulin is affected by flow, body mass, and dose size, as higher saturation tends to occur with increased tissue mass and dose (Figure 3.6 from Section 3.4.1).

T1D simulations (Figure 3.18) depict the differing effects of long-acting, rapid-acting, and regular delivery, including timing. T2D is only indirectly modeled, through an "intolerance" effect based on excessive (saturating) glycogen storage in tissues and indirectly through assumptions of body composition. However, it illustrates how "poor" lifestyle habits can cause gradual glucose accumulation in tissue compartments (Figure 3.19). Future directions for simulations could study longer time periods (e.g., weeks).

With regards to model capabilities and limitations, our model accurately depicts the reactive effects of exercise, i.e., those related to utilization of glucose for energy with HR as a separate, external input for tuning and validating predicted exertion if accessible (Chapter 4 and Figure 3.13, as a part of mitochondrial state validation). Anaerobic exercise elicits spikes via immediate glucose demand and hormonal action with higher glucose utilization as intensity increases, while aerobic efforts tend to utilize the mitochondrial state and glycolysis efficiency, often relying more so on a fuel mix (i.e. fat). Short periods of hyperglycemia may be evident due to release in stress hormones before or at the onset of exercise. The latter is suggested by case study data during anaerobic exercise in Chapter 4. Along with all other models, our model cannot yet predict the "anticipatory" adrenaline effect of a

short rise in BG, although with the addition of HR and a hormonal state this is possible.

4. PERSONALIZED ADAPTED MODEL FOR DIABETIC ATHLETES: IMPLEMENTATION OF A FEMALE TYPE 1 CASE STUDY

4.1   Introduction

A novel nonlinear 10-state lumped compartmental model was presented in Chapter 3 and aimed to provide a robust model with default parameters. Furthermore, it was designed to provide flexibility for variable body mass, muscle to non-muscle ratio, and Type 1 and Type 2 diabetes. The model is intended for both research and clinical use, particularly diabetes educators, to quantify BG effects of these lifestyle factors. The model could help inform delivery design of current artificial pancreas mechanism with a dual-hormone delivery, as well as develop continuous glucose monitor (CGM) feedback and prediction based on current activity and/or diet.

This chapter is motivated by the concept that a diabetic should be able to manage BG with exercise, diet, and for dual-hormonal control based on algorithm feedback of a personalized model, similar to that of machine learning mechanisms. It takes an important step towards refining the general BG regulation model of Chapter 3 to a new personalized version, particularly for trained athletes with Type 1 diabetes.

Oftentimes, from personal and peer anecdotal evidence, a highly-motivated diabetic keen on health-mindedness or athletic performance will know more about their personal adaptation mechanisms than their endocrinologist. This is something

that needs to change, if possible, so that diabetes educators and endocrinologists can provide quantified feedback to diversified patients.

   Current diabetes technology devices predict daily choices by varying inputs day-by-day. When daily choices become habitual a lifestyle body *type* becomes present—for example, one could be athletic, lean, overweight (indicator of Type 2 diabetes), inactive, or active.

   Exercise physiologists are able to quantify metabolic changes on the basis of body composition (i.e. increased muscle mass and/or basal metabolism) for various body types, which could inform a personalized model. Chapter 4 uses an athletic Type 1 female as an example for future adaptive modeling and device learning mechanisms.

   One key goal is to better inform clinicians to educate people with diabetes appropriately in regard to glucose regulation on the basis of lifestyle choices that may become habitual. This is possible with better understanding of lifestyle types in hope that a library of personalized adaptive models can be created. It is intended that current device technologies will become robust in that each can 'learn' its user to eliminate guesswork of bolus corrections, often used for appearance of hypo- and hyperglycemia. Additionally, such models can inform CGM 'trends.' Thus a second, longer-term goal is to provide the foundation for an "intelligent system" model framework that could directly inform a patient where their BG is headed, based on causation effects of lifestyle inputs. A particular user profile, if robust, could drive overall trends and baselines with instantaneous inputs (i.e. meal GI, stress, and/or exercise) affecting immediate BG.

4.2   Background and Motivation

It is well accepted that exercise directly influences BG concentration, in response to increases in muscle tissue demands for energy (in form of ATP) that result in consumption of glucose as a source of fuel. What needs characterization and modeling is the effect of exercise *type* as combined with an individual's personal metabolic and body composition parameters and current fed or fasting state. Many groups characterize exercise on the basis of VO2max and gauge substrate utilization (CHO vs. Fat) on the basis of RER and known % of total aerobic capacity. However, this is typically only consistent with aerobic exercise performed under conditions without other types of stressors (e.g., stress of competition).

An extensive study by Yardley (2012) that focused on exercise in TID attempted to demonstrate the effects of resistance vs. aerobic exercise and the timing of each. As seen in Figure 4.1 below, BG is utilized in general at a much faster initial rate during aerobic than resistance exercise (although ultimately about the same response is elicited). This is cause for investigation and seen in other sources. Resistance exercise incorporates other stress mechanisms beyond those associated with aerobic exercise (also dependent on the individual's lifestyle), oftentimes resulting in a slight 'spike' in BG at the onset or prior to a hard exercise training (often anaerobic) session. This phenomena has been seen throughout many studies (Yavari, 2012, and Harmer, 2008 and 2013) and is what clinicians warn against as a 'false' high due to catecholamine action and glycogen breakdown with adrenaline,

hormones, etc. when the 'flight or fight' mechanism normally associated with the sympathetic nervous system (SNS) occurs.

Heart rate is another means of characterization, and has been used to characterize exercise intensity and duration in a basic exercise model for glucose utilization, although a lack of research was recognized (Dalla Man, 2007). Most conclude that there is heightened insulin sensitivity and increased CHO oxidation, glycogen depletion, and hepatic production as exercise intensity increases.
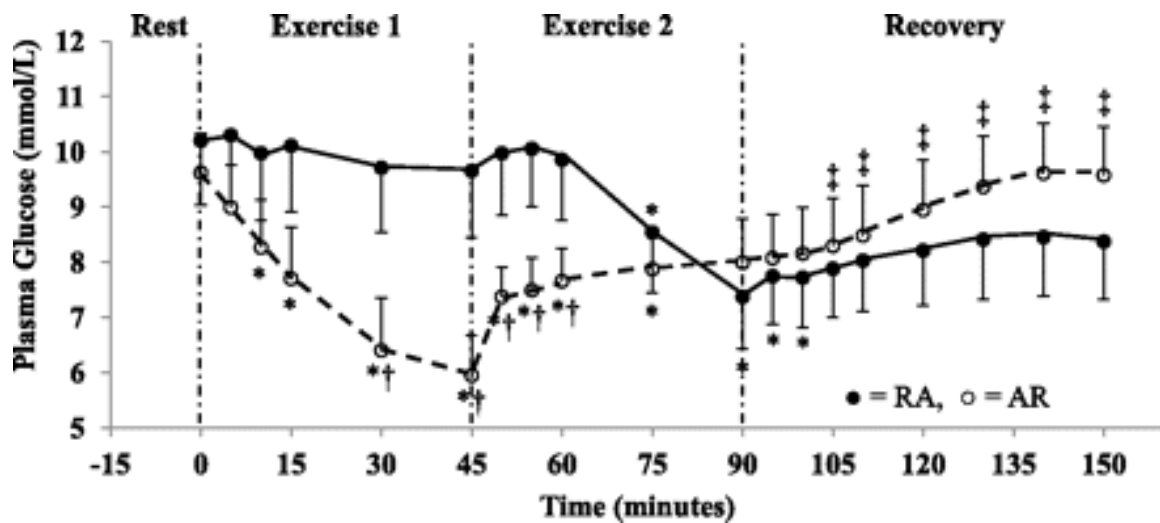
Figure 4.1: Yardley (2012) Resistance vs. Aerobic Exercise Training. From Yardley (2012) demonstrating the effects of performing resistance exercise before aerobic exercise (dark filled circle, RA) or resistance exercise after aerobic exercise (open circle, AR) in people with Type 1 diabetes.

Another source of glucose during exercise, perhaps more importantly, is skeletal muscle glycogen. It has been found that depleted glycogen levels results in the inability to sustain prolonged high-intensity exercise and that depletion of glycogen stores is dependent on its localization within the muscle cells (Nielsen, 2011).

As shown in Figure 4.2, other proposed contributions to a decrease in blood glucose levels (G in Figure 4.2) with prolonged exercise include a decrease in glycogenolysis (G_{gly}), which has been modeled using an equation dependent on exercise intensity and duration (Roy, 2007).

$$\frac{dG}{dt} = -p_1[G(t) - G_b] - X(t)G(t) + \frac{W}{Vol_G}[G_{prod}(t) - G_{gly}(t)] \quad (7)$$

$$- \frac{W}{Vol_G}G_{up}(t) + \frac{u_2(t)}{Vol_G}; \quad G(0) = G_b$$

$$\frac{dG_{gly}}{dt} = \begin{cases} 0 & A(t) < A_{TH} \\ k & A(t) \geq A_{TH} \\ -\frac{G_{gly}(t)}{T_1} & u_3(t) = 0 \end{cases}, \qquad \frac{dA}{dt} = \begin{cases} u_3(t) & u_3(t) > 0 \\ -\frac{A(t)}{0.001} & u_3(t) = 0 \end{cases}.$$

Figure 4.2: Roy (2007) Exercise Modeling. *From Roy, 2007:* Exercise modeling of BG taking into account exercise intensity and duration and effect on hepatic glucose production. Volume of non-muscle, muscle, and mitochondrial compartments is also accounted for as in the Schunk-Winters model. Parameters are defined as: p_1, rate at which glucose is removed independent of insulin, G_{prod}, hepatic glucose production induced by exercise, G_b, glucose concentration, G_{up}, glucose uptake, Vol_G, glucose distribution space, and A(t), the integrated exercise intensity (with critical threshold A_{th}).

Additionally, the dependence of glycogen depletion commencement time (t_{gly}) on exercise intensity (u_3 in Figure 4.2) is shown in Figure 4.3. Roy, 2007, uses an approach correlating glucose utilization with intensity, similar to what our model does with VO2max. This is a more robust and accurate approach than relying strictly on HR measures, as in Cobelli, 2009. However, HR has informational value, and is used to tune the *u3* input of our model, comparing to perceived intensity, which will be investigated below.
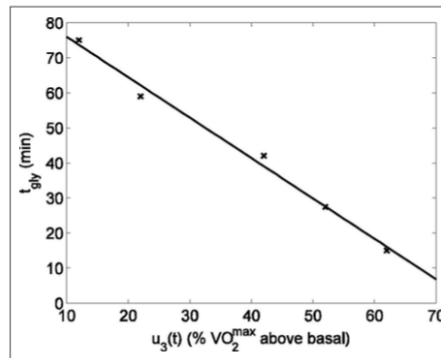
Figure 4.3: Roy (2007) Glycogen Depletion vs. Exercise Intensity. From Roy, 2007 plotting the muscle glycogen depletion commencement time vs. exercise intensity.

Post exercise late-onset hypoglycemia has also been widely documented in T1D and interestingly no link was found between those in good or excellent metabolic control, or those making the transition from an untrained to trained state (MacDonald, 1987); energy is a conservative quantity with consumption that can be predicted through tissue compartments, as in Chapter 3.

A recent review of exercise models describes principal energy substrates as muscular glycogen, plasma glucose (including liver production), plasma free fatty acids and intramuscular triglycerides with the CHO reserves (1200-2400 kcal) localized in the muscle (79%), liver (14%) in glycogen form and in blood (7%) as glucose (Derouich, 2002). This model incorporates early models which recognized increased insulin sensitivity with exercise simply by incorporating the lowering of glucose concentration during and after exercise and increasing the insulin use by cells (Bergman, 1981). In addition to simplified early models, the disappearance of glucose from blood to working tissue is dependent on the ability of the exercise to accelerate the flow of glucose via a factor that is independent of the increase of insulin, and a second factor (insulin sensitivity), which is a function of the increase

in insulin (Derouich, 2002). Energy remains conserved, and a variety of factors that will be discussed relate to the source of energy and its management.

In modeling T2D and the effect of exercise type, trends follow a similar pattern despite overall VO2max being lower on average. Therefore, the point at which threshold is reached and overall emphasis on CHO oxidation efficiency is lower. With less mitochondria and fewer capillaries, an unfit individual may burn more energy based on a lower oxidative capacity. A combination of both aerobic and resistance training led to an improvement in HbA1c and triglyceride content as opposed to aerobic or resistance training alone (Yavari, 2012). Hemoglobin A1C (HbA1C), related to oxygen transport capacity, is a common measure for how well-controlled an individual's BG has been for the previous 2-3 months, as it reflects average levels and whether or not red blood cells have become "glycated." Another recent hypothesis attributes insulin resistance in T2D and obese individuals by a deficiency and/or dysfunction of skeletal muscle mitochondria as a result of a decreased ability to oxidize fat (Kim, 2008). Exercise training results in improvement in insulin action and mitochondrial volume/function and hence is important for all people with diabetes, particularly those with T2D (Holloszy, 2011).

Exercise appears in later iterations of the Dalla Man (2007) and Cobelli (2009) model, and was kept as a simple and single input in the 12-13 state model as emphasis was placed on compartmental insulin kinetics. In fact, 3 different exercise models were proposed and implemented *in silico.* The 2009 version by the *Cobelli* group implemented three additional 'test' inputs for exercise. Model A assumes that exercise causes a rapid on-and-off increase in insulin-independent glucose clearance

and a rapid-on/slow-off effect on insulin sensitivity. Note that without separate muscle and non-muscle compartments, a possible source for this effect (e.g., flux between BG and muscle compartments based on demand-based GLUT4 transporter signaling as developed in Chapter 3 and discussed further in Section 4.2.1) could not be addressed. Model B relaxes the assumption that exercise causes a rapid on-and-off increase in insulin-independent glucose clearance. Model C is similar to model A, but also assumes that insulin action is increased in proportion to the duration and intensity of exercise. It was determined, that Models A and B predict different levels of exercise (based on heart rate) have the same effect on glucose utilization and Model C predicts a reasonable glucose infusion rate during euglycemic-hyperinsulinemic clamp simulations for both mild and moderate exercise. However, other literature suggests that exercise intensity, or different levels of exercise, does in fact have implications on glucose utilization (i.e., Brooks, 1994) and therefore Models A and B were recognized as limiting, and motivated the development of the Schunk-Winters exercise model (see Chapter 3). Heart rate (HR) is also debatable as an accurate measure of exercise level, as HR tends to fluctuate with other factors and is intrinsic to an individual. Hence, most exercise physiologists use factors such as percent of aerobic capacity. That being said, HR can be an accurate predictor if an anaerobic threshold and/or VO2max stress test has been performed and correlations between HR and particular training zones have been determined. This concept will aide in model personalization. For example, knowing anaerobic threshold and VO2max of an individual allows characterization of heart rate 'zones' 1-5 ranging from 'light, recovery' exercise (zone 1) to above anaerobic threshold

(zone 5). Often used in exercise physiology, zones can be correlated with respiratory exchange ratio (RER) in which an RER = 0.7, often during zones 1-2, is mainly fat utilization while zone 5, or RER $\geq$ 1.0, is mainly glucose utilization with a fuel mix in between (Knoebel, 1984). Zones are often used in regard to exercise planning and training, as they can be adjusted as one becomes trained, typically favoring higher fat utilization at elevated heart rates and shifting zones upward (Millan, 2014).

In 2013, a group associated with *Cobelli* and colleagues modified the *in silico* 2009 Padova type 1 simulator (Cobelli, 2009) to incorporate the effect of physical activity after demonstrating a doubling of insulin sensitivity and hence rate at which glucose enters cells (Schiavon, 2013). Subjects were put into two groups: one in the absence of and one with different degrees of reductions and durations of basal insulin infusion rates—it was shown an effective strategy is to reduce basal insulin by 50% 90 minutes prior to exercise and 30% during exercise to avoid hypoglycemia. However, currently, this is not possible in regard to current artificial pancreas design as exercise type and intensity is not accounted for, both of which may further adjust what changes need to be made in insulin dosing before, during, and after exercise. If type of exercise and relative intensity (which can be tuned with HR) and duration is inputted, theoretically a CGM or artificial pancreas design would be able to use a personalized model to predict BG fluctuations based on quantifiable trends (later shown in Figure 4.10). Reducing insulin during exercise is necessary; however, dependent on exercise *type* the amount of this decrease and timing would differ. For example, if a subject was performing high intensity sprint training, insulin reduction *before exercise* may be less than the 50% proposed above due to the

typical increase in BG at the onset of high intensity events. On the other hand,

insulin may be reduced *more* if exercise is going to be more aerobically based.

Limitations of current proposed exercise models include exercise energy

intensity as a function of HR implemented as a square wave – this is only useful for

steady-state aerobic exercise and varies amongst individuals in terms of threshold

values and zones. See Table 4.1 below and Figure 4.4 for limitations in using a

square wave approach. Anaerobic exercise is not accommodated by the 2009 Cobelli

model.

Table 4.1: Cobelli (2009) vs. Schunk-Winters HR informed Exercise Intensity

	Cobelli, 2009 **Characterization**	**Schunk–Winters HR Data (Phase 2 Case Study, Section 4.4)**
Baseline HR (bpm)	60	45
Mild Exercise, 15 min	1.5 x baseline = 90 bpm	128-145
Mild Exercise, 30 min	1.5 x baseline = 90 bpm	128-145
Moderate Exercise, 15 min	2 x baseline = 120 bpm	146-169
Moderate Exercise, 30 min	2 x baseline = 120 bpm	146-169
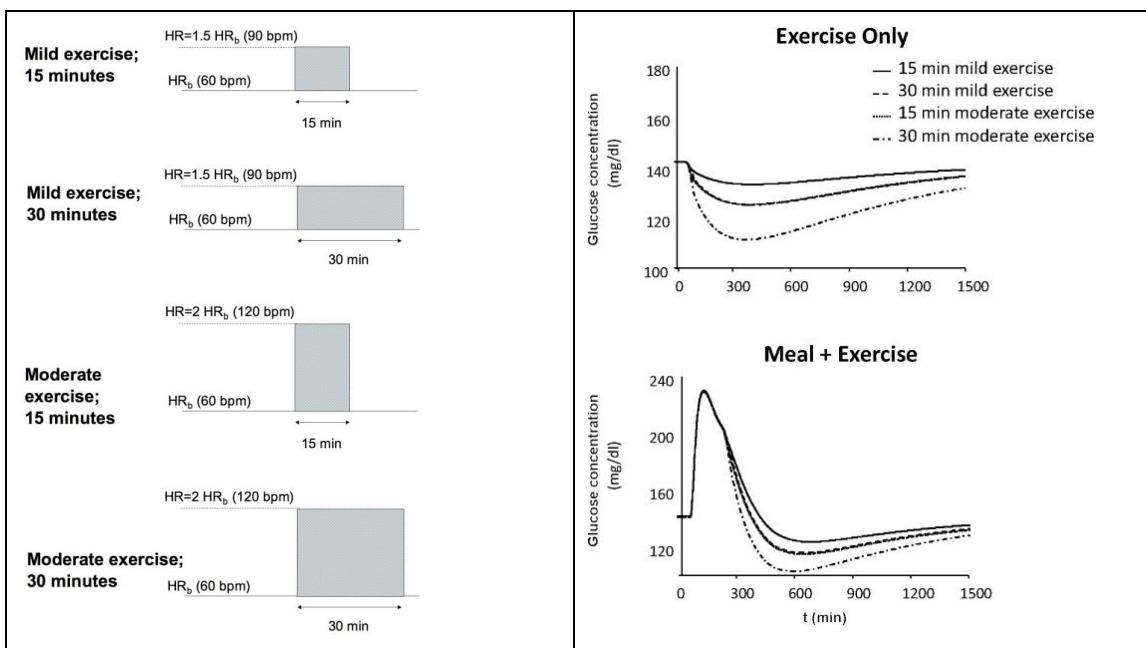
Figure 4.4: Cobelli (2009) Exercise Modeling Using Heart Rate. Cobelli (2009) simplistic approach to modeling exercise with the use of HR.

4.2.1 GLUT4 and Mitochondrial Biogenesis

An increase in the GLUT4 isoform of skeletal muscle tissue in addition to (and perhaps in part in conjunction with) an increase in mitochondrial content with endurance exercise results in roughly a linear increase in glucose uptake in response to the same insulin concentration. For example, a 2-fold increase in GLUT4 results in a 2-fold increase in glucose uptake in response to the same insulin concentration (Holloszy, 2011). GLUT4 expression is regulated in parallel with mitochondrial biogenesis in response to exercise-generated signals in skeletal muscle (Rockl, 2010). It is also important to note that GLUT4 has a short half-life ($t_{1/2}$) and the increase in GLUT4 concentration induced by exercise reverses rapidly (Richter, 2013).

4.2.2 Trained vs. Untrained Individuals

Skeletal muscle's glucose needs vary depending on activity level, and the glucose flux capacity depends on trained vs. untrained state. Hence, multiple mechanisms (other than the strictly insulin-mediated pathways) are available for glucose uptake. Particular motivation of a case study involving trained T1D's, based on personal experience and conversations with other elite T1D (DSP, 2015), stems from the ability to be carbohydrate/glycogen depleted in an insulin dependent state and still manage to avoid hypoglycemia during prolonged exercise. Despite early suggestions that a certain amount of insulin was necessary for muscle glucose transport in increase with contractions, it is now apparent that many other signaling

pathways are responsible and result in an additive effect on GLUT4 translocation, and hence glucose energy uptake of skeletal muscle during exercise (Richter, 2013).

Due to variations of fiber type amongst 'trained' individuals (i.e. greater proportion of slow Type I fibers of an endurance athlete vs. more and larger fast Type II fibers of sprinters and power athletes), it is recognized that although glycogen storage location may differ, total glycogen content within muscle can fluctuate considerably, and depends on diet and recent muscle use history (e.g., "carbo-loading" in athletes) (Costill, 1976). This was seen in Chapter 3, where the predicted muscle compartment levels would vary over the course of a 24-hr day, such as in Figures 3.17 and 3.18.

Endurance training effects (i.e. decreased resting HR, increased fat oxidation, etc.) generally follow similar trends (Nielson, 2011). However, aerobic endurance athletes may not rely on as much CHO oxidation if intensity is kept moderate for prolonged periods. High intensity training (i.e. >70-80% VO2max) requires a greater proportion of glucose fuel utilization, usually reached during intense interval training, maximal lifting, sprinting sessions, and in highly-trained athletes capable of maintaining such high VO2 and HR levels. A key adaptation is an increase in mitochondrial content, and hence oxidation potential in trained individuals (Holloszy, 2011). Some studies suggest an increase in mitochondrial demand and utilization may represent how exercise training enhances muscle insulin sensitivity, and fatty acid oxidation in both resting and exercise states (Befroy, 2008). Factors influencing increased insulin sensitivity are important for insulin models and clinically informing people with diabetes so that hypoglycemia can be prevented.

Summaries of varying adaptations of trained vs. untrained individuals between low,

moderate, and high intensity exercise is summarized below.

In studies comparing substrate utilization of untrained vs. trained subjects, a

variety of methods exist. Ahlborg et al., 1974, analyzed six healthy untrained

subjects during prolonged (4 hr) exercise on an upright bicycle at 30% of their

maximal oxygen uptake, focusing on leg metabolism of substrates including glucose,

lactate, pyruvate and individual amino acids (Ahlborg, 1974). Wolfe took varying

exercise intensity of 5 trained subjects and determined peripheral lipolysis, plasma

rate of appearance of FFA, total fat oxidation, and carbohydrate oxidation (Wolfe,

1998). The subjects were trained cyclists and performed 30 minutes at 85%VO2max

and 120 minutes at 25 and 65% VO2max randomized over a course of three days.

Table 4.2 Summary of Low Intensity Substrate Fuel Utilization in Trained vs. Untrained Subjects

Source	Characte rization	Overall Trend		Trained		Untrained	
		CHO	FFA	CHO	FFA	CHO	FFA
Ahlborg, 1974	~30% VO$_{2max}$ for prolonge d 4 hours	Contributi on fell from 40 to 30% between 90 to 240 min.	Account for majority of leg muscle metabolis m beyond 40 min to 62%.	—	—	*Rest: 4.51 mmol/l 40 min: 4.57 90 min: 4.30 180 min: 3.53 240 min: 3.12	*Rest: 0.66 mmol/l 40 min: 0.78 90 min: 0.93 180 min: 1.57 240 min: 1.83
Wolfe, 1998	25% VO$_{2max}$	—	—	15 μmol glucose/(kg *min), about 36% of total fuel	Total Fat Oxidation: 26.8 μmol FA/(kg*min); 25.8 FFA rate of appearance	—	—

*Refers to arterial concentration of substrate.

While in conflict with other literature that suggests a more proportional glucose-intensity relation (e.g., Figure 4.3), this study suggests that at low intensity endurance exercise, FFA oxidation is prevalent with only about 10% of total energy expended from carbohydrates (Holloszy, 1996). Sources also differ in regard to IMTG utilization (Ahlborg, 1974).

Table 4.3 summarizes studies of fuel utilization for trained versus untrained individuals for a moderate-intensity exercise session. Holloszy (1996) studied energy expenditure data during 0-30 minutes of exercise at 25, 65, and 85% of aerobic power and during 90-120 minutes of exercise performed at 25 and 65% VO2max. Confounding factors such as nutritional state, training level, and muscle glycogen supercompensation were taken into account for the 5 trained cyclists, adapted from the study used by Wolfe, making the studies comparable (Holloszy, 1996 and Wolfe, 1998). In a separate study, 9 untrained male subjects underwent a 12-week training program with measurements taken before and after training during exercise of 120 minutes at an average of 64% VO2max (Hurley, 1986). In terms of duration and intensity, this study is comparable—however, it is important to recognize possible confounding factors associated with untrained becoming 'trained' and lifestyle remodeling.

Table 4.3: Summary of Moderate Intensity Fuel Utilization in Trained vs. Untrained Subjects

Source	Characterization	Overall Trend		Trained		Untrained	
		CHO	FFA	CHO	FFA	CHO	FFA
Holloszy, 1996	50-75% VO_{2max}, 2 hours	10% Plasma Glucose, 20% Glycogen	<50% FFA, 20% IMTG (since prolonged)	—	Greater; IMTG~75% of FFA oxidized	—	IMTG ~50% of FFA oxidized
Hurley, 1986	$64 \pm 3\%$ of VO_{2max} for 2 hours	Glycogen becomes depleted quicker than BG	Function of concentration but in trained subjects FFA oxidation capacity increases; rely on IMTG	~415 kcal for energy from CHO after training	~600 kcal for energy from fat after training	~650 kcal for energy from CHO before training	~390 kcal for energy from fat after training
Wolfe, 1998	65% VO_{2max}	—	—	132µmol glucose/(kg *min)	Total Fat Oxidation: 42.5 µmol FA/(kg*min); 22.8 FFA rate of appearance	—	—

*Refers to arterial concentration of substrate.

At a moderate exercise intensity, more emphasis is placed on CHO oxidation, with total glucose utilization = BG + glycogen (Holloszy, 1996). IMTG utilization increases in some trained individuals. According to Hurley et al (1986) and calculated from RER, the proportion of caloric expenditure derived from fat increased from 35% before training, to 57% after training while keeping relative workload constant during exercise. Muscle glycogen utilization was 41% lower.

Kiens (1993) attributes the relative proportion of FFA uptake in exercising muscle as a saturable process enhanced by training; lower CHO utilization in the

trained leg was mainly a function of glycogenolysis reduction. As duration increases,

FFA uptake increases more rapidly in trained individuals and plateaus in non-

trained after 60 minutes.

Table 4.4: Summary of High Intensity Substrate Fuel Utilization in Trained vs. Untrained Subjects

Source	Characterization	Overall Trend		Trained		Untrained	
		CHO	FFA	CHO	FFA	CHO	FFA
Holloszy	>75% VO_{2max} up to 30 minutes	60% Glycogen; 10% Plasma	10% IMTG; 15-20% FFA	69% of Total	Decreasing; less release from adipose	75% of total	—
Wolfe, 1998	85% VO_{2max}	—	—	259µmol glucose/(kg*min)	Total Fat Oxidation: 29.6 µmol FA/(kg*min); 17.0 FFA rate of appearance	—	—

At high intensity, fat oxidation is no longer sufficient as a primary fuel source,

and carbohydrate oxidation is the dominant mode of most energy expenditure,

especially in untrained individuals (Ahlborg, 1974 and Kiens, 1993).

Sufficient data on the exercise physiology aspects of mass-conservation of

glucose with exercise allows for model personalization as long as intensity can be

characterized and inputted. The Schunk-Winters model (Chapter 3) uses an

approach to input exercise as an aerobic 'fuel-mix' demand source (in kcal/hr) or

from an anaerobic/daily activity standpoint (also in kcal/hr). The addition of a

mitochondrial demand consumption state allows the separation of muscle tissue

into multiple supply-demand based compartments to account for effects seen in

Tables 4.2-4.4 above and with case study results in Section 4.4 below.

4.3   Methods

The Chapter 3 Schunk-Winters model acts as the base compartmental model for Chapter 4 and model personalization. The main augmentations focus on the highlighted tissue compartments in Figure 4.5, the general model, and Figure 4.6, the skeletal muscle model proposed in Chapter 3. Further parameter personalization and an example of application to a T1D athlete are presented in Section 4.4 Case Study and Section 4.6, with personal adapted parameters used for simulations throughout results outline in Methods 4.3.2.
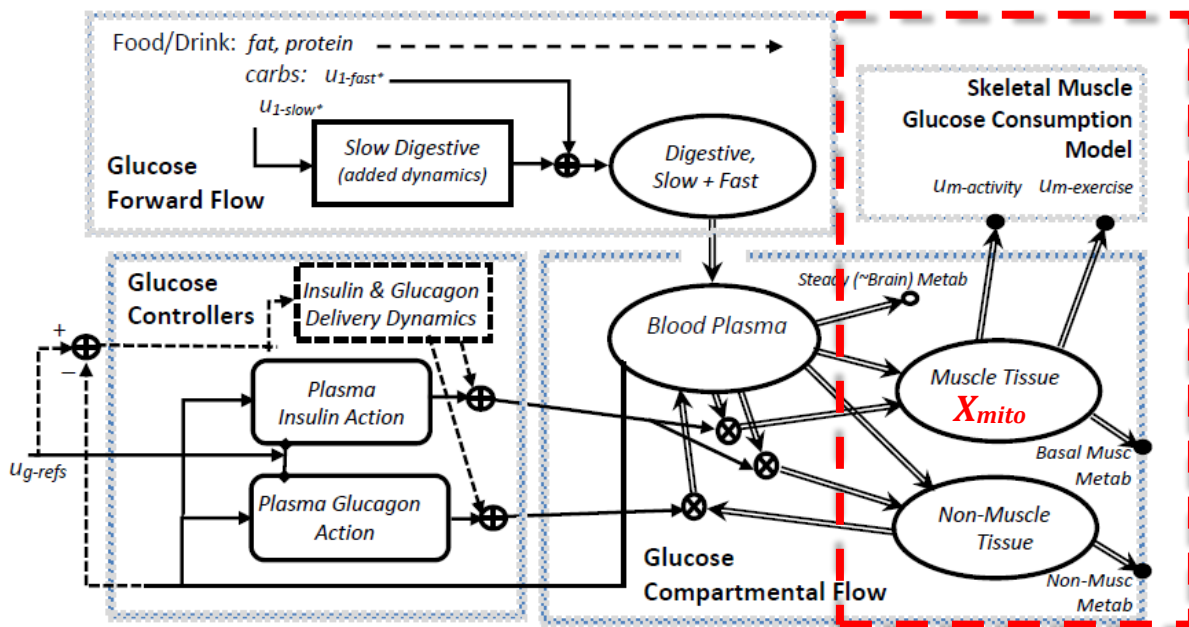
Figure 4.5: Schunk-Winters Model Structure with Exercise Focus. Thick lines represent material flow with storage and control action as unidirectional signals informed by rate parameters and oftentimes, nonlinear, by either Hill kinetics or multiplicative states. Nonlinear relations include both flux terms and heuristics that change fitting equations based on different state or input signal ranges.
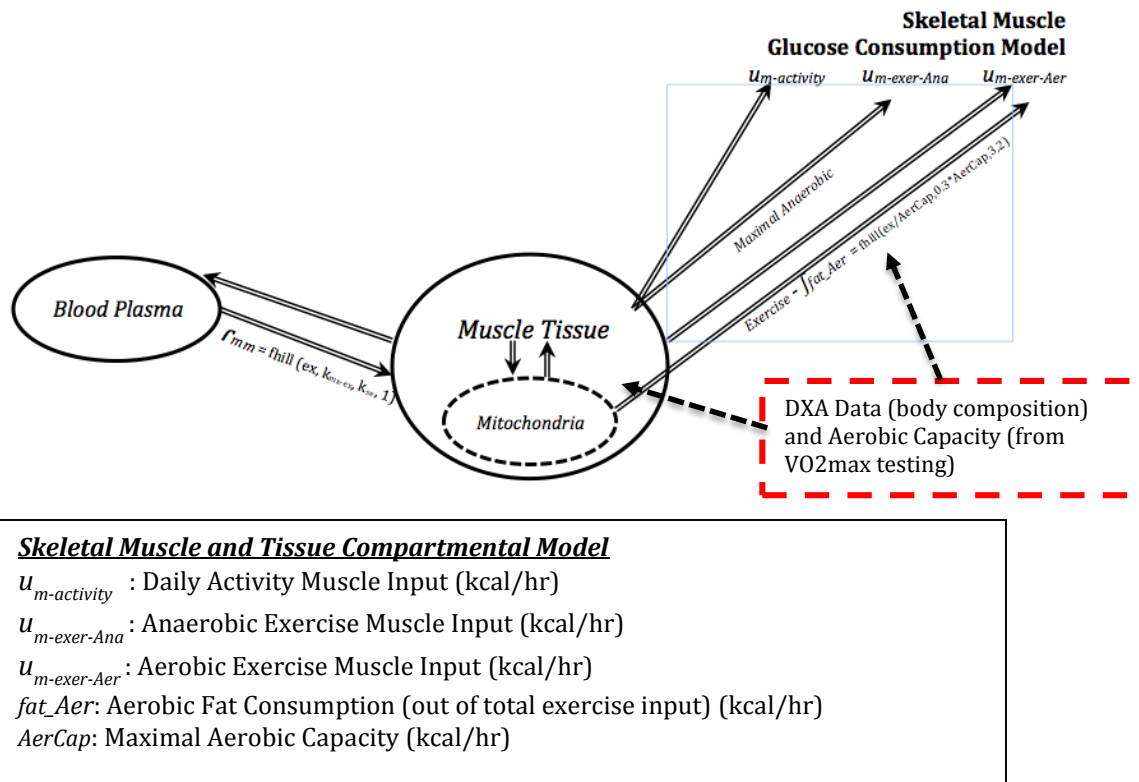
Figure 4.6: **Skeletal Muscle and Tissue Compartmental Model with Added Input**.

4.3.1   Case Study Phases 1 and 2 and Data Collection Protocol

Full protocol description, results, and logbook can be found in Appendices 7.2 and 7.3 for both phases, respectively. The subject completed an IRB-approved Case Study Phase 1 in June 2014 and Case Study Phase 2 in June-July, 2015.

The phase 1 case study was an *in silico* 24-hour study with the model output compared to BG monitoring of a 22-year-old T1D athletic female. 3 protocols and 1 control protocol were performed on the same day of the week for 4 consecutive weeks. BG was collected using the subjects OneTouch Ultra Blood Glucose monitor, requiring a finger prick every 30 minutes. Meal content (GI), exercise type, and meal timing were variables of interest. Controls included meal magnitude, exercise

duration, activity (time and relative intensity) and insulin injection, based on clinical prescription. Outputs mainly resulted in determining a need to differentiate exercise type and meal content in modeling. Limitations include inaccuracies due to finger pricks and sampling only 2 times per hour and no control for the female's menstrual cycle. This study opened up the need for Phase 2.

Phase 2 featured the addition of a continuous glucose monitor (CGM, specifically Dexcom G4 Platinum) and extended protocol length. The purpose of the study phases was to validate known BG trends in regard to particular meals and content (i.e. low vs. high GI) as well as differences in exercise type (intensity, duration, aerobic, and resistance variations) similar to that of Phase 1, but with longer duration to accommodate additions to both meal and exercise simulations. Known literature study inputs will be replicated for comparison and are referred to in the logbook of Section 6.4. Literature studies replicated include Yamamoto, 2014, Kotachev, 2014, and Cobelli, 2007 amongst others.

Prior to the primary part of this study of continuously monitoring blood glucose levels (Phase 2), clinically standard metabolic and physiological tests related to your body composition and baseline fitness levels took place (Phase 2). These were performed in several exercise laboratories on the Marquette University campus. An IRB-approved maximal oxygen consumption test (VO2max test) was performed on a treadmill. The subject wore a VO2 testing mask and followed the laboratory protocol of increasing the treadmill grade by 2% approximately every 2 minutes until volitional fatigue or the presence of any contraindication to the American College of Sports Medicine (ACSM) guidelines. Blood lactate was

measured before and after to ensure that the lactate threshold was reached. Body composition parameters and values were obtained with the use of a DXA machine and full-body scan (further explained in Appendix 7.5).

The main part of this research study involved a planned 8-day protocol for meals and exercise. Meal content was planned using glycemic index and load calculations to distinguish between "fast" and "slow" carbs.

4.3.2   Model Personalization

Parameters and inputs that shape the personal integration into the Schunk-Winters model are outlined below, and given in Table 4.5. These values are used for all simulations included in Section 4.4.2 results. They will form the basis for all future personal integration model parameter and input changes. New parameters (in addition to those changed below) are metabolism scaling that will scale both non-muscle and muscle tissue loss, and a stressor ratio parameter to inform the new additional input *uHM*, or any hormone effect associated with added stress, i.e. eliciting catecholamine action during exercise. This input is time dependent, with a default value of 1.0 and scaled by *stressrat*, or a pulse affecting the GLUT 2 bi-directional gradient at a given time. For example, in 4.4.2 results, this parameter is used to model circuit training. Both *metab* and *stressrat* will be defaulted at 1.0, with a scale from 1.0-1.5 for higher metabolism or higher stress situations, respectively. Stress ratios implemented for model simulations, particularly in regard to circuit and sprint training, are displayed in Figure 4.11a.

Table 4.5: Model Personalization Parameters

Schunk-Winters General Model	*Personal Integration Model*
Parameters	
Body Mass = **70 kg**	65
Muscle Mass = **30 kg**	30
Non-Muscle Mass = **25 kg**	20
Aerobic Capacity = **1000 kcal/hr**	1137
Mitochondrial Volume = **0.1**	0.3
Type 1 Ratio = **varies**	0.2
GLUT2 Forward Rate = **6.0**	6.0
Stressor Ratio (i.e. Exercise) = **1.0**	1.5
Maximum Fat Consumption Capacity = **300 kcal/hr**	341
Metabolism Scaling* = **1.0**	1.5
Basal Non-Muscle Tissue Metabolic Loss* = **2.5 g/hr**	**3.0 (Refer to Appendix 7.5 for body composition)**
Basal Muscle Tissue Metabolic Loss* = **1.5 g/hr**	2.25
HR Resting = **60 bpm**	45
HR Maximum = **200 bpm**	212
Inputs	
Exercise Duration and Single Intensity	Exercise Duration with Heart Rate Informed Intensity
Activity—Separate Input	Activity—Separate Input or During Exercise
Hormonal Input, ***uHM*** = 1.0	Hormonal Input, ***uHM*** = 1.0 *(Stressor Ratio); time dependent

* Metabolic Scaling is on the basis of basal metabolism and scales both muscle and non-muscle metabolic loss as a multiplicative entity.

An external heart rate input (if available) from a monitor or smart watch augments the exercise input portion of the model. The following code snapshot (Figure 4.7) from Matlab demonstrates the theory behind applying a Hill functional to map the *u3* reference input to the HR *u5* reference input. Heart rate is used to sculpt *u3* when compared to a reference input value to the user. The difference is used to add/subtract to *u3* to create a new and HR informed *u3*. HR is first normalized.

```
    urelHR(i) = (u(5,i)-HRrest)/(HRmax-HRrest);
    upredex(i) =(u(3,i)/AerCap);
    urelHR = upredex;
    kscale = 500;
    if urelHR(i) == 0
        u3new(i) = u(3,i);
    else
     deltu3(i) = kscale*(upredex(i) - urelHR(i));
     u3new(i) = u(3,i) + deltu3(i);
    end
```

Figure 4.7: Heart Rate Code Snippet. Code snippet from Schunk-Winters model.

Another aspect of the model involves varying a subject's fat oxidation

capacity, or the subject's potential ability to utilize fat as an energy substrate during

exercise. This often increases with training, along with mitochondrial volume, etc.

The following curves (Figure 4.8) demonstrate the model subtraction of fat from

total energy consumption, thereby leaving glucose consumption as the main input

(in kcal/hr). Although there is not a separate fat consumption state, the model

accounts for an increase in fat oxidation by a higher magnitude/rate subtraction as a

fat fuel Hill function from total energy consumption as seen below (Rynders, 2011).

This approach automatically adjusts the fuel mix, with fat a relatively higher

proportion for low-to-moderate and moderate intensity endurance activity, then

becoming less for high-exertion endurance activities. For example, the Hill function

could be adjusted to saturate at a higher value than 300 (~30% if Aerobic Capacity =

1000 kcal/hr), such as estimated as 341 Kcal/hr for the case study. For steady

aerobic exercise, even at higher intensity, this provides a reasonable approach for

fuel distribution as a function of endurance activity.
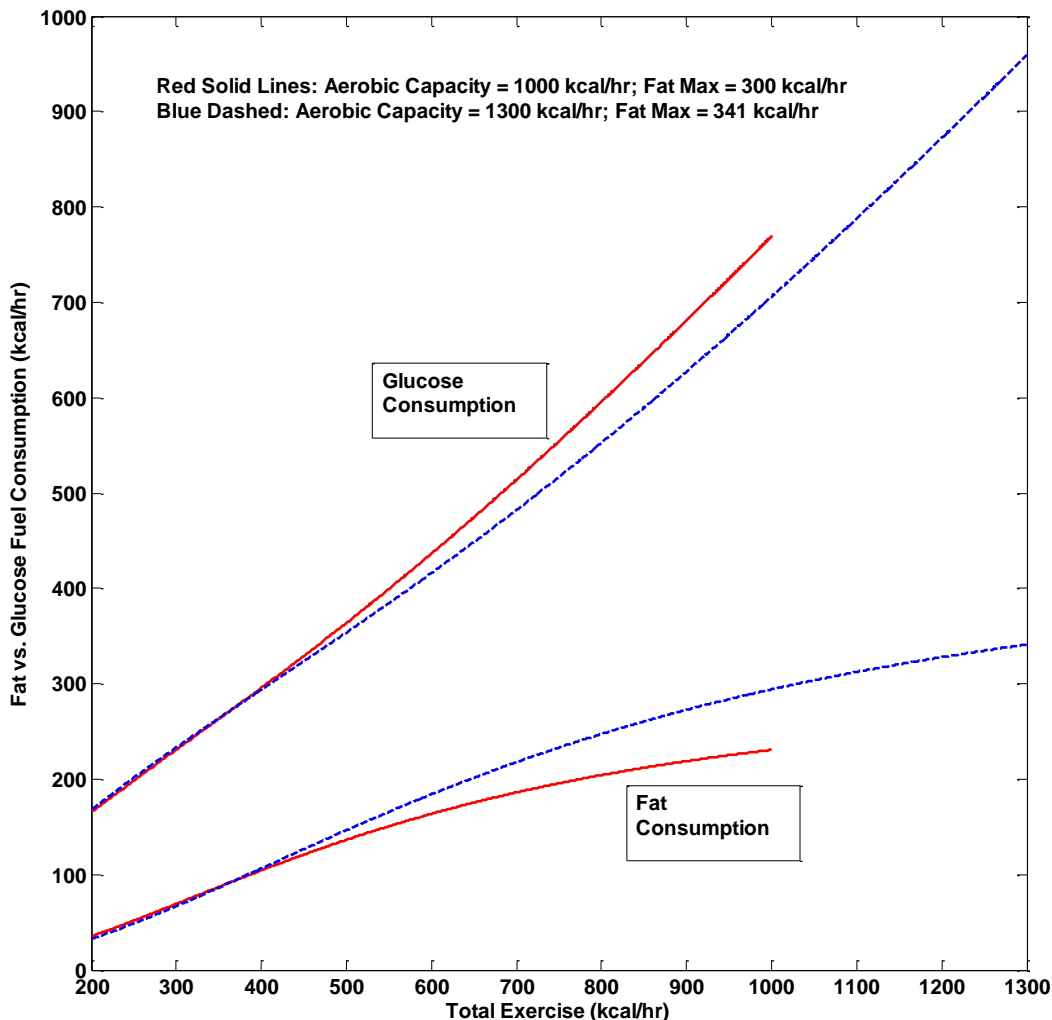
Figure 4.8: Glucose and Fat Consumption vs. Total Energy Expenditure. Fat and glucose energy consumption (kcal/hr) vs. total energy expenditure (kcal/hr) varying the fat consumption capacity from 30% of aerobic capacity (red lines) to 40% (blue lines). Dashed lines indicate glucose consumption, the main model input of total expenditure – fat consumption (solid lines).

Various types of exercise, particularly those similar to high intensity interval training, circuit training, and sprint intervals (i.e. repeating high intensity followed by rest), can be modeled using both *u3* and *u4* inputs thereby simulating both aerobic and anaerobic components . Such high-exertion exercise protocols, requiring discipline and concerted focus by the athlete, may be viewed as having a stress component outside of exercise stress. In such cases, an additional

multiplicative control function operating on tissues on the basis of anticipatory real-time sympathetic hormone effects (i.e. see hormone discussion in Section 3.4.7) similar to glucagon effect of transferring glucose to blood from non-muscle compartments via pathways such as hepatic over-and-above account for fluctuations associated with such exercise types as well. Effects are quantified in Section 4.4.2, case study phase 2 results.

Body composition variations have a large effect in terms of maximum saturation of Hill functionals, as limits are placed based on the amount of muscle and non-muscle volume (and hence glycogen/glucose storage) available. Additionally, a higher muscle volume directly effects mitochondrial volume, with both typically increased in a trained individual (can be verified by a DXA scan). In this case, aerobic efficiency and hence $u3$ effects are increased.

4.4   Case Study Results and Comparative Simulation

Section 4.4.1 highlights key Phase 1 results, limited in that Phase 1 was used to design Phase 2. Section 4.4. 2 includes Phase 2 results. Phase 2 results are separated into an exercise section (Figures 4.9 and 4.10) demonstrating CGM data acquisition, analysis, and model simulation replication. Exercise protocols are compared based on similar time duration. The following section and Figure 4.11 shows and example of a full-day protocol (Day 7), including CGM data and external heart rate input (Figure 4.11a), foodstuff logbook and spreadsheet, and Schunk-Winters replication (Figures 4.11b and c).

4.4.1   Phase 1 Results

Examples of useful Phase 1 results are shown in Figure 4.9; however, most

results were used to design the more extensive Phase 2 study. Timing of insulin

prior to a meal was a useful insight as well as lingering effects of exercise type. It

was clear that some hyperglycemia exists with resistance training but could not be

quantified due to a sampling frequency of every 30 minutes.
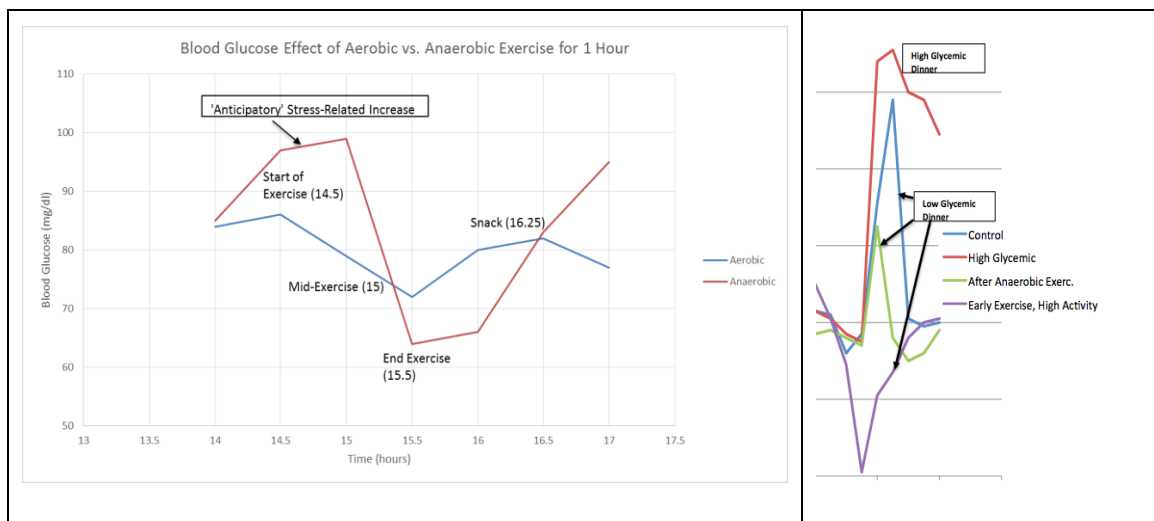
Figure 4.9: Phase 1 Case Study: Anaerobic vs. Aerobic Exercise and High vs. Low GI Dinner.
Snapshots from Phase 1. *Left:* Anaerobic vs. Aerobic Exercise for a 22-year old female T1D. *Right*:
High vs. Low GI Dinner. X-axis denotes time in hours. For the right plot, the time scale is over a period
of two hours—each tick = 30 minutes.

4.4.2   Phase 2 Results

All results from the following sources are provided in Section 6.5 and 6.6:

- DXA Scan
- VO2max Treadmill Test (Bruce Protocol)
    - o   Excel datasheet is available.
- CGM Data and Calibrations
- Garmin Heart Rate (HR) Snapshots
    - o   Excel HR files are available.

- Meals/Snacks
  - Magnitude, GI, proportion of CHO
  - Time/Duration
  - Excel datasheet available.
- Daily Logbook
  - Activity level/notes
  - Stress level
  - Resting HR
  - Corrections for BG

Figure 4.10 shows the process used for data analysis in a comparison of protocol days 4 and 8: long duration exercise. This example compares a long duration (~2 hour) anaerobic lifting workout to a long duration (~2.5 hour) aerobic run. CGM data is obtained alongside corresponding HR data. HR data is inputted into the Schunk-Winters model along with perceived intensity level of exercise (in kcal/hr as a proportion of maximal aerobic capacity) and all states are predicted as shown in Figure 4.10 (bottom). Figure 4.11 outlines HR variation, CGM data acquisition, and model prediction for four different exercise *types*.

4.4.2.1 VO2max and Body Composition

Table 4.6 and Table 4.7 provide VO2max test results and calculated aerobic capacity, as well as training zone characterization of the subject calculated from VO2max test results. Table 4.8 shows a general overview of subject body composition with all results in Appendix 7.5.

Other biological factors controlled for included the female menstrual cycle and insurance that the diet and exercise protocols would be as normal as possible to the subject's typical training and diet routine as to not affect basic body composition.

Table 4.6: VO2max and Aerobic Capacity Calculation

VO2max (mL/kg/min)	62.65
VO2max (kcal/kg/hr)	17.9
Aerobic Capacity (kcal/hr)*	**1137**
Anaerobic Threshold Parameters	
VO2 (ml/kg/min)	50.4
% VO2max	80.4
Speed @ 1% Grade (mph)	9-9.5
HR (BPM) at	170
Maximum HR (BPM)*	212
Resting HR (BPM)*	45
Maximal Fat Consumption (kcal/hr) Assuming ~30% Aerobic Capacity*	341

*Denotes Model Inputs

Table 4.7: Phase 2 Case Study Training Zone Characterization

Training Zones		%AT	Lower Bound (bpm)	Upper Bound (bpm)
1	Active Recovery	65-74	111	126
2	Easy Aerobic	75-85	128	145
3	Moderate Aerobic	86-95	146	169
4	Threshold	100-105	170	180
5	Maximal	106- max HR	180	191

Table 4.8: Subject Body Composition Overview

Date:	22-Jun-14
Height (in)	69.5
Weight (lbs)*	139
Age	23.2
Android (% Fat)	20.2
Gynoid (% Fat)	20.9
A/G Ratio	0.96
Total Body (%)*	15.4
BMI (kg/m^3)	20.2
Muscle Mass (kg)*	54.3
Non-Muscle Mass (kg)*	8.806

*Denotes Model Inputs

4.4.2.2   Exercise

Section 4.4.2.2 highlights key results pertaining to the Case Study exercise
sessions, with all data shown in Appendix 7.3. Figure 4.10 demonstrates an example
of personalized model progression to compare long endurance exercise, taking CGM
blood glucose clinical data, applying corresponding HR input, and replicating the
simulation inputs in a personalized version of the Schunk-Winters model so that
each state is displayed, and exercise physiology and biological glucose flow
mechanisms can be seen (i.e. mitochondrial consumption, flow to and from tissue
states, etc.). Heart rate is used to better tune and inform intensity based on taking a
perceived *u3* input and known aerobic capacity with any difference based on HR
fluctuation above or below this threshold as an added or subtracted entity.

Figure 4.11a-c compares type of exercise with a constant duration. An
aerobic tempo run at 60-70% maximum aerobic capacity is compared to circuit
training, a combined bike and run aerobic session, and sprint training. Circuit
training is further informed with the personalized parameter *stressrat* or a stressor
value of 1.5.

Anaerobic

Aerobic

Snack at 6:30 AM with
Long Aerobic in Pink
(lower curve) and
Anaerobic in teal.

6:00 AM   9:00 AM   12:0 PM
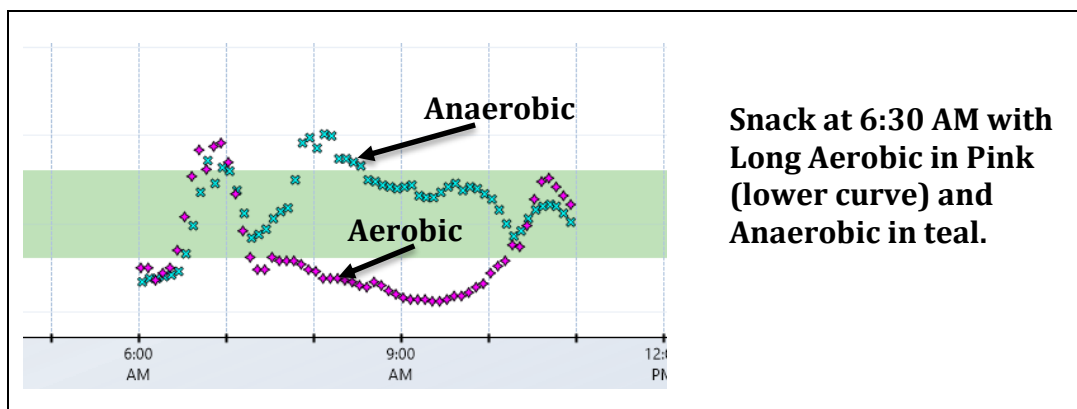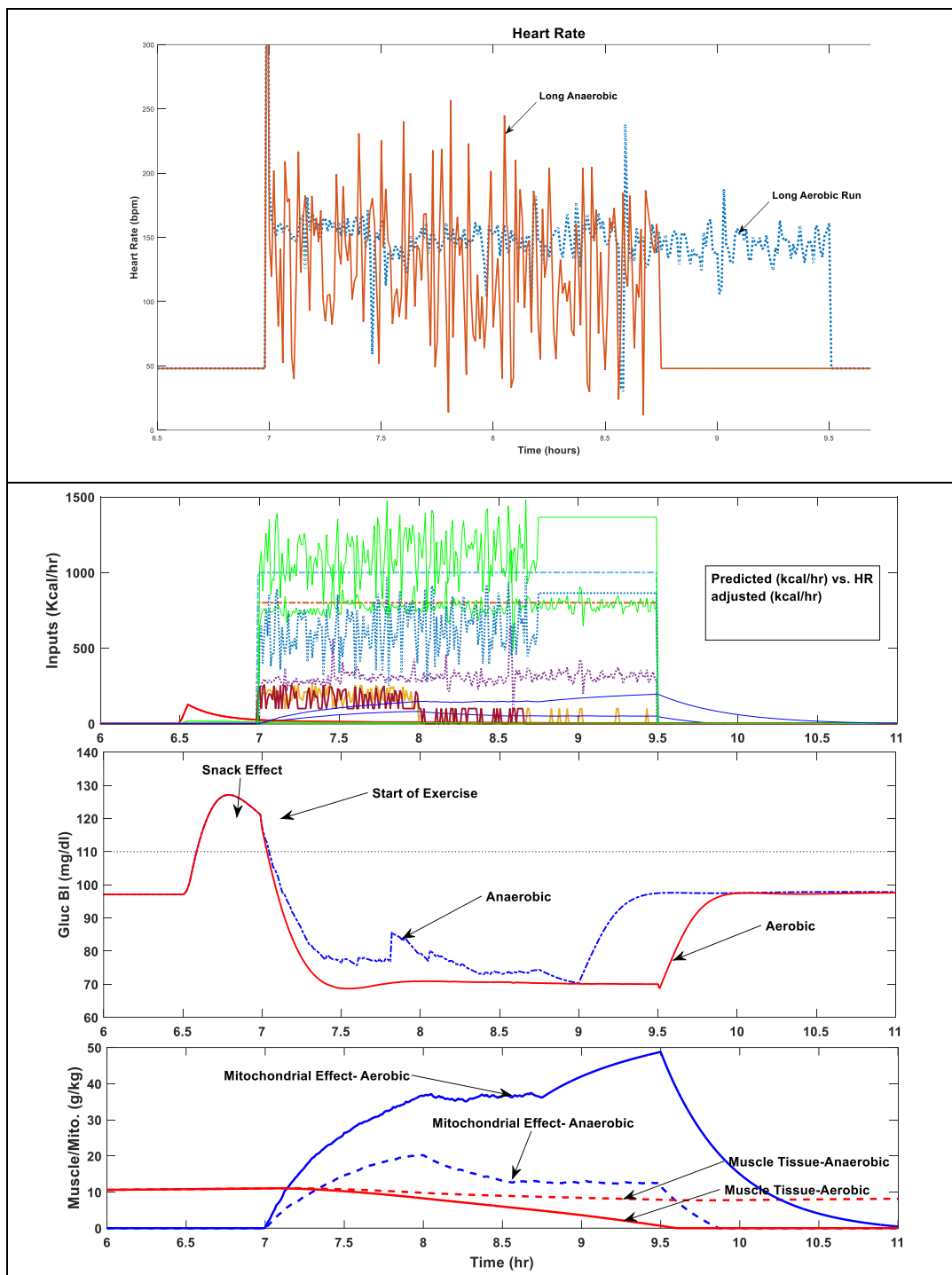
Figure 4.10: Phase 2 Case Study: Personalized Model Progression. Example of a personalized model progression taking Case Study Phase 2 CGM blood glucose clinical data *(Top)* for long-duration (2-2.5 hour) aerobic vs. anaerobic exercise and using corresponding HR data *(Middle)* to inform BG fluctuations and trends in summation with the model prediction*(Bottom).* If HR is higher (or lower) than the predicted exertion (i.e. ~500 kcal/hr for long aerobic and bouts of 800 kcal/hr or greater for anaerobic), the exercise and activity input is adjusted. Subject is a 65 kg T1D female with an increased mitochondrial content ratio (0.3) due to athletic training level (mitochondrial consumption shown in kcal/hr).

CGM (BG [mg/dl] vs. Time)	Heart Rate (bpm)	Additional Input
Protocol Day 2: Tempo Run		
		Stress Ratio = 1.5 Starting BG = 97 mg/dL Basal Insulin for Simulation = 1.0 U/hr Average HR = 162 bpm Training Zone 3
Protocol Day 3: Circuit Training		
		Stress Ratio = 2.0 Starting BG = 72 mg/dL Basal Insulin for Simulation = 2.0 U/hr Average HR = 164 bpm Peak HR = 183 bpm No Zone Characterization (HR spikes)
Protocol Day 6: Bike and Run		
		Stress Ratio = 1.0 Starting BG = 84 mg/dL Basal Insulin for Simulation = 1.5 U/hr Average HR = 143 bpm Training Zone 2
Protocol Day 7: Sprint Training		
		Stress Ratio = 1.8 Starting BG = 72 mg/dL Basal Insulin for Simulation = 2.0 U/hr Average HR = 163 (including rest) Peak HR = 182 Training Zone During Sprints = 4

Figure 4.11a: Exercise Type Comparison. Comparison of days 2, 3, 6 and 7 exercise sessions, CGM clinical data and external heart rate. The additional input column is used for Schunk-Winters simulation reference.
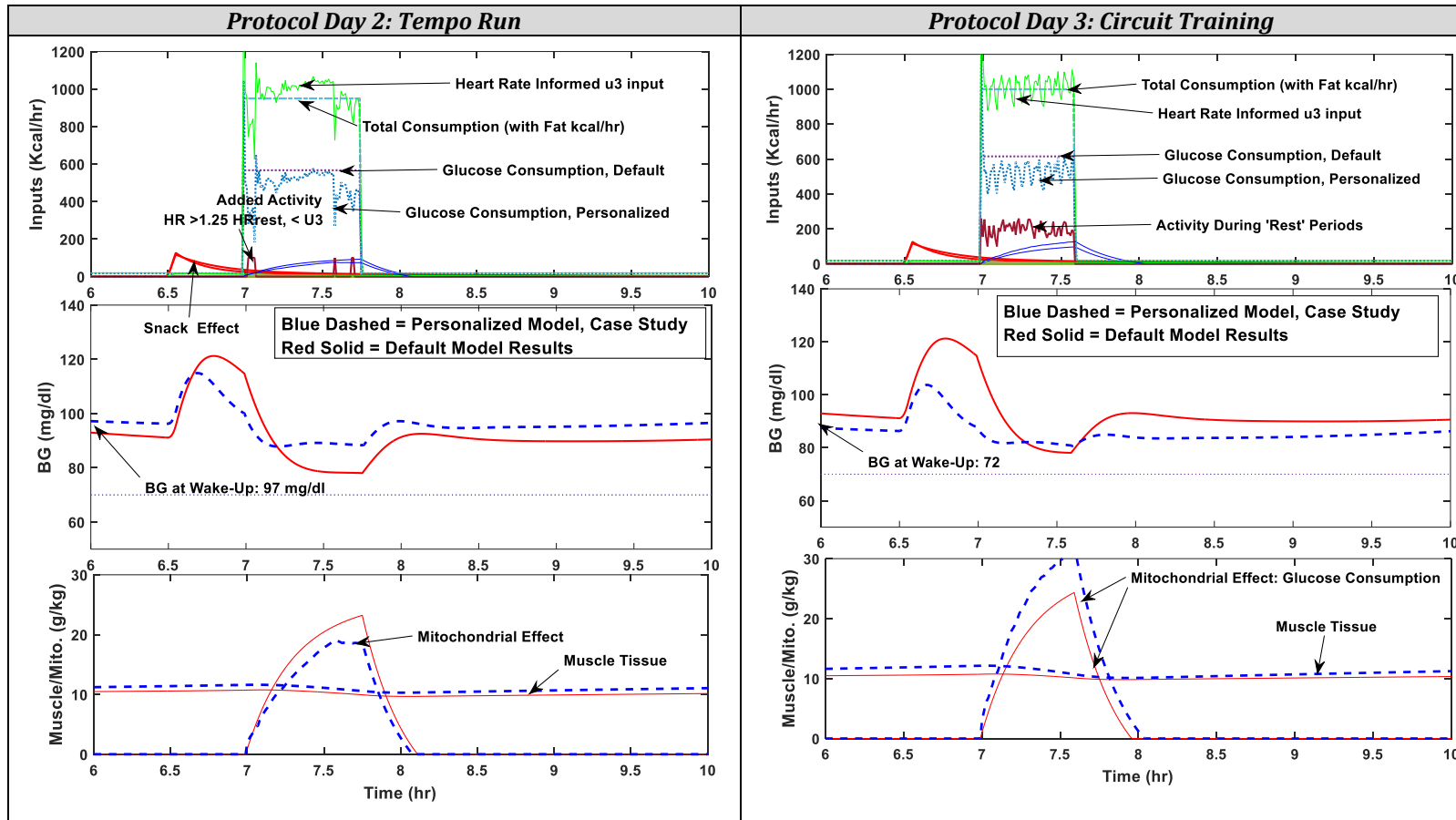
Figure 4.11b: Exercise Type Comparison. Simulation Comparison of days 2, and 3 exercise sessions. In all cases, the subject had a 15 g CHO snack at 6:30 AM with exercise beginning at 7:00 AM for 1 hour. Personalized model output is shown with blue-dashed lines, while default model output is shown in red solid.
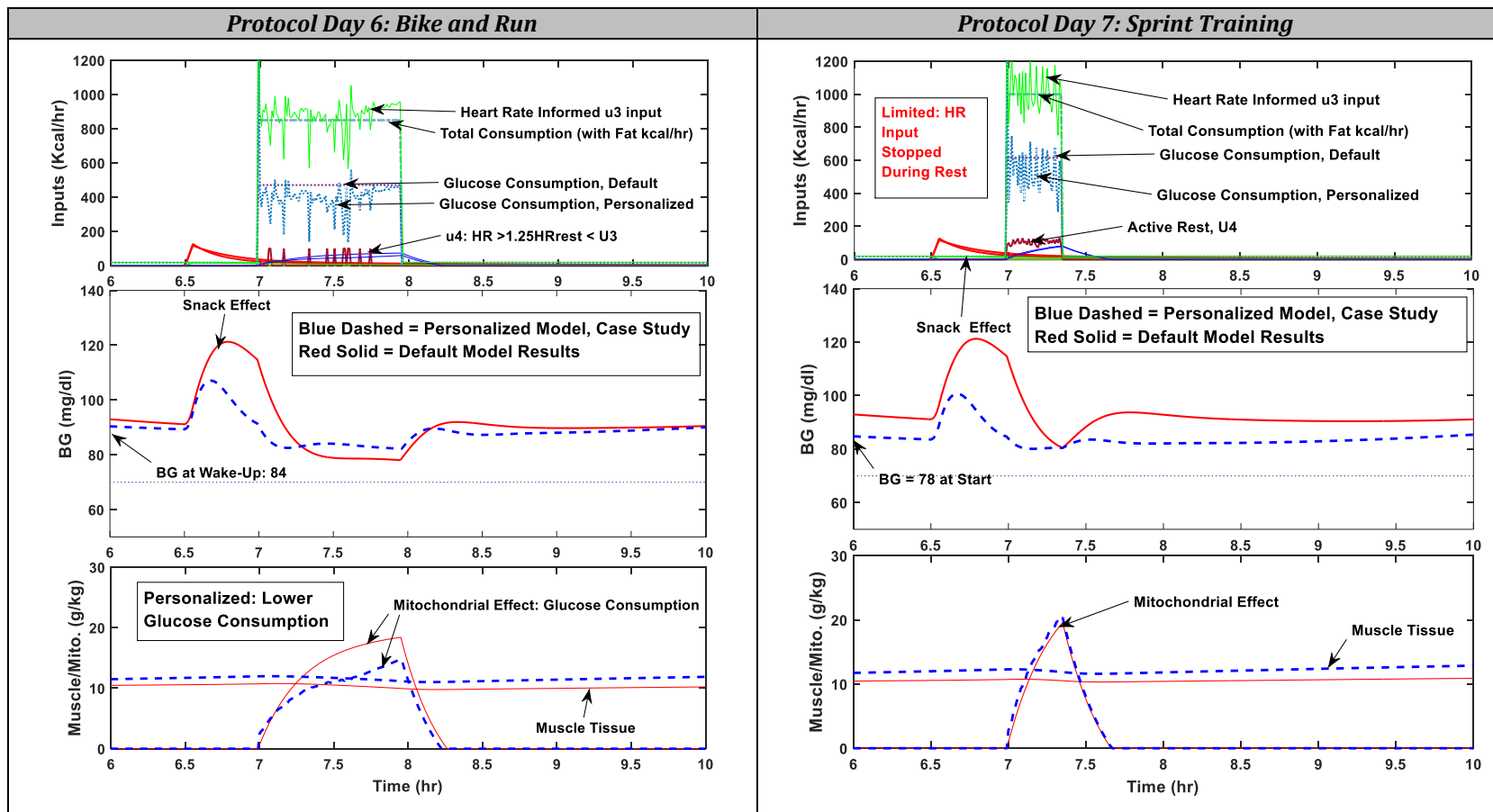
Figure 4.11c: Exercise Type Comparison. Simulation comparison of days 6 and 7 exercise sessions. In all cases, the subject had a 15 g CHO snack at 6:30 AM with exercise beginning at 7:00 AM for 1 hour. Personalized model output is shown with blue-dashed lines, while default model output is shown in red solid. The parameter *stressorrat* was used to inform any increased exercise-induced stress, triggering non-muscle to BG flux.

4.4.2.3   24-Hour Simulations

Figure 4.12 shows an example of a 24-hour simulation and replication. The provided example is for Protocol Day 7, which consisted of a track workout at 7 AM (4x400, 4x200, 1x400, 1x200, and 4x100) for about 40 minutes estimated at 700 kcal/hr, 3 meals, and 1 snack. In the simulation run, t =0 is 12:00 AM, as in the CGM graph. The subject data is found in Appendix Section 7.5 (23-year old T1D athletic female). Table 4.9 and 4.10 provide meal content information, including time, duration, and GI. Other full day CGM data and meal content are found in Appendix Section 7.4.
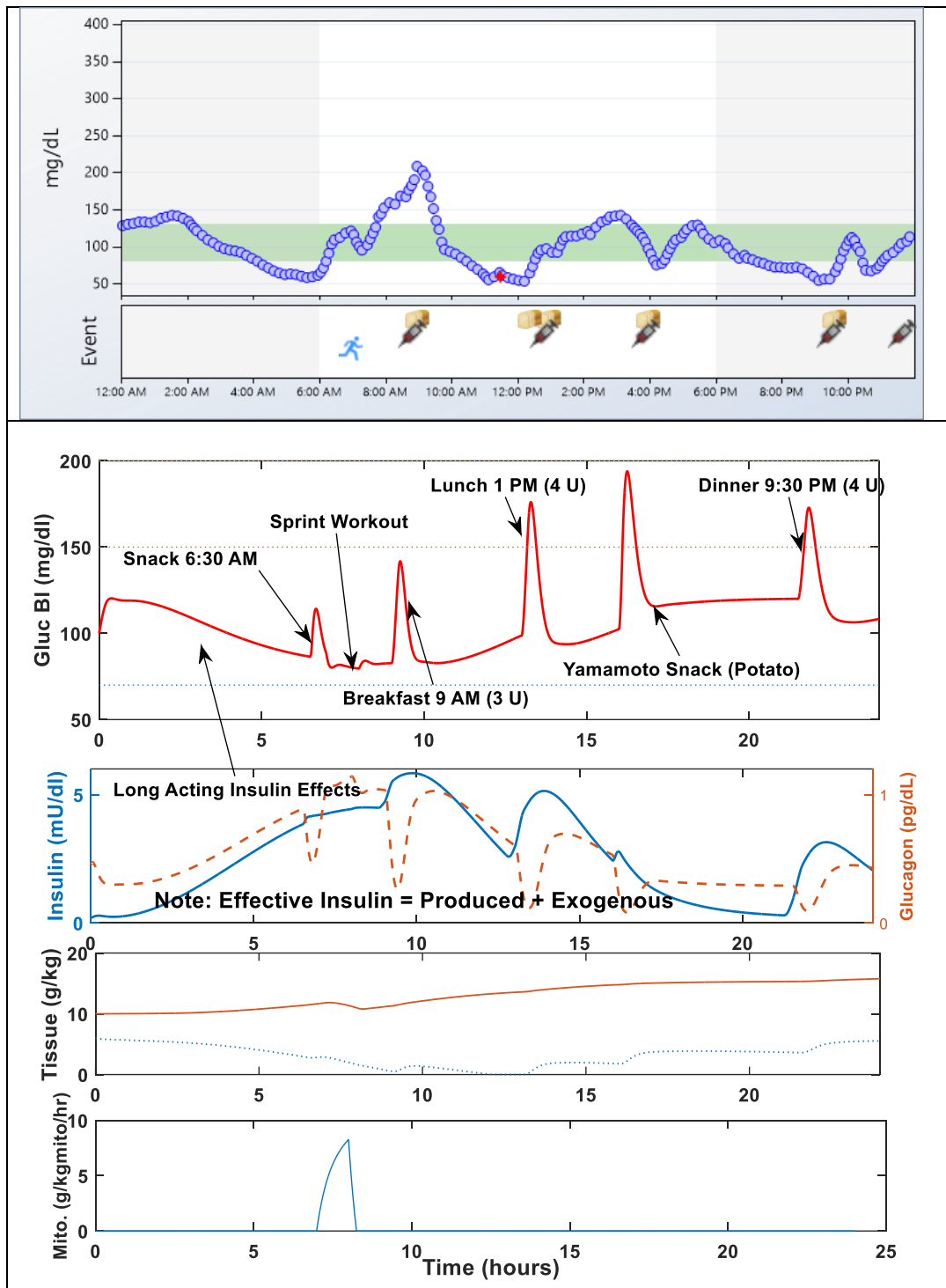
Figure 4.12: 24-Hour Case Study Simulation: Day 7. *(Top)* Dexcom Studio CGM plot for Protocol 7 (July 7, 2015), indicating CHO intake, insulin, and exercise. BG is plotted vs. Time. (***Bottom***) Model replication of Protocol 7 showing BG, effective insulin (amount produced with ratType1i = 0.2 + exogenous), tissue states, and mitochondrial effect.

Table 4.9: Protocol Day 7 Meal Content

Meal 1	Meal 2	Meal 3	Meal 4					
FOOD	**GI**	**Calories (kcal)**	**Serving**	**CHO (g)**	**Fiber (g)**	**Available CHO (g)**	**Fat (g)**	**Protein (g)**
Fiber One Protein	30	120	1 bar	17	5	12	6	6
Banana	60	100	1 banana	25	3.1	21.9	0	0
Eggs	0	140	2 eggs	0	0	0	8	12
Bread ,2 slices	60	140	2 slices	28	3	25	2	2.5
Peanut Butter	14	105	1 tbs	3.5	1	2.5	8.5	3.6
Grapes/ Berries	60	105	1 cup	28	0.5	27.5	0	0
Yoplait Strawberry	35	170	6oz	33	0	33	1.5	7
Cheese	0	110	1/3 cup	0.5	0	0	9	7
Turkey	0	60	4 slices	4	0	4	1.5	7.6
Kashi GoLean Crunch	55	95	1/2 cup	18	6	12	1.5	10
Instant Potato	83	333.6	67.3 g	50	3	47	12.6	5.6
Quinoa	53	174.75	3/4 cup	35	4	31	4	8
Chicken	10	200	4 oz	10	0	10	3	33.3
Bell Peppers	27	50	300g	8.4	3	5.4	0.6	3.6
Red Wine	15	130	1 glass	5	0	5	0	0
TOTALS		2033.4		265.4	28.6	236.3	58.2	50.2

Table 4.10: Protocol Day 7 Meal Duration and GI

Meal Duration	Meal 1	Meal 2	Meal 3	Meal 4
Time (min)	10	10	6	15
GI	65.4	50	83	43.9

4.5   Sensitivity Analysis

Sensitivity analysis was performed similar to Section 3.6 with sensitivity

coefficients calculated according to the following equation, varying each parameter

by +/- 10% (Lehman et al, 1982):

$$\frac{(B_+ - B_-)/B_o}{(P_+ - P_-)/P_o}.$$

Inputs are outlined in Table 4.11 below for the subject in the Phase 2 Case Study.

Table 4.11: Sensitivity Analysis Inputs (Subject: BW = 65 kg, rattype1i = 0.2)

Anaerobic Exercise Simulation	Aerobic Exercise Simulation	Snack + Exercise Simulation

• 2-Hour Lifting Workout (Case Study 2 Protocol Day 8)
  ○ 7:00-9:00 AM
• Bouts of 800 kcal/hr exertions informed by HR input
	• 2.5 Hour Long Run (Case Study 2 Protocol Day 4)
	  ○ 7:00-9:30 AM
	• 500-600 kcal/hr informed by HR input
		• 1 Hour Tempo Run (Case Study 2 Protocol Day 1)
		  ○ 7:00-8:00 AM
		• 15g CHO snack at 6:30 (kfast = 0.8, fraccarbs = 0.8)
		  ○ No insulin

It was determined from Appendix 7.6.2 that glucagon controllers were sensitive. Figure 4.13 below shows over plotted trajectories of varying Cga, the non-muscle glucagon controller for exercise protocol 2: circuit training. Other sensitive parameters included non-muscle and muscle GLUT2/GLUT4 gradient parameters, Kg2Max and Kmintol (X_g), tissue mass and basal tissue metabolism (X_{nm}), demand-based Hill saturation parameter Kmxex (all states) and insulin d-action (X_i). The subject Type 1 ratio was also varied in Figure 4.13 for the long aerobic exercise simulation (Protocol Day 4), demonstrating the effect if a subject's exact insulin production is not known. This estimate is often a function of the amount of insulin a T1D must take to maintain daily BG within the healthy range. Table 4.12 quantifies this sensitivity.
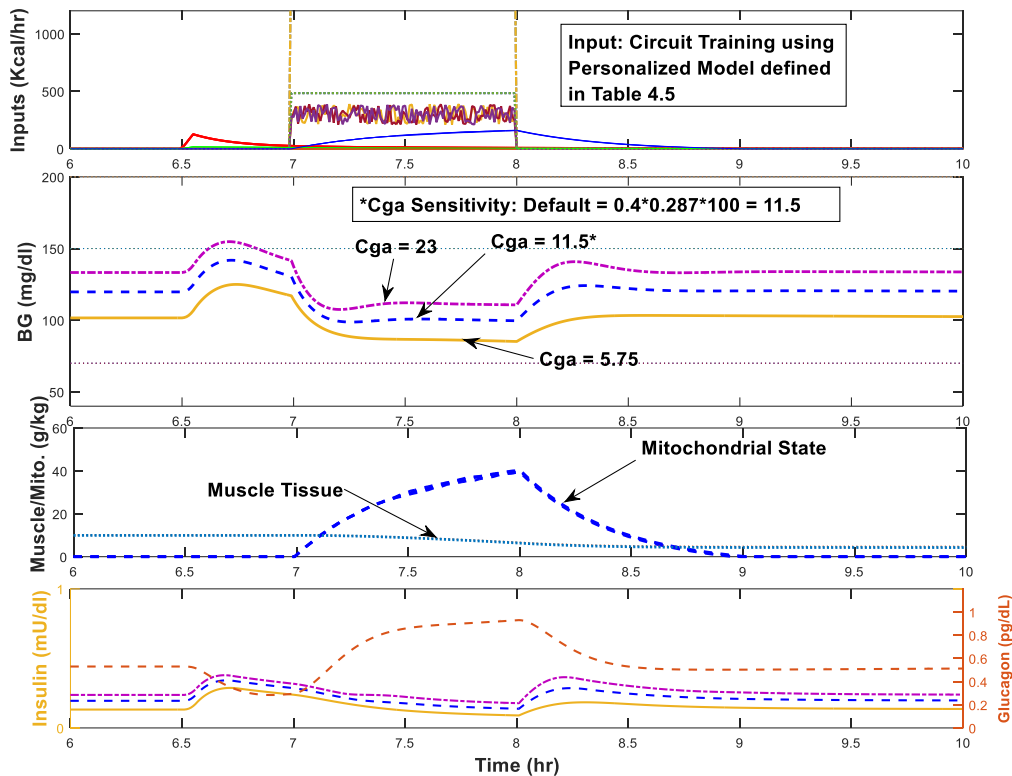
Figure 4.13: Model Sensitivity to Glucagon Control. Model sensitivity to Cga, the glucagon controller using the personalized model and parameters defined in Table 4.5.
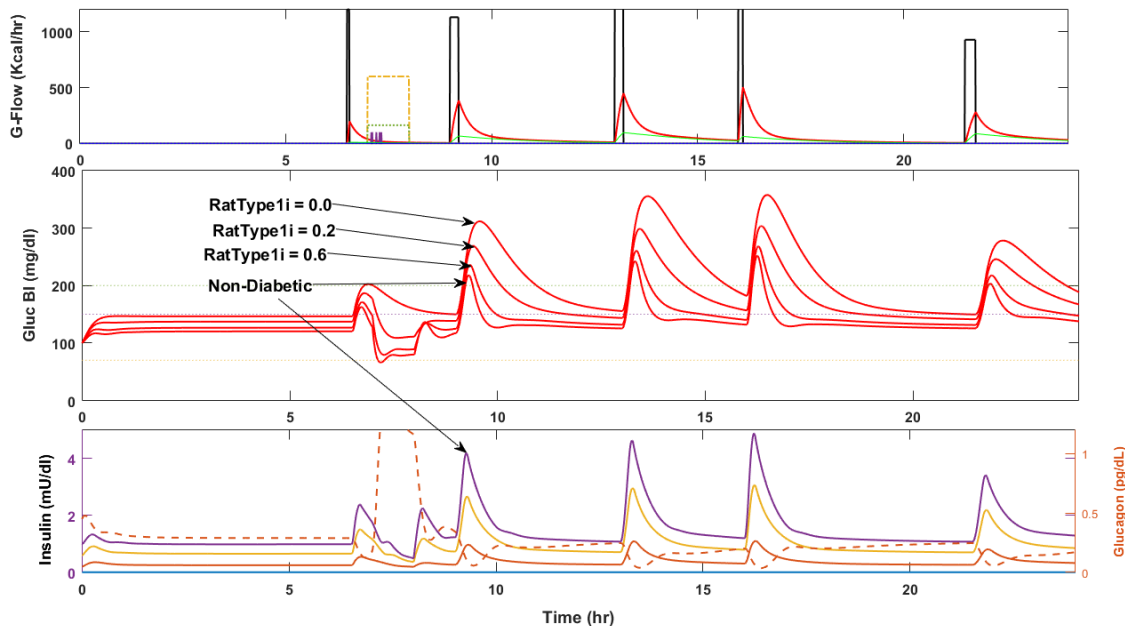
Figure 4.14: Model Sensitivity to Type 1 Diabetic Variations. Model sensitivity to ratType1i, the T1D ratio of remaining insulin production. Simulation is of 24-hour day 7, circuit training, similar to Figure 4.11 above.

Table 4.12: Sensitivity Coefficients for Parameter RatType1i*

	Xg	*Xnm*	*Xm*	*Xi*	*Xgn*	*Xmito*
Xmax	-2.20	0.00	-3.45	2.46	-5.03	-0.32
Xmin	0.00	-0.14	0.08	0.82	0.29	0.02
Before Exercise (6:30 AM)	-0.20	0.17	0.57	0.59	-0.13	0.02
During Exercise (8:00)	-2.11	0.34	2.08	2.97	-7.99	-0.16
Recovery (9:30)	-2.18	0.43	-4.71	2.48	-8.68	-0.30

*Long aerobic exercise simulation

4.6 *Personalized Parameters for Muscle Compartment and Trained Individuals*

Based on Section 4.4.2, particularly Figure 4.10, there are vast differences in

BG response to aerobic and anaerobic exercise due to reasons discussed in Section

4.2 including training effects. Training zones from Table 4.6 also are used to inform

u3 perceived exertion based on HR and % of VO2max. The 10th state, X_{mito}, was

added after some exercise effects, i.e. hyperglycemia at the onset and with high-

stress situations, could not be replicated in the Schunk-Winters model. The addition

also allows for GLUT4 action to bring glucose into muscle tissue when a *u3* input is

not occurring—this is a more realistic demand-based approach.

Section 4.3.2 outlined personalized parameters used for simulations to

replicate case study data. These values were decided after analyzing case study

results; however, were presented in 4.3.2 to outline parameters used for model

simulations throughout Section 4.4. Figure 4.15 shows a model comparison by

overplot of the new, personalized model for the case study subject compared to the

prediction using only default values. Values used were outlined in Section 4.3.2. The

only exception is a heart rate input, *u5*, is used in both cases, as opposed to only a

predicted *u3* for the default case.
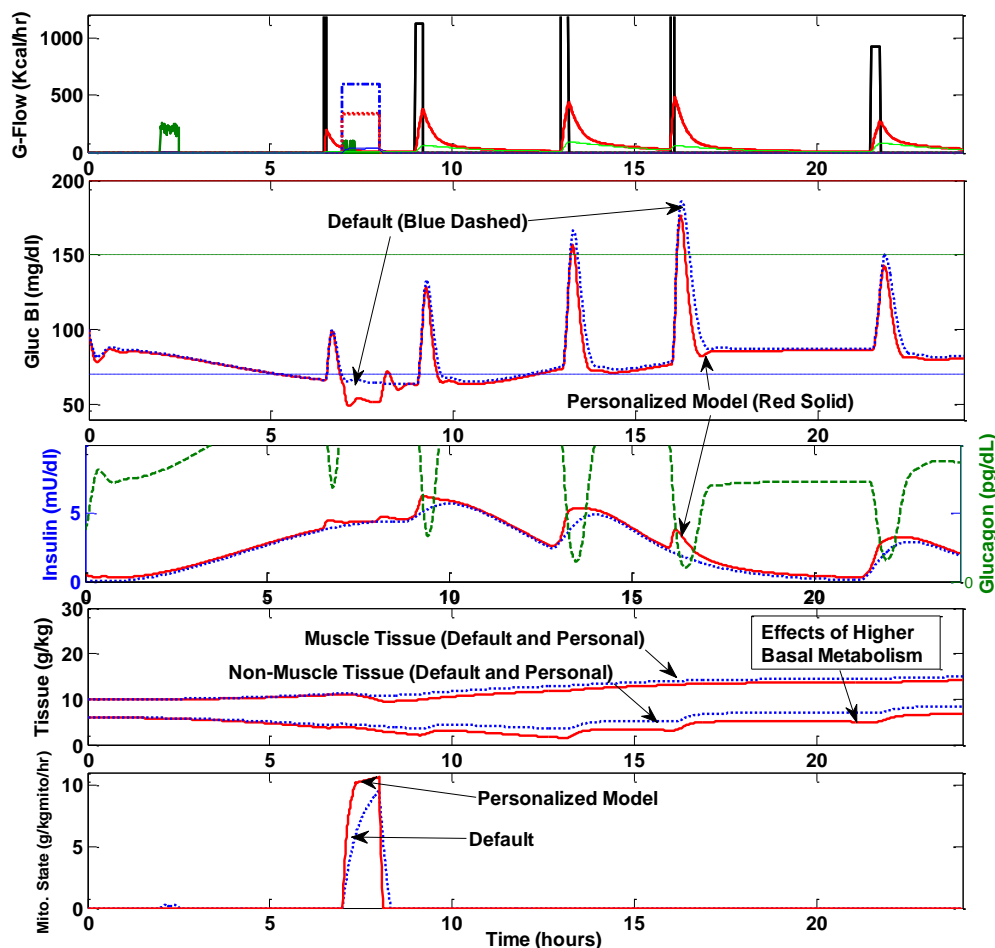
Figure 4.15: Comparison of Default and Personalized Model. Case study day 5 (Sprint Training) using default vs. personalized parameters described in Table 4.6.

4.7 Discussion

The aim of Chapter 4 is to form a basis for adaptive personalized modeling, to

further develop algorithms for those with T1D that live an active lifestyle. This could

potentially enable a CGM to have higher accuracy in predicting 'trends' or where BG

is headed based on external exercise inputs, body composition parameters, and overall lifestyle habits.

Meal effects were one area of focus for Phase 2 results, particularly in regard to digestive and insulin state model validation. Chapter 3 (Section 3.5) highlights some key results, comparing to literature. Here the focus was on controlled meal and snack inputs, often tied closely with studies from this literature, and often designed in tandem with exercise protocols (e.g., a snack a certain time prior, or a sustained lunch a few hours subsequent to exercise). Key insights can be seen in glycogen replenishment with post-exercise meals, which varied on the basis of exercise type and lingering sensitivity effects. Other insights further continued model validation for low vs. high GI food effects particularly in regard to Yamamoto (2014) snack simulation days. For example, the post-exercise meal after high-intensity circuit training did not elevate BG as significantly as the same post-exercise meal for the bike and run moderate aerobic protocol—BG levels remained below 140 mg/dL, whereas they became elevated close to 160 mg/dL post-aerobic. Insights here relate to total glucose consumption and glycogen depletion during exercise—it seems that on a time-dependent basis, anaerobic components of exercise present a lingering glycogen-depleting effect. Additionally, throughout all protocol days, low GI mixed meals again proved (as in Phase 1) to be the best option for BG management if a reduced amount of insulin intake is desired. For example, in comparing barley consumption on Day 3 of Phase 2 (GI = 25) vs. an instant white potato on Day 7 (GI = 83), BG remained significantly below the 'high' range for barley as opposed to the white potato. Additionally, hypoglycemia occurred about 2

hours post-potato—insulin was still in effect, but little to no slow absorbing carbohydrates from the potato were present.

Pre-test data involving the DXA body composition test and VO2max stress test point out differences of trained vs. untrained individuals recognized throughout the exercise physiology field. Particularly, muscle mass is close to and perhaps exceeds greatly non-muscle mass (or, only fat mass based on DXA results), resting HR is significantly lower, and VO2max and respective training zones are significantly higher (Tables 4.5 and 4.6 and Appendix 7.5). Trained individuals are more efficient in terms of energy utilization and typically demonstrate higher mitochondrial volume, which implies an ability to rely more heavily on sustained fat oxidation, especially in trained *endurance* athletes with adequate fat available as fuel (see Section 4.2.2). These phenomena are indicative of a need to characterize these adaptations and to design a model that has the capability for personalization— current models lack ability to model the flow of glucose as a source of energy for an athletic individual, particularly in regard to sports with varying intensities and durations.

Case study phase 2 was designed to better quantify differences in exercise type in terms of BG fluctuations, as well as characterize predictors for these changes (i.e. heart rate, level of training, fed state, etc.). After initial observation from Phase 1, Figure 4.10 made it clear that there is some anticipatory 'stress' effect that often results in hyperglycemia during intense exercise. Phase 2 confirmed the presence of this effect, particularly with fluctuations during circuit training, sprint intervals, and anaerobic lifting (see Figure 4.11). The original model was limited to only predict

generic end results—mainly, BG decrease due to glucose flux into the muscle compartment. Although the rate of which this decrease occurred as well as the magnitude could be quantified, there was no ability to show BG variation *during* exercise or post-exercise during recovery. The addition of the 10th mitochondrial state made this possible, especially for exercise involving aerobic components, as there is now a demand-supply mechanism between BG and tissue that can occur without activity or exercise present. The mitochondrial state is plotted in Figures 4.10 and 4.11 for varying types of inputs. Long endurance aerobic exercise showed a significant magnitude increase in mitochondrial action, as expected—primary energy is resultant from a fuel-mix and higher fat utilization in the personalized model. Long anaerobic efforts demonstrated a faster rate of mitochondrial consumption, but at a reduced magnitude than aerobic. Sprint training demonstrated the highest rate and magnitude of mitochondrial consumption and most significant decrease in muscle glucose. This idea is validated by CGM clinical data, as fluctuations ensue, but resulted in lowest ending BG level of the four protocol sessions. Sprint training has a high intensity aerobic component, despite rest periods. Additionally, tempo run training and combined bike/run protocols had varying mitochondrial consumption, particularly if effort variation occurred (i.e. at the end of tempo training). Circuit training showed high mitochondrial action for the personalized model, as expected due to higher mitochondrial volume.

It is important to note that sprint training HR data, Protocol Day 7, was not fully representative as HR was not recorded for the first four rest periods. The overall *u3* input that was used was shortened to match the HR duration, as well as

fluctuation characterization of just the recorded sprint events (i.e. *u3* informed).

This experimental limitation makes it difficult to capture BG effects shown in the

corresponding CGM data.

Figure 4.10 is important in comparing long endurance sessions, characteristic

of trained *endurance* athletes. Despite beginning snack and BG relatively constant,

different responses were elicited—a long aerobic workout was characterized by a

significant decrease in BG before settling at a steady value of around 65-70 mg/dl

with a steady (straight arrow) trend seen on the Dexcom G4 CGM. This is indicative

of the low to moderate intensity of running as a fuel-mix of fat and glucose energy

oxidation, thus conserving glucose. The average HR of 147 verifies this, as it falls in

Zone 3, or moderate aerobic, according to the subject's metabolic testing found in

Section 4.4. This trend continued for the entire 2.5 hour course (~19 mile run) with

a slight rise due to some fueling and other mechanisms such as hepatic production,

particular towards the end when stores become depleted. On the other hand, the

long anaerobic workout had a slightly different response, despite an initial trend of

decreasing BG similar to that of the long aerobic. In the anaerobic case, BG actually

elevated again after an initial decrease and continued to have fluxes throughout. The

overall trend and ending value was similar to that of long aerobic—around 75

mg/dl. The fluctuations are most likely due to varying intensities and fuel source

throughout, as HR was inconsistent (hence, zones do not apply here). Often, during

quick bursts of activity, there is an inefficient burning of glucose and hence a

separate form of glycolysis (i.e. without oxidation) is used for ATP production. Our

model has the ability to predict this with utilizing a low level *u3* input

simultaneously with the **u4** anaerobic activity input, as well as mitochondrial consumption.

In comparison of exercise type and intensity variation with constant duration (1 hour), Figure 4.11 provides CGM data of an athletic subject to quantify these variations. HR is also indicative of the varying intensity and exercise type in each case. It is clear that sprint intervals and circuit training have fluxes and even 'severe' cases of hyperglycemia briefly (>140 mg/dl), unlike forms of aerobic exercise, such as the tempo and run/bike combination. Sprint training is modeled as a form of **u3** exercise, and hence is tuned with HR which is clear in Figure 4.11, model prediction (*right*), as the model is able to predict initial rises due to onset of increased intensity and reaching threshold HR. The model is reasonably valid for tempo aerobic activity, and including the bike/run protocol. As expected, a higher **u3** aerobic input is indicative of higher mitochondrial action and consumption.

However, in regards to circuit training, some fluctuations were 'missed' most likely due to the HR difference not being a significant enough deviation from the *u3* reference value, although differences can be seen in the mitochondrial state. Most importantly, BG was much higher than could be expected from an energetic model that emphasized glucose consumption during exercise. An additional hormonal input, **uHM**, scaled by a stressor ratio is proposed in Chapter 4, particularly on the basis of circuit training and anaerobic results. Upon first iteration of Figure 4.11, circuit training appeared to have a similar Schunk-Winters simulation response as to sprint training. The two exercise types are similar in concept (high intensity with bouts of rest), but not in terms of anaerobic vs. aerobic basis. Hence, *stressorrat*, a

parameter formed to scale added stress other than only HR fluctuation, was implemented for the circuit training simulation of Figure 4.11b by increasing the rate at which glucose leaves x_g from x_{nm} via the GLUT2 flux pathway in a multiplicative manner with **uHM**. *Greft* and *Kg2Max* also have an effect due to increased sensitivity (Table 3.13) and as parameters involved in the GLUT2 Hill functional. *Stressorrat* works to inform exercise of additional catecholamine action (and general sympathetic neural system drive) that may be present and to generate an added flux of glucose. Figure 4.11 now shows improved results, similar to that predicted by CGM clinical data. This input and parameter will be used for future exercise interactions involving HR fluctuation characterized by both aerobic and anaerobic componentry that cannot be predicted by HR-informed **u3** alone.

In the 24-hour Phase 2 case study CGM output and model simulation/replication (Figure 4.12), the effects of insulin due to assumption that the subject produces ~20% (and takes the rest via injection) are dominant. The model is a strong predictor in regard to magnitude and steady-state, as well as for exercise (circuit training is shown in the example). The model predicts meal magnitude and the 'drop' overnight in BG (both start at the same time). As in Chapter 3, it is recognized that insulin control is a bit faster than seen in CGM data and *some* literature sources, however trends remain consistent. Other confounding factors, such as exact GI, etc. could be source of error/limitation to the model.

Due to a bit of uncertainty in regard to *ratType1i* (i.e. how much insulin production remaining for a T1D is often guesswork based on daily insulin amount required), sensitivity analysis was performed. It is clear this parameter is sensitive,

making it an important model input. Other sensitive parameters include glucagon control, exercise-based muscle gradient, and basal metabolism parameters.

Sections 4.3.2 and 4.6 and Table 4.8 solidify the model's ability to predict BG in a personalized and adaptive manner. These parameters refer to those that can be changed with emphasis on an *athlete*, while the inputs are also key in regard to exercise type, intensity, duration, and HR which furthers model capabilities compared to current BG predictive modeling techniques. Figure 4.9 demonstrates the ability to adjust the amount of maximum fat consumption and its effect on glucose consumption input to the model—an important adjustment for trained individuals with higher fat oxidation capacity. This idea explains why long distance endurance athletes tend to avoid severe cases of hypoglycemia as there is less reliance on BG for energy when fat can be used as a primary substrate during moderate intensity (i.e. 500 kcal/hr) for an extended period of time as seen in Protocol Day 8 CGM data (Figure 4.10). BG declines at the onset of a 2.5 hour running session, but tends to steady at around 75 mg/dl without any risk of hypoglycemia, assuming the subject is well-fed and maintains moderate intensity (i.e. does not start sprinting and elevating HR).

Figure 4.15 of Section 4.6 provides a key insight and summary of the purpose behind model personalization. Although the exercise session is small and meals are quite larger than normal for the simulated subject, it can be seen that even on an 'unhealthy' day, our model predicts that a trained individual demonstrates higher basal metabolism, higher aerobic capacity and potential for mitochondrial state consumption, and an overall more lifestyle-based and robust model.

As a result of personal experience, interactions with diabetes support and educational groups, endocrinologist's experience, and speaking with other elite athletes living with T1D, it is clear that adaptations and BG trends/management differ from many other T1D. Elite T1D athletes must use trial and error to predict BG and know what intensities/sports have the most drastic effect. In the future, a personalized model such as described here, augmented with adaptive learning algorithms to continually improve the personalized parameters, could work as a sort of "personal assistant" that provides ever-improving predictions that can help inform the athlete.

The Schunk-Winters model is not limited to athlete personalization—other parameters, such as GLUT2 gradient, tissue intolerance, and mass ratios can be adjusted for T2D implications and predictive of a more sedentary lifestyle. Additional applications involving conversion of excess glucose will be discussed in Chapter 5.

5. CONCLUSION AND FUTURE DIRECTIONS

Chapter 3, the general Schunk-Winters model, is intended for both research and clinical use, particularly diabetes educators, and to develop medical device technologies in order to eliminate guesswork of bolus corrections, often in error due to unknown food GI or exercise effects. This may help people with diabetes manage BG with exercise, diet, and dual-hormonal control based on algorithm feedback. Chapter 3 provides a model that can take a wider variety of lifestyle inputs than most CGM and artificial pancreas designs, enhancing where BG is headed *before* it occurs. For example, a device working under the Schunk-Winters default model would inform a person eating a 50g low GI meal vs. a 50g high GI meal differently, and furthermore make different predictions based on different consumption times for the same meal content. It can then be used to inform a person or an artificial pancreas algorithm to adjust any insulin bolus given—other models do not do this and hypoglycemia may occur in the low GI and slow consumption case, if the same insulin amount is taken for both high and low GI of the same CHO amount.

As discussed in Section 3.4.7, additional hormonal controllers may provide increased control in addition to strictly glucagon and insulin. Oftentimes, gradients of glucose to blood plasma exist, without means of foodstuff ingestion, etc. Additional hormone control could be categorized into 3 cases: 1) real-time rate controlling for both digestive rates (i.e. slow path) and glucagon tissue effects during periods of high BG, in particular slowing down glucose delivery fluxes (operating somewhat in tandem with insulin, e.g. similar to the role of amylin

hormone), 2) real-time 'anticipatory' for sympathetic nervous system "stress" effects, and 3) longer-term adaptive adjustments for energy storage.

The real-time anticipatory hormonal state would aid in quantizing stress hormones (catecholamine's such as epinephrine) and would most likely be a function of the GLUT2 non-muscle demand gradient, HR or other stress predictor. This concept was initiated in Sections 3.4.7 and a base implementation for this hormone, with additional input *uHM* and parameter *stressorrat,* acts as a multiplier of the GLUT2 bi-directional gradient for BG and non-muscle-tissue. With further tuning and other multiplying factors, the model now has capability of modeling inputted events that have an effect on BG other than foodstuff intake, activity, and exercise.

The third class is illuminated by 24-hour plus simulations and would be 'slow' due to excessive tissue glycogen buildup over time (e.g., over days, weeks, months) – an effect that can be highlighted in the present model because of framework glucose conservation. A steady state value at the end of a 24-hour day that is *consistently* higher than the initial value (which already may be high based on a previously simulated day) would indicate need for adaptive processes for dealing with excess glucose. This would involve characteristics similar to the hormone leptin, and would play a key role in the transport of excess glucose build up and tissue intolerance overtime, converting to fat (i.e. transport to the proposed fat compartment from BG). Such longer-term effects are especially relevant to study of the etiology of T2D.

Chapter 3 demonstrated that with proper modeling, there are in fact limitations with current device design, as with the initial GI example. This same idea can be applied to exercise, as indicated by the need of implementing *uHM.* For example, if a diabetic wearing a dual-hormonal controlled artificial pancreas begins high intensity exercise, a BG spike, or hyperglycemia, may occur. A device that does not account for exercise would provide insulin on the basis of elevated BG, which should not occur—a phenomenon known as a 'false high' to most diabetes educators. They recognize BG will most likely drop after exercise and that a corrective bolus should *not* be taken. However, if the educator is not present, a device should have this capability, as modeled in Chapter 3.

This was the motivation behind Chapter 4, which takes an important step towards extending the default BG regulation model of Chapter 3. By expanding personal input parameters and mechanisms such as ability to take external HR data and distinctions between exercise types, a 'library' of adaptive models can be formed. One example was shown in comparing the personalized model to the default in Section 4.6. By expanding a subject base, a majority of these curves could be built for *different* lifestyles. Once developed, as a form of adaptive learning, a particular user profile would drive overall trends and baselines with instantaneous inputs (i.e. meal GI, stress, and/or exercise) affecting immediate BG. Long-term, basal metabolism adjustment parameters play a role.

As discussed throughout Chapter 4, glucose and its conservation throughout the human body can, in most cases, single-handedly provide energy for human organ function and all processes. However, fat and protein are also key, with fat

breakdown as another energy source, along with fatty acid and protein supplementation. This can also affect the digestive state absorption parameters and fuel mix in regard to exercise. Although not a state in the model, fat consumption is subtracted off of total glucose exercise consumption and is increased in a trained individual. However, the addition of a 'fat' associated compartment and state could improve model capabilities and actually be modeled in conjunction with glucose consumption during exercise—i.e. completely quantifying 'fuel-mix' which occurs throughout daily activity, and especially with moderate intensity exercise. On the other hand, a fat compartment could provide a means of storage for excess glucose, thereby overcoming two model limitations: 1) fat buildup overtime and increase in BW and steady-state levels, as well as 2) a more personalized 'T2D' or 'unhealthy' lifestyle model.

An aim of the Schunk-Winters model is to take real-time glucose monitoring and experience from a T1D and aide in algorithm development for predictive modeling and artificial pancreas design in the future. Many opportunities exist to better improve current models, as most lack adaptation to athletes. As it stands, many elite T1D athletes are forced to learn by trial and error or through community advice, instead of relying on expensive medical devices which should provide this capability. Additionally, trends can be sport dependent. For example, T1D triathletes must take a separate approach for each sport in a multi-hour race. It is often noted in blog posts, etc. that one endurance sport can have vastly different BG response; for example, a runner who is *swimming* (i.e. their 'weaker' sport) would have a different **uHM** response during this portion than a practiced swimmer might. Other

factors also must be taken into account, such as body composition, fuel intake, and intensity. For this reason, programs such as the Diabetes Sports Project exist so as to better inform the diabetic population on BG effects and the difficulty in management during endurance sports of varying intensities, especially for those that are beginners (DSP, 2015). An algorithm such as the Schunk-Winters personalized model would be of interest so as to quantify effects and trends before they occur, thereby preventing trial and error.

Future versions could also involve the use of a Simulink (Matlab software extension) 'artificial pancreas' framework, as has been used throughout classroom design competitions. Future iterations and simulations could gain interactive insight from this Simulink framework, as it takes a multitude of inputs ranging from digestive foodstuff (and future GI additions), exercise, and body parameters. The ability for an interactive environment provides more efficient model personalization, as well as potential to be incorporated into a medical device.

Theoretically, algorithms such as those in Chapter 4 could also have market value for general, non-diabetic athletic performance. Algorithms would better inform performance, characterizing and predicting when one's blood glucose may be elevated, or, more importantly, when tissue is becoming depleted—therefore, proper timing for sports performance aides such as gels, drinks, etc. would be better informed. Chapter 3 demonstrates the importance of knowledge behind glycemic index control, as well as insulin type. Integrated into Chapter 4, modeling can inspire and inform sports performance for T1D athletes, as well as T2D beginning an exercise program, and potentially for non-diabetic population enhancement.

6. BIBLIOGRAPHY

Ahlborg G, Felig P, Hagenfeldt L, Hendler R, Wahren J. Substrate Turnover during Prolonged Exercise in Man. 1974;53:1080-1090.

American Diabetes Association. diabetes.org.

Aronoff SL. Glucose Metabolism and Regulation: Beyond Insulin and Glucagon. Diabetes Spec. 2004; 17(3): 183-189.

Befroy DE, Petersen KF, Dufour S, Mason GF, Rothman DL, Shulman GI. Increased substrate oxidation and mitochondrial uncoupling in skeletal muscle of endurance-trained individuals. PNAS. 2008; 105(43):16701-16706.

Berg JM, Tymoczko JL, Stryer L. Biochemistry. 5th Edition. New York: W H Freeman. 2002; 30.2.

Bergman RN, Phillips LS, Cobelli C. Physiologic evaluation of factors controlling glucose tolerance in man: measurement of insulin sensitivity and beta-cell glucose sensitivity from the response to intravenous glucose. J Clin Invest. 1981 Dec; 68(6):1456-67.

Boyadjiev N. Adaptation to submaximal physical training. Kinesiology. 2004; 2:154-164.

Brooks GA, Mercier J. Balance of carbohydrate and lipid utilization during exercise: the "crossover" concept. J of Appl Physiol. 1994; 76(6): 2253-2261.

Cobelli C, Mari A. Control of Diabetes with Artificial Systems for Insulin Delivery – Algorithm Independent Limitations Reveal by a Modeling Study. IEEE Trans Biomed Eng. 1985; 32 (10): 840-845.

Cobelli C, Dalla Man C, Breton MD. Physical Activity into the Meal Glucose—Insulin Model of Type 1 Diabetes: *In Silico* Studies. J of Diabetes Sci Technol. 2009; 3(1):56-67.

Costill DL, Fink WJ, Pollock ML. Muscle fiber compostioion and enzyme activities of elite distance runners. Med Sci Sports. 1976. 8: 96-100.

Dalla Man C, Cobelli C, Rizza RA. GIM, Simulation Software of Meal Glucose- Insulin Model. J of Diabetes Sci Technol. 2007; 1(3):323-328.

Dalla Man C, Cobelli C, Rizza RA . Meal Simulation Model of the Glucose-Insulin System. IEEE Trans Biomed Eng. 2007.

Dalla Man C, Micheletto F, Li D, Breton M, Kovatchev B, Cobelli C. The UVA/PADOVA Type 1 Diabetes Simulator: New Features. J of Diabetes Sci Technol. 2014; 8(1): 26-34.

Derouich, M., Boutayeb, A., 2002. The effect of physical exercise on the dynamics of glucose and insulin. J Biomech, 35, 911–917.

Diabetes Sports Project. *DSP.* 2015. http://www.diabetessportsproject.com/.

Dietary Reference Intakes for Energy, Carbohydrates, Fiber, Fat, Fatty Acids, Cholesterol, Protein, and Amino Acids (Macronutrients). The National Academy of Sciences, Institute of Medicine, Food and Nutrition Board. 2005.

Duun-Henriksen AK, Juhl R, Schmidt S, Norgaard K, Madsen H. Modeling the Effect of Exercise on Insulin Pharmacokinetics in "Continuous Subcutaneous Insulin Infusion" Treated Type 1 Diabetes Patients. DTU Compute Technical Report. 2013; 1-20.

Garcia A, Rack-Gomer AL, Bhavaraju NC, Hampapuram H, Kamath A, Peyser T, Facchinetti A, Zecchin C, Sparacino G, Cobelli C. Dexcom G4AP: An Advanced Continuous Glucose Monitor for the Artificial Pancreas. J Diabetes Sci Technol. 2013 Nov; 7(6): 1436-1445.

Gastin PB. Energy system interaction and relative contribution during maximal exercise. Sports Medicine. 2001; 37: 337-340.

Gesztelyi R, Zsuga J, Kemeny-Beke A, Varga B, Juhasz B, Rosaki A. The Hill equation and the origin of quantitative pharmacology. 2012; 66:427-438.

Guidelines for Exercise Testing and Prescription. 9th Edition. American College of Sports Medicine (ACSM). 2014.

Haidar A, Legault L, Dallaire M, Alkhateeb A, Coriati A, Messier V, Cheng P, Millette M, Boulet B, Rabasa-Lhoret R. Glucose-responsive insulin and glucagon delivery (dual-hormone artificial pancreas) in adults with type 1 diabetes: a randomized crossover controlled trial. CMAJ. 2013 Mar; 185(4): 297-305.

Harmer AR, Ruell PA, Hunter SK, McKenna MJ, Thom JM, Chisholm DJ, Flack JR. Effects of type 1 diabetes, sprint training and sex on skeletal muscle sarcoplasmic reticulum Ca^{2+} uptake and Ca^{2+}-Atpase activity. J of Physiol. 2013; 592(3):523-535.

Harmer AR, Chisholm DJ, McKenna MJ, Hunter SK, Ruell PA, Naylor JM, Maxwell LJ, Flack JR. Sprint training increases muscle oxidative metabolism during high-intensity exercise in patient with Type 1 Diabetes. Diabetes Care. 2008; 31(11):2097-2102.

Hernandez-Ordonez M, Campos-Delgado DU. An extension to the compartmental model of type 1 diabetic patients to reproduce exercise periods with glycogen depletion and replenishment, J Biomech, 41:744-752, 2008.

Holloszy JO. Muscle Metabolism during Exercise. Arch Phys Med Rehabil. 1982; 63: 231-234.

Holloszy JO. Regulation of Mitochondrial Biogenesis and GLUT4 Expression by Exercise. Compr Physiol. 2011; 1:921-940.

Holloszy JO, Coyle EF. Adaptations of skeletal muscle to endurance exercise and their metabolic consequences. J Appl Physiol. 1984; 56, 831-838.

Hovorka R, Shojaee-Moradie F, Carroll PV, Chassin LJ, Gowrie IJ, Jackson NC, Tudor RS, et al. Partitioning glucose distribution/transport, disposal, and endogenous production during IVGTT. Am J Physiol Endocrinol Metab. 2002 May; 282(5):E992-1007.

Hurley BF, Nemeth PM, Martin III WH, Hagberg JM, Dalsky GP, Holloszy JO. Muscle triglyceride utilization during exercise: effect of training. J of Appl Physiol. 1986; 60(2):562-567.

Jacobs PG, Youssef JE, Castle JR, Engle JM, Branigan DL, Johnson P, Massoud R, Kamath A, Ward WK. Development of a fully automated closed loop artificial pancreas control system with dual pump delivery of insulin and glucagon. IEE Conf Boston, Massachusetts. 2011; 397-400.

Janssen I, Heymsfield SB, Wang Z, Ross R. Skeletal muscle mass and distribution in 468 men and women aged 18-88 yr. J Appl Phys. 2000; 89: 81-88.

Jenkins DJA, Wolever TMS, Taylor RH. Glycemic index of foods: a physiological basis for carbohydrate exchange. Am. J. Clin. Nutr. 1981; 34, 362 – 366.

Rockl K, Witczak CA, Goodyear LJ. Signaling Mechanisms in Skeletal Muscle: Acute Responses and Chronic Adaptations to Exercise. IUBMB Life. 2015. 60(3): 145-153.

Kiens B, Essen-Gustavsson B, Christensen NJ, Saltin B. Skeletal Muscle Substrate Utilization during Submaximal Exercise in Man: Effect of Endurance Training. J of Physiol. 1993; 469: 459-478.

Kim J, Wei Y, Sowers JR. Role of Mitochondrial Dysfunction in Insulin Resistance. Ciruclation Research. 2008. 401-413.

Kjaer M. Epinephrine and some other hormonal responses to exercise in man: with special reference to physical training. Int J Sports Med. 1989; 10: 2-15.

Knoebel KL. Energy Metabolism. Physiology. Boston, MA: Little Brown & Co. 1984. 635-650.

Kovatchev B, Cobelli C, Renard E, Anderson S, Breton M, Patek S, et al. Multinational Study of Subcutaneous Model-Predictive Closed-Loop Control in Type 1 Diabetes Mellitus: Summary of the Results. J of Diabetes Sci Technol. 2010; 4(6): 1374-1381.

Lehman SL, Stark LW. Three algorithms for interpreting models consisting of ordinary differential equations: Sensitivity coefficients, sensitivity functions, global optimization. Mathematical Biosciences. 1982; 62(1): 107-122.

Li J, Kuang Y, Li B. Analysis of IVGTT glucose-insulin interaction models with time delay. Discrete Contin Dyn Syst Ser. 2001; 1: 103-124.

Li J, Kuang Y, Mason CC. Modeling the glucose-insulin regulatory system and ultradian insulin secretory oscillations with two explicit time delays. J of Theoretical Biol. 2006.

Maarbjerg SJ, Sylow L, Richter EA. Current understanding of increased insulin sensitivity after exercise –emerging candidates. Acta Physiol. 2011; 2002:323-335.

MacDonald MJ. Postexercise Late-Onset Hypoglycemia in Insulin-Dependent Diabetic Patients. Diabetes Care. 2006; 10:584-88.

Makroglou A, Li J, Kuang Y. Mathematical models and software tools for the glucose-insulin regulatory system and diabetes: an overview. Appl Numerical Mathematics, 2006; 56:559-573.

Melzer K. Carbohydrate and fat utilization during rest and physical activity. J Clin Nutr and Metab. 2011; 6: e45-e52.

Millan, I. Zone 2 Training for Endurance Athletes. Training Peaks, 2014.

Mohammed NH, Wolever TMS. Effect of carbohydrate source on post-prandial blood glucose in subjects with type 1 diabetes treated with insulin lispro. J Diabetes Research and Clinical Practice, 2004; 65:29-35. 8

Monro JA, Shaw M. Glycemic Impact, Glycemic Glucose Equivalents, Glycemic Index, and Glycemic Load: definition, distinctions, and implications. Amer J of Clinical Nutrition. 87(1):2375-2435.

Mukhopadhyay A, De Gaetano A, Arino O. Modeling the intra-venous glucose tolerance test: A global study for a single-distributed-delay-model. Discrete Contin Dyn Syst Ser, 2004; 2: 407-417.

National Diabetes Information Clearinghouse. Types of Insulin, Insert C. National Institute of Diabetes and Digestive and Kidney Diseases, National Institute of Health. 2012, http://diabetes.niddk.nih.gov/dm/pubs/medicines_ez/insert_C.aspx.

Neelakanta PS, Meta L, Roth Z. A Complex System Model of Glucose Regulatory Metabolism. Complex Systems. 2006.

Nielsen J, Holmberg HC, Shroder HD. Human skeletal muscle glycogen utilization in exhaustive exercise: role of subcellular localization and fiber type. J of Physiology. 2011: 2871-2885.

Northrop RB. Exogenous and Endogenous Regulation and Control of Physiological Systems. Chapman & Hall/CRC Press, Boca Raton FL., 2000.

Northrop RB. Introduction to Complexity and Complex Systems. CRC Press. 2011; 8, (4.2):258-277.

Ohlendieck K. Proteomics of skeletal muscle glycolysis. Biochimica et Biophysica Acta. 2010; 2089-2101.

Parillo J, Annuzzi G, Rivellese AA. Effects of meals with different glycaemic index on postprandial blood glucose response in patients with Type 1 Diabetes treated with continuous subcutaneous insulin infusion. Diabetic Med. 2011.

Powers S, Howley E. Exercise Physiology: Theory and Application to Fitness and Performance. 9th Edition. McGraw-Hill. 2014.

Richter EA, Hargreaves M. Exercise, GLUT 4 and skeletal muscle glucose uptake. Physiol Rev. 2013; 93:993-1017.

Roy A, Parker RS. Dynamic Modeling of Exercise Effects on Plasma Glucose and Insulin Levels. J of Diabetes Sci Technol. 2007;1(3):338-347.

Rynders CA, Angadi SS, Weltman NY, Gaesser GA, Weltman A. Oxygen uptake and ratings of perceived exertion at the lactate threshold and maximal fat oxidation rate in untrained adults. European Journal of Applied Physiology. 2011. 111: 2063-2068.

Sankaranarayanan S, Fainekos G. Simulating Insulin Infusion Pump Risks by *In-Silico* Modeling of the Insulin-Glucose Regulatory System. NSF Funded. 2012.

Sekigami T, Shimoda S, Nishida K, Matsuo Y, Ichimori S, Ichinose K, Shichiri M, Sakakida M, Araki E. Comparison between closed-loop portal and peripheral venous insulin delivery systems for an artificial endocrine pancreas. J Artif Organs. 2004 Feb; 7:91-100.

Shiavon M, Dalla Man C, Kudva YC, Basu A, Cobelli C. *In Silico* Optimization of Basal Insulin Infusion Rate during Exercise: Implication for Artificial Pancreas. J of Diabetes Sci Technol. 2013; 7(6):1461-1469.

Sorensen JT. A physiologic model of glucose metabolism in man and its use to design and assess improved insulin therapies for diabetes. Ph.D. Dissertation, Chemical Engineering Department, MIT, Cambridge. 1985.

Sturis J, Polonsky KS, Mosekilde E, Van Cauter E. Computer-model for mechanisms underlying ultradian oscillations of insulin and glucose. Amer J Physiol Endocrinol Metab, 1991; E801-E809.

Tonoli C. Effects of Different Types of Acute and Chronic (Training) Exercise on Glycaemic Control in Type 1 Diabetes Mellitus. Systematic Review: Sports Med. 2012; 42.

Walsh J, Roberts R, Heinemann L. Confusion Regarding Duration of Insulin Action: A Potential Source for Major Insulin Dose Errors by Bolus Calculators. J of Diabetes Sci Technol. 2014; 8(1) 170-178.

Wilinska ME, Chassin LJ, Schaller HC, Schaupp L, Pieber TR, Hovorka R. Insulin Kinetics in Type-1 Diabetes: Continuous and Bolus Delivery of Rapid Acting Insulin. IEEE Trans on Bio Eng. 2005; 52(1): 1-12.

Wolfe RR. Metabolic Interactions between glucose and fatty acids in humans. Amer Soc for Clinical Nutrition. 1998; 67.

Yamamoto Noguchi C, Furutani E, Sumi S. Mathematical model of glucose-insulin metabolism in Type 1 Diabetes including digestion and absorption of carbohydrates. SICE J of Control, Measurement, and System Int. 2014; 4(1) 001-007.

Yardley JE. Effects of Performing Resistance Exercise Before Versus After Aerobic Exercise on Glycemia in Type 1 Diabetes. Diabetes Care. 2012; 35.

Yavari A, Naiafipoor F, Aliasgarzadeh A. Effect of Aerobic Exercise, Resistance Training or Combined Training on Glycaemic Control and Cardiovascular Risk

Factors in Training or Patients with Type 2 Diabetes. Biology of Sport. 2012; 29.

7. APPENDICES

7.1 Model Parameters

Parameter	Value (default)	Literature Explanation	Units
Glucose Compartmental Flow			
bm	Varies (70)	Body Mass; for 70 Kg, muscle ~30, fat~15, brain ~1.3, liver ~1.4, blood plasma~3, RBC's ~2.2	Kg
wmu	Varies (30)	Body mass of muscle for normalizing f2	Kg
wnm	Varies (25)	Body mass of non-muscle for normalizing f3 (brain, liver, etc.)	Kg
ratBM	bm/70	Ratio of body mass to the default 70 Kg for scaling purposes	None
ratMUSC	wmu/30	Ratio for muscle relative to default value of 30 Kg	None
ratNONM	wnm/35	Ratio for non-muscle relative to default value of 35 Kg	None
ratmito	Varies (0.1)	Proportion of muscle mass that is mitochondria	None
wmito	ratmito*wmu	Mass of mitochondria	Kg
Stressrat	Varies (1.0)	Added stressor value for hormonal action, **uHM;** default of 1.0	None
kprop	0.2	Proportion of glucose consumption (activity) that reaches mitochondria	None
ratType1i	Varies	If Type 1, ratio of insulin still produced by beta cells; 1.0 = normal	Decimal %
ratType1g	Varies	If Type 1, ratio of glucagon still produced; 1.0 = normal	Decimal %
ratType2i	Varies	If type 2, ratio of insulin resistance	Decimal %
Ki	3.0	Insulin Elimination Rate	/hour
Kgt	1.0*0.287	Basal tissue elimination rate, scaled to grams	/hour
Knm_up	1.0	Non-Muscle Uptake (e.g. liver) without insulin signal	/hour
Grefi	70	Reference threshold of blood glucose in mg/dl for insulin control action; normal blood glucose is 80-120 and is cited in many sources	mg/dl
Grefg	110	Reference threshold of blood glucose for glucagon control action	mg/dl
Greft	90	Reference threshold of blood glucose for non-muscle flux direction (due to GLUT2)	mg/dl
Kg2Max	6.0	Maximum rate associated with non-muscle GLUT2 flux	/hr
Ktintol	12.0*ratNONM	Reference threshold for non-muscle tissue in mg/dl—estimated from J. Nielson's study before and after aerobic exercise	mg/dl

Kmintol	14.0*ratMUSC	Reference threshold for muscle tissue	mg/dl
Kbr**	((20/4(*ratNONM))	Blood glucose to steady consumption sink, no storage (mostly brain, also erythrocytes)	Kcal/hr/4 = g/hr
Metab	Varies (1.0)	Metabolism scaling; fit individuals range from 1.0-1.5 with default of 1.0	None
Gbt**	Metab*(10/4)*ratNONM	Basal elimination rate to non-muscle tissue scaled by amount of non-muscle tissue due to metabolism (but not brain)	g/hr
Gbm**	Metab*(6/4)*ratMUSC	Basal metabolic elimination rate to muscle tissue scaled by amount of muscle tissue	g/hr
Kbd	8*ratBM	Ratio of volume of blood plasma to volume of non-muscle tissue	(mg/dl)/g
wratm	(1/drat)/wmu	Scaling from glucose blood concentration (mg/dl) to glucose muscle tissue amount in grams, normal to mass of segment (g/Kg of muscle)	(g/kg)/(mg/dl)
Wratt	(1/drat)/wnm	Scaling from glucose blood concentration (mg/dl) to glucose non-muscle tissue amount in grams, normal to mass of segment (g/Kg of non-muscle)	(g/kg)/(mg/dl)
Gratm	0.01*wmu	Blood-Muscle Glucose Gradient (e.g. exercise demand)	mg/dl

Glucose Controllers

Cinm	0.3	Insulin Control Parameter, Non-Muscle Tissue; gain	None
Cim	0.4	Insulin Control Parameter, Muscle Tissue; gain	None
Cgnm	0.4*0.287*100	Glucagon Control Parameter, Non-Muscle Tissue scaled to pg/dl	Pg/dl
Cgm	0.001*0.287*100	Glucagon Control Parameter, Muscle Tissue scaled to pg/dl	Pg/dl
Kid	0.04	Derivative, d-action parameter	None
Insulindel	0.15	Delay of insulin action	Hours
Kg	0.4	P-Action for glucagon, from Cobelli	/hour
Kugf	5.0/ratBM	Forward rate (1/tau) of bolus (glucose-fast)	1/tau
Kugs	0.3/ratBM	Forward rate of bolus (glucose-slow)	1/tau
Kui	1.0/ratBM	Forward rate of bolus (insulin)	1/tau
Kgc	8	Glucagon Addition Rate	/hour
rat_ia	0.5 (varies)	Ratio of non-monomeric: to monomeric (slow:fast) insulin absorption paths	None
kai	0.02*60	Scaling for base rate constant (estimated from Cobelli, 2007)	
Ka2	rat_ia*kai	Rate constant of monomeric insulin absorption	/hour
Ka1	(1-rat_ia)*kai	Rate constant of non-monomeric insulin absorption	/hour
Kd	10*0.0164*60	Rate constant of insulin dissociation	/hour

Glucose Forward Mass Flow

drat	30	Conversion of digestive mass flow in grams into the blood	mg/dl
Kuga	2.0	Forward rate of bolus for slow glucose path; estimated with Cobelli model	1/tau
Kcarb	0.2	Carbohydrate scaling for dietary thermogenesis (normalized thermic effect of food)	

Gugf	0.98	Digestive effectiveness ratio, fast carbs	Decimal %
Gugs	0.88	Digestive effectiveness ratio, slow carbs	Decimal %
Exercise and Activity			
WorkEff	0.22 (varies)	Efficiency in performing physical work (typically 20-25%, higher for skilled tasks)	Decimal %
AerCap	1000 (varies)	Maximum capacity mapped to aerobic/mitochondrial metrics	Kcal/hr
Intens	Varies	Intensity of exercise out of maximum aerobic capacity	Kcal/hr
Kmusc	20.0	Rate of delivery to muscle	/hour
HRrest	Varies (60)	Resting heart rate	bpm
HRmax	Varies (180)	Maximum heart rate	bpm
Additional Hill Parameters			
K_{g2-Max}	10.0	Maximum Saturation for Glut 2 Pathway (muscle)	1/tau
k_{s-ex}	40.0	Half-way value for muscle gradient	1/tau
k_{mx-nm}	1.0	Maximum Saturation for Non-Muscle Intolerance	1/tau
K_{mx-m}	1.0	Maximum Saturation for Muscle Intolerance	1/tau
k_{s-ds}	5.0	Half-way value for slow digestive pathway (rising)	1/tau
k_{s-ds2}	10.0	Half-way value for slow digestive pathway (falling)	1/tau
k_{s-d}	5.0	Half-way value for fast digestive pathway (rising)	1/tau
k_{s-d2}	30.0	Half-way value for fast digestive pathway (falling)	1/tau
k_{s-ins}	12.0	Half-way value for endogenous insulin controller	1/tau
k_{s-gn}	2.0	Half-way value for endogenous glucagon controller	1/tau
hs_max	45	Maximum saturation for exogenous insulin infusion controller (magnitude)	1/tau
hs_ks	23	Half-way value for exogenous insulin infusion controller (magnitude)	1/tau
Hs_rate	20	Maximum saturation for exogenous insulin infusion controller (rate)	1/tau

**Add up to basal metabolism, e.g. Kbr+Gbt+G

7.2   Case Study Phase 1 Protocol

Case Study Control Protocol[a]

Time	Wednesday Protocol (4 consecutive weeks)
7:00 AM	Wakeup • 4 Units of Fast-Acting Insulin[f] (breakfast)
7:30 AM	Breakfast • GI =52.6 • 400 Calories • 55 g carbohydrates
10:30 AM	Snack (No Insulin) • GI = 70 • 120 Calories • 50 g carbohydrates
9:00 AM- 11:00 AM	Activity (soccer camp, walking, etc.)
12:30 PM	Lunch (5 units fast-acting insulin[f]) • 30 min. maximum • GI = 58 • 560 Calories • 66 g carbohydrates
2:30 PM	Exercise • Long, moderate aerobic running workout for 1 hour at 800 kcal/hr • Consistent distance (~8 miles)
4:15 PM	Snack (No Insulin) • GI = 20 • 100 Calories • 15 g carbohydrates
6:00-8:00 PM	Activity (beach volleyball…etc.) • Higher than morning activity
8:30 PM	Dinner (6 units fast-acting insulin[f]) • GI = 35 • 610 Calories • 65 g carbohydrates
Totals	• 15 Units Fast-Acting Insulin[f] • 14 Units Long-Acting Insulin[f] • 1800 Calories • 220 g carbohydrates

[a] BG was tested every 30 minutes upon waking, measured using a FDA approved glucose meter (OneTouch Ultra Mini, LifeScan Inc., Wayne, PA).
[b] Protocol 1 is control as outlined above.
[c] Protocol 2: high GI dinner with 690 calories (constant), 103 g carbohydrates (constant), and GI = 70.
[d] Protocol 3: track interval **anaerobic** running workout at 1100 kcal/hr with timing and duration constant.
[e] Protocol 4: lunch and exercise timing, with exercise occurring prior to lunch (snacks occur in same suit).
[f] Insulin dosage calculated based on clinical prescription of 1 unit per 12 g of carbohydrates.

7.3   Case Study Phase 2 Protocol

Dates: June 24-June 28, 2015, and July 5-July 9, 2015

IRB Approval: June 18, 2015

Simulation Day 1: 'Non-Exercise' Protocol 1 (Kotachev Morning Meal, Parillo Low Glycemic)
- Date: Monday, June 24, 2015
- 7:30 AM Breakfast: **KOTACHEV, CGM Simulation (starting night before)**
    - 50 g CHO bolus with optimal insulin bolus
        - Ensure Plus
    - GI = **44**
    - Total Calories = 350
    - Total Carbs = 50
    - Insulin = 4 U (following about a 1:15g CHO ratio; may be adjusted based on exercise)
- Fasting until ~ 1 PM to see full effects of meal
- 1 PM Lunch
    - **400 Calorie Meal A**
- 4 PM Snack (50 g CHO)
    - Yamamoto, White Bread
    - 50g CHO, 105 g portion size, GI = 76
- Dinner Meal Simulation Parillo Simulation-Starting BG: ~120 mg/dl
- See Excel Meal Substitute, Record time to replicate Day 5
    - Replicating Low GI: Pasta (90 g), beans (70g), Tomato (300 g), tuna fish (80g), olive oil(25g), apple(150g)
    - Meal Sub: Brown Rice, Chicken, Black Beans, Tomato/Veggies, Red Wine, Dark Chocolate
        - Total Cals: 796
        - Carbs: 102.4
        - GI = 36
- Bedtime at around 11 PM, Blood glucose around 120 mg/dl
- RECORD GI, TOTAL CHO INTAKE, TOTAL CALORIES, INSULIN IN EXCEL SPREADSHEET

Simulation Day 2: Exercise Protocol 1 (Aerobic Endurance Exercise)
- DATE: Thursday, June 25, 2015
- Wakeup 6 AM, adjust glucose levels accordingly
    - Banana and/or granola bar, **(15 g CHO typical)**
- 7 AM Run, <60 min. at moderate intensity continuously (~60% VO2max)
    - Thursday AM running group

- o Characterize intensity based on HR and VO2max test results
- 9 AM **Breakfast B (or equal amount)**
    - o Banana and/or similar fruit (calories, GI, etc.)
        - ▪ 100 calories, 25 g CHO, GI = 60
        - ▪ 0 g fat, 0 g protein
    - o 2 eggs
        - ▪ GI eggs = 0
        - ▪ 0 g CHO (eggs)
        - ▪ 8 g fat (eggs)
        - ▪ 8 g protein(eggs)
    - o Whole Wheat Toast (2 slices if eggs)1 TBS PB
        - ▪ 70 calories/slice
        - ▪ Toast, 1 wheat slices, 1 g fat, 14 g CHO, ~ 2 g protein, GI = 60
        - ▪ Peanut Butter = 105 calories, 8.5 g Fat, 3.5 g CHO, ~3.5 g protein, GI = 14
    - o GI = **57.1**
    - o Total Calories = 485 (eggs and toast)
    - o Total Carbs = 56.5 (eggs and toast)
    - o Insulin = 4 U (following about a 1:15g CHO ratio; may be adjusted based on exercise)
- Fasting until ~ 1 PM to see full effects of exercise + meal
- 1 PM Lunch (~400 kcal)
    - o **400 Cal Option A**
- 3 PM: Keep blood glucose consistent around **110 mg/dl (could change based on first day**
- 4 PM Snack (50 g CHO)
    - o Yamamoto protocol
        - ▪ Spaghetti, 50 g CHO portion (72.3g)
- Dinner (timing flexibility)
    - o About 800 Calories to fulfill daily calorie, protein, fat, CHO quota.
- Bedtime at around 11 PM, Blood glucose around 120 mg/dl

Simulation Day 3: **Exercise Protocol 2 (Circuit Training)**
- DATE: Friday, June 26
- Wakeup 6 AM, adjust glucose levels accordingly
    - o Banana and/or granola bar
- Circuit Training 7AM
    - o Work Capacity Circuit x 8
        - ▪ 100 Jump Rope, 20 Air Squats, 15 Push-Ups, 16 Step-Ups, 12 Burpees, 30 Full Sit-ups (1 round takes approx.. 3.5-4 minutes)
    - o This is routine to the subject and will be performed with a certified strength and conditioning coach at Marquette University.
- 9 AM **Breakfast B**
- Fasting until ~ 1 PM to see full effects of exercise + meal
- 1 PM Lunch (~400 kcal)

- o **400 Calorie Dalla Man Protocol (1 x BW in CHO = ~63 g CHO)**
- 3 PM: Keep blood glucose consistent around **110 mg/dl (could change based on first day**
- 4 PM Snack (50 g CHO)
  - o Yamamoto protocol
    - ▪ Barley, 50g CHO, 79.6 g portion size
- Dinner
  - o ~800 Calories or fulfill remaining nutritional goals
- Bedtime at around 11 PM, Blood glucose around 120 mg/dl

Simulation Day 4: **Exercise Protocol 3 (Long Aerobic Run)**
- DATE: Saturday, June 27
- Wakeup 6 AM, adjust glucose levels accordingly
  - o Banana and/or granola bar, **(15 g CHO typical)**
- 7 AM Run, ~1.5-2hr (or combined with 'brick' biking workout) at moderate intensity continuously (~60% VO2max)
  - o Lake Park with Badgerland Striders (14 miles)—subject to change
  - o Characterize intensity based on HR and VO2max test results
  - o Snack if subject starts to experience hypoglycemia (<60 mg/dl), 15 g CHO
- **Breakfast B (or equal amount) post-exercise**
- Fasting until ~ 1 PM to see full effects of exercise + meal
- 1 PM Lunch (~400 kcal)
  - o **400 Cal Option A**
- Afternoon/Nighttime (**Flexible)** Alcoholic Protocol Test
  - o 2-3 Alcoholic drinks recording CHO, timing, etc. This will be compared to the effect of only *one* drink resulting as part of a separate protocol day.
- **Remaining 2 meals will be based on individual's needs due to intense morning exercise. It will be important to record differences in choices/hunger effect of Days 4 and 8.**
- Bedtime and ending blood glucose flexible, but important for recording.

Simulation Day 5: **'Non-Exercise' Protocol 3 (Dalla Man, 2007, Parillo High GI)**
- DATE: Sunday, July 5
- 7:30 AM Breakfast: **KOTACHEV, CGM Simulation (starting night before)**
  - o 50 g CHO bolus with optimal insulin bolus
    - ▪ Ensure Plus
  - o GI = **44**
  - o Total Calories = 350
  - o Total Carbs = 50
  - o Insulin = 4 U (following about a 1:15g CHO ratio; may be adjusted based on exercise)
- Fasting until ~ 1 PM to see full effects of exercise + meal
- 1 PM Lunch- Kotachev, 75 g CHO meal (will repeat Day 7)

- o **Kotachev 75 g, 5 U insulin Simulation (~365 cal)**
- 4 PM Snack (50 g CHO)
  - o Yamamoto, Pineapple Juice
- 72.3 g portion size, 0.5 pg, GI = 46
- Meal Simulation #6: Parillo High Glycemic Index – Starting Glucose ~120
- Same time as Day 1 Dinner Meal
- See Excel Substitutes
  - o High GI: Rice, Artichoke, Tomato, Tuna Fish, White Bread, Banana
  - o Substitutions: White Rice, Chicken, Vegetables, Corn, ICEE from 711
- Bedtime at around 11 PM, Blood glucose around 120 mg/dl

Simulation Day 6: **Exercise Protocol 4 (Continuous Bike/Swim/Run <60 min.)**
- DATE: Monday, July 6, 2015
- Wakeup 6 AM, adjust glucose levels accordingly
  - o Banana and/or granola bar, **(15 g CHO typical)**
- 7 AM Workout, <60 min. at moderate intensity continuously (~60% VO2max)
  - o Characterize intensity based on HR and VO2max test results
- 9 AM **Breakfast B**
- Fasting until ~ 1 PM to see full effects of exercise + meal
- 1 PM Lunch (~400 kcal)
  - o **400 Cal Option A or similar**
- 3 PM: Keep blood glucose consistent around **110 mg/dl (could change based on first day**
- 4 PM Snack (50 g CHO)
  - ▪ Dalla Man, UVA/PADOVA Model Simulation
  - ▪ Protein bar, fulfilling 50 g CHO requirement
- Dinner (timing flexibility)
  - o About 800 Calories to fulfill daily calorie, protein, fat, CHO quota.
- Bedtime at around 11 PM, Blood glucose around 120 mg/dl

Simulation Day 7: **Exercise Protocol 5(Sprint Intervals)**
- Date: Tuesday, July 7
- Wakeup 6 AM, adjust glucose levels accordingly
  - o Banana and/or granola bar
- 7AM Sprint Intervals, < 60 minutes
  - o Track workout consisting of high intensity (~80-90% VO2max) intervals with full recovery in between
  - o 5x400's (1:15-1:20)
  - o 8x200's(35 seconds or faster)
- 9 AM Breakfast B
- Fasting until ~ 1 PM to see full effects of exercise + meal
- 1 PM Lunch (~400 kcal) –Repeated from Day 5
  - o **Kotachev 75 g, 5 U insulin Simulation (~365 cal)**

- 3 PM: Keep blood glucose consistent around **110 mg/dl (could change based on first day**
- 4 PM Snack (50 g CHO)
    - Yamamoto: Instant Potato, 50 g CHO, 67.3g
- Dinner- typical to subject, record first day and keep somewhat consistent or note variation
- Bedtime at around 11 PM, Blood glucose around 120 mg/dl

Simulation Day 8: Exercise Protocol 6 (Fatigue Inducing Anaerobic 'Brick')
- Performed last, in case of any lingering soreness. DATE July 8, 2015
- Wakeup 6 AM, adjust glucose levels accordingly
    - Banana and/or granola bar
- 7 AM Anaerobic (Lifting) Exercise Session (Duration 105 Minutes)
    - 4 sets of 8-10 seconds of heavy lifting exercise (last few repetitions should be stopped due to muscle fatigue and glycolytic limitations)
        - Set #1
            - Squats (50 kg), Pull-Ups (with 20 lb weight vest)
        - Set #2
            - Deadlifts (80 kg), Seated Rows (120 lbs)
        - Set #3
            - Push Press (35 kg), Back Extensions (10 kg)
        - Set #4
            - Cable Twists (10 kg), Split Lunges (100 lb)
        - Set #5
            - Hip Thrusters (90 kg), Kettle Bell Russian Twists (35 lb)
    - Significant rest between each set
        - 2-4 minutes
    - Bike sprint (gear 20 for 20 seconds) and row machine (8 pulls, ~10 seconds) in between each set
- Breakfast B (same time as Day 4)
- Fasting until ~ 1 PM to see full effects of exercise + meal
- 1 PM Lunch (~400 kcal)
    - **400 Cal Option A**
- Afternoon/Nighttime (**Flexible)** Alcoholic Protocol Test
    - 2-3 Alcoholic drinks recording CHO, timing, etc. This will be compared to the effect of only *one* drink resulting as part of a separate protocol day.
- **Remaining 2 meals will be based on individual's needs due to intense morning exercise. It will be important to record differences in choices/hunger effect of Days 4 and 8.**
- Bedtime and ending blood glucose flexible, but important for recording.

7.4   Logbook and Results

Recorded by CGM (replaced every 7 days; takes 2 hours to replace):
- Blood glucose (1 sample every five minutes)
  - TRENDS
- Calibration by finger prick every 12 hours
- Insulin amount and time stamp
- CHO amount and time stamp
- Exercise time and duration
  - Also record HR with Garmin

Recorded in EXCEL spreadsheet
- Meals/Food
  - GI, serving size, CHO, fat, protein

Summary Of Dates and Protocols Performed

Date	Main Protocol	Other Important Notes (Stress levels, etc.)
Day 1: June 24 (Wed)	Non-Exercise	*Minimal*
Day 2: June 25 (Thurs)	Aerobic < 60 min.	*Some midday*
Day3: June 26 (Fri)	Circuit Training <60 min.	*Yes- AM*
Day4: June 27 (Sat)	Intense Long Run/Brick	*Relaxing day*
Day5: July 5 (Sun)	Non-Exercise	*Some, driving to Chicago*
Day6: July 6 (Mon)	Swim (Flexible) < 60 min	*Stressful Working Day*
Day7: July 7 (Tues)	Sprint Training < 60 min	*Hard Workout*
Day8: July 8 (Wed)	Anaerobic Brick Workout	*Fluxes of Stress*

Approximate Caloric Intake Days 2, 3, 6, 7

Meal	Calories	CHO (grams)	Starting BG
1	~500 (Exercise)/ 350 (Non-Exercise)	50-56 g	100 $\pm$ 5 (before exercise), 85 $\pm$ 5 non-exercise
2	400 (+/-)	Varies	Dependent on protocol
3	200 (+/-)	50	120 mg/dl
4	800	Varies	Dependent on protocol
Total	1900		

*On days 4 and 8, caloric intake will be expected to be higher and will be documented accordingly.

Meal Timing

Meal	Exercise Day	Non-Exercise
1	9 AM	7:30 AM
2	1 PM	1 PM
3	4 PM	4 PM
4	Flexible	Flexible

Day Before Simulation Day 1

Day Before Protocol Set (Date: June 23)

Total Calorie and Carbohydrate Intake	1915 Calories, 256 g CHO
Exercise (Time/Intensity), Activity Level	Warmup strides, VO2max test Blood Lactate Levels: 1.5 and 18.8 mmol/L (before and after VO2max test) Schlitz Mile: 5:07, ~ 3 miles total with warm-up/cool-down
Food Logbook (and Insulin intake), Dinner should be similar to what is typical for subject and kept consistent throughout. **NOTE: For KOTACHEV Simulation, starting at 21:30, readings will need to be recorded**	Greek yogurt, 120 cal, 19 g CHO GoLean 1 cup, 220 cal, 41 g Peanut Butter, 1 TBS, 95 cal, 3 g Coffee Turkey Sandwich, 220 cal, 25 g CHO Pretzels, 220 Cal, 46 g CHO Coconut Water, 90 cal Nature Valley Bar, 140 cal, 10 g Chocolate Blueberries, 100 cal, 14 g Riesen, 40 cal, 7 g Banana, 100 cal, 23 g Beer, 300 cal, 20 g PB, 90 cal, 3 g ½ cup brown rice, 110 cal, 23 g 2 emergenc, 70 cal, 16 g bell peppers/tomatoes, 50 cal, 5g almond milk, 40 cal
Blood Glucose Level Before Bed (mg/dL)	76

Simulation Day 1- Non- Exercise Protocol 1

Description: Non-Exercise 1, Kotachev morning meal and Parillo Low GI

Protocol Day 1, Date: June 24 *(Dexcom Studio, half of this day saved as 6/24/14)*

Blood Glucose and Time of Wake-up, Breakfast Option	7:30 AM Ensure Plus Nutritional- wakeup 7 AM (4 U insulin at 7:20); 6 grapes 5 AM (low BG)
Lunch Notes	Insulin 10 min before with a few almonds; 4 U for 62 g; however only 70 mg/dl
3 PM Blood Glucose, adjusting for 4 PM Snack—Note this value and replicate	Yamamoto, White Bread ; 102—had a peach ~14 g total to get to 120 (NOTE: Insulin 4U) 5 min before; Before starting: BG 98 mg/dl (had to have a caramel at 4:45 since low!)
Food/Insulin/BG levels before dinner protocol and correction needed to reach 120 mg/dl ± 5 mg/dl	Grapes/cheese as snack to increase BG Start at 116 mg/dl Unfortunately a LATE dinner due to JDRF event (8:50 PM insulin, 6 U), ate at 9:06 PM NEW dinner window: 6:30 – 9 PM
Calibration Times and Levels/ Status of CGM and Sensor	Morning 7 AM, within 2 mg/dl; 8:30 PM, within 6 mg/dl
Blood Glucose Level Before Bed (mg/dL)	103
Total Daily Calorie, CHO, Fat, Protein Intake, GI	1965 Cal, 281 g CHO, 25 g Fat, 90 g Protein

FOOD	GI	Calories	SERVING SIZE	CHO (g)	Fiber (g)	Available CHO	FAT (g)	PROTEIN(g)	LOAD
Grapes	60	34	10 grapes	9	0.5	8.5	0.1	0.4	5.4
Ensure Plus	44	350	1 bottle	50	0	50	11	13	22
Turkey	0	60	4 slices	4	0	4	1.5	7.625	0
Bread ,2 slices	60	140	2 slices	28	3	25	2	2.5	16.8
Spinach	0	25	1/2 cup	3.5	0.7	2.8	0.5	1.625	0
Pretzels	83	100	1 oz	22	0.9	21.1	0	3	18.26
Almonds	7	80	0.5 OZ	4.5	2	2.5	6.5	2.5	0.315
Peach	28	59	1 peach	14	2.2	11.8	0.4	1.4	3.92
White Bread	71	250	105g (~4 slices)	50	0	50	3	8	35.5
Brown Rice	65	220	1 cup cooked	46	3.5	42.5	2	4.5	29.9
Chicken	10	200	4 oz	10	0	10	3	33.25	1

Black Beans	40	105	1/2 cup	21	15	6	0	5.25	8.4
Tomato/ Carrots	45	51	300 g	8.4	0.5	7.9	0.6	3.6	3.78
Red Wine	15	130	1 glass	5	0	5	0	0	0.75
Dark Chocolate	40	90	2 pieces	12	1.5	10.5	6	1	4.8
Celery/PB	14	105	1 tbs	3.5	1	2.5	8.5	3.625	0.49
Totals		1965		281.9	30.8	260.1	45	90.9	

Meal Duration	Meal 1	Meal 2	Meal 3	Meal 4
Time (min)	1	10	5	15
GI	44	64	71	59
CHO	50	62	50	102
FracCarbs	0.57	0.61	0.8	.51
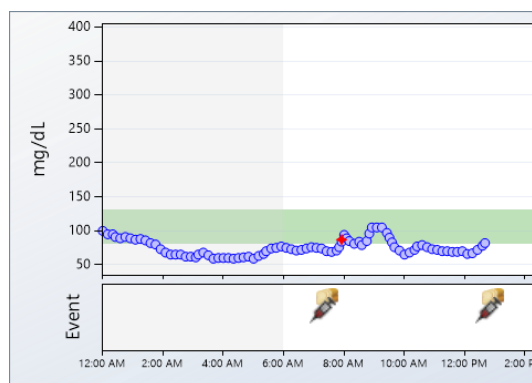
Wednesday, June 24, 2015

7:20 AM	Insulin 4 units
7:30 AM	Carbs 50 grams
12:50 PM	Insulin 4 units
1:00 PM	Carbs 62 grams
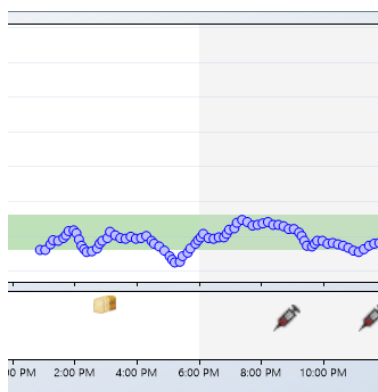
Tuesday, June 24, 2014

3:00 PM	Carbs 15 grams
8:52 PM	Insulin 4 units
11:36 PM	Insulin 12 units

Simulation Day 2- Exercise Protocol 1
Description: Aerobic Endurance Exercise <60 minutes Running

Date: June 25 (6/25/14 In Dexcom Studio)

Blood Glucose at 6 AM, Correction Needed to reach 100 ± 5 mg/dl	97—Cascade Farms granola bar (and a few banana chips) BG seemed slightly uncalibrated
Soreness and Fatigue Present?	No—a bit fatigued during
HR Before Exercise	After Warmup: 130
Peak HR	180
Average HR	162
Training Zone	3
Post-Exercise Meal	Hot Shower 8:35; 4 U insulin at 8:50, breakfast at 9:00 AM; Low glucose alarm at 11:00 AM (was actually 75)
BG at 1 PM lunch, corrections needed?	4 U, 119 mg/dl, took a bit late @ 12:54; ate at 1:00 (1:04 so 10 min post-insulin)
3 PM Adjustment to get BG to around 100 mg/dl (consistent each week)	Was ~120, took 2 U and ate a peach 3:15—111 mg/dl, 3:55—92, 4 U 5 min before
4 PM 50 g CHO snack	Yamamoto, Spaghetti
Dinner Notes and Timing (Note the flexibility here)	109 mg/dl (116 night prior); Insulin at 7:55, BG was a bit higher since had some chocolate (originally for dinner). however; started at similar value to 6/24, took 5 U and ate at 8:00 PM
Calibration Times and Levels/ Status of CGM and Sensor	Was off around 3 PM (registered too low) so calibrated
Total Daily Calorie, CHO, Fat, Protein Intake, GI	1990 cal, 293 g CHO, 37 g Fat, 90 g Protein
Blood Glucose Level Before Bed (mg/dL)	~116, steady, bed at 10:00

FOOD	GI	Calories	SERVING SIZE	CHO (g)	Fiber(g)	Available CHO	FAT (g)	PROTEIN(g)	LOAD
Cascade Farms Granola	30	90	1 bar	15	1	14	2.5	2	
Banana	60	100	1 banana	25	3.1	21.9	0	0	15
Eggs	0	140	2 eggs	0	0	0	8	12	0
Bread ,2 slices	60	140	2 slices	28	3	25	2	2.5	16.8
Peanut Butter	14	105	1 tbs	3.5	1	2.5	8.5	3.625	0.49
Grapes	60	105	1 cup	28	0.5	27.5	0	0	16.8
Greek Yogurt	33	140	1	15	0	15	0	12	4.95
Kash GoLean	55	142.5	3/4 cup	27	8	19	2.25	3.5625	14.85
Peach	28	59	1 peach	14	2.2	11.8	0.4	1.4	3.92
Spaghetti	41	270	72.3g	50	6	44	2	9	20.5
Chicken	10	200	4 oz	10	0	10	3	33.25	1
Black Beans	40	155	3/4 cup	30	20	10	0	7.875	12
Bell Peppers	45	50	300 g	8.4	0.5	7.9	0	0	3.78
Dark Chocolate	40	90	2 pieces	12	1.5	10.5	10	0	4.8
Red Wine	15	130	1 glass	5	0	5	0	0	0.75
Barley	25	160	1/3 cup uncooked	37	5	32	0.5	5	9.25
TOTALS		1986.5		292.9			36.65	90.2125	

Meal Duration	Meal 1	Meal 2	Meal 3	Meal 4
Time (min)	6	8	6	15
GI	65	60	47	42

Over Time ▾   Customize ▾

● Elevation   ⤢
1,000
750   661 ft
500
250
        4:10   8:20   12:30   16:40   20:50   25:00   29:10   33:20   37:30   41:40   45:50

● Pace   ⤢
0:00
10:00   Avg: 8:58 min/mi
20:00
        4:10   8:20   12:30   16:40   20:50   25:00   29:10   33:20   37:30   41:40   45:50

● Heart Rate   ⤢
200
150   Avg: 147 bpm
100
        8:20   12:30   16:40   20:50   21:00   29:10   11:20   37:30   41:40

Stats   Splits   Segments

Distance	Heart Rate	Elevation
6.34 mi Distance	**bpm** % of Max Zones	**254 ft** Elev Gain
		241 ft Elev Loss
Calories	**162 bpm** Avg HR	**581 ft** Min Elev
633 C Calories	**188 bpm** Max HR	**661 ft** Max Elev
	4.9 Training Effect ⓘ	

Timing

Pace   Speed

46:07
Time

46:02
Moving Time

1:02:02
Elapsed Time

7:16 min/mi
Avg Pace

7:16 min/mi
Avg Moving Pace

2:01 min/mi
Best Pace
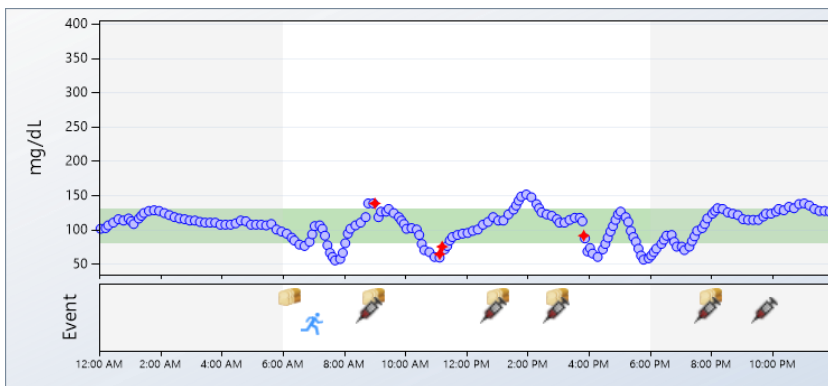
Thursday, June 25, 2014	
6:15 AM	Carbs 15 grams
9:00 AM	Carbs 56 grams
8:50 AM	Insulin 4 units
12:54 PM	Insulin 4 units
1:04 PM	Carbs 67 grams
3:00 PM	Carbs 14 grams
2:58 PM	Insulin 2 units
8:02 PM	Carbs 100 grams
7:55 PM	Insulin 5 units
7:00 AM	Tempo Run (50 minutes)
9:47 PM	Insulin 11 units

Simulation Day 3- Exercise Protocol 2
Description: Circuit Training at Al

Date: June 26 (Dexcom 6/26/14…Thursday)

Blood Glucose at 6 AM, Correction Needed to reach 100 ± 5 mg/dl	72, had granola bar (15g) and some berries; higher, ~135
Soreness and Fatigue Present?	No
HR Before Exercise	96 bpm
Peak HR	183 (spikes with circuits)
Average HR	164
Training Zone	3
Post-Exercise Meal	4 U at 8:50, had some low calorie Gatorade

BG at 1 PM lunch, corrections needed?	No—steady at 80; 4 U at 12:50, same lunch as 6/24
3 PM Adjustment to get BG to around 120 mg/dl (consistent each week)	~94 mg/dl, steady, no adjustments
4 PM 50 g CHO snack	Yamamoto, Barley
Dinner Notes and Timing (Note the flexibility here)	Dinner earlier, during USA game—hungrier today as well. 4 U at 7:10, dinner ~7:20, BG around 84 mg/dl
Calibration Times and Levels/ Status of CGM and Sensor	Had a low alarm at 5:30, maybe due to hot shower? It was actually 67 (not <55); otherwise, daily readings were accurate
Total Daily Calorie, CHO, Fat, Protein Intake, GI	1950 cals, 270 g CHO, 45 g Fat, 28 g Protein
Blood Glucose Level Before Bed (mg/dL)	116 mg/dl @ 10:45

Meal 1	Meal 2	Meal 3	Meal 4							
FOOD	GI	Calories	SERVING SIZE	CHO (g)	Fiber(g)	Available CHO	FAT (g)	PROTEIN (g)	LOAD
Cascade Farms Granola	30	90	1 bar	15	1	14	1	14	2.5
Banana	60	100	1 banana	25	3.1	21.9	0	0	15
Eggs	0	140	2 eggs	0	0	0	8	12	0
Bread ,2 slices	60	140	2 slices	28	3	25	2	2.5	16.8
Peanut Butter	14	105	1 tbs	3.5	1	2.5	8.5	3.625	0.49
Turkey	0	60	4 slices	4	0	4	1.5	7.625	0
Bread ,2 slices	60	140	2 slice	28	3	25	2	2.5	16.8
Spinach	0	25	1/2 cup	3.5	0.7	2.8	0.5	1.625	0
Pretzels	83	100	1 oz	22	0.9	21.1	0	3	18.26
Almonds	7	80	0.5 OZ	4.5	2	2.5	6.5	2.5	0.315
Barley	25	215	79.6g	50	5	45	1	7	12.5
Dove Dark Blueberries	50	200	42g	28	2	26	10	2	14

Black Beans	40	105	1/2 cup	21	15	6	0	5.25	8.4
Red Wine	15	130	1 glass	5	0	5	0	0	0.75
Chicken	10	200	4 oz	10	0	10	3	33.25	1
Corn Tortillas	52	120	2 tortillas	23	2	21	1.5	2	11.96
TOTALS		1950		270.5			45.5	98.875	

Meal Duration	Meal 1	Meal 2	Meal 3	Meal 4
Time (min)	8	6	4	15
GI	65.36437247	63.85379061	27.77777778	53.10294118
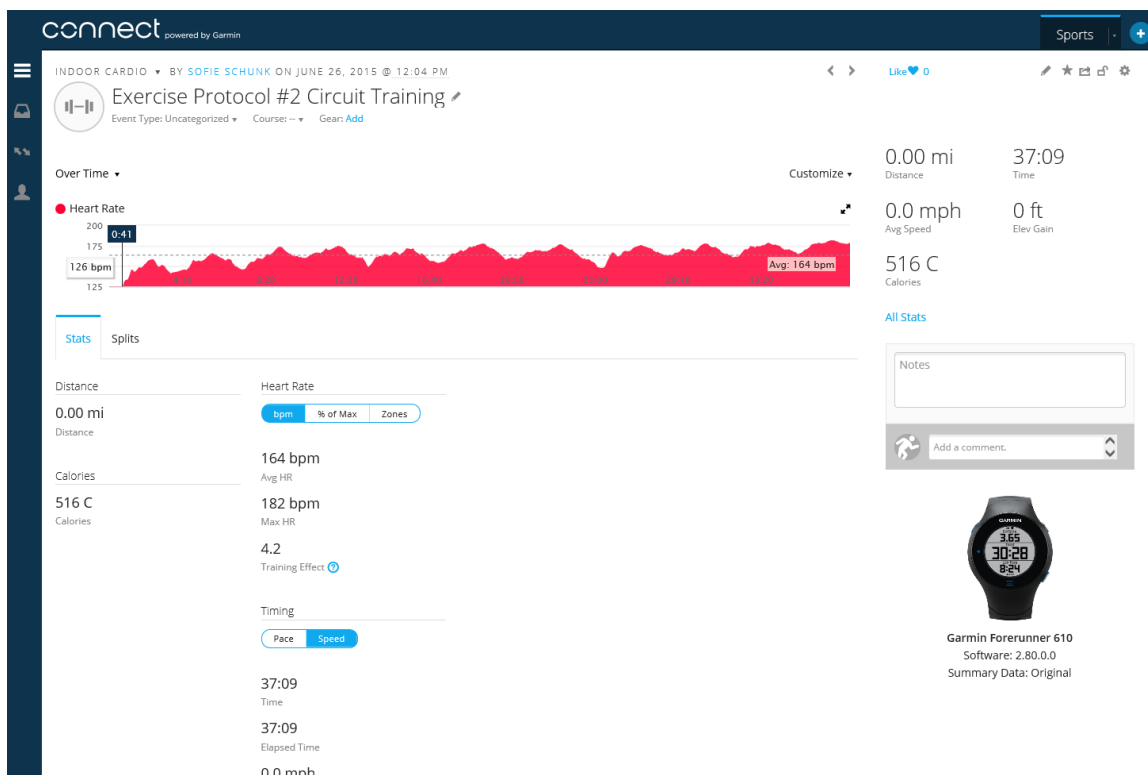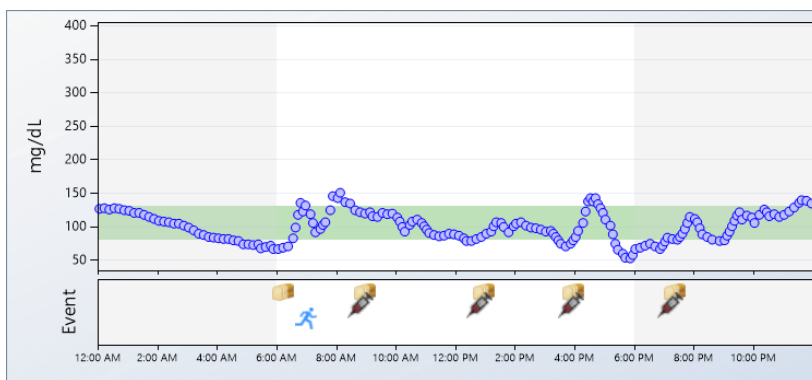
Thursday, June 26, 2014

9:00 AM	Carbs 56 grams
6:15 AM	Carbs 15 grams
8:50 AM	Insulin 4 units
7:02 AM	Exercise Medium (40 minutes)
12:50 PM	Insulin 4 units
1:00 PM	Carbs 63 grams
4:00 PM	Carbs 50 grams
3:55 PM	Insulin 4 units
7:23 PM	Carbs 85 grams
7:15 PM	Insulin 4 units

Simulation Day 4- Exercise Protocol 2
Description: Fatigue-Inducing Long Aerobic Brick Workout

Date: June 27 (Long Run, 19 miles, 2 hr 30 minutes)

Blood Glucose at 6 AM, Correction Needed to reach 100 ± 5 mg/dl	72, had granola bar (same one) and handful banana chips at 6:15; spiked to 144
Soreness and Fatigue Present?	Yes, back and arms, but did not affect running
HR Before Exercise	120
Peak HR	165
Average HR	150

Training Zone	3
Post-Exercise Meal	10:20, with insulin (4 U) at 10:10
BG at 1 PM lunch, corrections needed?	2:20 lunch, steady @ 92, no corrections but only 3 U since walking/exercising
3 PM Adjustment to get BG to around 120 mg/dl (consistent each week)	N/A (Cappucino, no insulin before, at 2:00 before lunch)
Dinner Notes and Timing (Note the flexibility here)/ Alcohol Protocol	Low BG around 5 PM, grapes and corona, no insulin; Dinner at Belair—tortilla chips appetizer (6:30), Insulin 4 U, 2 tacos—mahi mahi and Korean beef each with 2 corn tortillas Beers at Downer, Strawberry Margarita 2 Beers at bar after
Calibration Times and Levels/ Status of CGM and Sensor	Well Calibrated; left CGM in car from 11:50-12:20
Total Daily Calorie, CHO, Fat, Protein Intake, GI	2700 Calories, 321 g CHO, 52 g Fat, 97 g Protein
Blood Glucose Level Before Bed (mg/dL)	150 mg/dl @ midnight

Meal 1	Meal 2	Meal 3	Meal 4						
FOOD	GI	Calories	SERVING SIZE	CHO (g)	Fiber(g)	Available CHO	FAT (g)	PROTEIN(g)	LOAD
Cascade Farms Granola	30	90	1 bar	15	1	14	1	14	2.5
Almond Milk	0	80	1 Cup	4	1	3	2.5	2	
Watermelon	72	50		10	1	9	0	1	7.2
Banana	60	100	1 banana	25	3.1	21.9	0	0	15
Eggs	0	140	2 eggs	0	0	0	8	12	0
Bread ,2 slices	60	140	2 slices	28	3	25	2	2.5	16.8
Peanut Butter	14	160	1.5 tbs	5	1	4	12.5	7	0.7
Cappuccino	25	100	12 oz	12	0	12	4	8	3
Grapes	60	105	1 cup	28	0.5	27.5	0	0	16.8
Greek Yogurt	33	140	1	15	0	15	0	12	4.95
Kash GoLean	55	142.5	3/4 cup	27	8	19	2.25	3.5625	14.85

VegaOne Protein		90	23.3 g	4	0	0	0	15	0
Grapes	60	105	1 cup	28	0.5	27.5	0	0	16.8
Corona light	15	105	12 0z	5	0	5	0	0	0.75
Margarita	45	160	1 glass	15	0	15	0	0	6.75
Belair Tacos	52	450	2 tacos	40	2	38	15	20	20.8
Tortilla Chips	55	200	20 chips	40	1	39	5	0	22
Fat Tire	20	320	24 0z	20	0	20	0	0	4
TOTALS		2677.5		321	22.1	294.9	52.25	97.0625	

Meal Duration	Meal 1	Meal 2	Meal 3	Meal 4
Time (min)	6	10		20
GI	65	60		51.8556701

Garmin Forerunner 610
Software: 2.80.0.0
Elev Corrections ⓘ: Enabled ▾
Summary Data: Original

Distance

19.00 mi
Distance

Calories

1,511 C
Calories

Heart Rate

[bpm] [% of Max] [Zones]

147 bpm
Avg HR

164 bpm
Max HR

3.5
Training Effect ⑦

Timing

[Pace] [Speed]

2:30:00
Time

2:30:02
Moving Time

2:42:48
Elapsed Time

7:54 min/mi
Avg Pace

7:54 min/mi
Avg Moving Pace

6:19 min/mi
Best Pace

Elevation

561 ft
Elev Gain

567 ft
Elev Loss

581 ft
Min Elev

699 ft
Max Elev
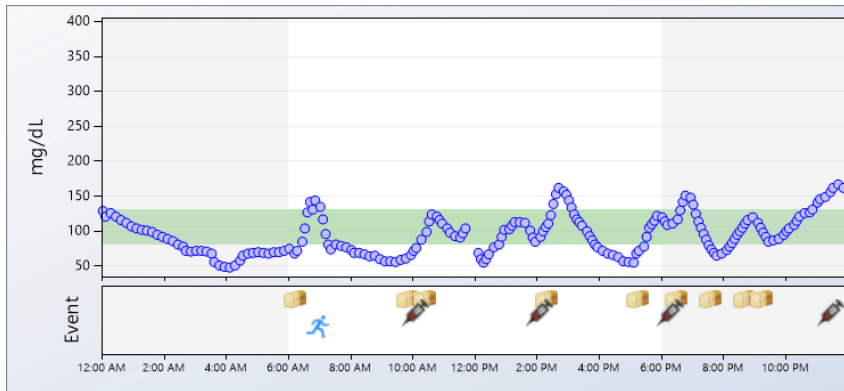
Friday, June 27, 2014	
6:15 AM	Carbs 15 grams
9:53 AM	Carbs 10 grams
7:00 AM	Exercise Light (150 minutes)
10:08 AM	Insulin 4 units
10:25 AM	Carbs 56 grams
2:07 PM	Insulin 3 units
2:20 PM	Carbs 60 grams
6:30 PM	Carbs 77 grams
6:20 PM	Insulin 4 units
5:17 PM	Carbs 15 grams
7:36 PM	Carbs 10 grams
8:43 PM	Carbs 10 grams
9:16 PM	Carbs 10 grams
11:30 PM	Insulin 11 units

Day Before Simulation Day 5

Date: July 4

Total Calorie and Carbohydrate Intake	2630 cals, 299 g CHO
Exercise (Time/Intensity), Activity Level	6 miles easy run with Lauren and Megan, low intensity
Food Logbook (and Insulin intake), Dinner should be similar to what is typical for subject and kept consistent throughout. **NOTE: For KOTACHEV Simulation, starting at 21:30, readings will need to be recorded**	PB (2 Tbs), 190 cals, 4 CHO Pretzels, 200 cals, 25 g CHO GoLean 190 cals, 40 g CHO Shrimp/Smoked Salmon, 200 cals, Chicken Noodle Soup, 140 cals, 20g Sourdough Bread, 210 cals, 43 g 4 Chocolates, 210, 21 g Banana, 100, 15 Bloody Mary, 120, 4 g Wine, 120, 2 g Chips/guac, 280 cals, 40 g Cake (small), 200 cals, 30 g Coors Light, 200 cals, 8 g Chicken Tenders, 170, 14 g Quinoa, 100, 15 g
Blood Glucose Level Before Bed (mg/dL)	126

Simulation Day 5- Non- Exercise Protocol 2
Description: Non-Exercise 1, Kotachev morning meal and Parillo High GI

Date: July 5

Blood Glucose and Time of Wake-up, Breakfast Option	7:30 AM Ensure Plus Nutritional (late night before, had some snacks); 187—high! slight exercise to ~80
Lunch Notes	In car driving, 4 Units, 12:50, 75 g Kotachev (added turkey)

3 PM Blood Glucose, adjusting for 4 PM Snack—Replicate Day 1 Value	Yamamoto, Pineapple Juice Somewhat up in the air BG At 3 PM—115 to 125 Fresh (premium brand) 100% juice
Food/Insulin/BG levels before dinner protocol and correction needed to reach 120 mg/dl ± 5 mg/dl	Went low at 5:45, had a bit of juice, rose to 81 Insulin, 6 U (consistent with Day 1) at 7:50 PM Dinner at 8:00 PM (Parillo High Glycemic) Low at 9:30—pretzels and PB
Calibration Times and Levels/ Status of CGM and Sensor	Within Range
Blood Glucose Level Before Bed (mg/dL)	~120, rose with grapes, pretzels
Total Daily Calorie, CHO, Fat, Protein Intake, GI	2016 cals, 296 CHO, 49.6 g fat, 50 g protein

Meal 1	Meal 2	Meal 3	Meal 4						
FOOD	GI	Calories	SERVING SIZE	CHO (g)	Fiber (g)	Available CHO (g)	FAT (g)	PROTEIN (g)	LOAD
Ensure Plus	44	350	1 bottle	50	0	50	11	13	22
Banana	60	100		25	3.1	21.9	0	0	15
Yoplait Strawberry	35	170	6oz	33	0	33	1.5	-28.125	11.55
Cheese	0	110	1/3 cup	0.5	0	0	9	7	0
Turkey	0	60	4 slices	4	0	4	1.5	7.625	0
Kashi GoLean Crunch	55	95	1/2 cup	18	6	12	1.5	-10.875	9.9
Tortilla Chips	55	100	8 chips	25	1	24	5	0	13.75
Pineapple Juice	46	160	72.3 g	50		50			23
White Rice, Instant	89	200	1 cup	40	2	38	3	4	35.6
Chicken	10	300	6 oz	0	0	0	14	43.5	0
Tomato/Veggies	27	51	300g	8.4	3	5.4	0.6	3.6	2.268
Corn	60	120	5.5v oz	28	12	16	0.5	0.875	16.8
Chobani Tube	85	100	2 tubes	15	0	15	2	10	12.75
Pretzels	83	100	1 oz	22	0.9	21.1	0	3	18.26
TOTALS		2016		318.9	28	290.4	49.6	53.6	

Meal Duration	Meal 1	Meal 2	Meal 3	Meal 4
Time (min)	1	5	3	15
GI	44	51.41043724	46	90.6155914
CHO (g)				91.4
FracCarbs				47.4
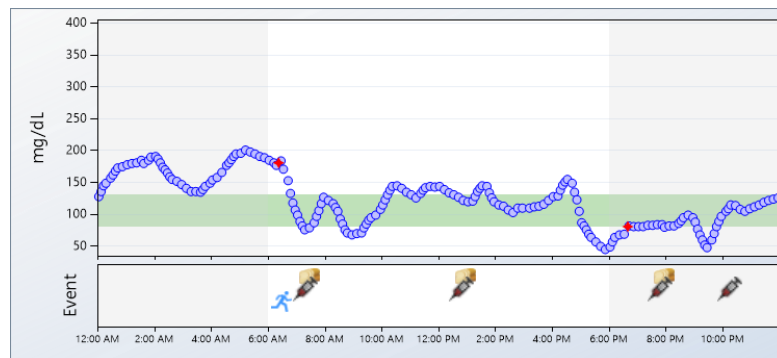
Sunday, July 5, 2015	
7:20 AM	Insulin 4 units
6:30 AM	Exercise Light (30 minutes)
7:30 AM	Carbs 50 grams
12:50 PM	Insulin 4 units
1:00 PM	Carbs 75 grams
7:50 PM	Insulin 6 units
8:00 PM	Carbs 100 grams
10:18 PM	Insulin 11 units

Simulation Day 6- Exercise Protocol 4
Description: Continuous Bike/Swim/Run <60 min

Date: July 6 (Bike 10 mi, Run 2 mi..45 minutes total)

Blood Glucose at 6 AM, Correction Needed to reach 100 ± 5 mg/dl	84, half of a granola bar; 115 at 6:40
Soreness and Fatigue Present? Exercise Chosen	No
HR Before Exercise**	119
Peak HR	~150? (HR monitor died, used app on phone)
Average HR	143
Training Zone	2
Post-Exercise Meal	BG slightly rising, 4 U insulin at 8:50
BG at 1 PM lunch, corrections needed?	~125, consistent from breakfast, 4 units

3 PM Adjustment to get BG to around 120 mg/dl (consistent each week)	~75, checked late (3:55—4 U insulin)
4 PM 50 g CHO snack	Dalla Man, UVA/PADOVA (Protein/ Granola Bar) Low at 5:45, 10 g CHO (pretzels)
Dinner Notes and Timing (Note the flexibility here)	Insulin, 5 U at 7:05 Dinner @7:15 PM
Calibration Times and Levels/ Status of CGM and Sensor	12 mg/dl, low during morning calibration
Total Daily Calorie, CHO, Fat, Protein Intake, GI	~2000 (1940), 261 g CHO, 51 g fat, 108 g Protein
Blood Glucose Level Before Bed (mg/dL)	125 mg/dl

**NOTE: Exercise was redone in order to get HR data

Meal 1	Meal 2	Meal 3	Meal 4						
FOOD	GI	Calories	SERVING SIZE	CHO (g)	Fiber (g)	Available CHO (g)	FAT (g)	PROTEIN (g)	LOAD
Fiber One Protein	30	120	1 bar	17	5	12	6	6	**5.1**
Banana	60	100	1 banana	25	3.1	21.9	0	0	15
Eggs	0	140	2 eggs	0	0	0	8	12	0
Bread ,2 slices	60	140	2 slices	28	3	25	2	2.5	16.8
Peanut Butter	14	105	1 tbs	3.5	1	2.5	8.5	3.625	0.49
Grapes	60	105	1 cup	28	0.5	27.5	0	0	16.8
Greek Yogurt	33	140	1	15	0	15	0	12	4.95
Kashi GoLean	55	142.5	3/4 cup	27	8	19	2.25	3.5625	14.85
Luna Protein Bar	33	350	2 Bars	48	7	41	11	21	15.84
Quinoa	53	174.75	3/4 cup	35	4	31	4	8	18.55
Chicken	10	200	4 oz	10	0	10	3	33.25	1
Bell Peppers	27	50	300g	8.4	3	5.4	0.6	3.6	2.268
Almonds	7	80	0.5 OZ	4.5	2	2.5	6.5	2.5	0.315
Dark Chocolate	40	90	2 pieces	12	1.5	10.5	10	0	4.8

TOTALS		1937.25		261.4	38.1	223.3	51.85	108.0375	

Meal Duration	Meal 1	Meal 2	Meal 3	Meal 4
Time (min)	1	6	12	20
GI	65.36437247	59.51219512	33	45.34175084

Stats   Splits   Segments ❷

Distance
10.19 mi
Distance

Calories
391 C
Calories

Heart Rate
bpm | % of Max | Zones

147 bpm
Avg HR

165 bpm
Max HR

3.1
Training Effect ❓

Elevation
322 ft
Elev Gain

322 ft
Elev Loss

581 ft
Min Elev

758 ft
Max Elev

● Heart Rate   No Overlay ▾

Over Time

● Pace

Avg: 7:22 min/mi

● Heart Rate

Avg: 160 bpm

| **Stats** | Splits | Segments |

Distance

3.00 mi
Distance

Calories

270 C
Calories

Heart Rate

| bpm | % of Max | Zones |

160 bpm
Avg HR

178 bpm
Max HR

3.3
Training Effect ⓘ

Elevation

3 ft
Elev Gain

2 ft
Elev Loss

581 ft
Min Elev

584 ft
Max Elev

Monday, July 6, 2015	
6:11 AM	Carbs 15 grams
8:50 AM	Insulin 4 units
9:00 AM	Carbs 57 grams
12:50 PM	Insulin 4 units
5:54 PM	Carbs 10 grams
4:00 PM	Carbs 50 grams
3:55 PM	Insulin 4 units
7:00 AM	Exercise Medium (45 minutes)

Simulation Day 7- Non- Exercise Protocol 5
Description: Sprint Intervals at Track

Date: July 7 (4x400's, 4x200's, 1x400, 1x200, 4x100's)

Blood Glucose at 6 AM, Correction Needed to reach 100 ± 5 mg/dl	Low, ~60, had 18 g granola bar at 6:00 (earlier than other days)
Soreness and Fatigue Present?	Some but didn't affect exercise
HR Before Exercise	130 after warmup
Peak HR	163

Average HR	182
Training Zone	3-4
Post-Exercise Meal	High, took an extra unit, 5 U
BG at 1 PM lunch, corrections needed?	Adjusted a bit with some berries to get ~96 (4 U)
3 PM Adjustment to get BG to around 120 mg/dl (consistent each week)	Took 2 units since at 140 mg/dl; dropped to ~118
4 PM 50 g CHO snack	Yamamoto, Instant Potato (4 U, 5 min before)
Dinner Notes and Timing (Note the flexibility here)	Something came up; no dinner until 9:30 PM, 3 U insulin, 58 g CHO
Calibration Times and Levels/ Status of CGM and Sensor	All seemed well calibrated
Total Daily Calorie, CHO, Fat, Protein Intake, GI	2003 calories, 263 g CHO, 53 g fat, 58 g Protein
Blood Glucose Level Before Bed (mg/dL)	120

Meal 1 FOOD	Meal 2 GI	Meal 3 Calories	Meal 4 SERVING SIZE	CHO (g)	Fiber (g)	Available CHO (g)	FAT (g)	PROTEIN(g)	LOAD
Fiber One Protein	30	120	1 bar	17	5	12	6	6	**5.1**
Banana	60	100	1 banana	25	3.1	21.9	0	0	15
Eggs	0	140	2 eggs	0	0	0	8	12	0
Bread ,2 slices	60	140	2 slices	28	3	25	2	2.5	16.8
Peanut Butter	14	105	1 tbs	3.5	1	2.5	8.5	3.625	0.49
Grapes/ Berries	60	105	1 cup	28	0.5	27.5	0	0	16.8
Yoplait Strawberry	35	170	6oz	33	0	33	1.5	-28.125	11.55
Cheese	0	110	1/3 cup	0.5	0	0	9	7	0
Turkey	0	60	4 slices	4	0	4	1.5	7.625	0

Kashi GoLean Crunch	55	95	1/2 cup	18	6	12	1.5	-10.875	9.9
Instant Potato	83	333.6	67.3 g	50	3	47	12.6	5.56	41.5
Quinoa	53	174.75	3/4 cup	35	4	31	4	8	18.55
Chicken	10	200	4 oz	10	0	10	3	33.25	1
Bell Peppers	27	50	300g	8.4	3	5.4	0.6	3.6	2.268
Red Wine	15	130	1 glass	5	0	5	0	0	0.75
TOTALS		2033.35		265.4	28.6	236.3	58.2	50.16	

Meal Duration	Meal 1	Meal 2	Meal 3	Meal 4
Time (min)	1	10	6	15
GI	65.36437247	50	83	43.90661479

Garmin Forerunner 610
Software: 2.80.0.0
Elev Corrections : Enabled
Summary Data: Original

connect powered by Garmin

Stats   Splits   Segments

Distance

2.86 mi
Distance

Calories

284 C
Calories

Heart Rate

bpm   % of Max   Zones

163 bpm
Avg HR

182 bpm
Max HR

3.7
Training Effect ⓘ

Timing

Pace   Speed

21:19
Time

18:34
Moving Time

40:07
Elapsed Time

7:28 min/mi
Avg Pace

6:30 min/mi
Avg Moving Pace

3:44 min/mi
Best Pace

Elevation

3 ft
Elev Gain

7 ft
Elev Loss

581 ft
Min Elev

584 ft
Max Elev

● Heart Rate   No Overlay ▾

Over Time ▾
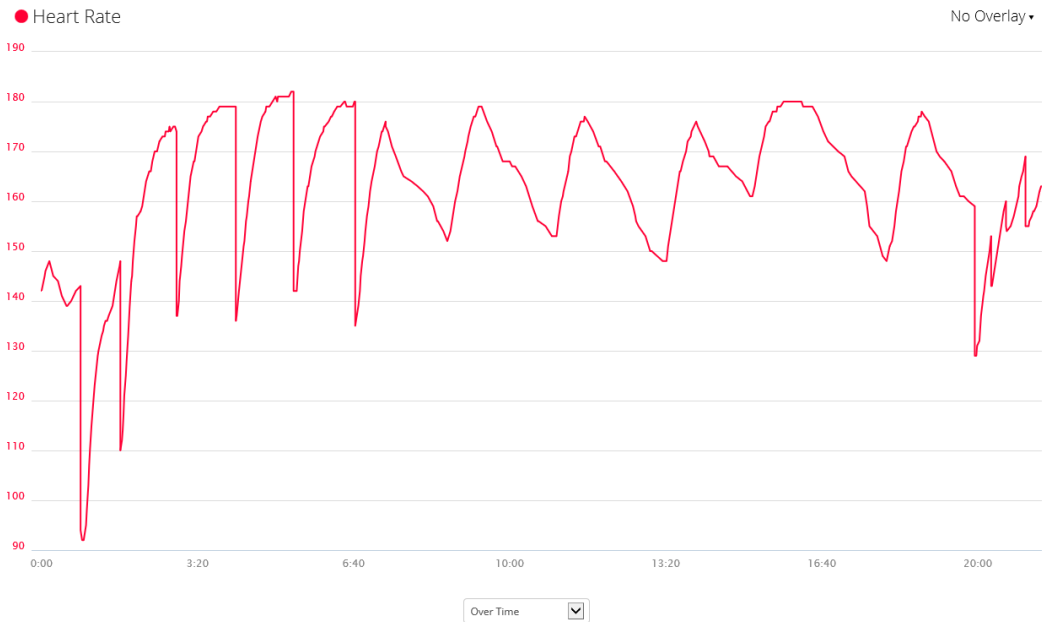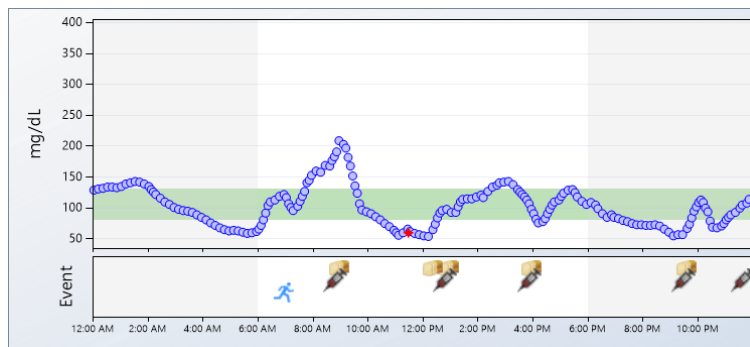
Tuesday, July 7, 2015

9:00 AM	Carbs 57 grams
8:50 AM	Insulin 5 units
1:00 PM	Carbs 75 grams
12:25 PM	Carbs 10 grams
12:50 PM	Insulin 5 units
3:55 PM	Insulin 4 units
4:00 PM	Carbs 50 grams
9:38 PM	Carbs 50 grams
9:30 PM	Insulin 4 units
7:00 AM	Exercise Heavy (45 minutes)
11:41 PM	Insulin 11 units

Simulation Day 8- Exercise Protocol 6
Description: Long Anaerobic Fatigue-Inducing Brick Workout

Date: July 8

Blood Glucose at 6 AM, Correction Needed to reach 100 ± 5 mg/dl	72, ate Fiber One Bar (15 g CHO)
Soreness and Fatigue Present?	Yes, some
HR Before Exercise	120 after jogging
Peak HR	169
Average HR	126
Training Zone	1-2
Post-Exercise Meal	A Couple of snacks (nuts, pretzels) right after; had meal, 4 U, similar breakfast
BG at 1 PM lunch, corrections needed?	Snacked on half a bagel then had meal (~1:00 snack, 1:45 meal)
3 PM Adjustment to get BG to around 120 mg/dl (consistent each week)	N/A
Dinner Notes and Timing (Note the flexibility here)/ Alcohol Protocol/Hot Environment	Chicken and Broccoli, 3 Units Chips at 5:00 PM 3 glasses wine between 7:00-9:00 Chocolate

Calibration Times and Levels/ Status of CGM and Sensor	Off by >10 after exercise in the morning
Total Daily Calorie, CHO, Fat, Protein Intake, GI	2209 cals, 274 g CHO, 47 g Fat, 94 g protein—more hungry today!
Blood Glucose Level Before Bed (mg/dL)	Had late snack, so ~105 but rising

Meal 1	Meal 2	Meal 3	Meal 4						
FOOD	GI	Calories	SERVING SIZE	CHO (g)	Fiber (g)	Available CHO (g)	FAT (g)	PROTEIN(g)	LOAD
Fiber One Protein	30	120	1 bar	17	5	12	6	6	5.1
Almonds	7	80	0.5 OZ	4.5	2	2.5	6.5	2.5	0.315
Pretzels	83	100	1 oz	22	0.9	21.1	0	3	18.26
Banana	60	100	1 banana	25	3.1	21.9	0	0	15
Eggs	0	140	2 eggs	0	0	0	8	12	0
Bread,2 slices	60	140	2 slices	28	3	25	2	2.5	16.8
Peanut Butter	14	160	1.5 tbs	5	1	4	12.5	7	0.7
Coconut Water		90	16 oz	22	0	22	0	0	0
Semi-Sweet Chocolate	40	70	1 tbs	10	0	10	4	1	4
Grapes	60	200	2 cups	52	3	49	0	0	31.2
Greek Yogurt	33	140	1	15	0	15	0	12	4.95
Turkey	0	60	4 slices	4	0	4	1.5	7.625	0
Broccoli	30	60	2 cups	12	3	9	0	0	3.6
Quinoa	53	174.75	3/4 cup	35	4	31	4	8	18.55
Chicken	10	200	4 oz	10	0	10	3	33.25	1
Red Wine	15	375	2.5 glasses	12.5	0	12.5	0	0	1.875
TOTALS		2209.75		274	25	249	47.5	94.875	

Meal Duration	Meal 1	Meal 2	Meal 3	Meal 4
Time (min)	15	10	N/A	30
GI	44.6	53.2		40.0
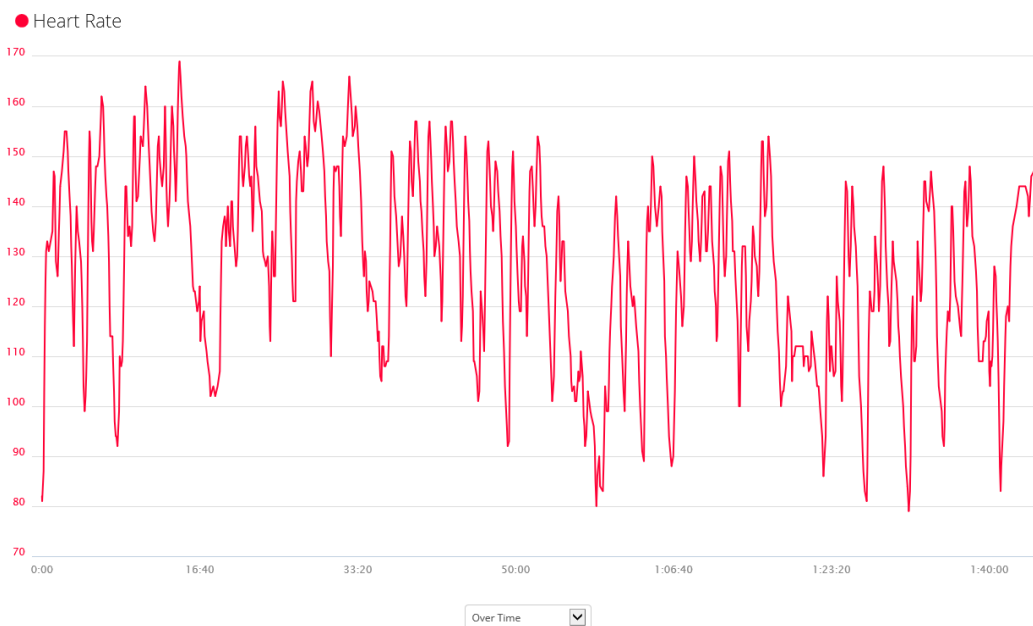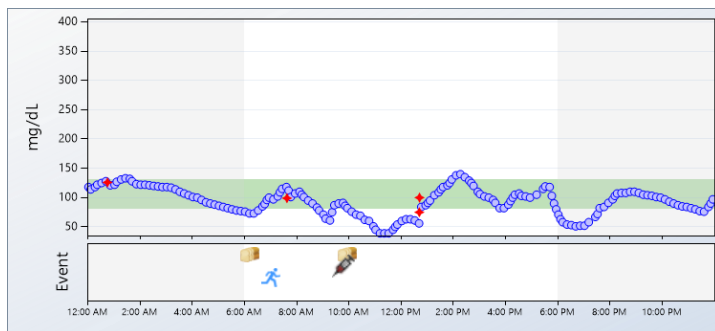
Wednesday, July 8, 2015

6:15 AM	Carbs 14 grams
7:03 AM	Exercise Heavy (105 minutes)
10:00 AM	Carbs 50 grams
9:50 AM	Insulin 4 units

7.5 DXA and VO2Max Data

EXERCISE PHYSIOLOGY & ATHLETIC TRAINING
MARQUETTE UNIVERSITY
MILWAUKEE, WI 53201

Patient:	Schunk, Sofie		Attendant:			
Birth Date:	4/8/1992	23.2 years	Patient ID:			
Height / Weight:	69.5 in.	139.0 lbs.	Measured:	6/22/2015	8:15:30 AM	(11.40)
Sex / Ethnic:	Female	White	Analyzed:	6/22/2015	8:15:32 AM	(11.40)

Total Body Tissue Quantitation
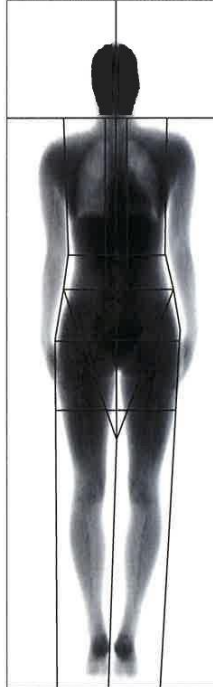
Reference Chart: No reference data for Total Body [Total] region. The selected Reference Population did not support Total Body Composition.

Composition Trend: Total
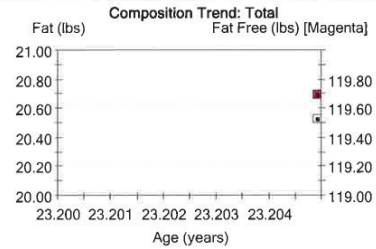
Trend: Fat Distribution

Measured Date	Age (years)	Android (%Fat)	Gynoid (%Fat)	A/G Ratio	Total Body (%Fat) [1]
6/22/2015	23.2	20.2	20.9	0.96	15.4

COMMENTS:

World Health Organization BMI Classification
BMI = 20.2 (kg/m²)

13	18.5		25	30	35
	Underweight	Normal	Overweight	Obese	
89	127		172	206	240

Weight (lbs.) for height = 69.5 in.

Image not for diagnosis

Printed: 6/23/2015 3:25:36 PM (11.40)76:0.15:153.85:31.2 0.00:-1.00
4.80x13.00 12.9:%Fat=15.4%
0.00:0.00 0.00:0.00
Filename: zkkcqnbk9.dfb
Scan Mode: Standard   0.4 µGy

1 -Statistically 68% of repeat scans fall within 1SD (± 0.8 % Fat, ±0.46 lbs. Tissue Mass, ±1.15 lbs. Fat Mass, ±1.34 lbs. Lean Mass for Total Body Total)
3 -Composition Matched for Age

GE Healthcare

Lunar Prodigy
DF+14985

EXERCISE PHYSIOLOGY & ATHLETIC TRAINING
MARQUETTE UNIVERSITY
MILWAUKEE, WI 53201

Patient:	Schunk, Sofie	**Attendant:**
Birth Date:	4/8/1992 23.2 years	**Patient ID:**
Height / Weight:	69.5 in. 139.0 lbs.	**Measured:** 6/22/2015 8:15:30 AM (11.40)
Sex / Ethnic:	Female White	**Analyzed:** 6/22/2015 8:15:32 AM (11.40)

BODY COMPOSITION

Region	Tissue[1] (%Fat)	Region (%Fat)	Tissue[1] (lbs)	Fat[1] (lbs)	Lean[1] (lbs)	BMC (lbs)	Total Mass (lbs)
Left Arm	15.2	14.4	7.72	1.17	6.55	0.45	8.2
Left Leg	15.3	14.5	22.35	3.42	18.93	1.29	23.6
Left Trunk	16.2	15.7	34.23	5.54	28.69	1.13	35.4
Left Total	15.4	14.7	68.28	10.53	57.75	3.33	71.6
Right Arm	15.2	14.3	7.33	1.11	6.22	0.46	7.8
Right Leg	15.3	14.5	22.45	3.43	19.01	1.26	23.7
Right Trunk	16.2	15.6	31.03	5.02	26.01	1.09	32.1
Right Total	15.3	14.6	65.21	10.00	55.21	3.41	68.6
Arms	15.2	14.3	15.06	2.29	12.77	0.91	16.0
Legs	15.3	14.5	44.80	6.85	37.95	2.55	47.3
Trunk	16.2	15.6	65.26	10.56	54.70	2.22	67.5
Android	20.2	19.9	8.99	1.81	7.17	0.14	9.1
Gynoid	20.9	20.3	22.27	4.65	17.61	0.69	23.0
Total	15.4	14.6	133.49	20.53	112.96	6.74	140.2

FAT MASS RATIOS

Trunk/ Total	Legs/ Total	(Arms+Legs)/ Trunk
0.51	0.33	0.87

1 -Statistically 68% of repeat scans fall within 1SD (± 0.8 % Fat, ±0.46 lbs. Tissue Mass, ±1.15 lbs. Fat Mass, ±1.34 lbs. Lean Mass for Total Body Total)
Filename: zkkcqnbk9.dfb

GE Healthcare

Lunar Prodigy
DF+14985

EXERCISE PHYSIOLOGY & ATHLETIC TRAINING
MARQUETTE UNIVERSITY
MILWAUKEE, WI 53201

Patient:	Schunk, Sofie	Attendant:			
Birth Date:	4/8/1992 23.2 years	Patient ID:			
Height / Weight:	69.5 in. 139.0 lbs.	Measured:	6/22/2015	8:15:30 AM	(11.40)
Sex / Ethnic:	Female White	Analyzed:	6/22/2015	8:15:32 AM	(11.40)

ANCILLARY RESULTS [Total Body]

Region	BMD [1] (g/cm^2)	Young-Adult (%)	Young-Adult T-Score	Age-Matched (%)	Age-Matched Z-Score	BMC (g)	Area (cm^2)
Head	2.410	-	-	-	-	480	199
Left Arm	1.173	-	-	-	-	202	172
Left Leg	1.533	-	-	-	-	584	381
Left Trunk	1.038	-	-	-	-	512	493
Left Total	1.328	-	-	-	-	1,510	1,137
Right Arm	1.245	-	-	-	-	208	167
Right Leg	1.483	-	-	-	-	573	386
Right Trunk	1.050	-	-	-	-	496	472
Right Total	1.362	-	-	-	-	1,545	1,135
Arms	1.208	-	-	-	-	411	340
Legs	1.508	-	-	-	-	1,157	767
Trunk	1.044	-	-	-	-	1,007	965
Ribs	0.806	-	-	-	-	315	391
Pelvis	1.281	-	-	-	-	410	320
Spine	1.110	-	-	-	-	282	254
Total	1.345	-	-	-	-	3,055	2,271

1 -Statistically 68% of repeat scans fall within 1SD (± 0.010 g/cm² for Total Body Total)
Filename: zkkcqnbk9.dfb

GE Healthcare

EXERCISE PHYSIOLOGY & ATHLETIC TRAINING
MARQUETTE UNIVERSITY
MILWAUKEE, WI 53201

Patient:	Schunk, Sofie	**Attendant:**			
Birth Date:	4/8/1992 23.2 years	**Patient ID:**			
Height / Weight:	69.5 in. 139.0 lbs.	**Measured:**	6/22/2015	8:15:30 AM	(11.40)
Sex / Ethnic:	Female White	**Analyzed:**	6/22/2015	8:15:32 AM	(11.40)

Total Body Bone Density

Reference Chart: No reference data for Total Body [Total] region. The selected Reference Population did not support Total Body Densitometry.

Region	BMD (g/cm²)[1]
Total	1.345

COMMENTS:

Image not for diagnosis

1 - Statistically 68% of repeat scans fall within 1SD (± 0.010 g/cm² for Total Body Total)

Printed: 6/23/2015 3:25:28 PM (11.40)76:0.15:153.85:31.2 0.00:-1.00
4.80x13.00 12.9:%Fat=15.4%
0.00:0.00 0.00:0.00
Filename: zkkcqnbk9.dfb
Scan Mode: Standard 0.4 µGy

Lunar Prodigy
DF+14985

Blood lactate level (mmol/l) at end of VO2max stress test. Lactic threshold was reached. Initial level was 1.7 mmol/l.

Vo2 Max Stress Test: June 23, 2015

Schunk	Sofie
Date:	6/23/15
Program	Exercise Science
Marquette	University
Milwaukee	WI
Speed Ramp Test (0.5 miles/min) @ 1% Grade	
Test Duration	11 min 08 sec

VO2max (mL/kg/min)	62.65
Anaerobic Threshold Parameters	
VO2 (ml/kg/min)	50.4
% VO2max	80.4
Speed @ 1% Grade (mph)	9-9.5
HR (BPM)	170

*Note: Entire RER Table and HR Values are Available
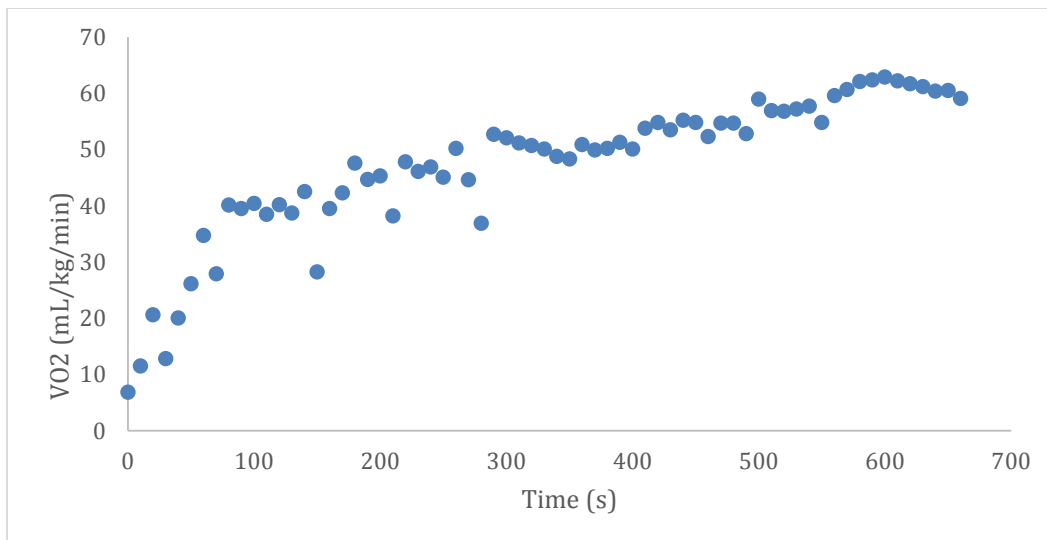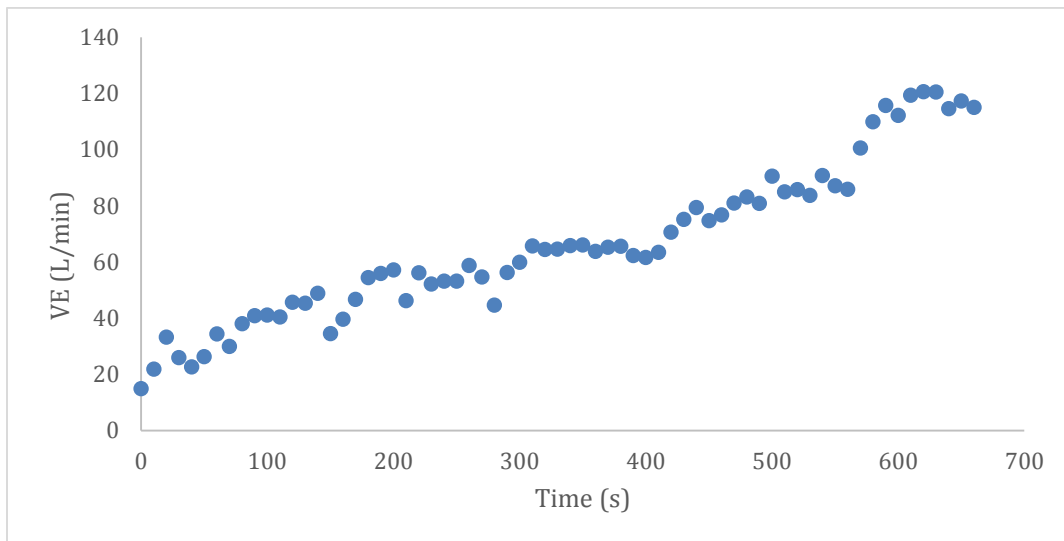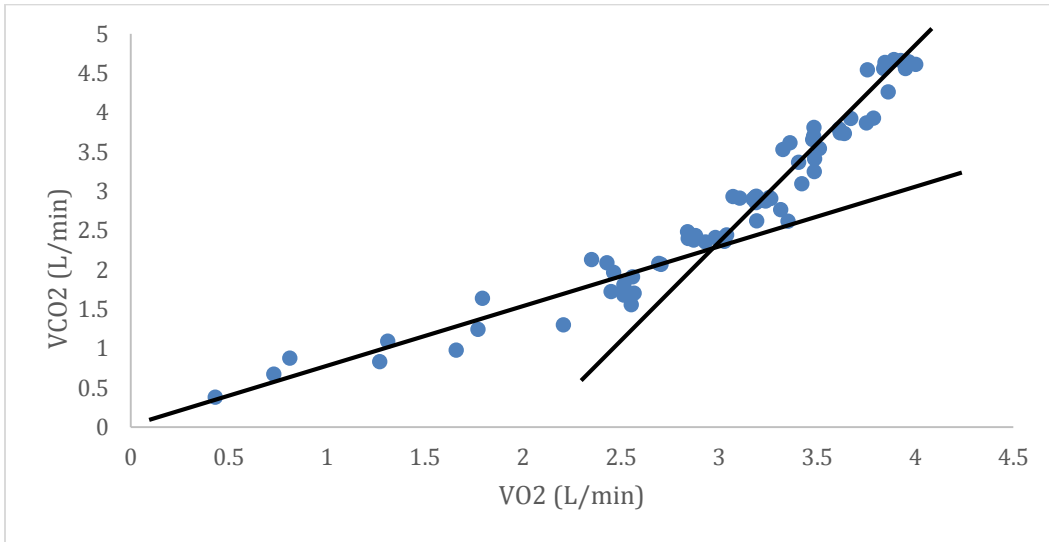
7.6 Sensitivity Analysis

7.6.1 Chapter 3 Sensitivity Analysis

Inputs

Meal	Snack	Exercise

• 700 kcal at 13 hours
• 30 minute duration
• 175 g CHO
    ○ GI = 50, 50% CHO
• Insulin bolus (Fast) = 50
	• 60 kcal at 10 hours
	• 6 minute duration
	• 15 g CHO
	    ○ GI = 80, 80% CHO
	• No Insulin
		• 600 kcal/hr for 1 hour
		• Aerobic Capacity = 1000
		• Simulation times
		    ○ 30 min before
		    ○ 30 min after start
		    ○ 18 min after end (Recovery)

Full Sensitivity Analysis Table Non-Diabetic—Most Sensitive Parameters (>0.4, **bold >1.0**)

	X_g	X_{nm}	X_m	X_d	X_{ds}	X_i	$X_{inj\text{-}m}$	X_{gn}	$X_{inj\text{-}nm}$	X_{mito}
					Meal Simulation					
$X_{min}{}^a$			—	—	—	**Ki 2.756** **Cia 3.007** **Cga -3.025** **Kgt -3.025** **Grefi 2.630** **Grefg -2.821** **Greft -2.999**	—		—	
$X_{max}{}^a$	**Ki 1.149** Cia -0.733 Kugs 0.578 Grefg -0.463 Kg2Max -0.476 Kmintol -0.784	**Wratt 1.068** Kmintol -0.523	Cib 0.589 Kmintol 1.306		Kugs 0.662	Ki -0.796 Grefi 0.612 **Grefg -1.272**			—	—

X_{BM}^b	**Ki -1.879** **-1.225** **Cib 3.090** **Cga 1.461** **Kgt 1.446** **Grefi -4.317** **Grefg 5.518** **Greft 1.872** Kg2Max -0.751 **Kmxex -1.233** Kse -0.921 **Kmintol -4.281** **Ratmito 1.079**	Ki -0.550 Cib 0.732 **Grefi -1.106** **Grefg 1.267** Gbt 0.504 Wratt 0.496 Kmintol 0.971	Ki -0.973 **Cib 1.296** Cga 0.620 Kgt 0.611 **Grefi -1.952** **Grefg 2.249** Greft 0.605 Kmxex -0.665 Kse -0.500 **Kmintol 1.690** Ratmito 0.645	—	—	**Ki -3.031** **Cia -1.147** **Cib 3.129** **Cga 1.311** **Kgt 1.296** **Grefi -4.489** **Grefg 4.857** **Greft 1.726** Kg2Max -0.707 **Kmxex -1.252** Kse -0.936 **Kmintol -4.060** **Ratmito 1.083**		**Ki -2.472** Cia -0.857 **Cib 3.297** Cga 0.768 Kgt 0.752 **Grefi -5.576** **Grefg 6.373** **Greft 1.191** Kg2Max -0.540 **Kmxex -1.338** **Kse -1.001** **Kmintol -4.043** **Ratmito 1.060**	—	
X_{DMR}^c		**Ki -1.311** **Cia -1.131** **Cib 2.198** Cga 0.796 Kgt 0.780 **Grefi -2.666** **Grefg 2.966** **Greft 0.894** **Gbt 1.486** **Kugf -1.035** Wratt -0.486 **KgwMax -1.315** **Kmxex -1.125** Kse -0.848 **Kmintol 2.995**	Ki -0.845 **Cib 1.201** Cga 0.533 Kgt 0.526 **Grefi -1.686** **Grefg 1.939** Greft 0.522 Kmxex -0.544 Kse -0.421 **Kmintol 1.622** Ratmito 0.506		**Kugs 0.717**	**Kid 0.890**		Ki -0.511 Cga 0.635 Kgt 0.636 **Grefi -1.025** **Grefg 1.301** Greft -0.615		
X_{DMF}^d	Ki 0.546 Cia -0.431 Kid -0.402	**Wratt 1.077** Kmintol -0.456	Cib 0.649 **Kmintol 1.137**		Kugs 0.600	**Ki -1.165** Grefi 0.455 Grefg -0.621		Ki -0.451 Cga -0.608 Kgt -0.609 **Grefi -1.002** **Grefg 1.444** Greft -0.582		
Snack Simulation										
X_{min}^a			—	—	—	**Ki 2.479** **Ciaa 2.697** **Cga -2.629** **Kgt -2.629** **Grefi 2.390** **Grefg -2.423** **Greft -2.658** **Kmintol 2.702**	—	Grefg 0.621	—	

X_{max}^a	**Ki 1.380** Cia -0.618 **Cga 1.197** **Kgt 1.200** **Grefi 1.424** **Grefg 4.366** Greft 0.991 Kmintol -0.471	—	Ki -0.940 **Cib 1.327** Cga 0.633 Kgt 0.625 **Grefi -1.760** **Grefg 2.242** Greft 0.603 Kmxex -0.611 Kse -0.459 **Kmintol 1.150**	Kugf 0.549	Kugs 0.972	**Ki -6.047** Cia -0.487 **Cga 1.927** **Kgt 1.932** **Grefi -8.041** **Grefg 6.924** **Greft 1.307** **Kid 1.261**				—
X_{BS}^b	Ki 0.776 Cia -0.479 Cga 0.920 Kgt 0.922 **Grefi 1.562** **Grefg 3.415** Greft 0.890	Ki -0.534 Cib 0.778 Cga 0.449 Kgt 0.444 **Grefi -1.049** **Greft 1.593** Greft 0.418 Gbt 0.451 Wratt 0.549 Kmintol 0.621	**Ki -1.014** **Cib 1.406** Cga 0.719 Kgt 0.710 **Grefi -1.994** **Grefg 2.534** Greft 0.666 Kmxex -0.684 Kse -0.513 **Kmintol 1.126** Ratmito 0.605	—	—	**Ki 54.629** **Cia 12.176** **Cib 7.400** **Cga -23.404** **Kgt -23.455** Grefi 109.876 Grefg -86.464 Greft -22.650 **Kg2Max 6.985** **Kmxex -3.746** **Kse -2.814** **Kmintol 8.313**		Ki 0.866 Cia -0.531 **Cga 1.026** **Kgt 1.028** **Grefi 1.744** **Grefg -2.752** Greft 0.991		
X_{DSR}^c	Ki 0.774 Cia -0.479 Cga 0.921 Kgt 0.923 **Grefi 1.559** **Grefg 3.416** Greft 0.891	Ki -0.536 Cib 0.778 Cga 0.448 Kgt 0.442 **Grefi -1.053** **Grefg 1.587** Greft 0.417 Gbt 0.452 Wratt 0.548 Kmintol 0.626	**Ki 1.014** **Cib 1.405** Cga 0.718 Kgt 0.708 **Grefi -1.995** **Grefg 2.530** Greft 0.666 Kmxex -0.684 Kse -0.513 **Kmintol 1.135**	—	—	**Ki 55.564** **Cia 12.392** **Cib 7.468** **Cga -23.805** **Kgt 23.587** **Grefi 111.732** **Grefg -87.947** **Greft -23.045** **Kg2Max 7.110** **Kmxex -3.786** **Kse -2.844** **Kmintol 8.532**		Ki 0.864 Cia -0.531 **Cga 1.026** **Kgt 1.028** **Grefi 1.739** **Grefg -2.746** Greft 0.991		
X_{DSF}^d	Grefi 0.608 **Grefg 1.054**	Ki -0.547 Cib 0.797 Cga 0.451 Kgt 0.446 **Grefi -1.076** **Grefg 1.604** Greft 0.426 Gbt 0.465	**Ki -1.009** **Cib 1.399** Cga 0.711 Kgt 0.702 **Grefi -1.987** **Grefg 2.510** Greft 0.661 Kmxex -0.680		Kugs 0.887	Ki -0.852 Grefi -0.985 Grefg 0.619 Kugf 0.450 Kid 0.836		Grefi 0.510 **Grefg -1.046**		

		Wratt 0.535 Kmintol 0.653	Kse -0.510 **Kmintol 1.152**							
Exercise Simulation										
X_{min}^c	—	—	—	—		Ki -0.510 Grefi -0.501 Grefg 0.674		Grefg 0.696	—	—
X_{max}^a	**Ki 1.819** **Cia -2.214** **Cib -1.456** **Cga 1.168** **Kgt 1.170** **Grefi 2.091** **Grefg 4.594** **Greft 1.611** Kg2Max -0.522 **Kmintol -1.315** **Kid -2.706**	—	Ki -0.550 Cib 0.994 **Cga 1.449** **Kgt 1.440** Grefi -0.993 **Grefg 4.197** Greft 0.675 Kmxex 0.591 Kse -0.557 Kmintol 0.692 **Ratmito -1.166**	—	—	**Ki -2.196** Cia -0.418 Cga 0.836 Kgt 0.839 **Grefi -2.160** **Grefg 2.902** Greft 0.541 Kmxex 0.915 Kid 0.745	—	**Ki 1.043** **Cia -1.337** Cib -0.901 **Cga 1.429** **Kgt 1.432** **Grefi 1.412** **Grefg -4.218** **Greft 1.160** Kg2Max -0.458 Kmintol -0.789 **Kid -1.682**	—	—
X_{BE}^e	Ki 0.810 Cia -0.469 Cga 0.913 Kgt 0.915 **Grefi 1.629** **Grefg 3.388** Greft 0.877	Ki -0.403 Cib 0.708 Cga 0.525 Kgt 0.520 Grefi -0.738 **Grefg 1.797** Greft 0.464 Wratt 0.602	Ki -0.941 **Cib 1.404** **Cga 0.772** Kgt 0.763 **Grefi -1.756** **Grefg 2.582** Greft 0.666 Kmxex -0.654 Kse -0.489 Kmintol 0.903	—	—	**Ki 42.380** **Cia 9.306** **Cib 6.628** **Cga -18.140** **Kgt -18.185** **Grefi 85.304** **Grefg -66.975** **Greft -17.457** **Kmxex -3.283** **Kse -2.465** **Kmintol 4.891**	—	Ki 0.916 Cia -0.527 **Cga 1.030** **Kgt 1.032** **Grefi 1.839** **Grefg -2.889** Greft 0.987	—	—
X_{DE}^f	Cga -0.951 Kgt -0.953 **Grefg -2.478** Kmxex 0.838	Cib 0.421 Cga 0.538 Kgt 0.535 Grefi -0.460 **Grefg 1.570** Wratt 0.743	Ki -0.533 Cib 0.893 Cga 0.976 Kgt 0.969 Grefi -0.996 **Grefg 2.902** Greft 0.572 Kse -0.432 Kmintol 0.585	—	—	**Ki 2.378** **Cga -1.293** **Kgt -1.297** **Grefi 3.298** **Grefg -3.808** Greft -0.541 Kmxex 0.475 Kid -0.911	—	**Kgt -1.197** **Kgt -1.199** **Grefg 1.085** Kmxex 0.874	—	—
X_R^g	Cga 0.838 Kgt 0.840 Grefi 0.539 **Grefg 2.788** Greft 0.470 Kmxex 0.548	Cga 0.464 Kgt 0.461 **Grefg 1.355** Wratt 0.825	Ki -0.567 Cib 0.996 **Cga 1.539** **Kgt 1.529** **Grefi -1.059** **Grefg 4.433**	—	—	Ki -0.958 Cga 0.614 Kgt 0.616 Grefi -0.910 **Grefg 2.101** Kmxex 0.827		Ki 0.509 **Cga 3.173** **Kgt 3.181** Grefi 0.890 **Grefg -2.388** Greft 0.983	—	

Kid -0.442		Greft 0.711 Kmxex 0.619 Kse -0.589 Kmintol 0.673 **Ratmito -1.310**			**Kid 1.033**		

[edge] For these cases, extremer behaviors occur at the beginning or end of respective time windows for the subtask event.
[a] All maximum behaviors occur at a peak during meal and snack simulation subtasks.
[b] Sensitivity behavior values were taken 0.5 hrs prior to this subtask (meal X_{BM}, snack X_{BS}), to document initial fluctuations.
[c] Rising sensitivity behavior measured at 0.3 hrs after start of this subtask (meal X_{DMR}, snack X_{DSR}).
[d] Falling sensitivity behavior measured at 1.0 hrs after the start of this subtask (meal X_{DMF}, snack X_{DSF}).
[e] Sensitivity behavior values were taken 0.3 hrs prior to exercise subtask event, to document initial fluctuations.
[f] Behaviors values taken during exercise subtask, 0.5 hrs after its start.
[g] Behavior values taken during exercise 'recovery' phase, at 0.25 hrs after the end of exercise (i.e., 1.25 hrs after its start).
[*] Exception to the >0.1 threshold.

Full Sensitivity Analysis Table T1D—Most Sensitive Parameters (>0.4, **bold >1.0**)

	X_g	X_{nm}	X_m	X_d	X_{ds}	X_i	$X_{inj\text{-}m}$	X_{gn}	$X_{inj\text{-}nm}$	X_{mito}
					Meal Simulation					
$X_{min}{}^b$	**Ki -5.444** **Cga -5.529** **Kgt -5.529** **Grefg -4.969** **Kd 5.133**	Ki 0.799 **Cib -1.153** **Grefg -1.120** Gbt -0.547 Wratt -0.655 **Kmintol -6.498** Ka1 -0.439 Kd -5.966	—	—	—	—	—	**Ki -1.042** Cia 0.959 Cga -0.792 Kgt -0.792 Grefg 0.800 Greft -0.542 Kmintol 0.797 Ka1 0.546 **Kd 2.294**	—	Kmintol 0.483
$X_{max}{}^b$	**Ki 1.605** Cga -0.655 Kgt -0.659 **Kugs 1.136** **Grefg -1.924** **Kmintol -1.237** **Ka2 -1.936** Ka1 -0.773 **Kd -2.294**		**Kmintol 2.073**		Kugs 0.662	Ki -0.866 Ka2 0.933 Ka1 0.429 **Kd 1.216**	Ka1 0.439 **Kd 1.555**	Cia -0.877 **Cga -1.464** **Kgt -1.468** Kugs 0.782 **Grefg -1.608** **Ka2 -1.446** Kd 0.458	**Ka1 1.418** **Kd 3.283**	—
$X_{BM}{}^c$	Grefg 0.550 Greft 0.418 Ka2 0.596	Wratt 0.743 **Kmintol 1.402**	**Kmintol 2.039** **Kd 1.007**	—	—	Ki -0.996 Ka1 0.571 **Kd 2.423**	Ka2 -0.733 Ka1 0.512 **Kd 2.543**	Ki -0.936 Cia 0.779 **Cga -1.026**	—	

		Kd 0.664						Kgt -1.027 Kmintol 0.806 Ka1 0.563 **Kd 2.304**		
X_{DMR}^d		**Grefg -1.579** Gbt 0.433 **Wratt -4.717** **Kmintol -4.846** Kd -6.107	Ki -0.420 **Kmintol 2.065** Ka2 -0.455 **Kd 1.081**		Kugs 0.717	Ki -1.057 Kd 0.574 **Kd 2.563**	Ka2 -0.877 Ka1 0.543 **Kd 2.683**	Ki -0.817 Cia 0.619 Cga -0.983 Kgt -0.984 Greft -0.459 Kmintol 0.600 Ka1 0.436 Kd 2.021	Ka1 0.930 **Kd 3.419**	
X_{DMF}^e	Kd -0.710	Grefg 0.455 **Wratt 1.914** Kg2Max 0.480 Kmintol 0.491 **Kd 1.656**	**Kmintol 2.154** Ka2 -0.473 Kd 0.821		K_{ugs} 0.600	Ki 0.617 **Ka2 1.260** **Kd -1.780**	—	Ki -0.772 Cia 0.579 Cga -0.935 Kgt -0.936 Greft -0.474 Kmintol 0.557 Ka1 0.408 **Kd 1.913**	Kd 0.431	Kmintol 0.406
					Snack Simulation					
X_{min}^b	Grefg 0.446	Wratt -0.434 KMintol -0.625 Kd -0.587	—	—	—		—	Ki -0.531 Cia 0.411 Cga -0.578 Kgt -0.578 **Grefi 2.390** Kmintol 0.413 **Kd -2.493**	—	
X_{max}^b	**Ki -2.927** **Cia 2.278** Cib 0.419 **Cga -3.595** **Kgt -3.600** **Grefg 11.472** **Greft -1.303** **Kmintol 2.281** Ka2 -0.425 Ka1 .1655 **Kd 7.322**	—	Ki -0.506 Cib 0.675 Grefg 0.649 **Kmintol 1.197** **Kd 1.181**	Kugf 0.549	**Kugs 0.972**	Ki -1.026 Ka1 0.588 **Kd 2.478**	Ka2 -0.971 Ka1 0.530 **Kd 2.563**	**Ki -2.160** **Cia 1.670** **Cga -2.350** **Kgt -2.353** Grefg 0.694 Greft -0.932 **Kmintol 1.680** **Ka1 1.226** **Kd 5.343**	Ka1 0.577 **Kd 1.734**	—
X_{BS}^c	**Ki -1.462** **Cia 1.094** **Cga -1.668** **Kgt -1.671**	Ki -0.410 Cib 0.585 Grefg 0.682 Wratt 0.764	Ki -0.538 Cib 0.726 Grefg 0.714	—	—	**Ki -1.026** Ka1 0.588 **Kd 2.478**	Ka2 -0.971 Ka1 0.530 **Kd 2.563**	**Ki -1.541** **Cia 1.140** **Cga -1.755** **Kgt -1.758**	Ka1 0.577 **Kd 1.734**	—

	Grefg -5.019 Greft -0.515 **Kmintol 1.122** Ka1 0.849 **Kd 3.562**	Kmintol 0.843 Kd 0.941	**Kmintol 1.056** **Kd 1.240**					Greft -0.534 **Kmintol 1.160** Ka1 0.891 **Kd 3.725**			
$X_{DSR}{}^{d}$	**Ki -1.522** **Cia 1.148** **Cga -1.745** **Kgt -1.747** **Grefg -5.285** Greft -0.550 **Kmintol 1.179** Ka1 0.894 **Kd 3.721**	Ki -0.408 Cib 0.580 Grefg 0.674 Wratt 0.766 Kmintol 0.865 Kd 0.938	Ki -0.533 Cib 0.718 Grefg 0.707 **Kmintol 1.080** **Kd 1.232**	—	—	**Ki -1.034** Ka1 0.592 **Kd 2.503**	**Ka2 -1.000** Ka1 0.536 **Kd 2.586**	**Ki -1.565** **Cia 1.167** **Cga -1.791** **Kgt -1.793** Greft -0.556 **Kmintol 1.192** Ka1 0.905 **Kd 3.797**	Ka1 0.580 **Kd 1.766**		
$X_{DSR}{}^{e}$	**Ki 1.668** **Cia -1.277** **Cga 1.277** **Kgt 1.278** **Grefg 4.2267** Greft 0.605 Kugf 0.799 **Kmintol -1.307** Ka1 -0.964 **Kd -4.094**	Ki -0.402 Cib 0.578 Grefg 0.664 Wratt 0.766 Kmintol 0.923 Kd 0.929	Ki -0.525 Cib 0.701 Grefg 0.685 **Kmintol 1.132** **Kd 1.218**		**Kugs 0.887**	**Ki -1.049** Ka1 0.598 **Kd 2.555**	**Ka2 -1.065** Ka1 0.546 **Kd 2.633**	**Ki -9.343** **Cia 7.058** **Cib 1.797** **Cga -9.803** **Kgt -9.815** **Grefg 6.947** **Greft -3.447** **Kugf -3.078** Ksds 0.633 **Kmintol 7.205** **Ka1 5.389** **Kd 22.855**	Ka1 0.586 **Kd 1.839**		
					Exercise Simulation						
$X_{min}{}^{b}$			—	—	—		—		—		
$X_{max}{}^{b}$	Cga 0.562 Kgt 0.563 **Grefg 2.168** Greft 0.988 Kg2Max -0.563	—	Ratmito 0.812	—	—		—		—		
$X_{BE}{}^{f}$	Cga 0.562 Kgt 0.563 **Grefg 2.168** Greft 0.989 Kg2Max -0.563	Grefg 0.891 Greft 0.415 Gbt 0.584 Wratt 0.416	Ratmito .5421	—	—		—		Grefg -0.529 Greft 0.529	—	—

$X_{DE}{}^g$	Cga 0.562 Kgt 0.563 **Grefg 2.168** Greft 0.988 Kg2Max -0.563	Grefg 0.784 Gbt 0.633	Ratmito 0.530	—	—		—	Grefg -0.529 Greft 0.529	—	
$X_R{}^h$	Cga 0.562 Kgt 0.563 Grefg 2.168 Greft 0.988 Kg2Max -0.563	Grefg 0.694 Gbt 0.674	Ratmito 0.819	—	—		—	Grefg -0.529 Greft 0.529	—	

edge For these cases, extremer behaviors occur at the beginning or end of respective time windows for the subtask event.
b All maximum behaviors occur at a peak during meal and snack simulation subtasks.
c Sensitivity behavior values were taken 0.3 hrs prior to this subtask (meal X_{BM}, snack X_{SM}), to document initial fluctuations.
d Rising sensitivity behavior measured at 0.3 hrs after start of this subtask (meal X_{DMR}, snack X_{DSR}).
e Falling sensitivity behavior measured at 1.0 hrs after the start of this subtask (meal X_{DMF}, snack X_{DSF}).
f Sensitivity behavior values were taken 0.3 hrs prior to exercise subtask event, to document initial fluctuations.
g Behaviors values taken during exercise subtask, 0.5 hrs after its start.
h Behavior values taken during exercise 'recovery' phase, at 0.25 hrs after the end of exercise (i.e., 1.25 hrs after its start).

7.6.2 Chapter 4 Sensitivity Analysis

Inputs (Subject: BW = 65 kg, rattype1i = 0.2, wmu = 30, wnm = 25)

Anaerobic Exercise Simulation	Aerobic Exercise Simulation	Snack + Exercise Simulation

• 2 Hour Lifting Workout (Case Study 2 Protocol Day 8)
   o 7:00-9:00 AM
• Bouts of 800 kcal/hr exertions informed by HR input
	• 2.5 Hour Long Run (Case Study 2 Protocol Day 4)
	   o 7:00-9:30 AM
	• 500-600 kcal/hr informed by HR input
		• 1 Hour Tempo Run (Case Study 2 Protocol Day 1)
		   o 7:00-8:00 AM
		• 15g CHO snack at 6:30 (kfast = 0.8, fraccarbs = 0.8)
		   o No insulin

Full Sensitivity Analysis Table—Most Sensitive Parameters (>0.4)

	X_g	X_{nm}	X_m	X_d	X_{ds}	X_i	$X_{inj\text{-}m}$	X_{gn}	$X_{inj\text{-}nm}$	X_{mito}
				Exercise Simulation 1 Long Anaerobic						
$X_{min}{}^b$		Cib Grefi Grefg Kmintol		—	—	**Ki** **Cia** **Cga** **Kgt** **Grefi** **Grefg** **Greft** **Kmintol**	—	Ki Cia Cga Kgt Grefi Grefg Greft Kmintol	—	
$X_{max}{}^b$	Ki Cia Grefg Kg2Max Kmintol	Wratt Kmintol	**Cib** **Kmintol**	—		**Ki** **Gref** **Grefg**	—		—	**Wmu**
Before Exercise (6:45)	**Ki** **Cia** **Cib** **Cga** **Kgt** **Grefi** **Grefg** **Greft** **Kg2Max** **Kmxex** **Kse** **Kmintol** **Ratmito**	Ki Cib **Grefi** **Grefg** Gbt Wratt Kmintol	Ki **Cib** **Cga** Kgt **Grefi** **Grefg** Greft Kmxex Kse **Kmintol** **Ratmito**	—	—	**Ki** **Cia** **Cib** **Cga** **Kgt** **Grefi** **Grefg** Kg2Max **Kmxex** Kse **Kmintol** **ratmito**	—	**Ki** Cia **Cib** Cga Kgt **Grefi** **Grefg** **Greft** Kg2Max Kmxex Kse Kmintol Ratmito	—	**Ki** Cia **Cib** Cga Kgt **Grefi** **Grefg** **Greft** Kg2Max Kmxex Kse Kmintol Ratmito **Wmu**
Halfway During Exercise (8:00)		**Ki** **Cib** **Cga** **Kgt** **Grefi** **Grefg** **Greft** **Gbt** **Kg2Max** **Kmxex** **Kse** **Kmintol**	**Ki** **Cib** **Cga** **Kgt** **Grefi** **Grefg** **Greft** **Kg2Max** **Kmxex** **Kse** **Kmintol** **Ratmito**		—	Kid	—	Ki Cga Kgt **Grefi** **Grefg** Greft	—	

Recovery (9:45)	Ki Cia Kid	Wratt Kmintol	**Cib** **Kmintol**	—	—	Ki Grefi Grefg	—	**Ki** **Cga** **Kgt** **Grefi** **Grefg** **Greft**		
Long Aerobic Exercise Simulation										
$X_{min}{}^{b}$	Grefg			—	—	**Ki** **Grefg**	—	Grefg	—	
$X_{max}{}^{b}$	Cga Kgt Grefg Kmxex Kse	—	**Ki** **Cib** **Cga** **Kgt** **Grefi** **Grefg** **Kmxex** **Kse** **Kmintol** **Ka1**	—	—	Ki Cga Kgt Grefg Kmxex	—	Cga Kgt Grefg Kmxex	—	**Grefg**
Before Exercise (6:45)	Cga Kgt Grefg Kg2Max	Grefg Gbt Wratt	**Ki** **Cib** **Cga** **Kgt** **Grefi** **Grefg** **Kmintol** **Ka1** **Ratmito**	—	—	**Ki** **Cga** **Kgt** **Grefg** **Kg2Max**	—	Cga Kgt Grefg	—	
Halfway During Exercise (8:00)	Cga Kgt Grefg Kmxex Kse	Grefg Gbt Wratt	**Ki** **Cib** **Cga** **Kgt** **Grefi** **Grefg** **Kmxex** **Kmintol** **Ka1**	—	—	**Ki** **Cga** **Kgt** **Grefg** **Kg2Max** **Kmxex** **Kse** **Ksds**	—	**Ki** **Cia** **Cga** **Kgt** **Grefg** **Kg2Max** **Kmxex** **Kse** **Ka2**	—	
Recovery (9:15)	Cga Kgt Grefg Kmxex	Grefg Wratt	**Ki** **Cib** **Cga** **Kgt**	—	—	Ki Cga Kgt Grefg	—	**Ki** **Cia** **Cga** **Kgt**	—	**Grefg**

	Kse		**Grefi** **Grefg** **Kmxex** **Kse** **Kmintol** **Ka1**			Kmxex		**Grefg** **Kg2Max** **Kmxex** **Kse** **Ka2**		
Exercise Simulation 3: Snack + Tempo										
$X_{min}{}^b$	—			—	—	Ki Grefg			—	
$X_{max}{}^b$	Cga Kgt Grefg	—	**Ki** **Cia** **Cib** **Cga** **Kgt** **Grefi** **Grefg** **Kg2Max** **Kmxex** **Kse** **Kmintol** **Ka2** **Ka1** **Ratmito**	—	—	Ki Cga Kgt Grefg Kg2Max Kid	—	—	—	**Wmu 1.120**
Before Exercise, after snack (6:36)	Cga Kgt Grefg Kg2Max	Grefg Gbt Wratt	Ki Cib Cga Kgt Grefi Grefg Kmintol Ka1 Ratmito	—	—	**Ki** **Cga** **Kgt** **Grefg** **Kg2Max**	—	Cga Kgt Grefg	—	**Wmu -0.972**
Halfway During Exercise (7:30)	Ki Cia Cga Kgt Kugs Grefg Kg2Max Kmxex Kse Ksds Ka2	Cib Grefg Gbt Ka1	**Ki** **Cib** **Cga** **Kgt** **Grefi** **Grefg** **Kg2Max** **Kse** **Kmintol** **Ka1**	—	—	**Ki** **Cia** **Cga** **Kgt** **Kugs** **Grefg** **Kg2Max** **Kmxex** **Ka2**	—	Ki Cia Cga Kgt Kugs Grefg Kg2Max Kmxex Kse Ka2	—	**Kugs**

| Recovery (8:15) | Cga 0.204
Kgt 0.204
Grefg 0.746 | Cga
Kgt
Grefg | **Grefg**
Gbt
Wratt | Ki
Cia
Cib
Cga
Kgt
Kugs
Grefi
Grefg
Kg2Max
Kmxex
Kse
Kmintol
Ka2
Ka1
Ratmito | — | **Ki**
Cga
Kgt
Grefg
Kmxex
Kid | — | **Cga**
Kgt
Grefg | — | **Kugs** |

[edge] For these cases, extremer behaviors occur at the beginning or end of respective time windows for the subtask event.

[b] All maximum behaviors occur at a peak during exercise subtasks.

8. CODE

```
% STARTER CODE, GLUCOSE 8- or 10-STATE
% States: x1: Glucose, Blood/plasma; also key regulated output
%         x2: Glucose, Tissue (non-muscle, lumped);
%         x3: Glucose, Muscle Tissue
%         x4: Glucose, Stomach (final path, fast & slow converge);
%         x5: Glucose, Stomach (slow food path, converges to x4)
%         x6: Insulin, Blood (controller; glucagon is ~mirror)
%         x7: Insulin, Local Tissue (for external input only), monomeric
%            insulin absorbtion
%         x9: Insulin, Local Tissue (for external input only), nonmonomeric
%            insulin absorbtion
%         x8: Glucagon, Blood (controller; insulin is ~mirror)
%         x10: Mitochondrial Consumption State
% Inputs: u1: Food ingestion (meals): Lines 36-38, via x4 (1st-ord filter)
%         u2: Insulin injection or pump: Lines 39-40, via x7 (1st-ord filt)
%         u3, exer: exercise of certian intensity in kcal/hr
%         u4,activity: activity as a randomized input of certian intensity
%                with max of 200 kcal/hr
%         u5: External Heart Rate (bpm)
%         uHM: Hormonal Stress

% Key Output: y:  Blood glucose (x1)
% Notes:  This is set up as 1 model, but has an embedded NL controller for
%         insulin & glucagon
%         Type I:  change ratType1i/g; add u(2,i) exogenous insulin
%         Type II: change (at minimum) starting levels, BM, wmu/wnm,
%         insulin rate, GLUT2 rate
clear all;

%PARAMETERS:
```

```
bm = 70;                % Body Mass, in Kg;  for 70, muscle ~30, fat ~15, brain ~ 1.3, liver 1.4 each, b-
plasma ~ 2.8, interstit ~ 10, RBCs ~2.2?
wmu = 30;               % BM of skeletal muscle, in Kg, ~40-45% healthy (less if obese), for normalizing in
f3, etc
wnm = 25;               % BM, "Non-Musc" in Kg, of: "BM - BMskeletal - BM_ECF - BM_brain+RBCs", for
normalizing in f2, etc
ratBM = bm/70.;
ratmito = 0.1; %proportion of muscle mass that is mitochondria; mitochondrial volume increases with
training
ratMUSC = wmu/30.;  ratNONM = wnm/25.;  % ratios for musc and non-musc relative to "normal"
wmito = ratmito*wmu; %Mass of mitochondria in kg
kprop = 0.2; %Proportion of glucose consumption (activity) that reaches mitochondria
stressrat = 1.0; %scaling for stressors for GLUT2; i.e. >1.0 will dump more glucose from non-muscle
                 %i.e. competitiveness of athletes >1.0; circuit/sprint
                 %training; 2.0 = MAXIMUM
metab = 1.0; %Basal Metabolism adjustment >1.0 = fit; <1.0 = unfit (default = 1.0); 2.0 = MAXIMUM


ratType1i = 1.0;     % If Type 1, ratio of insulin still produced by beta cells; 1.0 = normal, lower for
Type 1
ratType1g = 1.0;     % If Type 1, ratio of glucagon still produced by beta cells; 1.0 = normal, lower for
Type 1
ratType2i = 1.0;     % If Type 2, level of insulin resistance as ratio


Cia = .3; %1.0 %0.035;    % Insulin Control Param, Non-Muscle Tissue; Gain
Cib = 0.4; %1.0 %0.03;    % Insulin Control Param, Muscle;  now Cia + Cib = original C1; JW: .019 to .024
Cga = 0.4*.287*100;   % Glucagon Control Param, Non-Musc scaled to pg/mL
Cgb = 0.001*.287*100; % Glucagon Control Param, Muscle scaled to pg/mL
insulindel = 0.15;    % Delay in hours (Man-Cobelli use 10 min, 0.15=9 min)
Kid = 0.04;           % derivative


%NEW PARAMS FROM COBELLI INSULIN MODEL--INSULIN ABSORPTION
rat_ia = 0.5; %ratio of nonmonomeric:monomeric (slow:fast) insulin absorb. paths
kai = 0.02*60;
ka2 = rat_ia*kai; %rate constant of monomeric insulin absorption; originally 0.018*60
ka1 = (1-rat_ia)*kai; %rate constant of nonmonomeric insulin absorption converted to /hr from /min;
originally 0.0018*60
kd = 8*0.0164*60; %rate constant of insulin dissociation
```

```
Kg = 0.4;                  % /hr, Cg, ~P-action for glucagon, .4 or 1  NOT USED?
Ki = 3.0;                  % /hr, a4, Insulin elinimation rate
Kgt = 1.0*.287;            % /hr, a5, Basal tissue elimination rate JW: WHY???  NOT WELL-USED (Mult by Cia,
Cgb)?
Kugf = (5./ratBM);    % forward rate (~1/tau) of glucose bolus (JW: now min rate, mid-range max nearly
double)
Kugs = (0.4/ratBM);   % min slow path rate (~1/tau) of glucose bolus (can be as high as double this double)
Kugd = (5./ratBM);    % max digestive absorbtion rate (can be half of this at very low or high)
Gugf = 0.98;          % digestive effectiveness ratio, fast carbs
Gugs = 0.88;          % digestive effectiveness ratio, slow carbs
Kui = 1./ratBM;       % forward rate (1/tau) of insulin bolus
Kuga = 2.0;           % forward rate of bolus for slow glucose path
Kgc = 8.;             % /hr, glucagon addition rate
Knm_up = 1.0;         % /hr, non-muscle uptake (e.g., liver) without insulin signal
Kmusc = 20.0;         % rate of delivery to muscle - for example, "10" would be a time constant of 6 min
Grefi = 70;           % Ref thresh (BG) for insulin control
Grefg = 110;          % Ref thresh (BG) for glucagon
Greft = 90;           % Ref thresh (BG) for Non-muscle flux direction (due to GLUT2)
Kg2Max = 2.0;         % Max for Non-muscle GLUT2 flux (gradient, without control action
Ktintol = 12.*ratNONM;  % Ref thresh for non-musc tissue, g/Kg (  (typical body can store 2000 Kcal = 500 g
of glycogen
Kmintol = 14.*ratMUSC;  % Ref thresh for muscle (means 75% = 0.25 + 0.5 passed),
                        % insref = 30; %pmol/L; %glucref = 120; %glucagon max pg/mL


% Next three should add to basal metabolism, e.g., Kbr+Gbt+Gbm is "low side" of (glucose) basal metab (if
fully sedentary, no complex foods)
Kbr = ((20./4)*ratNONM);        % BG to steady consumption sink, no storage (mostly to brain, also
erythrocytes), in Kcal/hr/4 = g/hr
Gbt = metab*((10./4)*ratNONM);%/wnm;   % Non-musc tissue basal metabolic elimination (not brain, but liver,
cardiac, adipose...), Kcal/hr/4;
Gbm = metab*((6./4)*ratMUSC);%/wmu;    % muscle basal metabolic elimination rate, Kcal/hr/4;
Kcarb = 0.2;                    % NEW: Carb scaling for dietary thermogenesis (normalized digestive
thermic effect of food, using x5)

%ADDED HILL PARAMETERS
%note: for glut2 hill function, half is Greft and max is kg2max
```

```
kmxex = 10.0; %maximum gmgrad
kse = 40.0; %half gmgrad
kmxnm = 1.0; %max gtintol (half is ktintol)
kmxm = 1.0; %max gmintol (half is kmintol)
ksds = 5.0; %half slow digestive (max is kugs) - JW: not use?
ksds2 = 20.0; %half slow digestive falling (min is kugs)
ksd = 10.0; %half fast digestive (max is kugf)
ksd2 = 100.0; %half fast digestive falling (max is kugf)
  hs_max = 45;
  hs_ks = 23;
  hs_rate = 20;
% Mapping/scaling Params:
vratm = 0.1;        % ratio of volume_blood-plasma to volume_muscle tissue ... not used
vratt = 0.1;        % ratio of volume_blood-plasma to volume_non-muscle tissue ... not used
drat = 8.0*ratBM;   % NEW: Conversion of digestive mass flow in grams into ECF (blood plasma +
interstitial) in mg/dL, scaled by BW
wratm = (1/drat)/wmu;  % CHANGE: scaling from gluc blood conc (mg/dL) to gluc musc tissue amount in g, norm
to mass of segment (g/Kg_musc)
wratt = (1/drat)/wnm;  % CHANGE: scaling from gluc blood conc (mg/dL) to gluc non-musc tiss amount in g,
norm to mass of segment (g/Kg_n-m)

gratm = 0.01*wmu;   % for blood-muscle glucose gradient (e.g., exercise demand)
gratt = 0.01*wnm;   % not used
% NOTES:  % "normal" (70Kg BW) amount in blood plasma: (100 mg/dL)*(0.55*5L of blood) = (1 g/L)*(2.75L) =
2.75g ~ 3 g total (lit ~ 4g)
        % Adding in most of interstitial that is assumed to rapidly equilibriate for glucose: ~3.5*BP,
thus let ECF = 12.5 L, so norm ~ 12.5 g total
        % Consistent with Man-Cobelli: V = 1.88 dL/Kg * 70 = 132 dL = 13L
        % "normal" amount in muscle: 0.012*30Kg ~= 350 g (or 1400 Kcal) - ~25x more in musc than BP_ECF
        % "normal" amount in mon-musc (mostly liver): ~5 (3-8)?%*2.8Kg liver + ~1% adipose + other = 150
g other (lit)
        % side note: humans consume ~300 g/day, but OK with about 100 or so ... so multi-day store if no
exercise?
        % Ex, let density=1: if change of 10 mg/dL = 100 mg/L = 100 mg/Kg_ECF then 1300 mg transfer, or
1.4 Kg to 30 Kg = .047 g/Kg
        % Ex, conc grad: 100 mg/dL = 10 mg/L = 10 mg/Kg_ECF = .01 g/Kg_ECF) = .01*wmu g/Kg_tissue
```

```matlab
        % Ex, for drat: if 12.5 g/hr added to, say, 12.5 L of BP, then added 1 g/L or 100 mg/dL added in
1 hour, so mult by ~8

% PREP FOR SIMULATION:
delt = 0.01; tmin = 0;  tmax = 24;      % delt, tmax = 12 means 12 hours    JW CHANGE TO CHECK LONG_ACTING
t = tmin : delt : tmax;         % t=0 is wakeup (e.g., 8 AM); t=16=midnight
idel = insulindel/delt;      % number of samples for delay

%CHOOSE Sofie Protocol HR Input
%u = HRin_prot1(); %Tempo
 %u = HRin_prot2(); %Circuit Training
 %u = HRin_prot3(); %Long Run
%u = HRin_prot4(); %40 min bike + 20 min run
 %u = HRin_prot5(); %Sprint Intervals
 %u = HRin_prot6(); %Long Anaerobic
 u = HRin_noinput; %IF HR DATA IS NOT PROVIDED
 deltu3 = zeros(1,2401);

ug = 0.0; ui = 0.0;  ua = 0.0;  % init input matrix; residual produc levels
% %u = [ug*ones(1,length(t)); ui*ones(1,length(t)); zeros(1,length(t));  ua*ones(1,length(t))];
u1fast = ug*ones(1,length(t)); u1slow = ug*ones(1,length(t));  u1carb = ones(1,length(t));
% u = [ug*ones(1,length(t)); ui*ones(1,length(t)); zeros(1,length(t));  ua*ones(1,length(t));
zeros(1,length(t))];  % JW: added u5
u1fast = ug*ones(1,length(t)); u1slow = ug*ones(1,length(t));  u1carb = ones(1,length(t));
x = [zeros(5,length(t))];      % init state matrix size

% SETTING INPUTS (time and magnitude):
% Input 1: FOODSTUFF (MEALS)
nmeals = 6;  %define beginning:end of meals (every 10 is 6 min), total Kcal/hr rate, prop fast carbs (on
<0,1>):
mbeg(1) = 50;    mend(1) = 75;    mtot(1) = 800.;  kfast(1) = 0.8; FracCarbs(1) = 0.8;   % breakfast (in
Kcal/hr, area under curve is Kcal)
mbeg(2) = 500;   mend(2) = 550;   mtot(2) = 800.;  kfast(2) = 0.8;   FracCarbs(2) = 0.7; % lunch (in
Kcal/hr, area is ph*pw Kcals)
mbeg(3) = 1300;  mend(3) = 1350;  mtot(3) = 1400.;  kfast(3) = 0.5;  FracCarbs(3) = 0.5;  % dinner
mbeg(4) = 1800;  mend(4) = 1810;  mtot(4) = 600.;  kfast(4) = 1.0;   FracCarbs(4) = 1.0; % snack#1
```

```matlab
mbeg(5) = 1000;  mend(5) = 1010;  mtot(5) = 600.;  kfast(5) = 0.2;   FracCarbs(5) = 0.5; % snack#2
mbeg(6) = 800;    mend(6) = 810;  mtot(6) = 2000.;  kfast(6) = 0.5;   FracCarbs(6) = 0.8; % snack#3
xtot(1:nmeals,1:5) = 0.0;  scale4(1:nmeals) = 0; scale5(1:nmeals) = 0; lost4(1:nmeals) = 0.0;
for i = 1 : nmeals         % Pre-run to scale glucose conservation
    u1fast(i,length(t)-1) = 0.0; u1slow(i,length(t)-1) = 0.0;
    u1fast(i,mbeg(i):mend(i)) = mtot(i)*kfast(i);          % Area under fast meal curve in Carb-Energy
    u1slow(i,mbeg(i):mend(i)) = mtot(i)*(1-kfast(i));
    utotf(i) = (mend(i) - mbeg(i) + 1)*mtot(i)*kfast(i);
    utots(i) = (mend(i) - mbeg(i) + 1)*mtot(i)*(1-kfast(i));
    xx(4,1) = 0.0; xx(4,1:length(t)-1) = 0.0;                % Glucose, Stomach, fast meal path
    xx(5,1) = 0.0; xx(5,1:length(t)-1) = 0.0;
    % Glucose, Stomach, slow meal path
    for ii = 1 : length(t) - 1
        Gfast = fhill((xx(4,ii)),(Kugf/2),5,4) + fhillr((xx(4,ii)),(Kugf/2),30,4); % Kugf is mid-range max
        Gslow = Kugs + fhillr(xx(5,ii),Kugs,10,4);          % Kugs is min, mid-range max nearly double August
Fit
        f(4) = Gfast*(Gugf*(u1fast(i,ii)/4) - xx(4,ii)); % + x(5,ii); % 1st-order on glucose bolus, coud be
f8old  %JW changed!
        f(5) = Gslow*(Gugs*(u1slow(i,ii)/4) - xx(5,ii));
        %%
        for j =  4 : 5
            xx(j,ii+1) = xx(j,ii) + f(j)*delt;       % Euler integration
            xtot(i,j) = xtot(i,j) + xx(j,ii+1);
        end
    end
    scale4(i) = (xtot(i,4)/utotf(i));
    scale5(i) = (xtot(i,5)/utots(i));
end

for i = 1 : nmeals      % setting up input #1 (foodstuff)
    u1fast(1,mbeg(i):mend(i)) = mtot(i)*kfast(i);
    u1slow(1,mbeg(i):mend(i)) = mtot(i)*(1-kfast(i));
    if i < nmeals
    u1carb(1,mbeg(i):mbeg(i+1)-1) =FracCarbs(i);
    elseif i == nmeals
        u1carb(1,mbeg(i):length(t)) = FracCarbs(i);
    end
```

```matlab
end

% Input 2: Insulin Injections, as half-sine: 1: Regular (max in 2 hrs); 2: Fast (max in 1 hr); 3: Long-
acting (max in 6 hrs)
%ninjec = 3;   %define beginning:end of meals (every 10 is 6 min), total Kcal/hr rate, prop fast carbs (on
<0,1>):
% Prep:
t2r = [0 : 1 : 400];   u2r(1:length(t2r)) = sin(pi*(t2r/400));   % Regular half-sine
t2f = [0 : 1 : 20];    u2f(1:length(t2f)) = sin(pi*(t2f/20));   % Fast half-sine
t2s = [0 : 1 : 1200];  u2s(1:length(t2s)) = sin(pi*(t2s/1200));  % Slow half-sine
itype = [zeros(3,4)]; idose = [zeros(3,4)]; ibeg = [zeros(3,4)]; iend = [zeros(3,4)];
itbeg = tmin/delt;   itend = (tmax/delt)+1;
% Regular (max delivery in 2 hrs, through 4 hrs): give idose, ibeg
itype(1,1) = 1; idose(1,1) = 0; ibeg(1,1) = 10;    iend(1,1) = ibeg(1,1) + 400;
itype(1,2) = 1; idose(1,2) = 0; ibeg(1,2) = 475;   iend(1,2) = ibeg(1,2) + 400;
itype(1,3) = 1; idose(1,2) = 0; ibeg(1,2) = 2100;  iend(1,2) = ibeg(1,2) + 400;
% Fast-Acting (max delivery in 1 hr, ends 2 hrs): give idose, ibeg
itype(2,1) = 1; idose(2,1) = 0; ibeg(2,1) = 1;    iend(2,1) = ibeg(2,1) + 10;
itype(2,2) = 1; idose(2,2) = 0; ibeg(2,2) = 1325;  iend(2,2) = ibeg(2,2) + 20;
itype(2,3) = 1; idose(2,3) = 0; ibeg(2,3) = 475;   iend(2,3) = ibeg(2,3) + 20;
% Long-Acting (max delivery 6 hrs, ends 12 hrs): given idose, ibegitype(2,1) = 1; idose(2,1) = 5; ibeg(2,1)
= 100;    iend(2,1) = ibeg(2,1) + 400;
itype(3,1) = 1; idose(3,1) = 0; ibeg(3,1) = 10;   iend(3,1) = ibeg(3,1) + 1200;
itype(3,2) = 1; idose(3,2) = 0; ibeg(3,2) = 1800;  iend(3,2) = ibeg(3,2) + 1200;
for i = 1 : 3
    for ii = 1 : 4
        if iend(i,ii) > itend   % e.g., if end of day, then shorten array
            iend(i,ii) = itend;
        end
        if ibeg(i,ii) < itbeg
            ibeg(i,ii) = 0;
        end
        if idose(i,ii) > 0
            if i == 1   % regular
              u(2,ibeg(i,ii):iend(i,ii)) = u(2,ibeg(i,ii):iend(i,ii)) + 1.414*idose(i,ii)*u2r(1:(iend(i,ii)-
ibeg(i,ii)+1));
            end
```

```matlab
            if i == 2   % fast
                u(2,ibeg(i,ii):iend(i,ii)) = u(2,ibeg(i,ii):iend(i,ii)) + 1.414*idose(i,ii)*u2f(1:(iend(i,ii)-
ibeg(i,ii)+1));
            end
            if i == 3   % slow
                u(2,ibeg(i,ii):iend(i,ii)) = u(2,ibeg(i,ii):iend(i,ii)) + 1.414*idose(i,ii)*u2s(1:(iend(i,ii)-
ibeg(i,ii)+1));
            end
        end
    end
end


%IF/THEN CODE FOR DECIDING ON KA_RATE FOR SLOW VS FAST INSULIN PATHWAY
%k as a function of insulin type, tissue at area of injection/infusion, and
%increased blood flow of localized area
%Fast if fast-acting insulin, increased blood flow (i.e. heat, exercise)
%and lean tissue
%k_rate = k_type*k_tiss*k_flow
%by default k_tissue = k_flow = 1.0  % JW: not k_type
%RANGES: k_type: 3 subgroups
%         k_tissue: greater for people with excess body fat
%         k_flow: greater for decreased flow

% if itype(1,:) > 0
%     k_type = 0.2;
% elseif itype(2,:) > 0
%     k_type = 0.5;
% elseif itype(3,:) > 0
%     k_type = 0.8;
% end

% if ratMUSC >= 1.0
%     k_tissue = 0.2;
% elseif ratMUSC < 1.0
%     k_tissue = 0.8;
% end
```

```matlab
%WILL HAVE TO PUT AFTER EXERCISE INPUT
% if u3 > 0
%     k_flow = 0.2;
% elseif u4 > 0
%     k_flow = 0.5;
% else
%     k_flow = 1.5;
% end


% Input 3: Energy over time (power) consumed during Exercise (in Kcal/Hr)
    % Notes: - Steady: WorkWatts/WorkEff, e.g., if max is 256 W = 220 Kcal/Hr, 220/.22 = 1000 Kcal/hr
    %        - HRdiff in beats/min, e.g., if HRdiff = (HRmax-HRrest) = 170-70 = 100, then 10 Kcal/hr-HRdiff
    %        - RRdiff in beaths/min, e.g., RRdiff = (RRdiff-RRrest) = ...
    %        - PVO2Max: percent VO2max (can with resting being ~8% of this)
    %        - If at <25% of VO2max: kcal/hr*0.6 (but at some stage higher), 25-50%: *0.7; 50-60%: *0.8 (or
lower); >60%: *0.95
WorkEff = 0.22;              % Efficiency in performing physical work (typically 20-25%, higher for
skilled tasks)
AerCap = 1100;              % Max capacity, in Kcal/hr, can map to "aerobic/mitochondrial" metrics (each
with scaling capability):
uptime = 1;  downtime = 1;  % exercise up-time & down-time, without using metric such as HR - hour is 100
units
intens =0; slopeu = intens/uptime; sloped = intens/downtime; % steady aerobic intensity, in Kcal/Hr
u(3,350:(350+uptime-1)) = [slopeu*([1:uptime].*ones(1,uptime))];    % aerobic ramp up, for now
u(3,(350+uptime):450) = intens;              % USER: Add exercise with intensity = kcal/hr (glucose) burned
u(3,451:(451+downtime-1)) = [sloped*((downtime-[1:downtime]).*ones(1,downtime))];
%CHAPTER 4 EXERCISE INPUTS
HRrest = 60;
HRmax = 200;


%NEW HOROMONAL INPUT--Grow array to multiple levels--time dependent.
uHM = ones(1,2401);
uHM(700:800) = stressrat*uHM(700:800);


% Input 4: DAILY ACTIVITY (using randomization) for u(4,:), in Kcal/Hr
nactive = 3;   % "moving/fidgeting activity" time periods of the day where muscles consume glucose
```

```matlab
abeg(1) = 200;    aend(1) = 250;     actave(1) = 100.0;    alow(1) = 0.7;   ahi(1) = 1.3;
abeg(2) = 1100;   aend(2) = 1200;    actave(2) = 80.0;     alow(2) = 0.6;   ahi(2) = 1.4;
abeg(3) = 1600;   aend(3) = 1700;    actave(3) = 60.0;     alow(3) = 0.7;   ahi(3) = 1.3;
u4max = 50;       % assumed max Anaerobic in Kcal/hr before switch to mitochondrial/aerobic
for i = 1 : nactive
    u(4,abeg(i):aend(i)) = actave(i)*(alow(i) + ((ahi(i)-alow(i)).*rand(1,(aend(i)-abeg(i)+1))));
end

% nsens = 19;  salo = 0.9;  saloM1 = 1/salo; sahi = 1.1;  sahiM1 = 1/sahi; sadiff = sahi - salo;
% bt1 = 1250;  bt2 = 1325; bt3 = 1375;  % times for state magnitude behaviors
% btlo = 1250; bthi = 1500;  % time window for examining behaviors (bt1, bt2 should be within this range)
% bx_min = zeros(2*nsens+1,9);  bx_tmin = zeros(2*nsens+1,9);   % initializing behaviors for min
% bx_max = zeros(2*nsens+1,9);  bx_tmax = zeros(2*nsens+1,9);    % init behaviors for max
% bx_t1 =  zeros(2*nsens+1,9);  bx_t2 = zeros(2*nsens+1,9); bx_t3 = zeros(2*nsens+1,9);    % init behaviors
for magn at strategic times
% for isens = 1 : (2*nsens)+1
% % bm, Cia, Cib, Cga, Kgt, Kugs, Grefi, Grefg, Greft, Gbt, wratm, wratt,Gratm
%    switch (isens-1)
%        case 1;   Ki     = salo*Ki;        case 2;   Ki     = sahi*Ki;
%        case 3;   Cia    = salo*Cia;       case 4;   Cia    = sahi*Cia;
%        case 5;   Cib    = salo*Cib;       case 6;   Cib    = sahi*Cib;
%        case 7;   Cga    = salo*Cga;       case 8;   Cga    = sahi*Cga;
%        case 9;   Kgt    = salo*Kgt;       case 10;  Kgt    = sahi*Kgt;
%        case 11;  Kugs   = salo*Kugs;      case 12;  Kugs   = sahi*Kugs;
%        case 13;  Grefi  = salo*Grefi;     case 14;  Grefi  = sahi*Grefi;
%        case 15;  Grefg  = salo*Grefg;     case 16;  Grefg  = sahi*Grefg;
%        case 17;  Greft  = salo*Greft;     case 18;  Greft  = sahi*Greft;
%        case 19;  Gbt    = salo*Gbt;       case 20;  Gbt    = sahi*Gbt;
%        case 21;  wratm  = salo*wratm;     case 22;  wratm  = sahi*wratm;
%        case 23;  wratt  = salo*wratt;     case 24;  wratt  = sahi*wratt;
%        case 25;  Kg2Max = salo*Kg2Max;    case 26;  Kg2Max = sahi*Kg2Max;
%        case 27;  kmxex  = salo*kmxex;     case 28;  kmxex  = sahi*kmxex;   %new pars
%        case 29;  kse    = salo*kse;       case 30;  kse    = sahi*kse;   %new pars
%        case 31;  ksds   = salo*ksds;      case 32;  ksds   = sahi*ksds;   %new pars
%        case 33;  Kmintol= salo*Kmintol;   case 34;  Kmintol= sahi*Kmintol;  %new pars
%        case 35;  insulindel= salo*insulindel; case 36;  insulindel  = sahi*insulindel;   %new pars
%        case 37;  Kid= salo*Kid;               case 38;  Kid  = sahi*Kid;
```

```matlab
%       otherwise ; % no change, e.g., last run
%    end
%
% SETTING INITIAL CONDITIONS:
x(1,1) = 100.;                    % Glucose, Blood, x1=xG0
x(2,1) = (150*ratNONM)/wnm;  % Glucose, Non-Musc, AMOUNT, in g/Kg_non-m, e.g., 140 g/ 35 Kg = 4, & max ~20
(~3-8% liver, ~1% adipose)
x(3,1) = (300*ratMUSC)/wmu;  % Glucose, Musc, AMOUNT, in g/Kg_musc, e.g., 300 g/ 30 Kg = 10, & max ~600/30
= 20 (2%)
x(4,1)= 0.0;                     % Glucose Mass Flow, Stomach, fast meal path, in grams/hr glucose
x(5,1) = 0.;                     % Glucose Mass Flow, Stomach, slow meal path, in grams/hr glucose
x(6,1) = 1.0*ratType1i;        % Insulin, Blood, x6=xS0; default 1.0 mU/dL (7 mMol/L); for Type I, set to 0
JW CHANGE
x6(1:idel) = x(6,1);           % priming for delay
x(7,1) = 0.0;                   % Insulin, Tissue, forward path state, monomeric
x(8,1) = 0.45*ratType1g ;      % Glucagon, blood; ~70 in pg/mL or 0.7 in micro-g/dL or ; for Type I, lower
than 0.35  JW CHANGE
x1d = 0.0;
x(9,1) = 0.0;                   % Insulin, Tissue, forward path state, monomeric
x(10,1) = 0.0;                  % Mitochondrial consumption
%
%PART OF SENSITIVITY ANALYSIS
% bxmin(1:9) = x(1:9,1);  tbxmin(1:9) = btlo;  % seting up auto-behaviors
% bxmax(1:9) = x(1:9,1);  tbxmax(1:9) = btlo;

% LOOP FOR SIMULATION:
GG = [zeros(14,length(t))];
u1sum = 0; u1slowsum = 0;
x4sum = 0;  x5sum = 0;
for i = 1 : length(t)-1
  % NONLINEAR HILL Functionals:

  % For Controllers:
  % NEW NOTES:  Basal (non-meal) insulin level is about 1 mU/dL (70 pMol/L), and max is about 10 mU/dL
  GCi = ratType1i*fhillp1(x(1,i),6,Grefi,4);     % New control action: ratio, with k_1/2 higher
  GCi2 = u(2,i)*(ka1+kd);
```

```
  GCi_hs_mag = fhill(u(2,i),hs_max,hs_ks,1);  GG(10,i) = GCi_hs_mag; %Rate of exogenous infusion rate
(pmol/kg/min)
  GCi_hs_rate = fhill(x(9,i),hs_rate, kd, 1); GG(11,i) = GCi_hs_rate;
  if (x1d > 0)
      GCiD = Kid*x1d*ratType1i;  % rising, represents residual storage in pancreas, and "lead"
  else
      GCiD = 0.0;                % dropping, currently assumed 0
  end
  GCg = ratType1g*fhillrp1((x(1,i)),4,Grefg,4);     GG(2,i) = GCg;          % glucagon drive, sensing x1,
strong if low

  % For Digestive:
  %Gfast = 0.5 + fhill(x(4,i),0.5,10,2); % rate at which fast stomach glucose enters blood, either x4 or u1
(max overall is ~70 g/hr)
  %Gslow = fhill(x(5,i),75,20,2);
  %Gslow = 0.5 + fhill(x(5,i),0.3,4,2);  % rate for slow path
  Gabs = (fhill(x(4,i),(Kugd/2),ksds,4) + fhillr((x(4,i)),(Kugf/2),ksd2,4))*u1carb(1,i);  GG(8,i) = Gabs; %
Kugd is max, in mid-range
  Gslow = (Kugs + fhillr(x(5,i),Kugs,ksds2,4))*u1carb(1,i); GG(9,i) = Gslow;  % Kugs is min, mid-range max
nearly double August Fit

  % For Non-Muscle   NEW
  Gnm_glut2 = fhill((x(1,i)),Kg2Max,Greft,2) - (Kg2Max/2);   % bi-dir rate for non-musc, GLUT2 (mostly to
liver, also pancreas, intestines, ...)

  % For Intolerance (or could be used for glucose-to-fat conversion):
  Gtintol = fhillr(x(2,i),kmxnm,Ktintol,8)+0.0;   GG(4,i) = Gtintol; % NL Hill - tissue intolerance, mult,
1.0=none, <0.1,1>
  Gmintol = fhillr(x(3,i),kmxm,Kmintol,8)+0.0;    GG(7,i) = Gmintol; % NL Hill - muscle intolerance, mult,
1.0=none, <0.5,1>

  % For Muscle (and exercise):
  %NEW HR U5
  %Take u3 and put through LPF with time constant of 6 min
  %Perfect u3 and anticipated u3 informed by u5; as a function of u3
  %Derivative of u5; sum the two
```

```matlab
%    %U5 INPUT


        %Case Study Anaerobic Threshold (AT) = 170 bpm = 80% of HRmax, or (170-48)/(191-48) = 0.85
normalized
        %Case Study AEROBIC ZONES:   Active Recovery = 0.7*AT = 111-126 bpm
%                                    Easy Aerobic = 0.8*AT = 128-145 bpm
%                                    Moderate Aerobic = 0.9*AT = 146-169 bpm
%                                    Threshold = 1.02*AT = 170-180 bpm
% Maximal = 1.06*AT = 180-191 (max HR)


%normalize HR

%for j = 1:1:length(t)

%     if u(5,j) >= 128 && u(5,j) <= 145
%         u(3,j) = 0.8*AerCap;
%       elseif u(5,j) > 145 && u(5,j) <= 169
%           u(3,j) = 0.9*AerCap;
%       elseif u(5,j) > 169 && u(5,j) <= 180
%           u(3,j) = 1.02*AerCap;
%       elseif u(5,j) > 180
%           u(3,j) = 1.06*AerCap;
%       elseif u(5,j) == 0
%           u(3,j) = u(3,j);

       %NEW STEPS
      %1. Take steps zones and create a hill functional to map u3 ref to HR
      %ref; use delta hr to get delta u3 that adds or subtracts
      %normalize HR
    urelHR(i) = (u(5,i)-HRrest)/(HRmax-HRrest);
    upredex(i) =(u(3,i)/AerCap);
    urelHR = upredex; %IF NO HR DATA AVAILABLE delt will be 0
    kscale = 500; %scaling
    if urelHR(i) == 0
        u3new(i) = u(3,i);
```

```matlab
        else
         deltu3(i) = kscale*(upredex(i) - urelHR(i));
         u3new(i) = u(3,i) + deltu3(i);
        end
   %  end


       if u(5,i) >= 1.25*HRrest && u(5,i) < 130
       u(4,i) = 100; %200 would be 50 W
       end
%end




  %BAND PASS Filter for fluctuation?
%if (u3 is very high) & (u5 is very high) then (Gu35 is high)
Gsh2_u35 = u(3,i)*(fhill(u(3,i),1,500,2)) * fhill(u(5,i),1,0.85,4);  GG(12,i) = Gsh2_u35;     % "aerobic
effort"-related high stress hormone to f2
%if (u4 is very high) & (u4 is fluctuating) & (u5 is high) then (Gu45 is high)
Gsh2_u45 = (u(3,i)+ u(4,i))*(fhill(u(3,i) + u(4,i),1,100,2)) * fhill(u(5,i),1,0.5,2);   GG(13,i) =
Gsh2_u45;      % "anaerobic effort"-related high stress hormone to f2
%if (u5 is not low) & [(u3 is low) & (u4 is low) & (x4 is low)] then (Gu5 is higher)
Gsh_ant = fhill(u(5,i),1, 0.8, 4)*[fhillr(u(3,i),1,100,2) * fhillr(u(4,i),1,10,2) * fhillr(u(4,i),1,10,2) *
fhill(x(4,i),1,0.5,2)];  GG(14,i) = Gsh_ant; %HR is high and not exercising



if Gsh2_u35 > 0
    GfatAer = fhill(((u3new(i)/AerCap)), 0.4*AerCap, 0.2, 2);
else
    GfatAer = fhill(((u3new(i)/AerCap)), 0.3*AerCap, 0.3, 2);
end

  %GexerAer = 0.1*u(3,i) + fhill(u(3,i),10.0,500,1);  GG(5,i) = GexerAer;   % NL Hill - exercise
consumption rate (muscle),
 % GfatAer = fhill((u(3,i)/(AerCap)),0.3*AerCap,0.3,2); % proportion of fuel mix that is fats, normalized
  GexerAer = (u3new(i)) - GfatAer; GG(5,i) = GexerAer;    % assumed energy of glucose within fuel mix
  %if (u(3,i)) > 0  # JW COMMENTED OUT 7/24
```

```matlab
%       GexerAna = u4max;           % max out non-aerobic "activity" energy, to transition to need for aerobic
    %else
        GexerAna = 0;
    %end
    % Anaerobic max before aerobic, direct, assumed all glucose fuel, continues? Drops with slopeu?
    GexerTot = (GexerAer + GexerAna);           % total glucose energy (not yet in grams-equivalent)

    %Gmgrad = fhill(u(3,i),0.6,100,1) + fhill((x(1,i)-x(6,i)),0.04,100,1);       GG(6,i) = Gmgrad; % NL Hill -
blood glucose loss, with muscle demand gradient
    Kgrad = .0;
    Gmgrad = fhill(u(3,i)/4.0,kmxex*ratType1i,kse,1) - 0.1*fhillr(x(1,i), kmxex*ratType1i,kse,1); % +
Kgrad*(x(1,i)-(x(3,i)/gratm));       GG(6,i) = Gmgrad; % NL Hill - blood glucose loss, with muscle demand
gradient

    % State Equation Functionals (dx/dt=):
    f(1) = drat*x(4,i)- Kbr/wnm - ((Cia*Gtintol)+(Cib*Gmintol))*x(1,i)*x6(idel) - uHM(1,i)*Gnm_glut2*x(1,i) -
Gmgrad*(x(1,i)-(x(3,i)/gratm)) + (Cga+Cgb)*Kgt*x(8,i)*x(1,i); %- Gsh2_u45; % +uHRAer +uHRAna;  %*G4;
%x(2,i)-;  %+Gb %Gluc Bl
    f(2) = wratt*(uHM(1,i)*Gnm_glut2 + Cia*x6(idel)*Gtintol)*x(1,i) - wratt*Cga*Kgt*x(8,i)*x(1,i) - (Gbt +
(Kcarb*x(5)))/wnm ; % - uHRAer - uHRAna; %.2*x(4,i)*x(5,i); %+.6*x(4,i); %*G4; % non-muscle tissue
    f(3) = wratm*Cib*x(1,i)*x6(idel)*Gmintol - Gbm/wmu - wratm*Cgb*Kgt*x(8,i)*x(1,i) + wratm*(Gmgrad*(x(1,i)-
(x(3,i)/gratm)))  + ratmito*x(10,i); %g/kgmusc %+uHRAna +uHRAer %+kFAT*x(10,i); %+.4*x(4,i)*0.2*x(8,i)*G5;
% musc tissue
    f(4) = Gabs * ((u1fast(1,i)/4) + x(5,i) - Gugf*x(4,i)); % + x(5,ii); % Final common digestive rate
    f(5) = Gslow* ((u1slow(1,i)/4) - Gugs*x(5,i));    % Slow low-GI path
    f(6) = (ka2)*x(7,i) + (ka1)*x(9,i) - (Ki)*x(6,i) + GCi + GCiD ;  %+ Kid*x6(idel)+ (ka1)*x(9,i);  %
insulin in blood plasma, up via controller; fast monomeric path
    f(9) = (ka1*x(9,i)) - GCi_hs_rate + GCi_hs_mag;      % new insulin tissue state
    f(7) = (kd*(x(9,i)) - (ka2)*(x(7,i)));%GCi_hs; %*GCi_hs;
    f(8) = Kgc*(GCg - x(8,i));                     % glucagon in blood plasma (compare to f6)
    f(10) = (Kmusc*((GexerTot + kprop*u(4,i))/4 - x(3,i) - x(10,i)))/wmito; % kcpt*(GexerAna+u(4,i)) -
kFAT*(x(10,i)); %MITOCHONDRIAL CONSUMPTION STATE, GIVEN DEMAND

    %Generate Simulation Iteration of States

    for j =  1 : 10
      if x(j,i) < 0
```

```
    x(j,i) = 0.0;
  end
  x(j,i+1) = x(j,i) + f(j)*delt;        % Euler integration
  if j == 4
      x4sum = x4sum + x(4,i)*delt;  % integrating x4 to get total grams
      u1sum = u1sum + (u1fast(1,i)/4)*delt;
  end
  if j == 5
      x5sum = x5sum + x(5,i)*delt;  % integrating x5 to get total grams
      u1slowsum = u1slowsum + (u1slow(1,i)/4)*delt;
  end
%PART OF SENSITIVITY
%     if ((x(j,i+1) < bxmin(j)) & (i >= btlo) & (i <= bthi));   % behavior: finding low of state
%         bxmin(j) = x(j,i+1);  tbxmin(j) = i+1 - btlo;
%     end
%     if ((x(j,i+1) > bxmax(j)) & (i >= btlo) & (i <= bthi)); % behavior: finding high of state
%         bxmax(j) = x(j,i+1);  tbxmax(j) = i+1 - btlo;
%     end
%     if (i == bt1)              % behavior at t1
%         bxt1(j) = x(j,i+1);
%     end
%     if (i == bt2)              % behavior at t2
%         bxt2(j) = x(j,i+1);
%     end
%     if (i == bt3)              % behavior at t3
%         bxt3(j) = x(j,i+1);
%     end
  end
  x1d = (x(1,i+1) - x(1,i))/delt;
  for ii = 1 : idel-1
    x6(idel-ii+1) = x6(idel-ii);    % shifting for time delay
  end
  x6(1) = x(6,i+1);

end
```

```
u1 = u1fast + u1slow;
%FIGURE 1: 1) INPUT CURVES 2) X1 (BLOOD GLUCOSE)WITH THRESHOLD LINES
%           3) TISSUE GLUCOSE, MUSCLE AND NON-MUSCLE (X2, X3) AND
%              4) GLUCAGON AND INSULIN CONTROLLERS
% 24 HOUR SIMULATION
figure(1); set(2,'Color',[1 1 1]);
hold on;
 %tp = t(250:550);    up = u(:,250:550);    xp = x(:,250:550);   % ONE APPROACH: NEW VECTORS FOR PLOTTING
 tpbeg = 0; tpend = 24;                                                  % USE AXIS()
TO PLOT PART OF T VECTOR (EASIEST?)
subplot(5,1,1)                    % Meal input, stomach state x4:
  plot(t,u1(1,:),'k',t,x(4,:)*4,'r',t,u(3,:),'-.',t,u(4,:),'-',t,GG(5,:),':','LineWidth',1.5); hold on;
  plot(t,x(5,:)*4,'g',t,x(10,:)*4,'b')
  ylabel('G-Flow (Kcal/hr)','FontWeight','bold')
  axis([tpbeg tpend 0 1200])
subplot(5,1,2)                        % Glucose states:
   winl = [70*ones(1,length(t))];        % low glucose line
   winh = [150*ones(1,length(t))];       % somewhat high glucose line
   winhh = [200*ones(1,length(t))];      % very high glucose line, intol and/or to fat
  plot(t,x(1,:),'r','LineWidth',1.5); hold on;
  plot(t,winl,':',t,winh,':',t,winhh,':'); hold on;
  ylabel('Gluc Bl (mg/dl)','FontWeight','bold')
  axis([tpbeg tpend 40 280])

subplot(5,1,3)                        % Insulin input, states:
 [hAx,hLine1,hLine2] = plotyy(t,x(6,:),t,x(8,:)); hold on;     % ,t,u(2,:),':',t,x(7,:),':'
 set(hLine1,'LineStyle','-','LineWidth',1.5)
 set(hLine2,'LineStyle','--','LineWidth',1.5)
 ylabel(hAx(1),'Insulin (mU/dl)','FontWeight','bold') % left y-axis
 axis(hAx(1),[tpbeg tpend 0 5])   % NEW, CAN COMMENT OUT
 ylabel(hAx(2),'Glucagon (pg/dL)','FontWeight','bold') % right y-axis
 axis(hAx(2),[tpbeg tpend 0 1.2]) % NEW, CAN COMMENT OUT
 hold on;
subplot(5,1,5)
 plot(t,u(2,:),'r',t,x(9,:),'g',t,x(7,:)),'m'; hold on;
ylabel('Exogenous Insulin')
```

```matlab
  xlabel('Time (hours)','FontWeight','bold')
  axis([tpbeg tpend 0 20])
   subplot(5,1,4)                                    % Meal input, stomach state x4:
     plot(t,x(2,:),':',t,x(3,:));
     ylabel('Tissue','FontWeight','bold') %ADD MITOCHONDRIAL STATE HERE? SAME UNITS G/KG
     axis([0 tmax 0 50])

     %plot GG HILL FUNCTIONALS
% figure(2)
% subplot(3,2,1)
% plot(u(2,:), GG(10,:)) %RATE OF EXOGENOUS INFUSION
% subplot(3,2,3)
% plot(u(2,:), GG(11,:))  %MAGNITUDE OF EXOGENOUS INFUSION
% subplot(3,2,4)
% plot(t,GG(8,:), t,GG(9,:)) %FINAL DIGESTIVE AND SLOW DIGESTIVE
% axis([tpbeg tpend 0 10])
% subplot(3,2,5)
% plot(x(4,:),GG(8,:),'+') %FINAL DIGESTIVE AND INPUT
% subplot(3,2,6)
% plot(x(5,:),GG(9,:),'+') %SLOW DIGESTIVE AND INPUT


%INSULIN STATES
%figure(3);
%subplot (2,1,1)
%plot(t,x(6,:))
%ylabel('Plasma Insulin')
%subplot (2,1,2)
%plot(t,x(7,:))
%ylabel('Exogenous Insulin')
%xlabel('Time (hours)')

%PLOT MITOCHONDRIAL STATE
% figure(4)
% plot(t,x(10,:));
% ylabel('Mitochondrial State (g/kgmito/hr)')
```

```
%DEMONSTRATE HR CODE AND INFORMING U3
% figure(6)
% subplot(4,1,1)
% plot(t, u(5,:))
% title('Heart Rate')
% axis([5 10 0 200])
% subplot(4,1,2)
% plot((t),deltu3)
% title('Delt U3')
% axis([5 10 -200 200])
% subplot(4,1,3)
% plot(t,u(3,:),'g')
% plot(t,u(4,:),'r')
% title('U3 and U4')
% axis([5 10 0 800])
% subplot(4,1,4)
% plot(t,x(1,:),'k', t, x(2,:),'r', t, x(3,:),'b')
% title('BG and Tissue')
% axis([5 10 0 800])


%~~~~~~~~~~~~~~~~~~~~~~~~~~~~~~~~~~~~~~~~


%END OF SENSITIVITY ANALYSIS
%    bx_min(isens,1:8) = bxmin(1:8);  bx_tmin(isens,1:8) = tbxmin(1:8);  % getting min behaviors
%    bx_max(isens,1:8) = bxmax(1:8);  bx_tmax(isens,1:8) = tbxmax(1:8);  % getting max behaviors
%    bx_t1(isens,1:8)  = bxt1(1:8);   bx_t2(isens,1:8) = bxt2(1:8);  bx_t3(isens,1:8) = bxt3(1:8);     %
getting magn at times behaviors
%
%    switch (isens-1)    % switch back, after run
%       case 1;   Ki    = saloM1*Ki;        case 2;   Ki    = sahiM1*Ki;
%       case 3;   Cia   = saloM1*Cia;       case 4;   Cia   = sahiM1*Cia;
%       case 5;   Cib   = saloM1*Cib;       case 6;   Cib   = sahiM1*Cib;
%       case 7;   Cga   = saloM1*Cga;       case 8;   Cga   = sahiM1*Cga;
%       case 9;   Kgt   = saloM1*Kgt;       case 10;  Kgt   = sahiM1*Kgt;
%       case 11;  Kugs  = saloM1*Kugs;      case 12;  Kugs  = sahiM1*Kugs;
%       case 13;  Grefi = saloM1*Grefi;     case 14;  Grefi = sahiM1*Grefi;
```

```
%        case 15;  Grefg  = saloM1*Grefg;      case 16;  Grefg  = sahiM1*Grefg;
%        case 17;  Greft  = saloM1*Greft;      case 18;  Greft  = sahiM1*Greft;
%        case 19;  Gbt    = saloM1*Gbt;        case 20;  Gbt    = sahiM1*Gbt;
%        case 21;  wratm  = saloM1*wratm;      case 22;  wratm  = sahiM1*wratm;
%        case 23;  wratt  = saloM1*wratt;      case 24;  wratt  = sahiM1*wratt;
%        case 25;  Kg2Max = saloM1*Kg2Max;     case 26;  Kg2Max = sahiM1*Kg2Max;
%        case 27;  kmxex  = saloM1*kmxex;      case 28;  kmxex  = sahiM1*kmxex;  %new pars
%        case 29;  kse    = saloM1*kse;        case 30;  kse    = sahiM1*kse;  %new pars
%        case 31;  ksds   = saloM1*ksds;       case 32;  ksds   = sahiM1*ksds;  %new pars
%        case 33;  Kmintol= saloM1*Kmintol;    case 34;  Kmintol= sahiM1*Kmintol;  %new pars
%        case 35;  insulindel= saloM1*insulindel; case 36;  insulindel = sahiM1*insulindel;  %new pars
%        case 37;  Kid= saloM1*Kid; case 38;  Kid  = sahiM1*Kid;  %new pars
%    end
%
% end   % Param Sens Anal Loop (isens)
% sens_xmin = zeros(nsens,8); sens_txmin = zeros(nsens,8);
% sens_xmax = zeros(nsens,8); sens_txmax = zeros(nsens,8);
% sens_xt1  = zeros(nsens,8); sens_xt2   = zeros(nsens,8); sens_xt3   = zeros(nsens,8);
% for i = 1 : nsens
%     sens_xmin(i,:)  = ((bx_min((2*i)+1,:)-bx_min(2*i,:))./bx_min(1,:))/sadiff;
%     sens_xmax(i,:)  = ((bx_max((2*i)+1,:)-bx_max(2*i,:))./bx_max(1,:))/sadiff;
%     sens_txmin(i,:) = ((bx_tmin((2*i)+1,:)-bx_tmin(2*i,:))./bx_tmin(1,:))/sadiff;
%     sens_txmax(i,:) = ((bx_tmax((2*i)+1,:)-bx_tmax(2*i,:))./bx_tmax(1,:))/sadiff;
%     sens_xt1(i,:)   = ((bx_t1((2*i)+1,:)-bx_t1(2*i,:))./bx_t1(1,:))/sadiff;
%     sens_xt2(i,:)   = ((bx_t2((2*i)+1,:)-bx_t2(2*i,:))./bx_t2(1,:))/sadiff;
%     sens_xt3(i,:)   = ((bx_t3((2*i)+1,:)-bx_t3(2*i,:))./bx_t3(1,:))/sadiff;
% end
% sens_all = [ sens_xmin' ; sens_txmin' ; sens_xmax' ; sens_txmax' ; sens_xt1' ; sens_xt2'; sens_xt3' ];


%~~~~~~HILL FUNCTION CODE~~~~~
%   function [dfh] = fhill(df,kmax,ks,nh)
%     dfh = (kmax.*(df^nh))./((ks^nh) +(df^nh));
%   end
%
%     function [dfh] = fhillp1(df,kmax,ksp1,nh)
%   ks = (9*(ksp1.^(nh))).^(1/nh);    % mapping 10% to 50% for any nh
%   dfh = (kmax.*(df^nh))./((ks^nh) +(df^nh));
```

```matlab
%       end
%
%         function [dfh] = fhillr(df,kmax,ks,nh)
%      dfh = (kmax.*(ks^nh))./((ks^nh) +(df^nh));
%        end
%
%   function [dfh] = fhillrp1(df,kmax,ksp1,nh)
%    ks = ((1/9)*(ksp1.^(nh))).^(1/nh);      % mapping 10% to 50% for any nh
%    dfh = (kmax.*(ks^nh))./((ks^nh) +(df^nh));
%     end
%~~~~~~~~~~~~~~~~~~~~~~~~~~~~~~~~~~~~~~~~~~~~~~~~~~~~~~~~~~~~~~~~~~~~

%LITERATURE PLOTTING CODE%
%u(3,:) = u3new;
%Import Literature Data
%t_moh = xlsread('Ins_clindata.xlsx', 'GI_avg', 'A3:A11');
%moh_gluc_potato = xlsread('Ins_clindata.xlsx', 'GI_avg','M3:M11'); %GI 41
%moh_gluc_bread = xlsread('Ins_clindata.xlsx', 'GI_avg','N3:N11'); % GI 25
%moh_gluc_spag = xlsread('Ins_clindata.xlsx', 'GI_avg','P3:P11');% GI 46
%moh_gluc_bar = xlsread('Ins_clindata.xlsx', 'GI_avg','Q3:Q11'); %GI71
%moh_gluc_juice = xlsread('Ins_clindata.xlsx', 'GI_avg','O3:O11');%GI 83


%figure(1)
%% %Mohammed et. al. GI
%plot(t_moh,moh_gluc_potato); hold on;
%plot(t_moh,moh_gluc_bread); hold on;
%plot(t_moh,moh_gluc_spag); hold on;
%plot(t_moh,moh_gluc_bar); hold on;
%plot(t_moh,moh_gluc_juice); hold on;
%~~~~~~~~~~~~~~~~~~~~~~~~~~~~~~~~~~~~~~~~~~~~~~~~~~~~~~~~~~~~~~~~~~~~~
%%Aronoff, Blood Glucose, Insulin, and Glucagon, for normal and T1D 1)
%%before injection and 2) after
% aro_time_norm = xlsread('Ins_clindata.xlsx', 'Aronoff','A5:A17');
% aro_norm_BG = xlsread('Ins_clindata.xlsx', 'Aronoff','B5:B17'); %mg/dL
% aro_norm_ins = xlsread('Ins_clindata.xlsx', 'Aronoff','C5:C17'); %microU/mL
% aro_norm_gluc = xlsread('Ins_clindata.xlsx', 'Aronoff','D5:D17'); %pg/mL
%
```

```matlab
% aro_time_T1D = xlsread('Ins_clindata.xlsx', 'Aronoff','F5:F16');
% aro_T1Dinj_BG = xlsread('Ins_clindata.xlsx', 'Aronoff','G5:G16'); %mg/dL
% aro_T1Dinj_ins = xlsread('Ins_clindata.xlsx', 'Aronoff','H5:H16'); %microU/mL
% aro_T1Dinj_gluc = xlsread('Ins_clindata.xlsx', 'Aronoff','I5:I16'); %pg/mL
%
% aro_time_T1D2 = xlsread('Ins_clindata.xlsx', 'Aronoff','O5:O14');
% aro_T1Dninj_BG = xlsread('Ins_clindata.xlsx', 'Aronoff','K5:K16'); %mg/dL
% aro_T1Dninj_ins = xlsread('Ins_clindata.xlsx', 'Aronoff','L5:L16'); %microU/mL
% aro_T1Dninj_gluc = xlsread('Ins_clindata.xlsx', 'Aronoff','P5:P14'); %pg/mL
%
% subplot(3,3,1)
% plot(aro_time_norm, aro_norm_BG)
% title('Aronoff Normal BG')
% ylabel('mg/dL')
% subplot(3,3,2)
% plot(aro_time_norm, aro_norm_ins)
% title('Aronoff Normal Ins')
% ylabel('microU/mL')
% subplot(3,3,3)
% plot(aro_time_norm, aro_norm_gluc)
% title('Aronoff Normal Glucagon')
% ylabel('pg/mL')
%
% subplot(3,3,4)
% plot(aro_time_T1D, aro_T1Dinj_BG)
% title('Aronoff T1D BG after Inj')
% subplot(3,3,5)
% plot(aro_time_T1D, aro_T1Dinj_ins)
% title('Aronoff T1D Ins after Inj')
% subplot(3,3,6)
% plot(aro_time_T1D, aro_T1Dinj_gluc)
% title('Aronoff T1D Gluc after Inj')
%
% subplot(3,3,7)
% plot(aro_time_T1D, aro_T1Dninj_BG)
% title('Aronoff T1D BG before Inj')
% subplot(3,3,8)
% plot(aro_time_T1D, aro_T1Dninj_ins)
```

```matlab
% title('Aronoff T1D Ins before Inj')
% subplot(3,3,9)
% plot(aro_time_T1D2, aro_T1Dninj_gluc)
% title('Aronoff T1D Gluc before Inj')
%~~~~~~~~~~~~~~~~~~~~~~~~~~~~~~~~~~~~~~~~~~~~~~~~~~~~~~~


%%Yamamoto Subcutaneous vs. Intravenous (from Sekigami) Insulin Effect--Not sure how I feel about this
data;
%the source does not match what is presented and for children only
% t_yam_sub = xlsread('Ins_clindata.xlsx', 'Yamamoto_ins','A4:A16');
% t_yam_iv = xlsread('Ins_clindata.xlsx', 'Yamamoto_ins','C4:C11');
% sub_ins_eff = xlsread('Ins_clindata.xlsx', 'Yamamoto_ins','B4:B16');
% iv_ins_eff = xlsread('Ins_clindata.xlsx', 'Yamamoto_ins','D4:D11');
% plot(t_yam_sub, sub_ins_eff);hold on;
% plot(t_yam_iv, iv_ins_eff);
% ylabel('Subcutaneous vs. Intravenous Ins Effect (/min)');


% %~~~~~~~~~~~~~~~~~~~~~~~~~~~~~~~~~~~~~~~~~~~~~~~~~~~~~~~~
% %Shimoda Peripheral Venous Insulin at 0.1 U/kg and Plasma Insulin Response
% t_pvi =  xlsread('Ins_clindata.xlsx', 'Shimoda1','A4:A12');
% ins_conc = xlsread('Ins_clindata.xlsx', 'Shimoda1','B4:B12');
% plot(t_pvi, ins_conc)
% title('Insulin Concentration (pmol/l)')
```